

**DEVELOPMENT OF A NEW ENVIRONMENTALLY FRIENDLY
GLASS FIBRE REINFORCED COLD MIX MICROASPHALT
WITH HIGH RESISTANCE TO CRACKING AND
DEFORMATION**

By

Atif Rasheed

A thesis submitted in partial fulfilment of the requirements of Liverpool John
Moore's University for the degree of Doctor of Philosophy

August 2017

DECLARATION

The research reported in this thesis has been conducted at Liverpool John Moores University, Department of Civil Engineering, between February 2014 and April 2017. I declare that the work is my own and has not been submitted for a degree at another university and appropriate credit has been given where reference has been made to the work of others.

Atif Rasheed

Liverpool

August 2017

SUPERVISOR CERTIFICATE

I certify that this thesis entitled “**Development of a New Environmentally Friendly Glass Fibre Reinforced Cold Mix Microasphalt with High Resistance to Cracking and Deformation**” has been prepared under my supervision at Liverpool Centre for Materials Technology (LCMT), Built Environment Sustainable Technologies Research Institute (BEST), Faculty of Engineering & Technology, Department of Civil Engineering, Liverpool John Moores University (LJMU), as partial fulfilment of the requirements of Liverpool John Moores University for the degree of Doctor of Philosophy. Field of study: Civil Engineering: Transportation - Highways (Pavements).

Dr Hassan Al Nageim BSc (Hons), MSc, PhD, CEng, FCIHT, MPEC, FInsNDT, FHEA
Professor of Structural Engineering
Head of Liverpool Centre for Materials Technology
Faculty of Engineering & Technology
Department of Civil Engineering
Liverpool John Moores University
Liverpool

August 2017

Table of Contents

Title Page	i
Declaration	ii
Supervisor Certificate	iii
Table of Contents	iv
List of Figures	xii
List of Tables	xvii
List of Graphs	xviii
List of Equations	xx
Abbreviations / Acronyms	xxi
Glossary of Symbols	xxv
Acknowledgements	xxvii
Dedication	xxviii
Abstract	xxix
Chapter 1	Research Definition and Aim
Chapter 2	Literature Review of the Previous Studies
Chapter 3	Cold Bituminous Emulsion Mixture
Chapter 4	Microasphalt
Chapter 5	Preparation of Cold Mix Microasphalt and Laboratory Testing
Chapter 6	Critical Analysis of Test Results
Chapter 7	Site Trial for Control and Glass Fibre Reinforced Cold Mix Microasphalt
Chapter 8	Conclusions & Recommendations

Table of Contents

Chapter 1: Research Definition and Aim

1.1 Introduction.....	2
1.2 Background to Research.....	4
1.3 Problem Statement.....	5
1.4 Aim.....	5
1.5 Objectives.....	5
1.6 Research Approach.....	6
1.7 Research Outcome.....	8
1.8 Thesis Structure.....	8

Chapter 2: Literature Review of the Previous Studies

2.1 Introduction to Literature Review.....	11
2.2 Road Transport Infrastructure Importance.....	11
2.3 Recognition of the Problem.....	12
2.4 Review of Related Past Literature.....	13
2.5 Pavement Preservation.....	15
2.6 Preservation Strategies	16
2.7 Microasphalt for Pavement Preservation.....	18
2.8 Pavement Performance Indicators.....	19
2.8.1 International Roughness Index (IRI).....	19
2.8.2 Distress Index.....	20
2.9 Analysis of Severity of Consequences.....	21
2.10 Synthesis of the Reviewed Literature.....	22
2.11 Summary.....	23

Chapter 3: Cold Bituminous Emulsion Mixture

3.1 Road Construction Development.....	25
--	----

3.2 Bituminous Mixtures.....	27
3.2.1 Hot Mix.....	27
3.2.2 Warm and Half Warm Mix.....	29
3.2.3 Cold Mix.....	29
3.3 Challenges to Asphalt Technologies.....	30
3.3.1 CO ₂ and Fume Emission.....	31
3.3.2 Energy Saving.....	31
3.3.3 Working Conditions.....	32
3.3.4 Paving Season and Hauling Distance.....	32
3.3.5 Incorporating Recycled and Waste Materials.....	33
3.3.6 Mixture Performance.....	33
3.3.7 Cost.....	34
3.4 Contents of Bituminous Mixtures.....	34
3.4.1 Aggregate.....	35
3.4.2 Bituminous Binders.....	35
3.4.3 Additives.....	36
3.4.4 Recycling, Waste and By-Products Materials.....	36
3.5 Road Mixtures and Cold Mix.....	37
3.6 Bitumen Emulsion Mixtures.....	37
3.7 Current Status of Hot and Cold Mix.....	37
3.8 Bitumen and Water.....	40
3.9 Curing of Bitumen Emulsions.....	41
3.10 Applications of Bitumen Emulsions.....	41
3.10.1 Surface Dressing.....	41
3.10.2 Tack Coats.....	42
3.10.3 Fog Seal.....	42
3.10.4 Prime Coat.....	42
3.10.5 Slurry Seal and Microsurfacing.....	43
3.11 Cold Mix Asphalt.....	44

3.12 Bitumen Emulsion.....	45
3.13 Foamed Bitumen.....	47
3.14 How Cold Mix Works.....	48
3.15 Practical Use of Cold Mix.....	53

Chapter 4: Microasphalt

4.1 Pavement Structure.....	56
4.2 Deterioration of Pavement Layers.....	58
4.3 Background Information on Microasphalt.....	59
4.4 Microasphalt as a Preventive Maintenance Tool.....	61
4.5 Benefits of Microasphalt.....	61
4.6 Limitations of Microasphalt.....	63
4.7 The Future of Microasphalt.....	63
4.8 Fibres in Microasphalt.....	64
4.9 Scope of Novel Glass Fibres in Microasphalt.....	66
4.10 Summary.....	67

Chapter 5: Methodology, Preparation of Cold Mix Microasphalt and Laboratory Testing

5.1 General: Pavement Distresses.....	69
5.2 Cracking in Pavements.....	70
5.2.1 Reflective Cracking in Pavements.....	71
5.2.1.A Tack Coats.....	71
5.2.1.B Transverse Cracks in Pavements.....	72
5.3 Rutting in Pavements.....	73
5.4 Ravelling.....	74
5.5 Performance of Thin Asphalt Layers.....	75
5.6 Distresses in Microasphalt Road Surfacing.....	76
5.7 Methodology.....	77
5.8 Material Characterisation.....	77

5.9 Aggregate Characterisation.....	78
5.10 Filler Characterisation.....	81
5.11 Bitumen Emulsion Characterisation.....	82
5.12 Retarder Characterisation.....	87
5.13 Fibre Characterisation.....	88
5.14 Mix Design.....	94
5.14.1 Prescreening.....	95
5.14.2 Job Mix Design (Mixing Proportions).....	95
5.14.3 Final Testing.....	97
5.15 Optimum Binder.....	97
5.16 Sample Preparation and Curing Technology.....	98
5.17 Laboratory Testing.....	101
5.17.1 Semi-Circular (Three Point) Bending Test Protocol.....	101
5.17.2 Sample Preparation.....	103
5.17.3 Testing.....	108
5.18 Laboratory Testing.....	109
5.18.1 Wheel Tracking Test Protocol.....	109
5.18.2 Sample Preparation.....	111
5.18.3 Testing.....	112
5.19 Replacement of a Conventional Filler.....	115
5.20 Filler and Filler Supplementary Approach to Enhance Microasphalt.....	115
5.21 Alternatives: Waste and By-Product Active Fillers.....	117
5.22 Benefits of Cementitious Filler.....	119
5.23 Characterisation of OPC.....	119
5.24 Characterisation of PSA.....	120
5.25 Characterisation of CKD.....	121
5.26 Characterisation of RHA.....	122
5.27 Microstructure Characterisation of Active Fillers.....	124

5.28 Experimental Setup.....	124
5.28.1 PH.....	124
5.28.2 XRF Analysis of New Cementitious Filler.....	124
5.28.3 Specific Surface Area.....	126
5.28.4 Particle Size Characteristics.....	127
5.28.5 SEM Analysis of New Cementitious Filler.....	127
5.28.6 Density.....	130
5.29 Evaluation of SCB and WT Tests using Finite Element Modelling.....	130
5.29.1 Determination of Parameter for Finite Element Modelling.....	131
5.29.2 FEM for the SCB Test.....	135
5.29.3 FEM for the WT Test.....	142

Chapter 6: Critical Analysis of Test Results

6.1 Semi-Circular Bending Test Results.....	145
6.2 Semi-Circular Bending Test Analysis.....	152
6.3 Crack Propagation Rate.....	154
6.4 Wheel Tracking Test Results.....	156
6.5 Discussion.....	158
6.6 Chemical and Physical Test Results for the Active Fillers.....	159
6.6.1 XRF Analysis for OPC.....	160
6.6.2 XRF Analysis for PSA.....	162
6.6.3 XRF Analysis for CKD.....	164
6.6.4 XRF Analysis for RHA.....	166
6.6.5 Particle Size Distribution of Fillers.....	167
6.6.6 Main Oxides Percentages for Fillers.....	168
6.6.7 Chemical & Physical Characteristics of Fillers.....	169
6.6.8 SEM Analysis of OPC Powder & Mastic.....	170
6.6.9 SEM Analysis of PSA Powder & Mastic.....	171
6.6.10 SEM Analysis of CKD Powder & Mastic.....	172

6.6.11 SEM Analysis of RHA Powder & Mastic.....	174
6.6.12 SEM Analysis of Blend (PSA, CKD & RHA) Mastic.....	176
6.7 Discussions.....	177
6.7.1 Alkaline Nature.....	178
6.7.2 Cementitious Action.....	179
6.7.3 Specific Surface Area and Particle Size.....	179
6.7.4 Morphology.....	180
6.8 Summary on Filler Development.....	180
6.9 New Cementitious Filler Test Result Analysis.....	181
6.10 Test Results for the FEM.....	187
6.11 Experimental and FEM Results for the SCBT.....	193
6.12 Experimental and FEM Results for the WTT.....	195
6.13 Summary of Findings on FEM.....	196

Chapter 7: Site Trial for Control and Glass Fibre Reinforced Cold Mix Microasphalt

7.1 Introduction.....	199
7.2 Field Trial.....	199
7.3 Ingredients.....	202
7.4 Application.....	202
7.5 Applicator Settings.....	205
7.6 Weather.....	205
7.7 Site Inspection the Next Day.....	205
7.8 Site Sample Testing.....	206
7.9 Summary.....	208
7.10 Site Inspection at 12 Months on 23 rd September 2015.....	209
7.11 Site Inspection at 25 Months on 24 th October 2016.....	212

Chapter 8: Conclusions & Recommendations for Further Research

8.1 Conclusions.....	219
----------------------	-----

8.2 Recommendations.....	224
8.2.1 Recommendations for Implementation.....	224
8.2.2 Recommendations for Further Research.....	225

References

References.....	227
-----------------	-----

List of Figures

Figure 2-1: Consequences of Deferred Maintenance (Bennett, 2009).....	13
Figure 2-2: Pavement Condition vs Time (Galehouse, 2002).....	17
Figure 2-3: IRI Roughness Scale (Sayers et al., 1986).....	20
Figure 2-4: Remaining Service Life of Two Pavement Sections (Baladi et al., 2004)....	21
Figure 3-1: Asphalt Mixture Market (EAPA, 2010).....	31
Figure 3-2: Classification of Mixture Technologies by Temperature Range and Fuel Usage (D'Angelo et al., 2008).....	32
Figure 3-3: A Suspension of Bitumen Droplets in Water.....	45
Figure 3-4: Bitumen Emulsion Preparation Process.....	46
Figure 3-5: Bitumen Emulsion - Colloid Mill.....	46
Figure 3-6: Bitumen Emulsion Droplets.....	47
Figure 3-7: Foamed Bitumen Preparation Process.....	47
Figure 3-8: Foamed Bitumen.....	48
Figure 3-9: Mechanics of Cold Mix.....	49
Figure 3-10: Internal Void Structure of Cold Mix (Left) and Hot Mix (Right).....	50
Figure 3-11: Volumetrics for Cold and Hot Mixes.....	51
Figure 3-12: Strength Gained by Cold Mixes Since Construction.....	52
Figure 3-13: Difference Between Cold Mix (Left: Grey) and Hot Mix (Right: Black).....	53
Figure 4-1: Typical Pavement Structure.....	57
Figure 4-2: Vertical Elastic Strain in Cold Mix Pavements.....	58
Figure 4-3: Tensile Strain in Cold Mix Pavements.....	58
Figure 4-4: Machine Laying Microasphalt on Site.....	59
Figure 5-1: Cracking Phenomena in Pavements.....	70
Figure 5-2: Reflective Cracking in Asphalt Concrete Pavement.....	71
Figure 5-3: Longitudinal Crack in Pavement.....	72
Figure 5-4: Reasons for Longitudinal Cracking.....	72
Figure 5-5: Transverse Crack in Pavement.....	73
Figure 5-6: Rutting Phenomena in Pavements.....	73

Figure 5-7: Causes of Rutting in Pavements.....	74
Figure 5-8: Rutting in Asphalt Concrete Pavement.....	74
Figure 5-9: Ravelling in Asphalt Concrete Pavement.....	75
Figure 5-10 (a): Sieve Shaker.....	81
Figure 5-10 (b): Aggregates in the Container.....	81
Figure 5-11: Bitumen Emulsion Jerrycan.....	83
Figure 5-12: Bitumen Emulsion Sample in the Container.....	84
Figure 5-13: Bitumen Emulsion Examined with the Help of High Resolution Microscope.....	84
Figure 5-14: Latex and Asphalt Particles 3-D Structure at Magnification Level of 100µm.....	84
Figure 5-15: Emulsion Modification Process.....	85
Figure 5-16: Surfactant Action in Modified Asphalt emulsion.....	86
Figure 5-17: Bitumen Emulsion Production Facility.....	86
Figure 5-18: Emulsification of Bitumen Emulsion in Progress.....	86
Figure 5-19: Bitumen Emulsion Production in Silos.....	87
Figure 5-20: Drums Filled with Bitumen Emulsion.....	87
Figure 5-21: Glass Fibre Manufacturing Process	89
Figure 5-22: Glass Fibre Doff.....	89
Figure 5-23: Chopped Glass Fibres.....	89
Figure 5-24: Glass Fibres in Different Cut Lengths.....	90
Figure 5-25: SEM Images of Glass Fibres.....	90
Figure 5-26: Universal Tensile Testing Machine.....	93
Figure 5-27: Fractured Glass Fibre Filament after the Test.....	94
Figure 5-28: Microasphalt Mix Prepared in the Laboratory.....	96
Figure 5-29: Principles of SCBT.....	102
Figure 5-30: Schematic of the Experimental Setup for SCBT.....	103
Figure 5-FC: Process for preparation of a sample to testing of a specimen.....	104
Figure 5-31: Hydraulic Standard Roller Compactor (CRT-RC-H2).....	106
Figure 5-32: Core and Beam Saw (CRT-SAW150).....	107

Figure 5-33: Compressed Sample for SCB Test.....	108
Figure 5-34 (a): SCB Test Assembly with Sample under Test.....	109
Figure 5-34 (b): Condition of the Sample after the Test.....	109
Figure 5-35: Principle of WTT.....	110
Figure 5-36-1: Hobart Mixer.....	112
Figure 5-36-2: Wheel Tracking Test Sample.....	112
Figure 5-37: Automatic Wheel Tracking Tester (HYCZ-5).....	113
Figure 5-38: Schematic of the Experimental Setup for Wheel Tracking Test (BACTIA, HYCZ-5, Operation Manual, 2013).....	113
Figure 5-39: Wheel Tracking Test in Progress.....	114
Figure 5-40: Condition of the Sample after the Test.....	114
Figure 5-41: Conventional Filler OPC and New Candidate Fillers PSA, CKD & RHA.....	118
Figure 5-42: XRF Analysis of Candidate Fillers.....	125
Figure 5-43 (a): Specific Surface Area Apparatus.....	126
Figure 5-43 (b): Samples in the Test Tubes.....	127
Figure 5-44: Particle Size Analyser.....	127
Figure 5-45-1: Different Interactions of an Electron Beam with a Solid Target (Ramachandran & Beaudoin, 2001).....	129
Figure 5-45-2: SEM Analysis of Candidate Fillers.....	129
Figure 5-46: Principle of Poisson's Ratio (Greaves et al., 2011).....	131
Figure 5-47: Marshall Sample Mould and Base Plate.....	132
Figure 5-48: Marshall Hammer.....	133
Figure 5-49: Marshall Samples.....	133
Figure 5-50: Poisson's Ratio Test Setup.....	134
Figure 5-51 (a): Shape of Cohesive Element CPE4 (First-order Interpolation).....	136
Figure 5-51 (b): Shape of Cohesive Element C3D8 (Second-order Interpolation).....	136
Figure 5-51 (c): Abaqus FE Mesh for the SCB Test Specimen.....	136
Figure 5-52: Layout of the FE Model.....	137
Figure 5-53: Crack Evolution Process in the SCBT.....	139

Figure 5-54: Crack Evolution Damage in the SCBT.....	141
Figure 5-55: Layout of the FE Model.....	142
Figure 6-1: Balling Phenomenon in Microasphalt.....	149
Figure 6-2: Left FEA Diagram Shows the Distribution of Tensile Stresses and Right One Shows the Distribution of Compressive Stresses (Molenaar & Molenaar, 2000).....	153
Figure 6-3: Graphic Illustration of Cracking Phenomena in 3D Space for SCB Test and Stress Concentration within the SCB Specimen.....	153
Figure 6-4: Particle Size Distributions for the Selected Fillers.....	168
Figure 6-5: Main Oxides Percentages for the Selected Fillers.....	169
Figure 6-6: SEM Analysis of OPC Powder & Mastic.....	171
Figure 6-7: SEM Analysis of PSA Powder & Mastic.....	172
Figure 6-8: SEM Analysis of CKD Powder & Mastic.....	174
Figure 6-9: SEM Analysis of RHA Powder & Mastic.....	175
Figure 6-10: SEM Analysis of Blend (PSA, CKD & RHA) Mastic.....	177
Figure 6-11: Stress Concentration Zone 3D FE Modelling for the CMM in the WTT.....	192
Figure 6-11 (a): Stress concentration zone 3D FE modelling for the CM - WTT (A)	188
Figure 6-11 (b): Stress concentration zone 3D FE modelling for the CM - WTT (B)	188
Figure 6-11 (c): Stress concentration zone 3D FE modelling for the 0.2% GFRM blend - WTT (A).....	190
Figure 6-11 (d): Stress concentration zone 3D FE modelling for the 0.2% GFRM blend - WTT (B).....	190
Figure 6-11 (e): Stress concentration zone 3D FE modelling for the GCF - 0.2% GFRM blend - WTT (A)	192
Figure 6-11 (f): Stress concentration zone 3D FE modelling for the GCF - 0.2% GFRM blend - WTT (B)	192
Figure 7-1: Site Trial Location on Talbot Road, Leeds.....	199
Figure 7-2: Location Map of Site Trial Section on Talbot Road, Leeds.....	200
Figure 7-3: Myriad of Extensive Cracks.....	201
Figure 7-4: Condition of Talbot Road before Application of Control and Fibre Reinforced Microasphalt.....	201

Figure 7-5: Schematic for Application of Glass Fibre Reinforced Microasphalt.....	202
Figure 7-6: Two Reels of Glass Fibre with a Chopper (Open Cover).....	203
Figure 7-7: Schematic of Glass Fibres Blended in the Mix Acting as a Stress Absorbing Membrane Interlayer (SAMI).....	203
Figure 7-8: On Site Glass Fibres Inclusion in the Microasphalt.....	204
Figure 7-9: Site Sample Broken Open to Show the Two Forms of Fibre.....	207
Figure 7-10: Two Forms of Glass Fibre and Aggregates Recovered from a Site Sample.....	208
Figure 7-11: Appearance of Roughly the same Area as the Initial Photo before Application given in Section 7.2 above.....	210
Figure 7-12: Condition of Talbot Road on Inspection at 12 months, Fibreless Section on Left and Closer Look on Surface Texture of Fibre Reinforce Section on Right.....	210
Figure 7-13: Temperature for Leeds, UK (WeatherSpark, 2015).....	211
Figure 7-14: Precipitation for Leeds, UK (WeatherSpark, 2015).....	212
Figure 7-15: Reflective Cracking (Transverse) in Fibreless Section.....	213
Figure 7-16: Reflective Cracking (Longitudinal) in Fibreless Section.....	213
Figure 7-17: Minor Ravelling in Fibreless Section.....	214
Figure 7-18: Glass Fibre Reinforced Section.....	215
Figure 7-19: Glass Fibre Reinforced Section near Hump.....	215
Figure 7-20: Temperature for Leeds, UK (WeatherSpark, 2016).....	216
Figure 7-21: Precipitation for Leeds, UK (WeatherSpark, 2016).....	217

(Courtesy: photographs captured with professional Nikon D90 digital single reflex (DSLR) camera)

List of Tables

Table 5-1: Aggregate Physical Properties.....	79
Table 5-2: Typical Aggregate Gradings (Caltrans, 1999).....	79
Table 5-3: Ingleton Typical Aggregate Gradation.....	80
Table 5-4: Properties of Bitumen Emulsion (Ralumac).....	83
Table 5-5: Properties of Retarder Dope.....	88
Table 5-6: Specifications of Glass Fibre.....	91
Table 5-7: XRF (quantitative) Analysis of Glass Fibres (GF).....	92
Table 5-8: Optimum Binder Content for the Microasphalt Mixes.....	97
Table 5-9: Specifications of Hydraulic Standard Roller Compactor (CRT-RC-H2).....	106
Table 5-10: Specifications of Core and Beam Saw (CRT-SAW150).....	107
Table 5-11: Semi-Circular Bending Test Conditions.....	108
Table 5-12: Wheel Tracking Test Conditions.....	114
Table 5-13: Most Important Oxides of Cement (Domone and Illston, 2010).....	120
Table 5-14: Relaxation Test Conditions.....	134
Table 6-a: Effect of Fibre Length.....	147
Table 6-b: Effect of Fibre Quantity.....	150
Table 6-1: XRF (Quantitative) Analysis of OPC.....	161
Table 6-2: XRF (Quantitative) Analysis of PSA.....	163
Table 6-3: XRF (Quantitative) Analysis of CKD.....	165
Table 6-4: XRF (Quantitative) Analysis of RHA.....	167
Table 6-5: Chemical and Physical Characteristics of Selected Fillers.....	170
Table 7-1: Specifications of Tandem Roller Compactor.....	205
Table 7-2: Results of Site Samples.....	206

List of Graphs

Graph 3-1: Effect of Fluid Content on Compaction.....	51
Graph 5-1: Tensile Strain and Deformation versus Asphalt Thickness (Thom, 2012).....	76
Graph 5-2: XRF Analysis of Glass Fibre.....	92
Graph 5-3: Tensile Strength of a Glass Fibre Filament.....	94
Graph 6-1: Flexural Load as Function of Vertical Displacement.....	145
Graph 6-a: Error Bars for Displacement at Peak Force.....	147
Graph 6-2: Effect of Glass Fibre Length in Microasphalt.....	148
Graph 6-b: Error Bars for Displacement at Peak Force.....	150
Graph 6-3: Effect of Fibre Quantity in Microasphalt.....	150
Graph 6-4: Optimised Length and Quantity of Glass Fibre in Microasphalt versus Control Microasphalt.....	152
Graph 6-5: Crack Growth Rate in Microasphalt with varying Quantity of Glass Fibre.....	156
Graph 6-6: Wheel Tracking Test for Control and Glass Fibre Reinforced Microasphalt.....	158
Graph 6-7: XRF Analysis of OPC.....	161
Graph 6-8: XRF Analysis of PSA.....	163
Graph 6-9: XRF Analysis of CKD.....	165
Graph 6-10: XRF Analysis of RHA.....	167
Graph 6-11: Effect of Green Cement Filler in Microasphalt (SCBT).....	184
Graph 6-12: Effect of Green Cement Filler in Microasphalt (WTT).....	186
Graph 6-13: Experimental and FEM Results for the CM - SCBT.....	193
Graph 6-14 (a): Experimental and FEM Results for the 0.1 % GFRM Blend - SCBT.....	193
Graph 6-14 (b): Experimental and FEM Results for the 0.2 % GFRM Blend - SCBT.....	194
Graph 6-14 (c): Experimental and FEM Results for the 0.4 % GFRM Blend - SCBT.....	194
Graph 6-15: Experimental and FEM Results for the GCF - 0.2 % GFRM Blend - SCBT.....	194
Graph 6-16: Experimental and FEM Results for the CM - WTT.....	195

Graph 6-17: Experimental and FEM Results for the 0.2 % GFRM Blend - WTT.....	196
Graph 6-18: Experimental and FEM Results for the GCF - 0.2 % GFRM Blend - WTT.....	196

List of Equations

Equation 3-1: Analytical Method for Prediction of Cold Mix Stiffness Modulus.....	52
Equation 3-2: Determination of Parameter (n).....	52
Equation 5-1: Volume Fraction.....	105
Equation 5-2: Aspect Ratio.....	105
Equation 5-3: Poisson's Ratio.....	131
Equation 6-1: Stress.....	154
Equation 6-2: Stress Intensity Factor.....	154
Equation 6-3: Crack Growth Rate.....	155

Abbreviations / Acronyms

American Emulsion Manufacturers Association (AEMA)

American Society of Civil Engineers (ASCE)

American Society for Testing and Materials (ASTM)

Aspect Ratio (AR)

Asphalt Institute Report (AIR)

British Standards (BS)

Crack Growth Rate (CGR)

Cement Kiln Dust (CKD)

Climate Change Levy (CCL)

Cohesive Element (CE)

Cold Bituminous Emulsion Mixture (CBEM)

Cold Mix Asphalt (CMA)

Cold Mix Microasphalt (CMM)

Computer Aided Engineering (CAE)

Computer Aided Pavement Analysis Three Dimensional (CAPA-3D)

Control Microasphalt (CM)

Conventional Mineral Filler (CMF)

Damaged Zone (DZ)

Deformation Process Zone (DPZ)

Departments of Transportation (DOTs)

Emulsion Content (EC)

Energy Dispersive Spectroscopy (EDS)

European Asphalt Pavement Association (EAPA)

European Standards (EN)

Evolution of Damage (ED)

Federal Highway Administration (FHWA)

Finite Element (FE)

Finite Element Analysis (FEA)

Finite Element Modelling (FEM)

Fly Ash (FA)

Fracture Process Zone (FPZ)

Generalised Finite Element Modelling (GFEM)

Georgia Department of Transportation (GxDOT)

Glass Fibre (GF)

Glass Fibre Reinforcement (GFR)

Glass Fibre Reinforced Microasphalt (GFRM)

Granulated Ground Blast Furnace Slag (GGBFS)

Green Cement Filler (GCF)

Rice Husk Ash (RHA)

Her Majesty's Stationery Office (HMSO)

Highway Authority and Utility Committee (HAUC)

Hot Mix Asphalt (HMA)

Inorganic (INORG)

International Roughness Index (IRI)

International Slurry Surfacing Association (ISSA)

International Organization for Standardization (ISO)

Life-Cycle Cost Analysis (LCCA)

Linear Elastic Fracture Mechanism (LEFM)

Liverpool John Moores University (LJMU)

Loaded Wheel Deformation Contours (LWDC)

Minnesota Department of Transportation (MnDOT)

National Asphalt Pavement Association (NAPA)

National Cooperative Highway Research Program (NCHRP)

Optimum Binder Content (OBC)

Ordinary Portland Cement (OPC)

Organisation for Economic Co-operation and Development (OECD)

Paper Sludge Ash (PSA)

Poisson's Ratio (ν)

Polycyclic Aromatic Compounds (PAC's)

Primary Filler (PF)

Pulverised Fuel Ash (PFA)

Ralumac Emulsion (RE)

Reclaimed Asphalt Pavement (RAP)

Remaining Service Life (RSL)

Rice Husk (RH)

Roller Compactor (RC)

Rut Potential (RP)

Scan Electron Microscopy (SEM)

Stone Mastic Asphalt (SMA)

Supplementary Cementitious Materials (SCMs)

Secondary Filler (SF)

Semi-Circular Bending (SCB)

Semi-Circular Bending Test (SCBT)

Silica Fume (SF)

Stress Absorbing Membrane Interlayer (SAMI)

Stress Concentration Zone (SCZ)

Stress Induced Concentration Areas (SICA)

Styrene Butadiene Styrene (SBS)

Texas Department of Transportation (TxDOT)

Transport and Road Research Laboratory (TRRL)

United Kingdom of Great Britain and Northern Ireland (UK)

United States Environmental Protection Agency (USEPA)

United State of America (USA)

Voids in Minerals Aggregate (VMA)

Warm Mix Asphalt (WMA)

Wheel Tracking (WT)

Wheel Tracking Test (WTT)

X-ray Fluorescence (XRF)

Young Modulus (E)

Glossary of Symbols

Units

Ampere (A)

Degrees Celsius ($^{\circ}\text{C}$)

Gram Per Litre (g/l)

Hertz (Hz)

Hour (hr)

Kilogram (kg)

Kilogram Per Cubic Metre (kg/m^3)

Kilometre (km)

Kilopascal (kPa)

Kilowatt (kW)

Megagram Per Cubic Metre (Mg/m^3)

Megapascal (MPa)

Micrometer (μm)

Millimeter (mm)

Milligram Per Cubic Metre (mg/m^3)

Minute (min)

Nanoampere (nA)

Nanogram Per Cubic Metre (ng/m^3)

Number (No)

Percentage (%)

Seconds (s)

Seconds Per Minute (s/min)

Volts (V)

Chemical Formulas

Aluminum Oxide (Al_2O_3)

Calcium Oxide (CaO)

Carbon Dioxide (CO_2)

Chlorine (Cl)

Dicalcium Silicate ($3\text{CaO}\cdot\text{SiO}_2$)

Iron Trioxide (Fe_2O_3)

Magnesium Oxide (MgO)

Phosphorus Pentoxide (P_2O_5)

Potassium Oxide (K_2O)

Silicon Dioxide (SiO_2)

Sulphur Trioxide (SO_3)

Tricalcium Aluminate ($3\text{CaO}\cdot\text{Al}_2\text{O}_3$)

Tricalcium Silicate ($3\text{CaO}\cdot\text{SiO}_2$)

Tetracalcium Aluminoferrite ($4\text{CaO}\cdot\text{Al}_2\text{O}_3\cdot\text{Fe}_2\text{O}_3$)

ACKNOWLEDGEMENTS

I would like to express my deepest gratitude to my Director of Studies, **Professor Hassan Al Nageim**, for his excellent guidance, encouragement and advice he has provided throughout my postgraduate research studies at Liverpool John Moores University. I have been extremely lucky to have a research supervisor who cared so much about my work, and who responded to my questions and queries so promptly. It is not often that one finds an advisor and colleague that always finds the time for listening to the little problems and roadblocks that unavoidably crop up in the course of performing research. His technical and editorial advice was essential to the completion of this research and has taught me innumerable lessons and insights on the workings of academic research in general.

His mentorship was paramount in providing a well-rounded experience consistent my long-term career goals. He encouraged me to not only grow as an experimentalist and a professional engineer but also as an independent thinker. This aptitude not only increased my curiosity but also enabled me to apply a scientific approach to tackle complex problems through niche and unique research work which aims at addressing longer-term needs of the industry with self-criticism on it. I am not sure many postgraduate research students are given the opportunity to develop their own individuality and self-sufficiency by being allowed to work with such independence.

In particular, I also wish to thank the following individuals and organizations: **Dr Clare Harris** and **Dr Linda Seton**, my research team supervisors, for their help and guidance, throughout the work. The laboratory staff at the university, especially **Malcom Feegan** and **John Sinclair**. Industrial partner, **John Richardson** and **Sommerville Wright** for generously providing the resource materials bitumen emulsion, aggregates, fibres and chemicals to carry out the research work.

DEDICATION

This thesis is dedicated to my parents, **Abdul Rasheed** and **Musharraf Rasheed** and my younger brother and sister, **Adil Rasheed** and **Amber Rasheed**. Thank you for the sacrifices you have made to give me the freedom to undertake this work. They were always supporting me and encouraging me with their best wishes.

ABSTRACT

Nowadays, the pavement industry plays an important role in the global transportation infrastructure and stimulates economic growth in both advanced and emerging countries. Nevertheless, most of these transportation infrastructures are paved with using hot mix asphalt (HMA) technology. Apropos to this, the use of cold bituminous emulsion mixtures (CBEMs) for road maintenance is increasingly gaining interest. These mixtures offer advantages in several ways: environmentally friendly, energy saving, cost effectiveness, safety and enhanced production processes. Today in the UK, the use of cold mix attracts less interest, as these mixtures show low strength to resist traffic loading due to rainfall.

Microasphalt is a cold mix applied wearing course which is deemed as an important player in the maintenance of the nation's roadways. This research was designed to investigate the cracking and deformation resistance properties of microasphalt both with and without a novel glass fibre applied. The effect of varying the length of glass fibres (aspect ratio) and varying the percentage of quantity of glass fibres (volume fraction) in the microasphalt mix was probed. The investigation was divided into three main areas of study. They were i) the physical, ii) chemical characterisation of glass fibres, aggregates, bitumen emulsion, primary & secondary filler, and iii) mechanical testing of control microasphalt, glass fibre reinforced cold mix microasphalt and green cement filler microasphalt.

Chemical testing involved a regime to show the affinity between aggregates and bitumen emulsion in the presence of water. Chemical composition of glass fibres and secondary filler was also examined. Physical testing included the common tests for demonstrating the properties of glass fibres. These tests included the tensile testing and scanning electron microscopy (SEM) test. Microasphalt was chosen as a suitable road material for testing the effects of the glass fibre to retard the reflective cracking and rutting pavement distresses in a bituminous emulsion material as it is a uniformly graded stone matrix mixture and is currently enjoying increased acceptance Europe-wide as a high-quality surfacing material. Tests applied included the semi-circular bending (SCB) and wheel tracking tests. All necessary equipment was available to the researcher at Liverpool John Moores University (LJMU).

Observations made during the testing programme showed that for the first time the glass fibres displayed a useful improvement in the cracking and deformation properties of microasphalt over the control microasphalt. This was also validated through mass production prototyping of glass fibre reinforced cold mix microasphalt in road trial sections. In addition, paper sludge ash (PSA), cement kiln dust (CKD) and rice husk ash (RHA) were used as a novel secondary filler to; i) replace ordinary Portland cement (OPC) currently used for replacing limestone filler and ii) improve the mechanical properties and durability of cold mix microasphalt (CMM). The blended secondary filler (PSA, CKD and RHA) played a vital role in accelerating the hydration process of the microasphalt paste and thus produced a resilient thin surfacing material. Microanalysis techniques, namely SEM and x-ray fluorescence (XRF), were used to investigate the role and mechanism of active fillers in CMM.

The newly developed material was subjected to seasoned testing protocols and showed an achievement of 15% and 33% in the tensile strength of reinforced microasphalt at maximum load failure and ultimate failure respectively compared to the control microasphalt based on the results of the three-point bending test and an improvement of 83% in the deformation for reinforced microasphalt from the wheel track test compared to the control microasphalt. The results obtained in this research work which also covers a study using finite element modelling (FEM), appear to open up a new era of CMM and are based completely on sustainable techniques for both light and heavily trafficked road and highway pavements.

Chapter

1

Research Definition and Aim

1.1 INTRODUCTION

Highway and road transportation facilities are growing rapidly due to the massive global developments and characteristics of our modern transportation needs. The advancement in vehicles is an example of huge development; this includes increases in speed, safety and comfort. Furthermore, the characteristics of door to door service, decision freedom and general time consumed contribute to this development. Accordingly, the modern lifestyle has forced the automobile manufactures to increase the production of private and commercial vehicles; the International Organization of Motor Vehicle Manufacturers reported that within the last 10 years, global annual vehicle production increased from 69.22M to 94.97M (IOMVMs, 2016). Consequently, the construction of new highways and roads plus maintenance of the existing networks are in high demand and certainly this will eventually reflect on pavement structure to accommodate such demand.

Annual investment in highway, street, and bridge construction represents one of the major public investments; in Europe, it has reached €80 billion, while in the USA it is \$110 billion (NAPA & EAPA, 2011). More or less all daily activities use highway and road infrastructure facilities, thus the authorities in charge worldwide provide sound instructions to ensure high standards of the product (pavements). For many years in the UK and worldwide, pavement surface and/or structural layers were traditionally constructed from HMA, and this material has shown satisfactory characteristics in terms of serviceability and durability.

Recently, global warming, CO₂ emissions and the continuing increases in energy costs have presented real problems, which are putting pressure on industry in general. Another pressure in the paving industry in addition to the above is the health and safety issue, with the use of unsafe high temperatures plus exposure to fumes and dust during HMA production. All these raised significant discussions to find more economic and sustainable alternatives. Hence, warm mix asphalt (WMA) technology has attracted many researchers and huge efforts have been expended to develop such a mixture. Generally, WMA has slightly reduced CO₂ emissions and energy consumption, however, cost and other issues need to be proven (Bouteiller, 2010).

On the other hand, to date there is no cold mix asphalt (CMA) with characteristics that are acceptable to road engineers. Nevertheless, globally, many researchers and pavement specialists believe that upgrading CMA can be a move in the right direction, due to the comparative economic, environmental and manufacturing process characteristics of CMA in contrast to HMA (Bouteiller, 2010). Thus, an understanding of CMA characteristics and control of the said mix's shortfalls is a challenge that should be met.

Generally, the major shortfalls of CMA are low early strength, long curing time, high void content and high sensitivity to rain at the early stage (Leech, 1994) and (Needham, 1996). Thus, CMA has attracted little attention from the pavement authorities of some countries; e.g. in the UK, CMA is restricted for reinstatement work of low trafficked roads and footways (HAUC, 2010). However, in countries like the USA and France more attention has been devoted to characterise CMA (Asphalt Institute, 1989) and (Bouteiller, 2010). Although the development of CMA started in the early 1970s, economic and environmental impacts have recently begun to provide pressure for more development. However, continuing studies into CMA could offer unique asphalt mixtures.

Synchronously, throughout the transportation industry there is an ongoing need to improve the quality of the surfacing material provided for the maintenance of flexible pavements. Flexible bituminous pavement constitutes a very large part of the transportation network facility; therefore, the performance and durability of bituminous material needs constant upgrading to meet the socio-economic and environmental demands of the transportation network user.

Further, in many countries, there are insufficient supplies of pavement materials suitable for high stability, low deformation bituminous road surfacing. Often these countries need to import expensive materials to meet their construction needs. It follows then, that road construction and maintenance can become a burden on local and national economies. Poorer quality bituminous surfaces are no longer acceptable, for they can fail under the stresses applied by modern vehicles. The use of these materials could therefore be costly in repair bills and in the resulting delays.

Guidelines, specifications and regulations rule out the use of these materials in all but the least severe applications, in many countries.

It can be seen therefore that there is a need to improve the performance of cold mix microasphalt so it can be used in a wider range of applications. This research seeks to i) improve the cracking resistance and deformation properties of microasphalt by testing a glass fibre and ii) to investigate the use of waste filler as a replacement to the Ordinary Portland cement in microasphalt and thus provide more environmentally friendly material.

1.2 BACKGROUND TO RESEARCH

In the current economy, infrastructure maintenance among different assets has become a mammoth challenge for highway agencies because of funding scarcity, increased competition and the anticipated need for prioritising resource allocations. As a consequence, goals to maximise the benefits for taxpayers within the limited funds need to be thoroughly reviewed.

Developed in Germany in the late 1960s and early 1970s, microsurfacing was pioneered as a way to apply a conventional slurry in thick enough layers to fill wheel ruts. Microsurfacing is now used throughout Europe, the US, and Australia and is making inroads into many other areas (Allan, 2002 and ISSA, 2010).

The research stems from ongoing work at Liverpool John Moores University (LJMU), in collaboration with an industrial partner and Knowledge Transfer Partnerships UK funding programme. The work concentrated mainly on new techniques for improving the surface course material using novel glass fibres, chemical additives and green cement. The work was for application in the fields of high quality flexible pavements mixtures and for other more general maintenance uses. An interest generated by the factors mentioned in the introduction, together with a general interest in materials-science further encouraged this research. The aim was to understand and improve the mix material at a chemical and microstructure level to increase the overall mechanical strength and cracking resistance of microasphalt.

Preliminary studies showed that the performance of bituminous pavement depends upon the bonding between the bitumen binder and the aggregate particles and that this bonding is a function of both physical and chemical properties. The purpose of this research was therefore, to investigate a method of improving the crack resistance and deformation properties of cold mix microasphalt.

1.3 PROBLEM STATEMENT

Companies applying the material are facing the problem of early crack development and deformation within the microasphalt life span. LJMU was approached by an industrial partner to overcome this problem; producing microasphalt with high resistance to cracking and deformation.

1.4 AIM

The aim of this research is twofold:

- a) To overcome the cracking and deformation problems associated with the microasphalt and produce a new high value glass fibre reinforced microasphalt with high resistance to cracking and deformation.
- b) To replace the conventional OPC used in the microasphalt by a secondary cementitious (cost effective and environmentally friendly) material

1.5 OBJECTIVES

The research objectives cover the following key aspects:

- 1) To carry out a background study to establish the properties of microasphalt.
- 2) Developing curing & compaction technology for sample preparation to predict cracking and deformation of conventional microasphalt.

-
-
- 3) Carry out laboratory testing using the above to optimise the amount of novel fibres in the microasphalt in terms of cracking and deformation.
 - 4) On the optimised microasphalt, replace the conventional OPC with the novel secondary cementitious material of similar chemical and mechanical properties.
 - 5) Use finite element programme Abaqus version 6-16-3 to simulate the laboratory findings.
 - 6) Use the laboratory findings to confirm (to provide understanding) for the high performance of the newly developed material on site and monitor its performance over a complete winter-summer cycle.
 - 7) Providing the company with the best practice report.

1.6 RESEARCH APPROACH

In order to achieve the aim of the research the following methodology has been devised:

1. Familiarisation with best practices and current standards for microsurfacing. This stage will culminate in a preliminary study based on current practices in the quality assessment of highways and on the specifications, creating baseline information to benchmark against work conducted in further stages. Detailed literature survey of previous studies on microsurfacing. This stage will gather and review studies conducted on microsurfacing and critical assessment of cracking and other mechanical and durability performance parameters i.e. resistance to deformation will be done through knowledge acquired in stage 1.
2. Characterisation and optimisation of the existing and new material in terms of the key physical and chemical properties using BS EN relevant codes of practice. Based on the literature review, previous work conducted and the laboratory investigation:

-
-
- a. Optimise novel fibre physical properties such as length (aspect ratio), quantity (volume fraction) and tensile strength together with its surface chemical characteristics.
 - b. Developing sample preparation and curing technology. This is a very challenging new research work conducted for the first time.
 - c. Optimise final mix product and carry out tests namely; semi-circular bending test for determination of crack resistance and wheel tracking test for permanent deformation.
3. Laboratory testing, producing new high value glass fibre reinforced microasphalt. This stage includes:
 - a. Assessing the ability of the microasphalt to resist cracking due to traffic loadings using a semi-circular bending (SCB) fracture test according to BS EN 12697-44. This will include a:
 - i. Control standard microasphalt.
 - ii. Novel glass fibre reinforced microasphalt (at different glass fibre additions of lengths: 6mm, 12.5mm, 16mm and 25mm and quantities: 0.1%, 0.2%, 0.3% and 0.4%).
 - iii. Novel filler (i.e. secondary cementitious waste filler) reinforced microasphalt.
 - b. Measure the rut resistance by tracking a loaded rubber wheel back and forth across the microasphalt; wheel tracking (WT) test to simulate the effect of traffic loading according to BS EN 12697-22.
 - c. Critical analysis of test results. This stage includes a comprehensive investigation into cracking, and rutting properties revealed from the testing will be conducted.
-
-

-
-
4. Use the experimental program results to simulate a three-dimensional (3D) finite element (FE) model, to interpret and to analyse the failure mechanisms in the SCB test as well as the WT test.
 5. Analysis of results from the site trial for understanding the new characteristics of the developed new microasphalt with high resistance to cracking and deformation.

1.7 RESEARCH OUTCOME

To successfully develop a high value glass fibre reinforced cold mix microasphalt for highways with high mechanistic values to retard the reflective cracking and deformation in asphalt pavements.

1.8 THESIS STRUCTURE

This thesis will review the literature on CMA and microasphalt science and technology together with the laboratory scale investigations to develop a new glass fibre reinforced microasphalt (GFRM) followed by prototyping of new material in road trial sections. The thesis includes the following chapters:

- Chapter 1: is an introduction to the subject. It covers the current pavement materials impact, and aims and objectives of this study.
- Chapter 2: is a review of the previous studies on pavement maintenance, preservation strategies and consequences of deferred pavement maintenance. This chapter also highlights the current materials for pavement maintenance.
- Chapter 3: reviews bitumen emulsion characteristics and applications.
- Chapter 4: includes details of microasphalt characteristics, types and applications. This chapter includes a review of the previous studies that attempted to improve microasphalt.

-
-
- Chapter 5: describes the methodology of this research work, selected microasphalt design procedures; i) new technology for sample preparation and ii) the test methods selected to characterise the microasphalt mechanical and durability properties in terms of cracking resistance and deformation.
 - Chapter 6: shows a sequential optimisation process of different factors related to glass fibres by means of semi-circular bending (SCB) test results to produce novel GFRM. The chapter includes discussion of the performance of the optimised GFRM in terms of other mechanical properties, namely fracture toughness performance and deformation. It contains further development of microasphalt incorporating different waste materials as replacement for conventional mineral filler. In addition, the chapter presents the optimization of incorporated waste filler and comprises the use of microanalysis tools to explain the variation in mechanical and durability property of microasphalt. Finally, the chapter reports on the use of experimental program results to validate a three-dimensional (3D) finite element (FE) model, to interpret and to analyse the failure mechanisms in the semi-circular bending test (SCBT) and wheel tracking test (WTT).
 - Chapter 7: demonstrates the prototyping of newly developed material on site.
 - Chapter 8: presents the conclusions and the recommendations for further work.

Chapter

2

**Literature Review of the Previous
Studies**

2.1 INTRODUCTION TO LITERATURE REVIEW

Well maintained highways are imperative for meeting the transportation needs of any nation. During the past few years, the amount of traffic on the highway system has increased significantly (Adams and Kang, 2006). Due to ever increasing growth in vehicle miles travelled, the maintenance budgets have failed to provide a safe, efficient and reliable highway network for road users and consequently, pavement preservation continues to capture the attention of transportation engineers to find cost-effective maintenance solutions (Galehouse, 2002).

The Federal Highway Administration (FHWA) states that each dollar spent at a particular instant on preventive maintenance, saves up to six dollars in the future (FHWA, 2000). According to another study, every dollar spent on the pavement preservation today, results in saving of \$4 - \$5 or even in some case up to \$10 against rehabilitation (Baladi et al., 2002). All these dynamics stimulate transportation agencies to establish pavement preservation programs.

2.2 ROAD TRANSPORT INFRASTRUCTURE IMPORTANCE

In recent years preservation of the existing transportation infrastructure asset has been the prime focus of state transportation agencies across the United States (Nasseri et al., 2009). It is witnessed that as the country's infrastructure deteriorates, sustainability within the confines of operating and maintenance budgets becomes a grey area. If any project is conceived with initial construction cost only thus ignoring probable maintenance perspectives, then it may result in the selection of a maintenance alternative which is more costly over the long run (Lee, 2002).

As a result, this will over-burden an ever-shrinking transportation budget and will reduce the overall quality and safety of the network (Peshkin et al., 2004). This implies that pavement preservation will be instrumental in addressing system needs by keeping good roads operational, instead of allowing them to deteriorate to the point of no return and this aim is being pursued by transportation agencies as their prime objective (Galehouse et al., 2003).

2.3 RECOGNITION OF THE PROBLEM

In the current economy, infrastructure maintenance among different assets has become a massive challenge for highway agencies because of funding scarcity, increased competition and the anticipated need for prioritizing resource allocations (Haider and Dwaikat, 2011). As a consequence, goals to maximize the benefits for taxpayers in the limited funds need to be thoroughly reviewed.

According to the report published by American Society of Civil Engineers, one of the major challenges being faced by maintenance managers in state Departments of Transportation (DOTs) today is to preserve the road networks at an acceptable level of serviceability subject to the stringent yearly maintenance and rehabilitation budgets (Khurshid et al., 2010).

It is vital that transportation agencies evaluate all the needed trade-offs to ensure that asset preservation programs and projects yield maximum cost-effectiveness. Thus, quantifying these trade-offs is the main aim of asset management (Wittwer et al., 2004 and Khurshid, 2010).

Rehabilitation and maintenance treatments are normally applied by highway agencies to slow down the deterioration process and restore condition of their assets. They often seek to do this at the optimal time so that the asset does not reach a very advanced state of deterioration (Sharaf et al., 1988). However, one cannot rule out the possibility that in actual practice, funding, political, legal or institutional constraints may impede the application of a treatment at an optimal time. For instance, if a highway agency is facing any problem on the pretext of limited funding, then it may defer a maintenance or rehabilitation treatment (NCHRP, 1979).

Often, such deferments have consequences that include poorer asset performance and lead to a reduced level of service, early deterioration, high user cost, and accelerated asset deterioration and an earlier than usual need for high level treatments such as replacement (Sharaf et al., 1988 and Khurshid, 2010). Therefore, maintenance managers must strive to allocate sufficient budgets among competing alternatives, or

else pavement condition can drastically worsen. Figure 2-1 depicts the real dilemma being confronted by the transportation agencies where a decision is to be taken between two options i.e. either to have good road infrastructure or to face the consequences of deferment.



Figure 2-1: Consequences of deferred maintenance (Bennett, 2009)

It is also highlighted that an intervention can be deferred not only because of funding, political, legal or institutional restraint but also due to an agency's strict implementation of time-based preservation schedules that entails application of an intervention at pre-specified time intervals; due to the indistinct nature of asset deterioration (Earl, 2009).

2.4 REVIEW OF RELATED PAST LITERATURE

Even though there is an abundance of literature available related to the establishment of optimal asset preservation profiles, relatively very few studies have analysed quantitatively the consequences of deferred preservation (NCHRP, 1979 and Khurshid, 2010). According to Kuennen (2005) experience shows that every \$1 spent on pavement preservation before the point of rapid deterioration eliminates or delays

spending \$6 - \$10 in future rehabilitation or reconstruction costs. Similarly, another study in a discussion of pavement preservation benefits has used hypothetical examples based on past experiences to graphically illustrate the effects of deferring pavement preservation (Galehouse et al., 2003).

A further study was conducted in which data from in-service pavements was used and Sharaf et al., (1988) quantified the extent to which delayed maintenance and repair leads to higher costs in the long term. They suggested that timely preservation intervention could result in a four-fold saving in overall maintenance and repair costs over the life cycle (Sharaf et al., 1988). According to a NCHRP (1979), research study highlighted the critical issues related to the analysis of deferred pavement maintenance and it was found that highway agencies seeking to quantify the consequences of deferred preservation were often stymied due to lack of clear baseline conditions to measure the changes in maintenance service levels, and thus accentuated that baseline to determine the service level to be established.

In a study, Chasey used dynamic simulation techniques to elucidate the system which demonstrated the wide economic impact of deferred highway maintenance (Chasey, 2002). During the study a hypothetical example was used to exemplify the effects of maintenance expenditure (or delays thereof) on the benefits of highway revenue and investment cost-effectiveness. Although interesting expenditure-benefit trade-offs were provided at a system-wide level, the consequences of delaying specific treatments were not addressed.

It is an admitted fact that under restricted budgets, highway agencies are inclined to delay the repair and maintenance of pavement without analysing, or sometimes realizing, the effects of such decisions on future repair and maintenance costs. By now, several studies have been carried out to address the issue of deferring pavement maintenance and its economic effects. During early 1970's in the United States, a detailed study was conducted (TxDOT, 1984) which divulged that within the following couple of decades the road network would deteriorate to an extent that 60% of the highways would reach the stage of functional failure unless adequate treatment was applied.

The World Bank has from time to time conducted different studies and according to a survey report it was revealed that 45 billion dollars was essentially required to reconstruct the road networks in 85 countries (Peterson, 1987). The study also indicated that if timing of maintenance was controlled and necessary preventive maintenance was executed, the cost could have been reduced to 12 billion dollars.

The study helped in concluding that if the maintenance of pavement is deferred from when it is in a relatively good condition until the time pavement deteriorates to a poor condition, this would result in an inflated maintenance cost by about 400 - 500 %. Other studies (Sharaf et al., 1987 and 1988) reported that every unit of maintenance cost spent at the proper time can save 4 - 7 units of maintenance cost, if maintenance is not deferred until the failure condition.

A number of research studies in the past have furnished various analytical tools that can be applied to estimate the performance level and corresponding cost of applying an intervention at a specified time during asset life (Walls & Smith, 1989; Sharaf et al., 1987; Irfan et al., 2009; and Pasupathy et al., 2007). To address this gap an attempt was made to formulate a methodology to assess the repercussions of deviating from the optimal timing of intervention (Khurshid et al., 2009). The rationale was to help the road agencies by equipping them with sufficient knowledge so that they can make well informed decisions regarding investment timing by considering the implicit performance and cost trade-offs that are associated with each timing decision.

2.5 PAVEMENT PRESERVATION

A pavement preservation program as described by the FHWA experts' task group is a network level, long-term treatment program that augments pavement performance by using an integrated, cost-effective set of strategies to lengthen pavement life, improve safety and meet road user expectations (Geiger, 2005). A comprehensive pavement preservation program includes preventive maintenance, minor rehabilitation (non-structural) i.e. functional overlay, and routine maintenance strategies.

Preventive maintenance is planned such that it provides cost-effective treatments to an existing roadway network and appurtenances that preserves the system, slows down future deterioration, and maintains or improves the functional state of the asset without increasing structural capacity (FHWA, 1999). Minor rehabilitation consists of non-structural improvements made to the existing pavement sections to remove the age-related, top-down surface cracking due to environmental impact.

Since these rehabilitation techniques are of a minor nature with no change in structural capacity of the asset affected, therefore these types of rehabilitation techniques are placed under the ambit of pavement preservation. Routine maintenance consists of work that is planned and executed on a routine basis to maintain and preserve the operational condition of the highway or to respond to specific conditions and events that restore the highway system to an acceptable level of service (Geiger, 2005).

FHWA's definition does not include major rehabilitation that is proposed to reinstate serviceability or structural capacity. The real and obvious difference between a pavement preservation and a major rehabilitation scheme is that preservation deals with the functional condition of a pavement whereas rehabilitation addresses the structural condition of the road (Zimmerman & Peshkin, 2003).

Another definition states that pavement preservation is intended to arrest low-level deterioration, retard progressive failure, and lessen the need for routine maintenance and service activities (O'Brien, 1989). According to a new definition, pavement preservation is described as a strategy which can reduce the need for costly maintenance in the long term (Deborah et al., 2004).

2.6 PRESERVATION STRATEGIES

The advantages of pavement preservation can be expressed in terms of anticipated service life extension before rehabilitation or after executing necessary reconstruction. The concept is illustrated in figure 2-2. It can be inferred that pavement preservation improves the condition of a treated pavement until it returns to the condition before the treatment is applied. Extended service life or the life extension given to the original

pavement actually reflects the period over which the pavement condition was improved by applying a treatment (Galehouse, 2002).

The range of expected life of pavements varies widely among the highway authorities. The real task is to maximize the life extension by selecting the right strategy for the pavement condition with a premise that pavement strategy is applied at the optimal time i.e. not too late because otherwise it will lose its importance (Galehouse, 2002). Some highway agencies use remaining service life (RSL) as a main criterion for deciding the applicability of a pavement preservation strategy. Pavements with less remaining service life are not considered as good candidates for preservation. The threshold for pavement preservation is relatively different from that of other maintenance. In order to make a decision, the life extension obtained from pavement preservation strategies needs to be compared with the life extension achieved from other maintenance strategies such as major rehabilitation or reconstruction (Galehouse, 2002).

But the transportation agency management must be aware of the fact that the timing for pavement preservation is very critical and distinct from that of major rehabilitation or reconstruction. Transportation agencies would prefer to have a pavement preservation program that takes account of these concepts of life extension to support the planning of pavement preservation strategies.

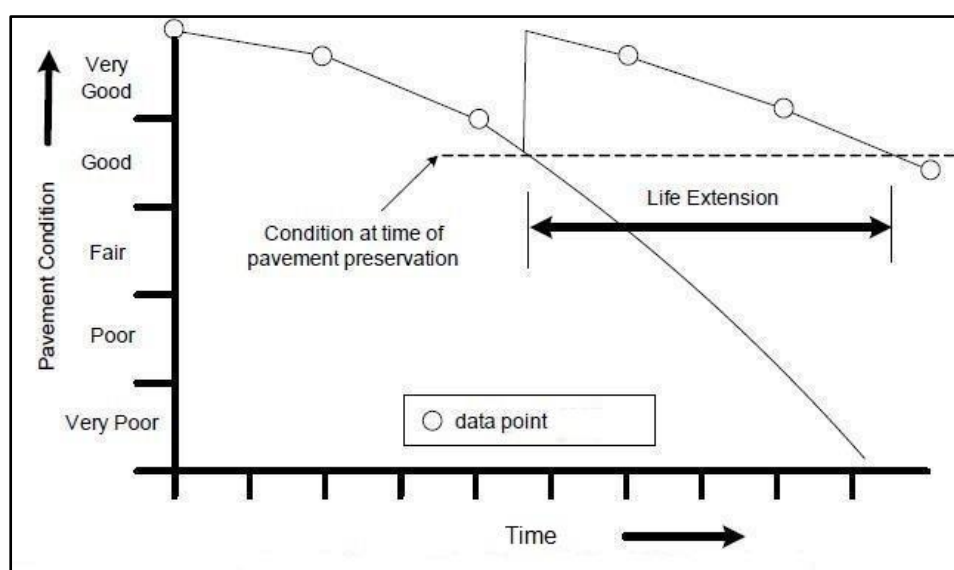


Figure 2-2: Pavement Condition vs Time (Galehouse, 2002)

2.7 MICROSURFACING FOR PAVEMENT PRESERVATION

Introduced to the United States in 1980 after Dr. Frederick Raschig presented his new slurry system at the International Slurry Surfacing Association (ISSA) convention, microsurfacing is now used throughout Europe, the US, and Australia and is making inroads into many other areas (Allan, 2002 and ISSA, 2010). The main benefit achieved from microsurfacing over alternative pavement treatments results from the polymer-modified asphalt emulsion that chemically speeds loss of moisture. This enables it to set in less than one hour in most instances, requires no rolling, and allows traffic to return to the roadway quickly.

Microsurfacing is a road maintenance tool that involves laying a mixture of dense-graded aggregate, asphalt emulsion (about 7% residual binder by weight of mix), water, polymer additive, and fillers (about 1% of weight of total dry mix) to correct or prevent certain deficiencies in pavement conditions (Hein et al., 2003). The treatment may be as thin as 3/8 inch (9.5 mm), or it can fill wheel ruts up to 2 inches (50.8mm) deep using multiple passes. Because of the similar ingredients used in microsurfacing as in slurry seals, microsurfacing is sometimes referred to as a “polymer-modified slurry seal.” The difference historically, however, is that slurry seals cure through a thermal process while microsurfacing uses a chemically controlled curing process (Campbell, 2007).

Improvements in rutting and friction characteristics are the most frequently mentioned benefits gained from micro-surfacing (Pederson et al., 1988; Watson & Jared, 1998; Hixon & Ooten, 1993; Erwin & Tighe, 2008; and Labi et al., 2007). Hixon & Ooten (1993) found a 40% reduction in the amount of original rutting and substantial increases in the friction characteristics of the pavement.

In the Texas Department of Transportation study, microsurfacing was shown to perform most efficiently at reducing bleeding and increasing pavement condition index (Freeman et al., 2002). Similarly, to Freeman et al., Temple et al., (2002) found that microsurfacing produced a higher pavement condition index (PCI) and maintained it longer than chip sealing.

Microsurfacing allows for rapid opening of roadways to traffic, often within 1 hour or less of its application under a range of conditions (Holleran, 2001). Reports of a great reduction in ride roughness support microsurfacing's immediate benefits (Moulthrop et al., 1996), while additional benefits are seen over time as microsurfacing effectively addresses rutting, increases ride quality, and has a significant service life (Labi et al., 2007). Labi et al., (2007) found that the superiority of microsurfacing in terms of cost is most evident when treatment life is the measure of effectiveness, and least evident when increased pavement condition is used compared to thin HMA overlays.

This further strengthens the fact that the benefits seen with microsurfacing are appreciated over time when compared to alternative treatments. Microsurfacing is aesthetically pleasing to people as it restores a black appearance to roadways (Watson & Jared, 1998). Microsurfacing requires no adjustment of curb lines, manholes, guide rails, or bridge clearances due to its thin lift height (Reincke et al., 1989).

2.8 PAVEMENT PERFORMANCE INDICATORS

Pavement performance indicators help to explain the characteristics of pavement distresses in terms of condition for example transverse profile, skid resistance factors etc. They are normally expressed in the form of dimensionless technical parameters or through a dimensionless index. Some common pavement performance indicators are discussed in the following sub-sections.

2.8.1 INTERNATIONAL ROUGHNESS INDEX (IRI)

The International Roughness Index (IRI) is a scale for roughness based on the simulated response of a generic motor vehicle to the roughness in a single wheel path of the road surface. Change in pavement surface roughness over a period of time has remained one of the most important performance indicators. Refer to figure 2-3 for IRI roughness scale (Sayers et al., 1986).

It is germane to mention that one of the main objectives of every highway agency is to provide a comfortable ride to its road users, and pavement roughness is a very good indicator to assess that whether this criterion is fulfilled (Kargah-Ostadi

& Stoffels, 2010). In fact, studies following the AASHTO Road Test revealed that approximately 95% of the information about pavement serviceability is attributed to surface roughness (Shahin, 1994).

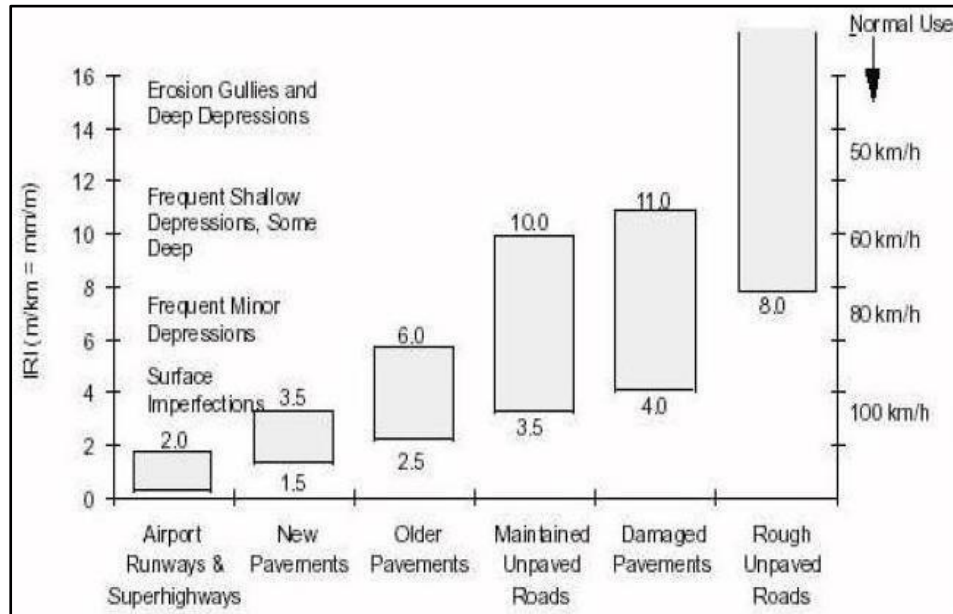


Figure 2-3: IRI Roughness Scale (Sayers et al., 1986)

2.8.2 DISTRESS INDEX

The remaining service life of a given pavement is the predicted number of years from the time of the analysis to the year when that section is expected to accrue distress points equal to the threshold value (i.e. when pavement preservation strategy is essentially required) as shown in figure 2-4 (Baladi et al., 2004). The remaining service life (RSL) is normally calculated using the pavement distress data or the distress index determined with the help of cracking, rutting and IRI parameters.

It is to be noted that any pavement section that falls below the threshold value has a zero remaining service life. The pavements which are left unattended thus deteriorate more rapidly. However, implementing the correct preservation strategy at the correct place and time helps in controlling the deterioration at the lowest cost. Since the timing of pavement preservation impacts the cost-effectiveness, therefore, only pavements which meet a minimum RSL criterion

are considered eligible for preservation treatment. In some highway departments RSL is deemed as an important parameter for selecting the appropriate pavement preservation strategy.

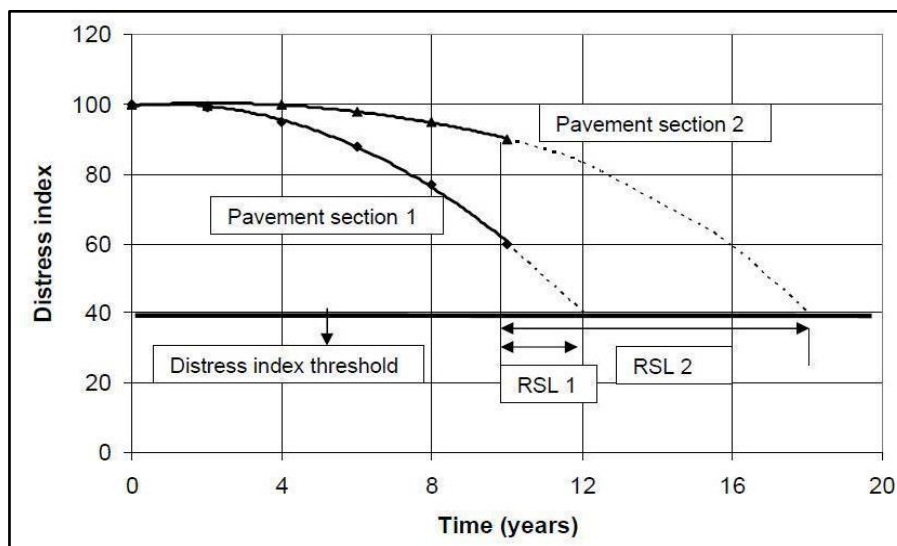


Figure 2-4: Remaining Service Life of Two Pavement Sections (Baladi et al., 2004)

However, the criterion for the minimum RSL varies widely among transportation departments. At Minnesota Department of Transportation (DOT), pavement preservation treatments are applied on pavements with an RSL greater than eight years (MnDOT, 2003). At the Michigan Department of Transportation, pavements having an RSL of two or more years are considered as potential candidates for pavement preservation treatment (MxDOT, 2003). The important point to be noticed here is that RSL is an important criterion for pavement preservation eligibility.

2.9 ANALYSIS OF SEVERITY OF CONSEQUENCES

The analysis suggests that for any given length of deferment, the consequences of deferring the intervention (increases in cost and IRI, and decrease in cost-effectiveness) are more severe in the case of thin overlay (maintenance) than they are for functional overlay (rehabilitation). This suggests that the effect of maintenance, at least of thin overlays, is probably more beneficial than was previously thought.

Another important aspect is that irrespective of the treatment, the severity of consequences of deferment is greater for lower class highways (i.e., local council roads) than that for higher class highways (i.e., trunk roads). This may be because in spite of the lower loadings of the lower-class highways, they have lower construction and design standards compared to their higher-class counterparts. Obviously, the debilitating effect of the lower design standards of these roads outweighs the redeeming effect of their lower traffic loadings.

Moreover, the higher standards of higher class highways are consistent with a lower deterioration rate compared to lower class highways. As such, lower class highways are more vulnerable to suffering the effects of delayed maintenance or rehabilitation, compared to the higher-class roads.

This reveals that the later an intervention is applied (with respect to optimal performance level) the more it would increase the likelihood of leading the pavement to a performance level which might require the next higher degree of intervention, respectively.

2.10 SYNTHESIS OF THE REVIEWED LITERATURE

Microsurfacing is shown to be most effective under certain conditions as Labi et al., (2007) demonstrated that treatment effectiveness is influenced by climate, traffic loading and highway class, with greater long-term effectiveness generally associated with lower freeze and traffic conditions, and lower pavement class. While this appears to indicate microsurfacing would not be suitable for use on high-traffic roadways, there is a comparable decrease in efficiency of other treatments under heavy traffic loads. Thus, the literature review shows that there is a lack of adequate past literature specific to the area and this has therefore, not been a prime focus of past research.

Further, reflective cracking is the most serious threat to microasphalt. As other types of cracks may not be structural, much of the debate centres on addressing this type of crack with microasphalt. Marquis (2004) does not claim microasphalt will stop reflective cracking but does report that microasphalt slows the progression of

reflective cracking. However, other studies are not as optimistic about microsurfacing's ability to positively affect cracking as Kazmierowski and Bradbury (1995) declared that it does not inhibit reflective cracking or provide structural support. It is suggested that premature failure of microsurfacing is normally due to placement on unstable, cracked, dirty, or poorly prepared surfaces resulting in delamination (Anderson, 2009). Additionally, in a study performed for the Texas Department of Transportation (TxDOT) on six maintenance treatments, microsurfacing was shown to perform the worst at stopping cracks when the base pavement was in poor condition upon application (Freeman et al., 2002).

2.11 SUMMARY

Synthesis of the reviewed literature leads to the conclusion that there is still a need to thoroughly evaluate the use of microasphalt as a robust pavement maintenance material and an endeavour can be made to address this grey area.

A reasonable conclusion may be that microsurfacing may at times be used on structurally deficient roads, but it is done so as a stopgap and to limit water intrusion into existing cracks until money is available for more extensive repairs. This fact makes applying microsurfacing treatments at the correct time of the pavement lifecycle paramount, before structural issues develop.

No thorough and fundamental investigations to predict and/or improve microasphalt resistance to cracking and deformation were found.

Chapter

3

Cold Bituminous Emulsion Mixture

3.1 ROAD CONSTRUCTION DEVELOPMENT

Over the course of history, human activities have developed and increased day by day. Consequently, this has raised the need to transport people and goods from one place to another. The invention of the wheel in Mesopotamia in about 5000 BC and the development of the axle that linked two wheels, contributed to the evolution of civilizations by facilitating communications between different communities and increasing the exchange of goods and the sharing of ideas and experiences (O’Flaherty, 2007).

Historically, the Babylonians built the earliest roads using natural asphalt as a binder; also the Egyptians constructed roads to transport stones during the building of the pyramids (Watson, 1994). The Chinese built the Silk Route, which is amongst the best known roads, in about 2600 BC; and the Persian Empire also benefited from this route through its lands for trade between China and Europe (Kendrick et al., 2004). In Europe, in about 2500 BC, roads were built using log-rafts; such roads have been discovered in Britain: one crosses the Somerset peat bogs to Glastonbury. Also, similar roads have been discovered in the Swiss Lakeside Villages and across the Pangola Swamps in Hungary (Kendrick et al., 2004). In Indian civilization, brick paving with proper piped surface water drainage systems dating from about 3000 BC has been discovered.

The most professional roads were built by the Roman Empire around 312 BC. The Romans built 29 major radial roads to connect Rome to other cities and encampments (O’Flaherty, 2007). Generally, they cut deep ditches, then layers of chalk, flint, sand and gravel were constructed to form embankments beneath the final surface, which was finished with huge stone slabs. The Roman roads system extended as a loop from Spain through France, Germany and Italy to Turkey, also through Syria to Tangier in the north west of Africa. The total length of the roads system was approximately 78,000 kms. However, this roads system represents the most organized roads system until the 17th century in Europe.

The development of the coach during the 16th century led to the start of the stagecoach services between Edinburgh and Leith in 1610. Also, steady-development in manufacturing industries during the 18th century put huge pressure on the British Parliament, which responded by passing a number of statutes aimed at improving and extending the road network. By 1706, over 1,100 Turnpike Trusts had been created, with responsibility for 36,800 kms of roads (O’Flaherty, 2007). The duties of these Trusts were constructing and maintaining a specified road length, also to levy tolls upon certain types of traffic. At the same time, France had applied the same Roman construction principles to build streets in Paris and elsewhere in France.

During the 18th century a new road builders’ era commenced, started by Robert Phillips when he submitted his suggestion “A dissertation concerning the Present State of the High Roads of England” to the Royal Society in 1736. Phillips suggested a solid road surface of a beaten gravel layer resting on a well-drained base. Another well-known English road maker was John Metcalf, who built 290 km of roads in Yorkshire. Metcalf believed in good foundation and drainage; he arched carriageways to help surface water drainage; also, on weak/soft ground, he used a sub-base raft of bundled heather. Additionally, the contributions of two Scottish road engineers, namely Thomas Telford and John Macadam, were extremely important in the development of road construction methods and traffic stream carriages, and for the first time, roads were being built to suit the requirements of the traffic. Regarding construction methods, Macadam’s varied from Telford’s in that the formation was shaped to the road camber, while the sub-base was formed to camber in Telford’s method. Also, Macadam’s method was a cheaper form of construction.

Road development was negatively affected after the first operation of the railways in 1825, as the numbers of passengers who were using stagecoaches started to decrease continually; consequently, the Turnpike revenues decreased. However, at the beginning of the 20th century, and especially after the end of World War I, attention to the development of roads and highways was renewed; this interest in road development resulted from the development in motor vehicles (O’Flaherty, 2007). The development started with the spreading of tar on roads to control dust created by vehicles’ movement and then to reconstructing existing roads.

However, the development in vehicles in terms of extra weight and speed led to the need for new roads and highways; as a result, for example, dual carriageway roads were constructed, and road geometric designs were advanced. Also, vehicle development put a huge stress on pavement constructors to build structures that could resist high stresses and bad weather conditions. Accordingly, construction techniques were advanced; more structural layers were built; and the structural layers and subgrade were compacted using different materials to improve their mechanical properties and reduce cost. During the 20th century significant developments in road and highway construction were achieved to satisfy the traffic requirements. Today, roads and highways represent a great achievement, but of course the development will not stop as material and technology developments progress knowledge.

3.2 BITUMINOUS MIXTURES

The upper courses which distinguish asphalt pavement from the other pavement types normally consist of specified mineral aggregates bound by bituminous material with or without additives. These blends of aggregate and bitumen are called “Bituminous Mixtures”. There are many functions for each course and there are multiple requirements accordingly, thus different mixtures have been developed to satisfy specific requirements, such as crack resistance, resistance to permanent deformation, resistance to fatigue, resistance to wear, resistance to water ingress, high skid resistance, etc. Additionally, significant efforts to develop new mixtures that satisfy the above points and achieve economic and environmental benefits are on-going. Accordingly, different technologies are currently available to manufacture bituminous mixtures. The main differences in these technologies are the preparation and compaction temperatures, which will be discussed in the following sections:

3.2.1 HOT MIX

The structural layers of modern roads consist of graded aggregate mixtures held together by a binder of some description. In the majority of cases in developed countries, the binder used today in the structural layers is bitumen. The material most often used to make bitumen bound layers is known as hot mix due to it being made and laid at elevated temperatures. Although bitumens

are manufactured to have a range of viscosities, the grades used in the structural layers of roads are almost solid at ambient temperatures. In order to mix with the aggregate mixture, bitumen must first be liquefied by heating.

HMA is a bituminous mixture prepared and compacted at elevated temperatures, generally between 110 and 180°C. These elevated temperatures are necessary to dry the aggregates, coat the aggregates with the bitumen binder, get the required workability, and grant enough time to compact the HMA course. On the other hand, these temperatures are highly dependent on the bitumen binder grade: of course, hard bitumen needs high and soft bitumen needs low temperatures. Additionally, the selection of bitumen grade is highly dependent on the ambient temperature in the construction region: the hard bitumen is suitable for hot climate regions and the soft bitumen is more suitable for cold regions. However, the bitumen should be solid enough during hot seasons to prevent bleeding; at the same time, it should be relatively soft in cold seasons to prevent cracking.

HMA is prepared by adding the hot bitumen to the hot aggregates (coarse, fine and filler), then mixing the blend to a stage where all the aggregates are fully coated with bituminous binder. Then, the mixture is transported to the required site and then spread by paver machine. After that, the laid material is compacted under certain temperature ranges which are compatible to certain viscosity ranges, again depending on bitumen grade. These ranges are limited because over the upper limits the mixture will be very soft, and under the lower limits the mixture will not compact correctly to reach the required density and air voids. Bitumen test data chart (Heukelom, 1969) shows the temperature viscosity relationship for binders and the ideal mixing and laying viscosities and denotes the required mixing and laying mix temperatures. Air void and density are limited with respect to the mixture's mechanical properties. Finally, after compaction is finished, the road can open to traffic as soon as the mixture has cooled down to ambient temperature.

3.2.2 WARM AND HALF WARM MIX

Decreasing the HMA mix and compaction temperatures could result in several economic, environmental, and even performance advantages. Therefore, early research studies have been trying to reduce the mixing/compaction temperature of HMA since 1956 when Professor Ladis Csanyi produced foamed binder (Csanyi, 1957). Then, Mobil Oil Australia in 1968 introduced a modification on the Csanyi process by adding cold water rather than steam into the hot bitumen (Button et al., 2007). After the Rio De Janeiro conference on the environment and sustainable development in 1992 which highlighted that climate change was mainly due to the impact of industry in generating CO₂, significant studies were conducted in the pavement materials field to reduce the mix and compaction temperatures.

In 1995, Shell Bitumen filed a patent on the use of the two stage mixing technique to produce warm mix asphalt (Harrison and Christodulaki, 2000). Two years later, at the German Bitumen Forum, warm-mix asphalt (WMA) technology was introduced, basically to lower HMA production temperature by 25°C to 55°C (D'Angelo et al., 2008). Jenkins et al. (1999) introduced a new process: they named it “Half-Warm Foamed Bitumen Treatment”. This process involved applying the foamed bitumen on heated aggregate to less than 100°C. However, the early results encouraged researchers to develop a number of WMA technologies to allow asphalt mixtures to be mixed and compacted at significantly lower temperatures. In fact, the WMA technology has become popular recently due to its economic and environmental advantages (Rubio et al., 2012). Generally, the technologies used to produce WMA can be classified in three main groups by applying organic additives, chemical additives, and water-based or water-containing foaming processes.

3.2.3 COLD MIX

Cold mix is defined as “a hydrocarbon mix made with aggregate, a hydrocarbon binder and possibly dopes or additives with characteristics such that the aggregate can be coated without drying or heating”, (Serfass, 2002).

Hydrocarbon binder could be cutback or emulsified bitumen; according to the hazardous effects of cutback, regulations limit its use in pavement mixtures (Leech, 1994). Thus, bitumen emulsion significantly covered all applications of cold mix asphalt.

France is the largest producer of bitumen emulsion in Western Europe, and the applications of CMA have been used there since the 1960s, mainly in strengthening and re-profiling of lightly trafficked highways. The continuous French developments in CMA resulted in “grève émulsion” which has been proven as a structural layer for moderately trafficked roads (Read and Whiteoak, 2003). In the USA, early works during the 1970s on stabilized paving mixtures with emulsified bitumen achieved by Chevron (1977) resulted in a published practical guideline for producing emulsion-stabilized mixes. Also, the Asphalt Institute produced different manuals related to bitumen emulsion (Asphalt Institute, 1979), CMA (Asphalt Institute, 1989), and thickness design for CMA (Asphalt Institute, 1991). In the UK, the use of CMA is largely restricted to surface treatment such as surface dressing, slurry surfacing, and reinstatement work on low trafficked roads and walkways (Read and Whiteoak, 2003). CMA will be discussed in detail in the following sections of this chapter.

3.3 CHALLENGES TO ASPHALT TECHNOLOGIES

So far, HMA occupies the major market of the paving industry worldwide, while CMA/WMA production percentages are still very low, comparatively (EAPA, 2010), as can be seen in figure 3-1. This might be due to the widespread practice and high investment spent in the HMA industry. Although HMA has been proven in terms of suitable performance, this is the time to move to more economic and environmentally friendly technologies. The following aspects may represent the most significant challenges in modern asphalt technologies:

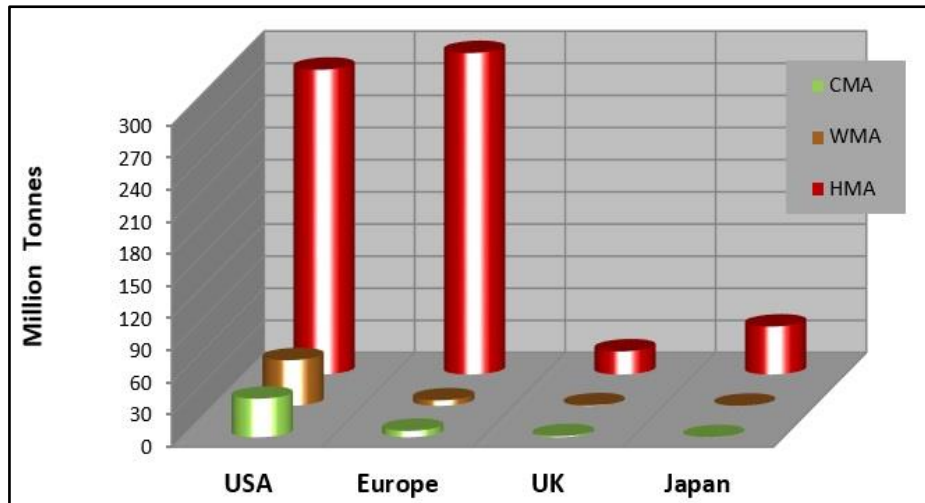


Figure 3-1: Asphalt mixture market (EAPA, 2010)

3.3.1 CO₂ AND FUME EMISSION

Generally, HMA is produced at (150-190°C), and for hard bitumen in stone mastic asphalt (SMA) it might reach 180-250°C (NAPA and EAPA, 2011). The production temperatures for WMA and HWMA are (100-140°C) and (60-100°C), respectively and no heating is required for CMA (Rubio et al., 2012). Emissions are directly related to production temperature, consequently, each metric tonne of HMA, WMA and CMA produces 21, 13 and 3kg of CO₂, respectively (Bouteiller, 2010). Records indicate that there are no emissions from bitumen at temperatures below 80°C; even as high as 150°C, emissions are only about 1 mg per hour; considerable emissions were recorded at 180°C (D'Angelo et al., 2008). Additionally, the asphalt plant fume emissions limit the position of the plant in rural areas. Therefore, introduction of new technologies with less CO₂ and fume emission is a real challenge.

3.3.2 ENERGY SAVING

As can be seen in figure 3-2 (D'Angelo et al., 2008), there are 11-35% savings in fuel used for burners during WMA preparation compared to HMA. Another study indicated the saving could reach 60 to 80% (Kristjansdottir, 2006). However, this saving is so far dissipated due to the requirements for plant modification. Of course, for CMA there is a 100% saving in burner fuel.

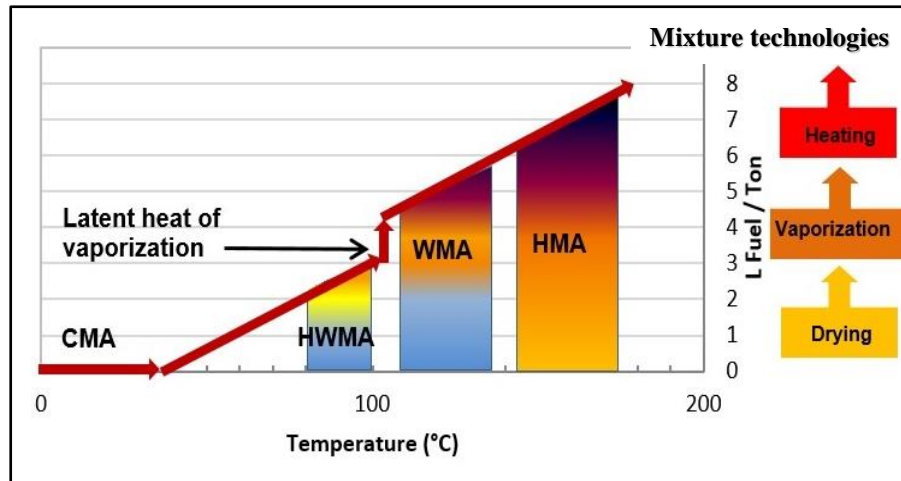


Figure 3-2: Classification of mixture technologies by temperature range and fuel usage (D'Angelo et al., 2008)

3.3.3 WORKING CONDITIONS

The reduction of emissions and fumes directly provides health and safety benefits for workers, who are harmed due to exposure to the fumes during asphalt production processes. Chauhan et al. (2010) reported that paving workers typically are exposed to 0.1 to 2mg/m³ of bitumen fumes, which includes 10 to 200ng/m³ of benzo(a)pyrene; toxic gas. However, working conditions improve when there is less exposure, as occurs with WMA and CMA technologies. In fact, in non-open-air sites, such as tunnels, workers' exposure to fumes represents a huge challenge. Also, the reduction in mixing and compaction temperatures could contribute to more comfortable working conditions, and might encourage workers to stay in their jobs for longer (Rubio et al., 2012).

3.3.4 PAVING SEASON AND HAULING DISTANCE

Paving season and hauling distance present another challenge restricting the paving engineers as there are high differences between the cold season ambient temperatures and HMA, resulting in a dramatic drop in mixture temperature. However, the introduction of WMA has reduced this restriction (Rubio et al., 2012). Consequently, this extends the paving season and increases the hauling

distances (You et al., 2007). CMA could offer superior characteristics in this issue as it can be prepared in ambient temperatures. Some developed CMA could remain workable for days or even weeks (Read and Whiteoak, 2003). In fact, hauling distance represents no problem for CMA, but rain was the main challenge for CBEM (Needham, 1996).

3.3.5 INCORPORATING RECYCLED AND WASTE MATERIALS

Many benefits can be gained by introducing reclaimed asphalt pavement (RAP) into HMA. Previous studies claimed that the use of RAP can assist in addressing the rise in initial cost of aggregates i.e. sustaining natural resources, and minimizing the impact on landfill (McDaniel et al., 2002, Aravind and Das, 2007, Karlsson and Isacson, 2006). Furthermore, these studies reported that the properties of RAP mixtures have been proven to be equivalent to new asphalt concrete pavements. The challenge in using RAP to produce HMA is that, in order to avoid deterioration of the aged binder, RAP should not be subjected to relatively high temperatures; also there is a certain percentage of RAP needed to conserve the volumetric and mechanical properties; some studies suggest RAP up to 50% of total aggregate weight (McDaniel et al., 2002). However, research studies have proved the opportunity to incorporate 75% of RAP into WMA with comparable properties to virgin mixtures (Mallick et al., 2008 and Bonaquist, 2011). At the same time, recently cold in-place recycling has been developed significantly and its validity has been proven worldwide (Kim and Lee, 2006; Sebaaly et al., 2004; Bergeron, 2005).

3.3.6 MIXTURE PERFORMANCE

Successful pavement material should perform satisfactorily against traffic and the environment. The continuous modifications of HMA led to the development of specifications and quality controls that help to produce a high-performance material, which is capable of resisting different failure phenomena, e.g., cracking, rutting, fatigue, wearing, etc. On the other hand, comprehensive studies on WMA reported that such mixes appear to perform

similarly to or, in some sites, better in contrast to HMA in short-term periods (3 years); very few sections showed poor performance (D'Angelo et al., 2008). In fact, more time is required to prove the long-term performance of new WMA technologies, but to date, no considerably negative long-term performance has been reported in the USA (Chowdhury and Button, 2008). At the same time, continuous developments have been made to overcome the shortcomings in CMA performance.

3.3.7 COST

Although there is a significant reduction in the energy required to produce WMA and CMA, to date, the initial cost could be more in comparison to HMA. Also, limited experience of such mixes could add other costs, e.g. royalties. These additional costs might come from additives required to improve mixture performance, and asphalt plant modifications (Rubio et al., 2012). However, these technologies could bring cost benefits if they prove better under long-term performance. New unique alternatives are in great demand to increase mixture performance without adding extra cost. On the other hand, continuing increases in energy costs may denote a challenge for HMA technology, which may facilitate the utilization of the other technologies accordingly.

In summary, pavement materials science has wide ranging challenges which restrict the nomination of the most appropriate technology. Generally, the huge modern impacts of environmental and economic limitations represent feasible challenges to solve. However, further development of WMA and CMA could minimize their cost and optimize their performance to replace HMA in the future and meet the environmental and economic challenges.

3.4 CONTENTS OF BITUMINOUS MIXTURES

The general content of bituminous mixtures is aggregates, binder, and/or additives and air voids. One major factor in the selection of material for bituminous mixtures is the availability of these materials locally, thus extensive research works (Nikolaides, 1983; Thanaya, 2003; Ibrahim and Thom, 1997) have been carried out to explore the

applicability of local materials for each pavement course. Additionally, from the relatively wide studies and experiences gained, detailed specifications have been created to ensure high quality pavement. On the other hand, waste and by-product materials have recently been involved as alternatives or additives in bituminous mixtures due to their economic and environmental impact.

3.4.1 AGGREGATE

Aggregate is the main volumetric constituent of bituminous mixture, i.e. it represents more than 90% of the total mix weight. It can be supplied from natural crushed rock, gravel, sand and reclaimed asphalt pavement. Aggregate characteristics play a key role in final mixture behaviour. Thus, European standard BS EN 13043 (BSI, 2002) which include descriptions for aggregate sieve sizes, categories, properties and test methods for all European countries, was produced to specify the required properties of aggregate for use in bituminous mixtures of roads, airfields and other trafficked areas. Also, the PD 6682-2 (BSI, 2009) was published as a guideline for BS EN 13043 to recommend the aggregate test methods, gradations limits, categories, properties, etc.

3.4.2 BITUMINOUS BINDERS

Bitumen is a black to dark brown sticky material, composed principally of high molecular-weight hydrocarbons (Robinson and Thagesen, 2004). It can be found as a natural material, but the majority of today's bitumen is produced from the distillation of crude oil. Practically, bitumen should be of low viscosity when applied to aggregate to produce a bituminous mixture. So far, there are four methods to make bitumen behave as a mobile liquid, namely heating, blending with solvent, foaming, and emulsifying.

Traditionally, HMA (which uses heated bitumen) has been used successfully for structural pavement layers wherever the required equipment is available to produce quality products. Solvents such as petroleum products are used in asphalt mixtures for small and remote areas as a cost effective method, as well

as being used to produce the bond/tack coat. It has to be said that the flammability (safety) and environmental issues have restricted the use of cutback bitumen (Robinson and Thagesen, 2004). Foamed asphalt binder is used for stabilizing granular materials and in cold place recycling. Also, recently a significant application of foamed asphalt is used in WMA (Rubio et al., 2012). Emulsified asphalt is largely used for surface treatment and the bond/tack coat (Read and Whiteoak, 2003).

3.4.3 ADDITIVES

Recently, different additives have been developed to improve bitumen properties, assist in bituminous mixture preparation or enhance the bituminous mixture performance. Rubber and polymers are the best-known additives to improve bitumen performance. Unfortunately, such additives either have a cost impact; i.e. polymers, or they tend to increase mixing temperature; i.e. rubber (Robinson and Thagesen, 2004). The efficiency of additives in lowering the mixing and compaction temperatures has been proven in WMA preparation technology, but the cost impact is prohibitive (Rubio et al., 2012). Hydrated lime is cited as a bituminous mixture improver; it is considered by experts as a significant anti-stripping agent (Gorkem and Sengoz, 2009).

3.4.4 RECYCLING, WASTE AND BY-PRODUCTS MATERIALS

Due to the huge economic and environmental benefits of using these materials, recently they became very common for replacing primary materials. This helps to protect virgin resources and also minimizes the impact on landfill. During the last 60 years, secondary materials were used in pavement construction, mainly as aggregate substitution. For example, many researchers (Wu et al., 2007; Pasetto & Baldo, 2010; Sorlini et al., 2012) have proved the validity of the use of steel slag in asphalt mixtures as a replacement for a certain percentage of primary aggregate. Thanaya (2003) showed the suitability of using glass as a fine aggregate. Additionally, incorporating crumbed rubber in asphalt mixture has shown a better permanent deformation and a low

temperature cracking resistance (Lee et al., 2008; Pasquini et al., 2011; Xiao et al., 2009). Furthermore, no significant variance was found in permanent deformation, tensile strength and moisture susceptibility of asphalt mixes containing waste fibres and other contended virgin fibres (Anurag et al., 2009; Putman and Amirkhanian, 2004). Waste fly ashes have shown advantages when added to asphalt mixtures (Xue et al., 2009; Di and Liu, 2012). However, great care should be taken to avoid health hazards and soil contamination when incorporating waste materials.

3.5 ROAD MIXTURES AND COLD MIX

In the UK, traditional methods of road construction are employed in nearly all of the structural layers of road building projects. These involve the use of hot mixtures of aggregate and bitumen for which manufacturing and laying plant are well established and the technology has a proven record. However, over the last decade, there has been a realization that cold processes, which use bitumen emulsion in place of hot bitumen, have a part to play. A number of countries, such as the United States of America, France and those in Scandinavia, have made use of cold processes for many years, but current technology only allows them to be used for particular applications in certain situations. In the United Kingdom, bitumen emulsions are used only in surface overlay processes and bitumen emulsion based mixtures are in their infancy.

3.6 BITUMEN EMULSION MIXTURES

An alternative method of liquefying bitumen is to emulsify it in water. In this case, no heating of the binder nor aggregate mixture is necessary and mixing and laying are carried out at ambient temperature. This process has been in existence since the early part of the twentieth century and emulsions were actually used as binders for formerly unbound road.

3.7 CURRENT STATUS OF HOT AND COLD MIX

Bitumen emulsions are used today in a variety of road construction techniques, but mainly only for surface overlays. In most situations, the material used for the structural

layers of roads in the UK is hot mix. Several countries use the emulsion based alternative, which has been generically termed "cold mix", in a number of discrete applications but, even in these countries, the majority of paving is hot mix. In the United Kingdom, the road construction industry is only now starting to look to cold mix and lay materials, under pressure from environmentalists and new specifications for reinstatement materials (HAUC, 1992).

Cold mix is not utilized in the UK, for example, for a number of reasons. First and foremost, hot mix does an excellent job when manufactured and laid correctly. A great number of hot mix plants exist in developed countries and consequently materials are readily available. Hot mix technology is well developed even though this is based on empirical laboratory and field data rather than fundamental principles. Engineers and contractors have a great deal of experience with hot mix materials, enabling them to have confidence in the performance of a structure comprised of hot mix. Even advocates of cold mix would not claim that it is yet ready to be used in all situations in which hot mix is used and, without the use of modifiers, there is still a shortfall in performance in terms of mechanical properties (Needham, 1996). Cold mix has very little stiffness during its early life and can, therefore, be damaged if trafficked at that time. Emulsion based mixtures also have an inherent susceptibility to water damage, due to the fact that unset bitumen emulsions are partially water soluble and the binder can, therefore, be washed away by rainfall resulting in a very weak material. There are, however, arguments for the use of cold mix and the debate is gaining momentum. Many of the arguments have an environmental basis.

As aggregates do not have to be dried for use in emulsion mixtures, dust emissions are eliminated. Hot mix can also lead to gaseous emissions, which are potentially harmful to health (Van Gorkum et al., 1993) and the environment, if proper control measures are not employed. Some efforts are currently being made to contain emissions from both mix plant and paver.

As well as very large organic molecules, bitumen contains many low molecular weight hydrocarbons and polycyclic aromatic compounds (PAC's) which are vaporised at high temperatures such as those experienced during hot mix production, transport and

laying. Hydrocarbons contribute to atmospheric pollution although this is small scale compared to other sources. Hydrogen sulphide is also released from hot bitumen, with some types being worse than others. In the open, this gas is not present at dangerous levels but in bulk storage tanks it can build up to levels at which it becomes hazardous to health.

However, it is the PAC's which are of more concern as those with 3 to 7 fused rings are known or suspected carcinogens. In particular, benzo (a) pyrene and benz (a) anthracene are considered to be powerful carcinogens. However, the concentrations of these chemicals in bitumen are very low (Morgan & Mulder, 1995). A number of studies have been carried out to assess the potentially harmful effects of these compounds (Lien, 1993; Jorgensen et al., 1993; Brandt et al., 1993). The current consensus is that there is little risk from the carcinogenic compounds in bitumen, but the fact that these materials are present at all is still cause for concern. This seems to be supported by the fact that manufacturers of mix production and laying plant are still attempting to develop systems to prevent the release of fumes. These emissions can be eliminated completely by the use of bitumen emulsion mixtures, as bitumen is only heated during the emulsification process and here it is very easy to contain harmful gases.

Energy and, therefore, cost savings can also be realized through the use of cold mixtures. According to BS 4987, hot mix production requires that the binder is heated to temperatures in excess of 140°C. Aggregate mixtures must also be dried and heated to similar temperatures. In the case of cold mix, the emulsification process requires energy to heat the bitumen and drive the emulsion mill, but once made, the emulsion can be used cold and no drying or heating of the aggregate mixture is necessary. As hot mix plants are more complicated than cold mix versions, they are not normally considered to be portable. This means that transport costs are generally higher for hot mix as both raw materials and finished product have to be carried over longer distances. A number of reports have shown that cold mix uses about half the energy of hot mix on a tonne for tonne basis (OECD, 1984; AIR, 1993; USEPA, 1978). Additionally, investment in cold mix plant is far lower than in the more complicated hot mix plant which, although it is not an important factor in countries with an

established network of hot mix facilities, is particularly advantageous in developing countries.

Emulsion mixtures also offer potential improvements in performance. Hardening of binder through oxidation and other processes, which can occur during the heating process (James & Stewart, 1991) and can lead to embrittlement and cracking, is avoided. Polymers in latex form can be easily incorporated which is not possible with hot mix.

Finally, cold mix has logistical advantages over hot mix, in that it can be stockpiled or transported over longer distances and it is not necessary to use insulated trucks for shorter journeys. It is, therefore, very useful for small scale reinstatement work or for projects in remote areas.

3.8 BITUMEN AND WATER

An emulsion is a dispersion of fine droplets of one liquid in another liquid. In contrast to solutions, the two liquids are coexistent rather than mutually mixed. In the case of a bitumen emulsion, these are bitumen, which is a liquid with a very high viscosity, and water. Normally, in good quality bitumen emulsions, the droplets are in the order of 1 to 30 μm in diameter with the majority $>1 \mu\text{m}$ and the largest volume or mass between 5 and 10 μm . The bitumen content is normally in the region of 60 to 70% but can be as low as 40% or as high as 80%. The globules of bitumen are termed the disperse phase, as they are discreet droplets, and the water is the continuous phase in which the droplets are suspended.

Under normal circumstances, an oil, such as bitumen, and water, are totally immiscible. This is due to the chemistry of the two materials. Bitumen is composed of two groups of organic molecules called asphaltenes and maltenes (Whiteoak, 1991). The system can be regarded as colloidal, with the asphaltenes being dispersed in the maltenes. Asphaltenes are molecules of very high molecular weight, ranging from 1,000 to 100,000, composed of mainly carbon and hydrogen with some nitrogen, sulphur and oxygen. They are amorphous solids which are fairly polar due to the

unsaturate (C=C double bond), nitrogen, sulphur and oxygen content. These are dispersed in the maltenes which can be further broken down into three types of molecules; saturates, aromatics and resins. The saturates are non-polar straight chain and branched aliphatic hydrocarbons which make up between 5 and 20% of the bitumen.

3.9 CURING OF BITUMEN EMULSIONS

After a bitumen emulsion has coalesced or broken it must fully cure or set for the binder to recover its original physical properties and water resistance. The process seems to be mainly dependent on the evaporation of water but it is not fully understood. Curing is to a large extent dependent upon climatic conditions in the field. Wet and cold conditions have an adverse effect on curing whereas hot, dry conditions have a beneficial effect. Additional rolling can assist in the expulsion of water but only up until a density at which the minimum achievable void content of the mixture has been reached. At this point the excess water merely fills the available air voids and no pressure can be exerted on the water to squeeze it out.

3.10 APPLICATIONS OF BITUMEN EMULSIONS

The range of surfactants available, impart different characteristics to the emulsions they produce. Emulsions with different setting characteristics are necessary for different applications.

3.10.1 SURFACE DRESSING

Surface dressing, or chip sealing as it is known in some countries, is a cost-effective process used for improving the texture of, and sealing small cracks in, deteriorating pavement surfaces (TRRL, 1981). It also corrects minor irregularities in profile but does not give any structural improvements. A rapid setting cationic emulsion is used for this application (coded K1-70 in the UK, where K= cationic, 1= rapid setting, 70 = 70 % bitumen) as the binder must cure quickly to allow early trafficking and sweeping to remove excess chips.

The technique involves applying warm (60 °C) bitumen emulsion to the road surface by spraying and then immediately placing single sized aggregate chippings onto the unbroken emulsion. A number of variations on the basic theme have been developed which can involve several layers of emulsion and aggregate.

3.10.2 TACK COATS

A tack coat is a very light spray of diluted bitumen emulsion used to provide a bond between an old surface and a newly applied layer. It is considered to be good practice to use a tack coat whenever an old surface is overlaid as weathered bitumen can lose its adhesive properties (AEMA, 1979). A tack coat emulsion must be able to penetrate any surface cracks or unbound material before breaking, but it must set quickly to allow the new, layer to be applied. Tack coats are also used in patching operations. After all loose material has been removed from an excavation, the emulsion is applied to the base and sides. This helps to keep the patch in place and provides a watertight seal between the patch and the surrounding pavement.

3.10.3 FOG SEAL

A fog seal is similar to a tack coat in composition but it is used as a surface treatment itself rather than an aid to another resurfacing process (AEMA, 1979). Fog seals are used on surfaces which have become deficient in binder and are therefore susceptible to loss of chippings or ravelling, or to seal minor cracks. If applied conscientiously and in good time, fog seals can extend the life of a pavement considerably.

3.10.4 PRIME COAT

A prime coat is an application of bitumen to a granular base in preparation for a bituminous overlay (AEMA, 1979). Cut-back bitumen (bitumen diluted with

solvent to lower its viscosity) and bitumen emulsion are both used. A prime coat serves several purposes:

- i. coats and bonds loose particles
- ii. hardens or toughens the surface
- iii. waterproofs the surface
- iv. plugs voids in the aggregate surface
- v. provides adhesion between the base and overlying course

3.10.5 SLURRY SEAL AND MICROSURFACING

Slurry sealing and microsurfacing are two very similar techniques which are used as surface treatments to improve surface texture and correct minor irregularities (AEMA, 1979). The only difference between the two is that microsurfacing uses larger aggregate sizes and is used in thicker layers. Unlike surface dressing, these processes can be used on high speed roads as they give a surface with a very even profile with good skid resistance and a secure finish. The level of technology is very highly developed as systems are designed very specifically for certain road conditions, aggregates and climate.

Slurry seal and microsurfacing mixtures comprise finely graded aggregate mixtures, water, cement and bitumen emulsion. There are three different aggregate mixture designs which are used for different applications. The coarsest, Type III is used for surface corrections and to impart skid resistance. The second, Type II, is slightly finer and is used to correct severe ravelling and loss of binder. The finest mixture, Type I, is used for crack filling and pre-treatment for hot mix or surface dressing overlays (Needham, 1996). A slurry seal mixture is produced by first pre-wetting the aggregate mixture with water. This ensures that when the emulsion is added it does not immediately break onto the aggregate due to absorption of the emulsion water into the aggregate. Additive or dope solution may then be added which controls the rate of break of the mixture to a high degree of accuracy when used correctly. This consists of a weak solution of emulsifier which neutralizes the negative sites on the

aggregate to some extent thus slowing down the reaction with the emulsion itself. Ordinary Portland cement is often added to control the breaking process and improve the setting behaviour and final properties of the seal. The addition levels of dope solution and OPC must be carefully pre-determined and controlled to obtain the desired mixing, breaking and setting rate of the mixture (Needham, 1996). Finally, the emulsion is added and mixed for a short time. Emulsions used in slurry sealing were traditionally slow to medium setting but in recent years the need for quick set slurries has led to the use of rapid setting emulsions.

Slurry seal can be applied either by hand or a specialized paving machine. The hand method is used on small scale jobs and involves dumping a mixture onto the pavement and spreading it out using squeegees. Slurry seal machines are very sophisticated mix pavers. The mixture components are stored within the machine, mixed together and laid in a continuous process. Slurry seals must set within a 1 hour to be acceptable. No rolling is carried out and the seal is merely allowed to cure due to chemical breaking and evaporation of the water.

3.11 COLD MIX ASPHALT

Conventional hot mix materials have excellent mechanical properties but:

- i. the aggregate has to be heated and dried thoroughly,
- ii. this means that certain potential aggregates are excluded,
- iii. the material has to be placed and compacted before it cools.

It would therefore be extremely useful to find an alternative which could be mixed with cold, wet aggregate. There might be significant environmental benefits as well as a reduced energy demand. There are two options:

- i. Bitumen Emulsion
- ii. Foamed Bitumen

3.12 BITUMEN EMULSION

Bitumen emulsion is a ‘suspension’ of bitumen droplets in water, created as follows:

Break the bitumen into very small droplets, typically 1-20 microns in size (see figure 3-3 below).

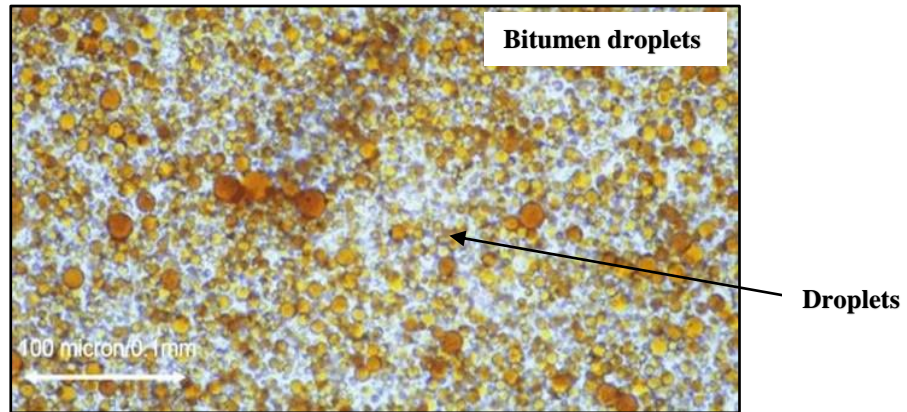


Figure 3-3: A suspension of bitumen droplets in water

This requires a Colloid Mill (which unfortunately is expensive and uses up significant energy). Figure 3-4 illustrates the procedure for preparation of bitumen emulsion and figure 3-5 shows the colloid mill used in the bitumen emulsion preparation process.

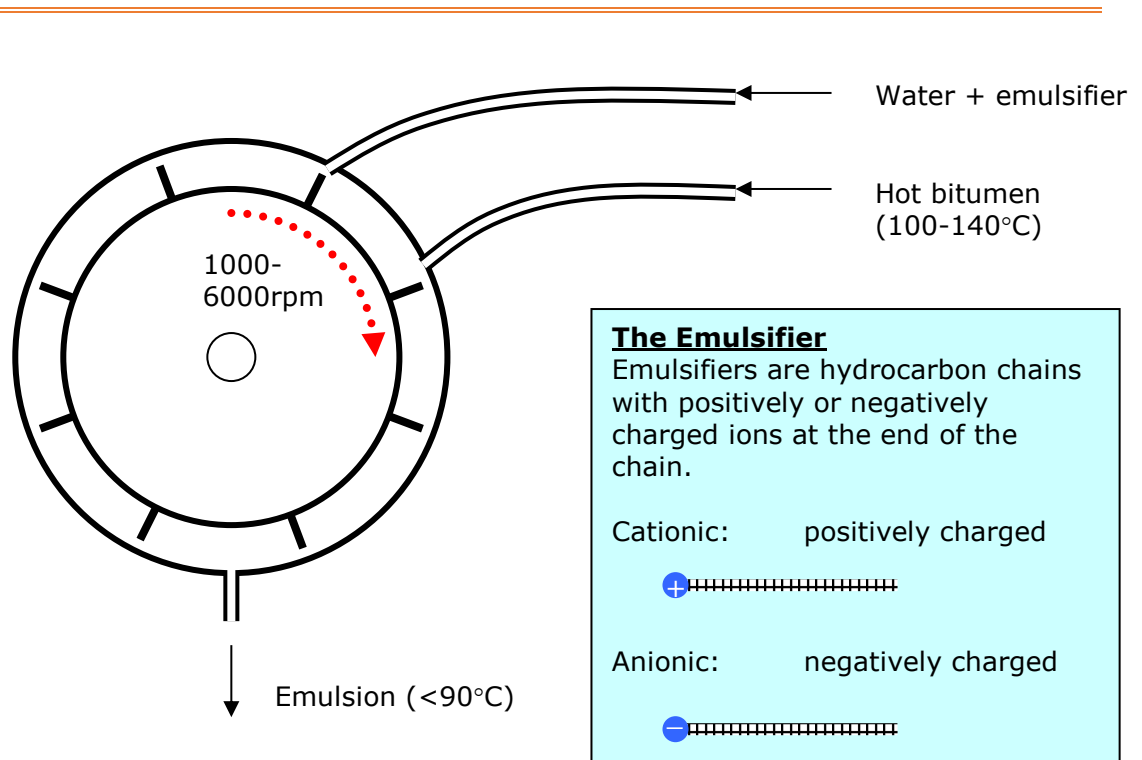


Figure 3-4: Bitumen emulsion preparation process



Figure 3-5: Bitumen emulsion - colloid mill

The emulsion works because the polymer parts of the emulsifier molecules attach themselves to the bitumen droplets (see figure 3-6). This leaves each droplet surrounded with charge and means that droplets repel each other (Capitao et al., 2012).

These forces are enough to prevent droplets coalescing (combining) since bitumen and water have very similar specific gravities (1.00 and 1.03 respectively).

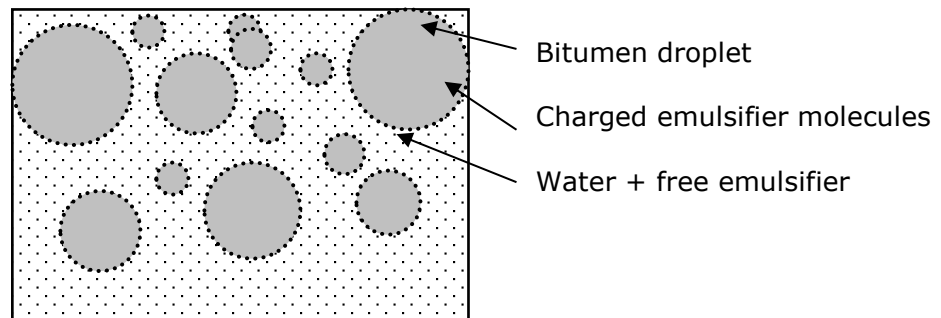


Figure 3-6: Bitumen emulsion droplets

Typical proportions are 40-70% bitumen and the advantage of emulsions is they can last for months (with the occasional stir).

3.13 FOAMED BITUMEN

Bitumen foaming is an alternative technique to produce a binder which is workable at normal ambient temperatures. This is done as illustrated in the figure 3-7 below:

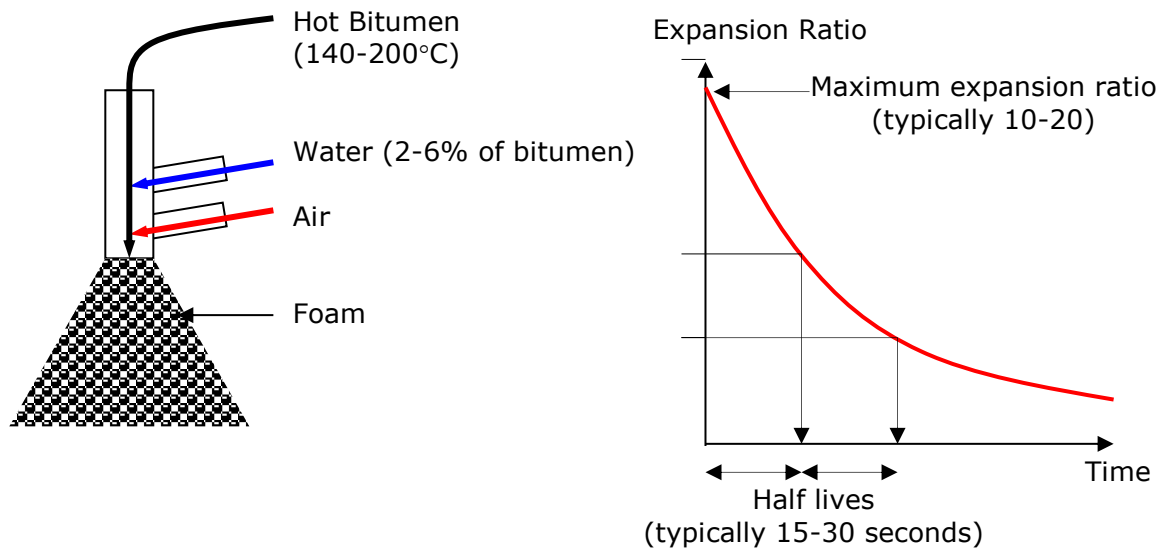


Figure 3-7: Foamed bitumen preparation process

The advantage of foamed bitumen over emulsion is it doesn't need so much water and the disadvantage is it has to be used within about a minute i.e. straight into the mixer (Capitao et al., 2012). Figure 3-8 shows the general appearance of foamed bitumen prepared through the above process.

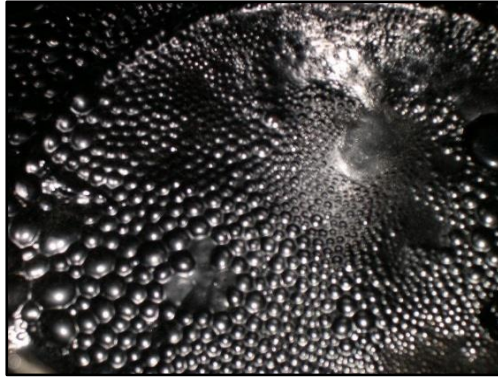


Figure 3-8: Foamed bitumen

3.14 HOW COLD MIX WORKS

For both emulsion and foamed bitumen to achieve reasonable mixing, the aggregate must be wet. The water content required is typically 2-3%. The problem is that the binder (bitumen droplets in emulsion or flakes of bitumen foam) is attracted to the water, which is mostly found amongst the fine aggregate particles (figure 3-9 illustrates in detail, how coalescing of bitumen droplets onto the aggregate occurs in the cold mix). Resultantly, coarse particles often don't get coated properly with bitumen, leaving a partially bound material (Capitao et al., 2012).

In detail:

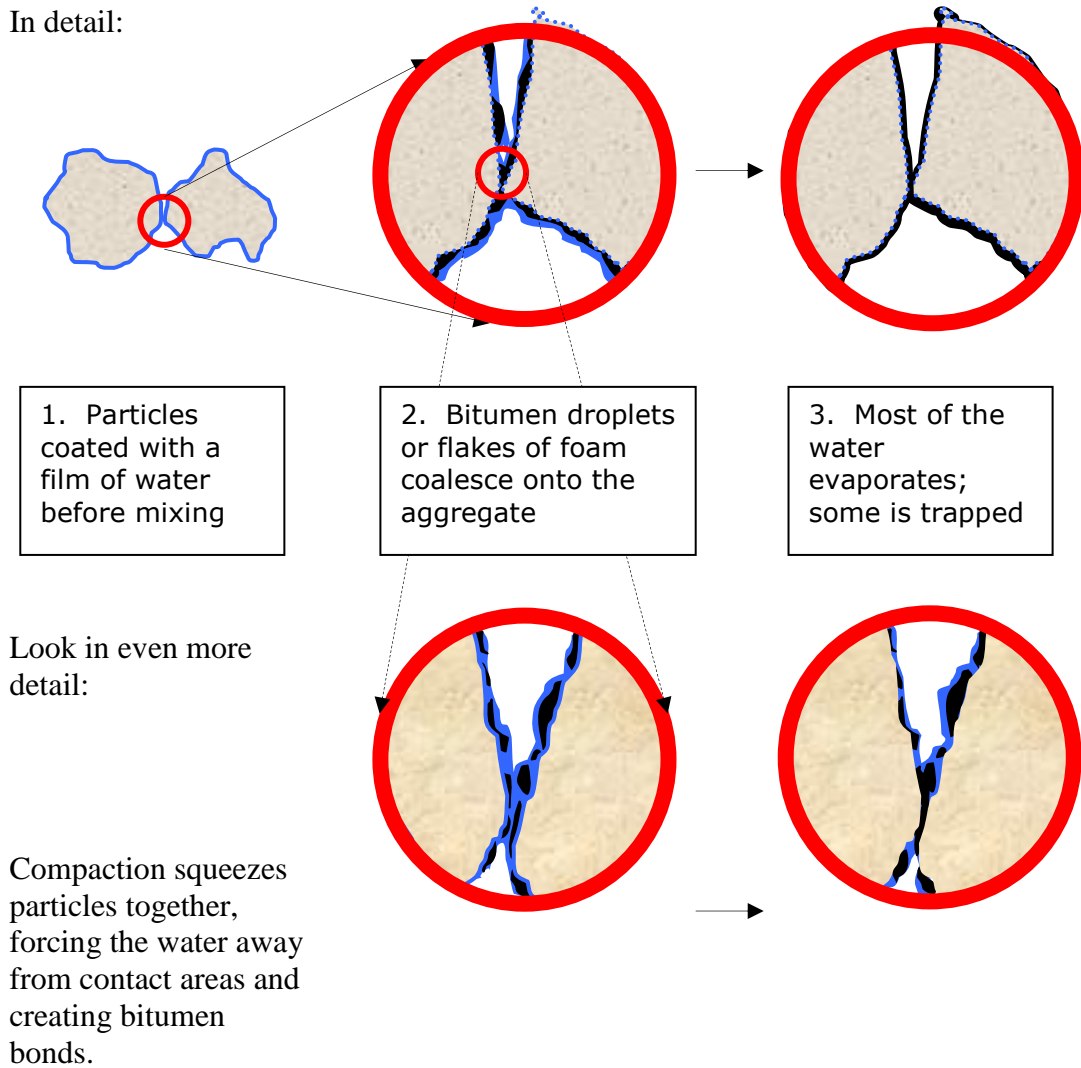


Figure 3-9: Mechanics of cold mix

The final trapped water content is usually 0.5-1.0% (by mass). The rest of the water can, in theory, evaporate; but this is highly weather dependent. Cold mix therefore needs good weather. Figure 3-10 shows the internal void structure of cold and hot mixes after compaction.

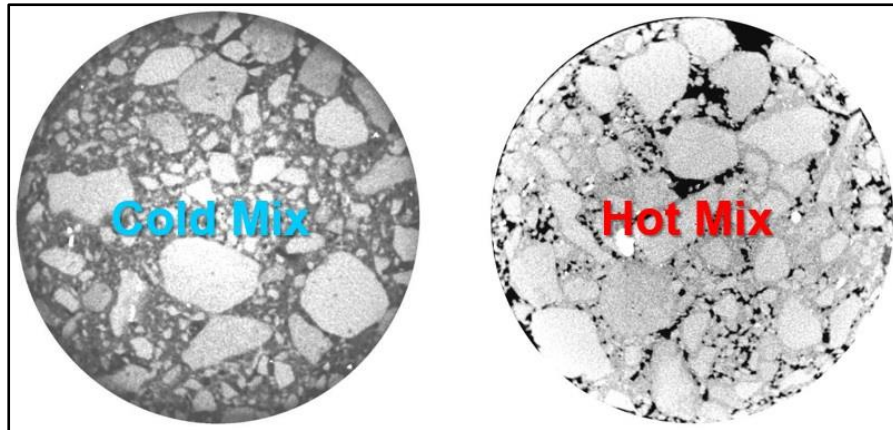


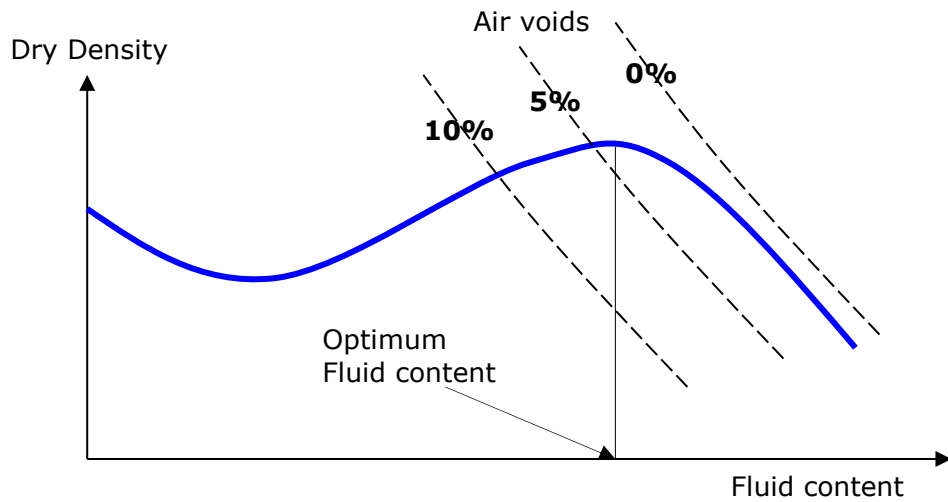
Figure 3-10: Internal void structure of cold mix (left) and hot mix (right)

Additives

Because the UK is not always warm and dry, it is common to add a small percentage (1-2%) of cement, lime or fly ash to the mixture in order to take up some of the water, helping the bitumen to attach itself to the aggregate.

Volumetrics

Good compaction is needed, and this depends on the fluid content (fluid means water or emulsion or more debatably – foam residue). Optimum compaction is achieved at an optimum fluid content. This is typically about 6% (by mass). An emulsion, can be up to 70% bitumen, which means that the upper limit on bitumen content is just under 2.8% compared to a typical 4-5% for a hot mix asphalt (Thom, 2012). If more bitumen is required then lower density has to be accepted. Graph 3-1 shows the effect of fluid content on the compaction.



Graph 3-1: Effect of fluid content on compaction

Foamed bitumen needs a slightly higher initial aggregate water content to get good mixing. This ends up with more or less the same limit as for emulsion.

Figure 3-11 illustrates the volumetrics for cold and hot mixes:

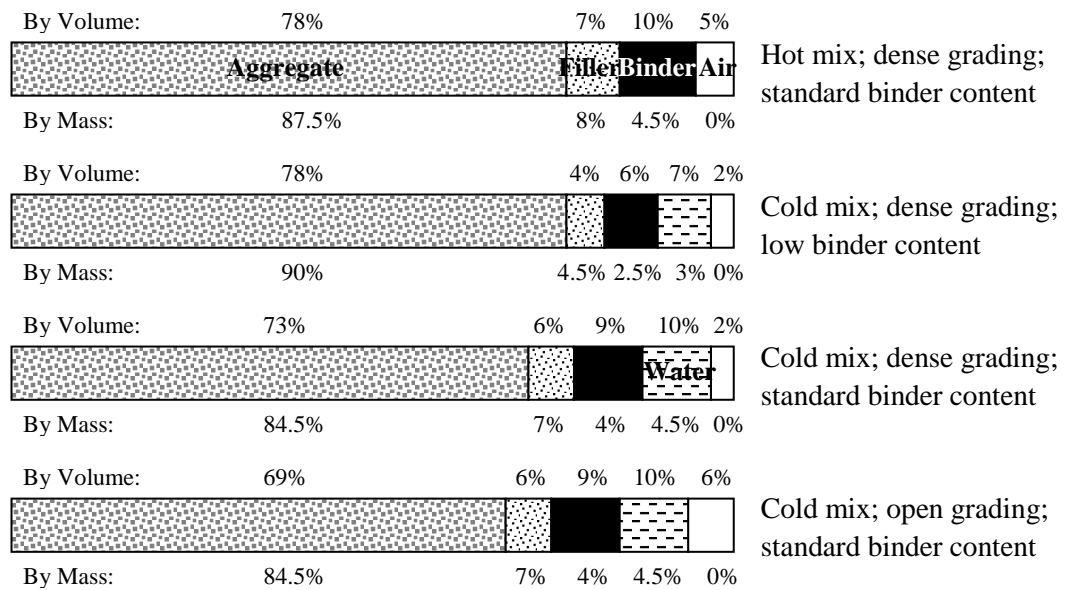


Figure 3-11: Volumetrics for cold and hot mixes

The same equations (Equation 3-1 & 3-2) below can be used for predicting the stiffness modulus of a cold mix as for hot mix by analytical method (Thom, 2012). A trapped water pocket has just the same effect as an air void.

$$E_{\text{mixture}} = E_{\text{binder}} \times [1 + (257.5 - 2.5\text{VMA}) / (n \times (\text{VMA} - 3))]^n \text{ [in MPa]} \quad (3-1)$$

where: $n = 0.83 \times \log_{10}[4 \times 10^4 / E_{\text{binder}}]$ and (3-2)

VMA is in %; E_{binder} is in MPa

Fatigue and deformation resistance in cold mixes are both also likely to be poorer than for hot mix. An important difference between cold mix and hot mix is the curing phenomenon i.e. cold mix takes more time to gain strength.

Hot mix has; i) high strength as soon as it has cooled down (e.g. 2 hours), ii) quite rapid stiffening for a few weeks as traffic slightly reorientates particles for maximum effectiveness, and iii) slow stiffening thereafter due to binder ageing.

Cold-mix has; i) initially little more than a granular material, ii) binder effect clear within 24 hours, iii) continuing slow strength gain over a period of up to 6 months, iv) unfortunately, it is not really practical to keep traffic off the road for 6 months while the material stiffens up therefore, there is a danger of early life damage taking place - but this is very hard to predict. So long as the traffic is light, no permanent damage will occur.

A study by Thom (2012) illustrates how strength is gradually acquired by cold mixes over a period of time (see figure 3-12).

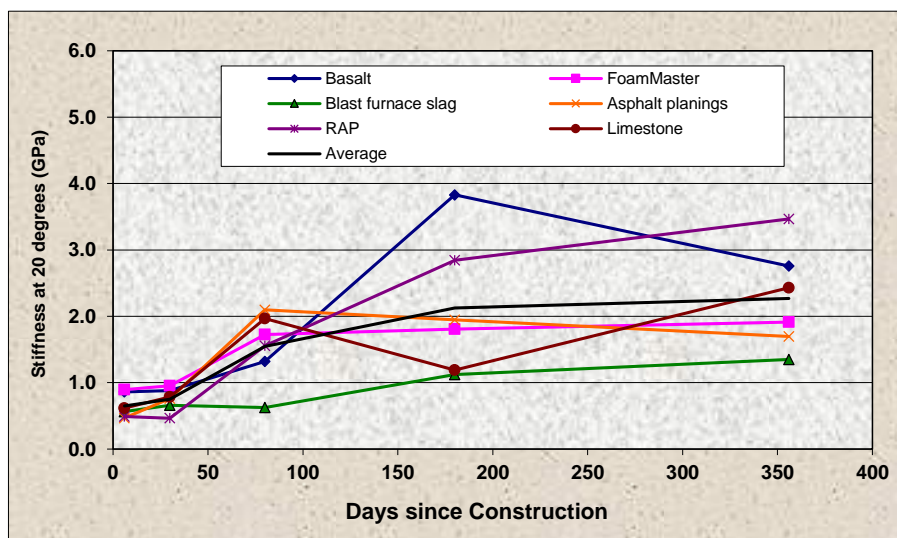


Figure 3-12: Strength gained by cold mixes since construction (Thom, 2012)

Figure 3-13 illustrates the difference between cold mix and hot mix.



Figure 3-13: Difference between cold mix (left: grey) and hot mix (right: black)

3.15 PRACTICAL USE OF COLD MIX

Summary of key points:

- a) The binder content will be lower than for a hot mix.
- b) The void content is likely to be higher than an equivalent hot mix.
- c) This means that cold mix will usually be less stiff, less resistant to deformation and have lower fatigue life.
- d) Water needs to evaporate before sealing the surface. This means that the aggregate grading used should be reasonably open.
- e) It is important to limit early trafficking.
- f) All of these points mean that there is a significant risk associated with cold mix.

Why to use cold-mix:

- a) The range of possible aggregates is extended. For example, construction and demolition waste, incinerator ash, crushed concrete and recycled asphalt planings (RAP) can all be used.
- b) Cold-mix technology is ideal for in-situ recycling.

-
-
- c) Cold-mix can have a storage life of several months.
 - d) Lower energy usage gives environmental benefits.

For these reasons, cold mix is a popular choice for minor roads particularly in remote locations.

Chapter

4

Microasphalt

4.1 PAVEMENT STRUCTURE

A pavement is a structure designed to allow trafficking, usually of wheeled vehicles. Most pavements are roads, but airfields, industrial hardstandings, cycle tracks etc. are all included. The main purpose of the pavement or pavement layers is to minimize stresses generated by traffic on the subgrade to such a level where no deformations occur (Read and Whiteoak, 2003). Simultaneously, the pavement layers themselves should be withstanding the stresses and strains which are imposed on each layer for the entire life of the pavement. Typically, modern pavement structures are either flexible, rigid or a composite of the two. Normally bituminous, hydraulic bound or concrete layers are built on foundation courses depending on the design decision. The decision and selection of course and layer type is generally dependent on common practices, availability of materials, site characteristics, etc. It should be noted that a layer is an element of a pavement laid in a single operation, while a course is a structural element of a pavement constructed with a single material; a course may be laid in one or more layers.

Key points are:

- a) Pavements are high-volume constructions; the materials used must therefore be cheap and environmentally acceptable.
- b) There is no exact definition of failure; they simply have to remain 'serviceable'.
- c) The definition of serviceability will vary from application to application.
- d) Maintaining serviceability is an important part of pavement engineering.

A typical pavement structure is illustrated in figure 4-1.

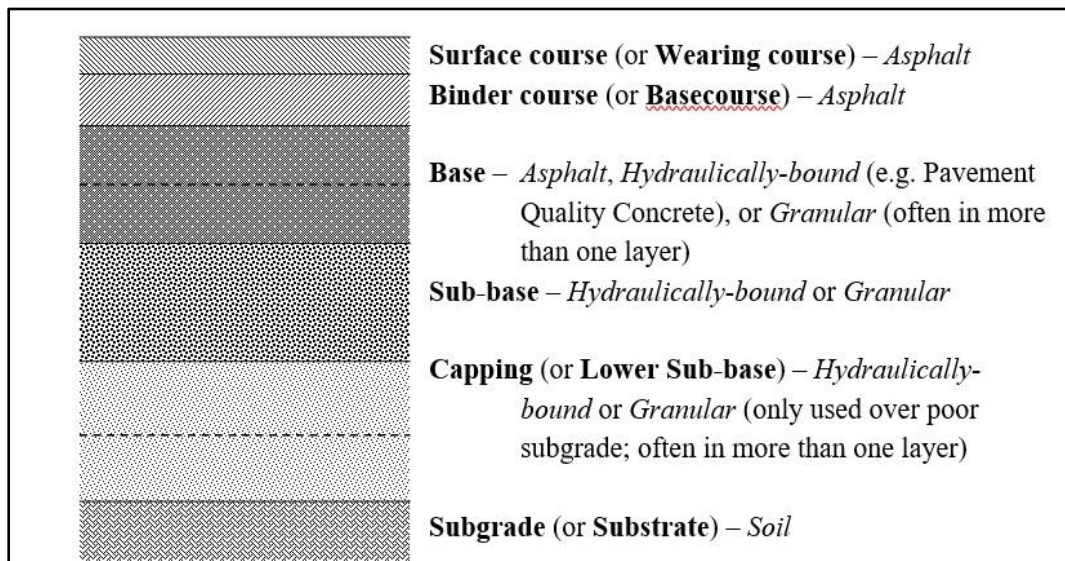


Figure 4-1: Typical pavement structure

The subgrade (existing subsoil) is the naturally occurring soil upon which the road is constructed. This layer is sometimes compacted to improve its bearing capacity. The foundation is the platform upon which the more expensive layers are placed. It can be seen from the above figure that each succeeding layer is more expensive than its predecessor. The foundation carries the load-bearing layers of the pavement, namely the binder course and base course layers. A capping layer may sometimes be placed on top of the subgrade to improve the load-carrying capacity of the latter, and this is followed by the sub-base which consists of either unbound or bound materials. The layers above this form the main structural element of the pavement and are often composed of graded aggregate and binder based on various recipes. The lower load-bearing layer is termed the base course and this is followed by the surfacing layer or layers, i.e. binder course and surface course (Watson, 1989). The base course must be able to sustain the stresses and strains generated within itself without excessive or rapid deterioration of any kind. The base course might comprise hydraulically bounded granular materials. The binder course is present to allow asphalt contractors to achieve the high standards of surface regularity commonly required by current asphalt specifications. Finally, the surface or wearing course has to provide a smooth, skid-resistant running plane having adequate resistance to the onset of defects,

including most commonly deformation and cracking, to the extent that the lifespan of the layer does not fall below acceptable levels (Highway Agency, 1999).

4.2 DETERIORATION OF PAVEMENT LAYERS

Whenever there is a moving load on pavements, it causes stress in the pavement layers underneath. This stress resultantly produces strain in the pavements and thus induces vertical elastic strain at the top of the subgrade which causes deterioration in the pavement with time. This vertical elastic strain further generates tensile strain at the bottom of the surface course i.e. just under the wheel load which can result in deterioration of the pavement layers. The maximum tensile strain in the asphalt layers of a pavement under a wheel load is related to cracking. Therefore, strength of the pavement layers must be sufficient to prevent excessive cracking from developing. Figure 4-2 illustrates the phenomenon of vertical elastic strain in cold mix pavements while figure 4-3 demonstrates the mechanism of tensile strain in cold mix pavements.

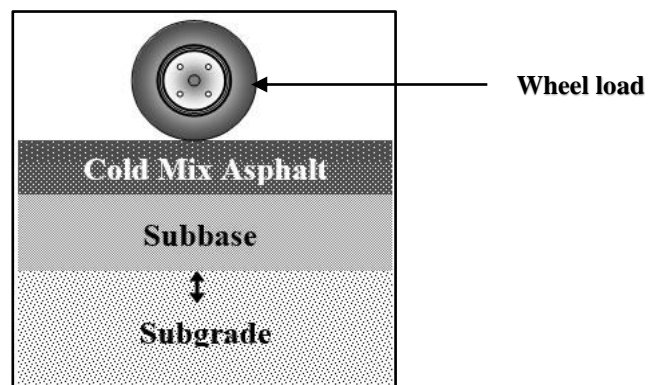


Figure 4-2: Vertical elastic strain in cold mix pavements

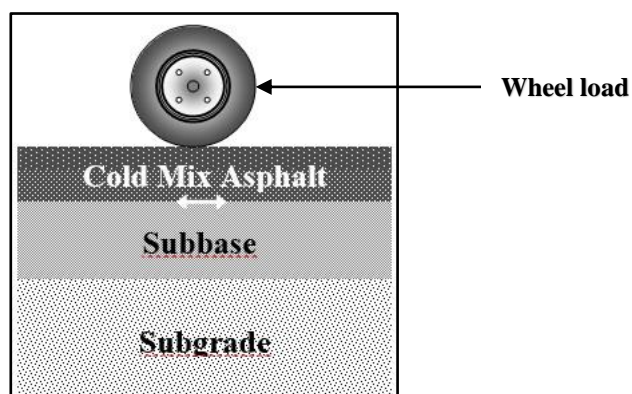


Figure 4-3: Tensile strain in cold mix pavements

4.3 BACKGROUND INFORMATION ON MICROASPHALT

Microasphalt is a high-performance surface treatment composed of a mixture of polymer modified emulsified asphalt, dense-graded crushed fine aggregate, mineral filler, break control additives and water (FPP, 2012). The emulsifiers and additives allow microasphalt to be placed at thicknesses up to 50 mm and the surface to be traffic ready in less than an hour. Type II gradation with maximum aggregate size of 6.4 mm is most commonly used for moderate-to-heavy traffic areas. Type III gradation with maximum aggregate size of 9.5 mm with more aggressive texture is typically used on heavy traffic roadways. Type II and Type III gradation details have been provided in table 5-2 in chapter 5. These gradations can be placed at a thickness slightly over the maximum aggregate size depending on the evenness of the existing road surface. Since being pioneered in Germany in the late 1960s and early 1970s, microasphalt now is recognized as one of the most cost-effective surface treatments (ISSA, 2012).

Microasphalt is made and applied to existing pavements by a specialized machine, which carries all components, mixes them on site in a pugmill, and spreads the mixture onto the road surface. Figure 4-4 shows the machine laying microasphalt on site.



Figure 4-4: Machine laying microasphalt on site

The Georgia Department of Transportation (GxDOT) documented the use of microasphalt in 1996 on I-285 in Atlanta in an effort to address ravelling, cracking and

improve the surface appearance before the 1996 summer Olympics. The microasphalt was determined to have performed well when checked two years later, providing excellent smoothness and good friction, with a minimal increase in pavement noise levels (Watson & Jared, 1998).

Micro surfacing can be successfully used for both corrective and preventive maintenance (Smith & Beatty, 1999). It has been reported that micro surfacing is generally more cost-effective than thin HMA overlays (Labi et al., 2007). In the study results based on Indiana data, the only exception to micro surfacing being more effective than thin HMA overlays is when both traffic volume and climate severity are high. Decision trees and matrices for the purpose of selecting optimal treatments on the basis of rational costs and benefits are recommended. The micro surfacing mixture design normally defines the amount of polymer modified emulsion and mineral filler (cement or lime commonly used) as functions of the amount of mineral aggregate. Successful micro surfacing projects depend on strict adherence to technical specifications and design guidelines (Watson & Jared, 1998; ISSA, 2005; and ASTM, 2005).

There is an ongoing search for improved micro surfacing mixtures. The use of a softer asphalt grade has been incorporated to create a more flexible micro surfacing mixture and test cells were constructed at the Minnesota Road Research facility near Albertville, Minnesota (MnDOT, 2005). After six months, approximately 71% of transverse cracks and 5% of longitudinal cracks had reflected through the micro surfacing. Early results from this research showed that the soft binder micro surfacing design had a moderate effect in decreasing transverse reflected cracks but was more effective in decreasing longitudinal reflective cracking.

Scientists and engineers are constantly trying to improve the performance of asphalt pavements. Modification of the bituminous binder is one approach taken to improve pavement performance. Since 1960s, microasphalt pavement surfaces have been used in Germany. Microasphalt has spread and gained acceptance all over the world; because of its performance characteristic, the use of microasphalt has increased in usage and is a material of choice amongst road authorities and the asphalt industry.

4.4 MICROASPHALT AS A PREVENTIVE MAINTENANCE TOOL

For the task of creating and maintaining a country's infrastructure, especially in today's age of tight budgets and ecological sensitivity, it is crucial that existing roads last as long as possible in order to utilize resources as efficiently as possible. Preventive maintenance of existing roadways has been shown to be the most financially efficient use of available resources (Syed et al., 1999). Many studies have been done with the goal of developing a set of criteria which will accurately guide decision makers in choosing a preventive maintenance strategy that produces the most cost-effective improvements in pavement quality and life (Li & Madanu, 2009; Pasupathy et al., 2007; Chan et al., 2008).

Microasphalt is generally classified as a preventive maintenance treatment as opposed to a corrective maintenance treatment (Geoffroy, 1996). Due to this classification by agencies involved in road repair and maintenance, microasphalt is most often used as a surface treatment to correct rutting, improve surface friction, and extend pavement life by sealing any cracks in the pavement surface (Pederson et al., 1998).

4.5 BENEFITS OF MICROASPHALT

Microasphalt generally receives positive reports in scientific literature. Most studies done on the effectiveness of microasphalt encourage its use as a preventive maintenance treatment (Van Kirk, 2000; Erwin & Tighe, 2008). Per contra, emphasis is placed on the importance of applying microasphalt at the correct time in a pavement's life cycle to achieve maximum durability and cost-effectiveness before the pavement has deteriorated structurally (Rajagopal & George, 1990). One of the early studies done on microasphalt in the United States foreshadowed the favourable conclusions of further research by recommending that microasphalt be approved for routine use in restoring flexible pavements to fill surface ruts and cracks, seal the surface, and restore skid resistance (Pederson et al., 1988). Hicks et al., (1997) also documented microasphalt as an appropriate maintenance strategy for more types of

pavement distress than any other commonly used strategy, as well as having a longer life expectancy than all but thin HMA overlays which cost 30% more.

Microasphalt performance is strongly affected by workmanship and the condition of the pavement at the time of application. When used as a preventive maintenance treatment, on pavements in relatively good condition, micro-surfacing may last 7 years (Van Kirk, 2000), although longer life times have been claimed (Van Kirk, 2000). On average, however, the life expectancy of a microasphalt treatment is 5 years. When applied in ruts, the life of the treatment is dependent on the stability of the microasphalt, the traffic level, and the condition of the underlying pavement.

The main mechanism of failure is wear. Through wear the surface oxidizes and is abraded over time. Premature treatment failure occurs from placement on highly deflecting surfaces, cracked surfaces, pavements with base failures, and on dirty or poorly prepared surfaces (resulting in delamination).

Distress modes that can be addressed using microasphalt include:

- a. Ravelling: Loose surfaces or surfaces losing aggregate may be resurfaced using microasphalt.
- b. Oxidized pavement with hairline cracks: These surfaces may be resurfaced using microasphalt.
- c. Rutted pavements: Deformation resulting from consolidation of the surfacing only. Rutting due to base failure or significant plastic deformation of the pavement cannot be treated except as a temporary measure.
- d. Rough pavements with short wavelength: These irregularities may be treated with microasphalt, provided the frequency of the irregularities is shorter than the spreader box width.

4.6 LIMITATIONS OF MICROASPHALT

Selecting effective ways to maintain roadway networks is paramount to pavement managers and decision makers. Cost and expected treatment life as a function of pavement condition are some of the key relevant parameters when conducting life cycle cost analysis in order to compare maintenance and rehabilitation alternatives. Microasphalt has been an effective maintenance treatment for decades. This technique has evolved over the years to be able to be used on roads with the requirements of rapid construction and quick return to traffic. Similarly, with any surface treatment, specifying agencies and users have shown interest to improve durability and design life so that the surfacing can last longer. Cracking resistance is often a challenge as the propagation of cracks from the existing pavement is difficult to mitigate. It would therefore be of great value to find ways to improve the durability and cracking resistance of microasphalt.

Distress modes that cannot be addressed using microasphalt include:

- a. Cracking (including reflection cracking)
- b. Base failures of any kind
- c. Pavement layers that exhibit plastic shear deformation

Microasphalt will not alleviate the cause of these distresses. As a result, the distresses will continue to form despite the application of a microasphalt.

4.7 THE FUTURE OF MICROASPHALT

Currently both economic and ecological efficiency are hot-button issues receiving enormous attention in politics, the private sector, and the media. With increasing demands on the world's infrastructure, it is imperative for decision makers to utilize funds wisely (Peshkin et al., 2004) while also balancing the demands of citizens for environmental sensitivity. Of the preventive maintenance treatments that can effectively and efficiently prolong the service life of roadways, microasphalt is best poised to meet the increasing demands placed upon such projects. Much has been

written on how to determine when microasphalt should be applied to pavements in order to limit the application of treatments to pavements too deteriorated to benefit (Broughton et al., 2012). The other key factor contributing to the success of microasphalt is workmanship.

4.8 FIBRES IN MICROASPHALT

Reinforcement generally consists of incorporating certain materials with some desired properties within other materials which lack those properties. Fibre reinforcement was used as a crack barrier rather than a reinforcing element whose function is to carry the tensile loads as well as to prevent the formation and propagation of cracks (Maurer & Malasheskie, 1989).

The concept of using fibres to improve the behaviour of materials is not new. The modern developments of fibre reinforcement started in the early 1960s. A multitude of fibres and fibre materials were introduced and are continuously being introduced in the market as new applications such as polyester fibre, asbestos fibre, glass fibre, polypropylene fibre, carbon fibre, cellulose fibre, etc (Serfass et al., 1996).

The principal functions of fibre as reinforcement material is to provide additional tensile strength in the resulting composite. This may increase the amount of strain energy that can be absorbed during the fatigue and fracture process of the microasphalt mix.

Attempts at using non-synthetic fibres in pavement have been reported in the literature. Cotton fibres and asbestos fibres were used but these were degradable and were not suitable as long term reinforcement (Bushing & Antrim, 1968). Metal wires have also been proposed but they were susceptible to rusting with the penetration of water (Tons & Krokosky, 1960). Asbestos was also used until it was deemed as a health hazard (Kietzman, 1960; Marais, 1979).

The addition of fibre as a way to improve the micro surfacing mixture characteristics was also evaluated and tried with success many years ago in France (Vivier & Brule,

1992). The addition of fibre results in short and long-term benefits. It initially increases the viscosity of the emulsion making it possible to use a gap graded gradation without segregation or emulsion run-off. After curing, the fibre network reinforces the gap graded mixture increasing shear strength and wear resistance. The flexural tension test can be performed as an indication of cracking resistance (ISSA, 1989). This is an empirical test that measures how far the specimen bends before cracking. Other tests methods typically performed on Portland Cement Concrete beams to measure flexural strength and toughness could possibly be adapted to micro surfacing mixtures for cracking resistance evaluation (ASTM, 1987; ASTM, 1997; Shaikh, 2012).

From the literature review fibre reinforced bituminous mixes have shown mixed results. It was noticed that relatively little published information concerning fibre modified microasphalt is available. Most studies that included fibres in asphalt mixtures had a limited number of trials, and investigating the effects of fibre modification was in many cases secondary to the main purpose of the studies.

Some fibres have high tensile strength relative to bituminous mixtures, thus it was found that fibres have the potential to improve the cohesive and tensile strength of bituminous mixes. They are believed to impart physical changes to bituminous mixtures by the phenomena of reinforcement and toughening (Brown et. al, 1990). This high tensile strength reinforcement may increase the amount of strain energy that can be absorbed during the fatigue and fracture process of the mix. Finely divided fibres also provide a high surface area per unit weight and behave much like filler materials. Fibres also tend to bulk the bitumen so it will not run off the aggregates during construction.

Previous researches (Brown et. al, 1990; Maurer & Malasheskie, 1989; Wu, et. al, 2006) showed that the addition of the fibre into bitumen increases the stiffness of the asphalt binder resulting in stiffer mixtures with decreased binder drain-down. Fibre modified mixtures show improved properties compared to the control mix. Fibres appear to have the potential to improve fatigue life and deformation characteristics by increasing rutting resistance (Yi & McDaniel, 1993). The tensile strength and related

properties of mixtures containing fibres was found to improve in some cases and not in others (Jenq et. al., 1993).

In terms of workability, mixtures with fibre show a slight increase on the optimum binder content (OBC) compared to the control mix (Bindu, 2012). This is similar to the addition of very fine aggregates. The quantity of bitumen needed to coat the fibres is dependent on the absorption and the surface area of the fibres and is therefore affected not only by different concentrations of fibres but also by different fibre types (Button & Lytton, 1987). In addition, the degree of homogeneity of dispersion of the fibres within the mix will also determine the strength of the resulting mixtures (Mills & Keller, 1982).

The results obtained from different field studies show that the addition of fibre has a benefit since it will help to produce a more flexible mixture and thus one that is more resistant to cracking (Jiang & McDaniel, 1993).

4.9 SCOPE OF NOVEL GLASS FIBRES IN MICROASPHALT

With new developments, the production of glass fibre reinforced bituminous mixtures can be cost competitive as compared with modified binders. The use of glass fibre reinforced bituminous mixes may increase the construction cost, however it may also reduce and save the maintenance cost.

However, due to lack of understanding on the reinforcing mechanisms as well as ways of optimising glass fibre properties (e.g., fibre diameter, length, aspect ratio and surface texture etc.) performance enhancement of asphaltic mixtures reinforced by these glass fibres was found to be marginal. Depending on the characteristics of glass fibres, the effect of glass fibre addition to microasphalt can be very variable. For example, if the glass fibres are too long, it may create the so called “balling” problem (i.e., some of the glass fibres may lump together) and the glass fibres may not blend well with the microasphalt. If the fibres are too short, then the fibres may not provide any reinforcing effect and may just serve as an expensive filler in the microasphalt mix.

4.10 SUMMARY

The above literature review suggests that research is required to identify additives that will enhance the already considerable usefulness and durability of microsurfacing in order to increase its cost-effectiveness. Additionally, research is needed to improve the “greenness” of microasphalt through the use of unique and sustainable ingredients.

In view of the above, it is thought that the addition of glass fibres to asphalt mixtures enhances material strength and fatigue resistance while adding ductility. Because of their mechanical properties, glass fibres might offer a potential for microasphalt.

This research aims to investigate the properties of glass fibre reinforced microasphalt, which may have the benefit of improving the performance of road pavement. To evaluate the effect of the fibre content in microasphalt mix, laboratory investigations were conducted on the samples with and without fibres. The testing undertaken in this research comprised resistance to fatigue cracking by using SCBT and deformation by the WTT.

Chapter

5

Methodology, Preparation of Cold Mix Microasphalt and Laboratory Testing

5.1 GENERAL: PAVEMENT DISTRESSES

Pavement distress is a surface deterioration which indicates a decline in the pavement's surface condition or structural load-carrying capacity such as cracking, rutting, ravelling etc. (Yoder & Witczak, 1975). As pavements age and experience traffic repetitions, pavement distresses begin to accumulate. Also, distresses can compound themselves; for example, a crack can allow water to enter the pavement and lead to the development of a pothole or stripping (Yoder & Witczak, 1975).

The applied traffic loading on pavements is usually much smaller than the bearing capacity i.e. strength of the material. Therefore, one load application does not fail the pavement, but causes a small amount of deterioration. However, it depends on level of load application and state of pavement. This deterioration gradually increases until it reaches an unacceptable level. So, it is important to perform timely maintenance. However, before the appropriate repair strategy can be applied to a distressed asphalt pavement, the type and extent of the deterioration must be understood, and the cause of the distress must be identified. The engineer must be able to evaluate fully the factors that affect the design of pavements and should also be able to extend the principles to situations that are not fully covered by current design techniques.

It is the intent of this section to illustrate various types of pavement distress. Before methods of evaluation can be discussed, it is necessary to have an understanding of the types of pavement distress that can occur. In particular, it is important to ascertain whether certain types of pavement distress are progressive, leading to eventual failure of the road or whether they are non-progressive. It is also worthwhile at this point to review the two types of failure i.e. structural and functional. The first of these is designated functional failure wherein the pavement can no longer carry out its intended function. The other type is called structural failure and indicates a breakdown of one or more of the pavement components. The two types of failure do not necessarily go together. Functional failure depends primarily upon the degree of surface roughness (Yoder & Witczak, 1975).

5.2 CRACKING IN PAVEMENTS

Cracking is generally a series of interconnecting cracks caused by fatigue failure of the asphalt concrete surface under repeated traffic loading. Conventional theory has it that cracking begins at the bottom of the asphalt surface (or stabilized base) where tensile stress and strains are highest under a wheel load.

It is a fact that a relationship is generally found between tensile strain in asphalt under load and the number of load applications until failure occurs; it is therefore quite logical that the maximum tensile strain in the asphalt layers of a pavement under a wheel load should be related to cracking (Thom, 2012).

Cracking can occur:

A – at the bottom of the asphalt immediately under the load;

B – near the surface just outside the loaded area;

C – at the surface in the tyre tread contact zone.

Cracking type A is generally assumed to be dominant (Thom, 2012). Figure 5-1 shows the areas under load resulting in strain in cold mix asphalt.

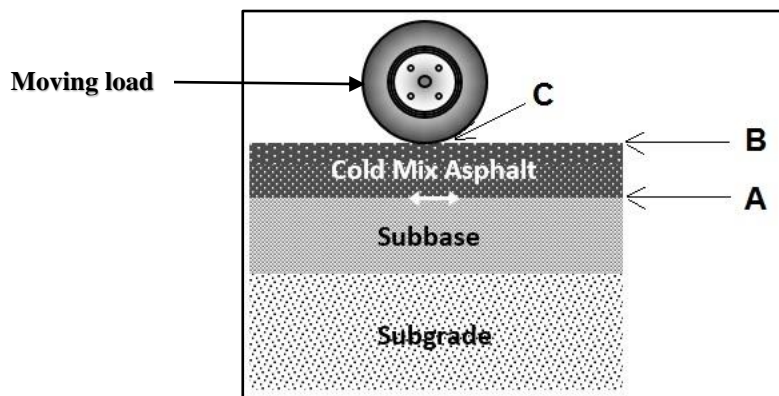


Figure 5-1: Cracking phenomena in pavements

5.2.1 REFLECTIVE CRACKING IN PAVEMENTS

Even if there are no traffic induced cracks i.e. longitudinal cracks in the asphalt, there may be thermally induced cracks i.e. transverse cracks (Thom, 2012). These represent discontinuities in the support given to the asphalt layers, which means we are very likely to find a crack appearing through the asphalt at those points. This is reflective cracking (Thom, 2012).

The cracks propagate to the surface initially as a series of parallel longitudinal or transverse cracks. After repeated traffic loading, the cracks connect, forming many-sided, sharp-angled pieces that develop a pattern resembling chicken wire (FHWA, 1998). Figure 5-2 shows the reflective cracking in pavement.

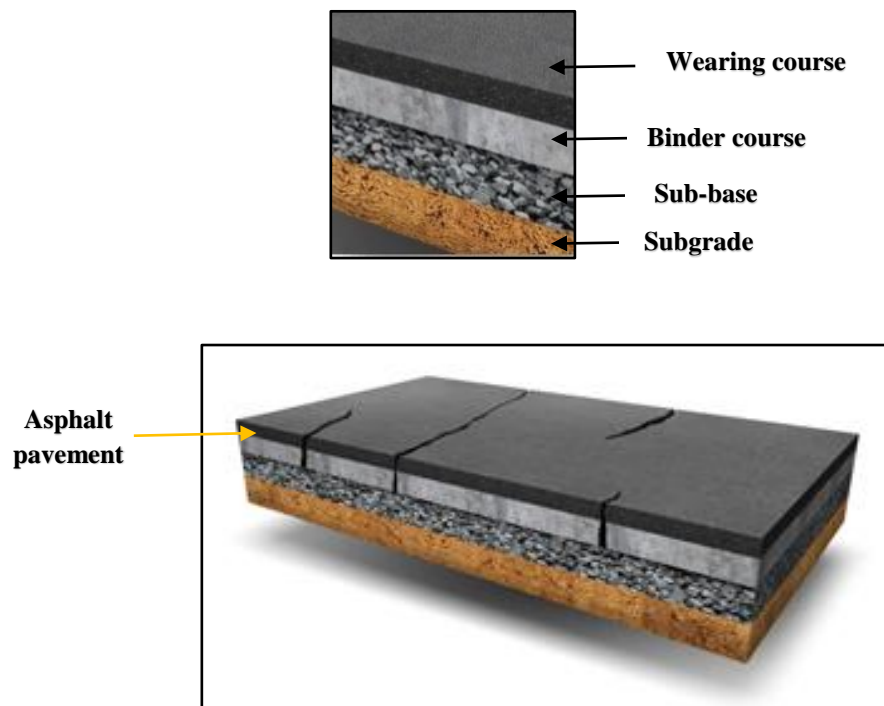


Figure 5-2: Reflective cracking in asphalt concrete pavement

5.2.1.A LONGITUDINAL CRACKS IN PAVEMENTS

The fact that this cracking is in the wheel path proves that it is the traffic which is causing the damage. If there are several cracks within the zone of the wheel path then the effect is almost certainly shallow, possibly associated with debonding between asphalt layers (Thom, 2012). In many cases, crack depth

is shallow. If it is low or variable, then this implies significant damage and/or debonding (Thom, 2012). Figure 5-3 shows a longitudinal crack in a pavement and figure 5-4 illustrates the reasons for longitudinal cracking i.e. dynamic traffic loading.

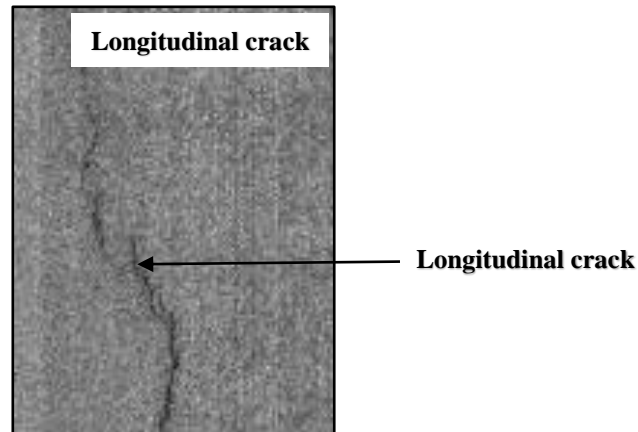


Figure 5-3: Longitudinal crack in pavement

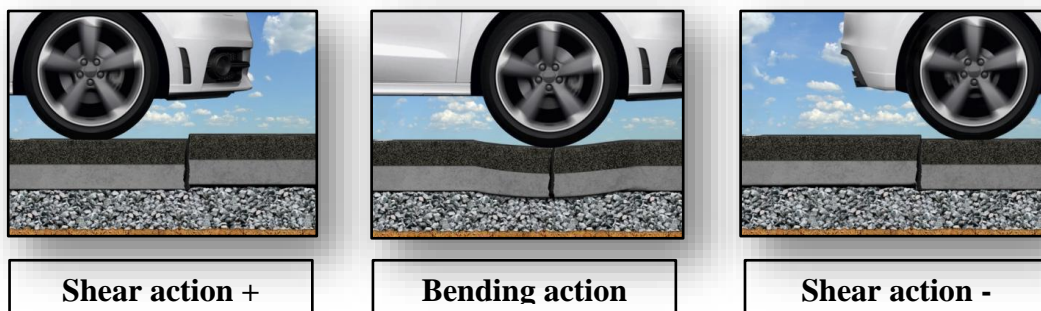


Figure 5-4: Reasons for longitudinal cracking (Montestruque, 2002)

5.2.1.B TRANSVERSE CRACKS IN PAVEMENTS

Straight and regularly spaced transverse cracks are typically reflective cracks from joints in an underlying pavement (Thom, 2012). If the shape is less regular, they may either be reflective cracks over a base or else low temperature cracking of the asphalt. If reflective cracking is suspected, the crack distribution should be measured. If there is a concentration in the wheel paths then traffic is clearly playing an important part; if not, then the effect is almost entirely thermally driven. Short transverse cracks may also have

originated as construction defects and they may be progressing due to binder embrittlement (Thom, 2012). See figure 5-5 for an example of transverse cracking in a pavement.

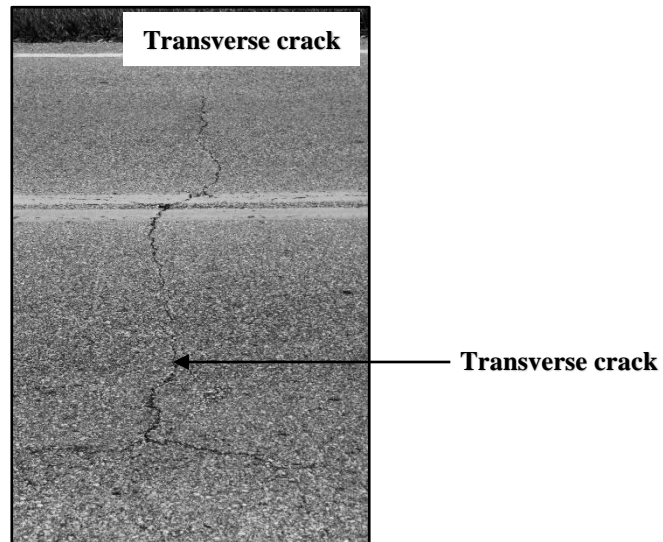


Figure 5-5: Transverse crack in pavement

5.3 RUTTING IN PAVEMENTS

A rut is a surface depression in the wheel paths. Pavement profile may raise along the sides of the rut. Rutting stems from a permanent deformation in any of the pavement layers or in the subgrade, usually caused by consolidation of un-bound as well as bound layers with local changes in density or plastic flow of asphalt-bound layers and may get densification reduction in air voids and hence a local reduction in volume. Figure 5-6 explains the phenomena of surface rutting in pavements.

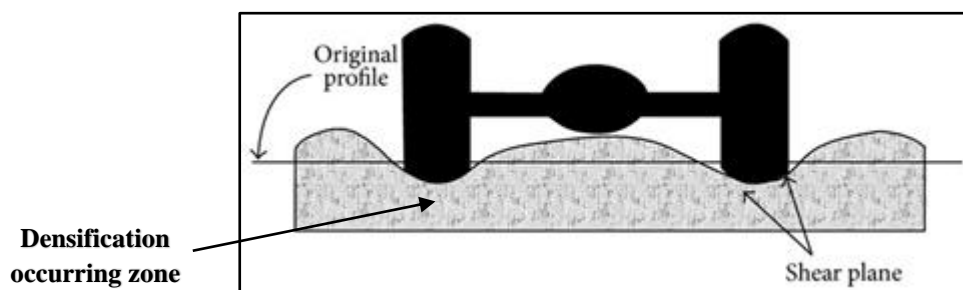


Figure 5-6: Rutting phenomena in pavements

If ruts are narrow with shoulders, the problem is near the surface (surface course or binder course probably); the wider the rut, the deeper the problem. If an asphalt layer appears rich in binder, especially if that binder is soft, that is likely to be the cause of the problem. Figure 5-7 illustrates the causes of non-structural and structural rutting in pavements and figure 5-8 shows on-site rutting in asphalt concrete pavement.

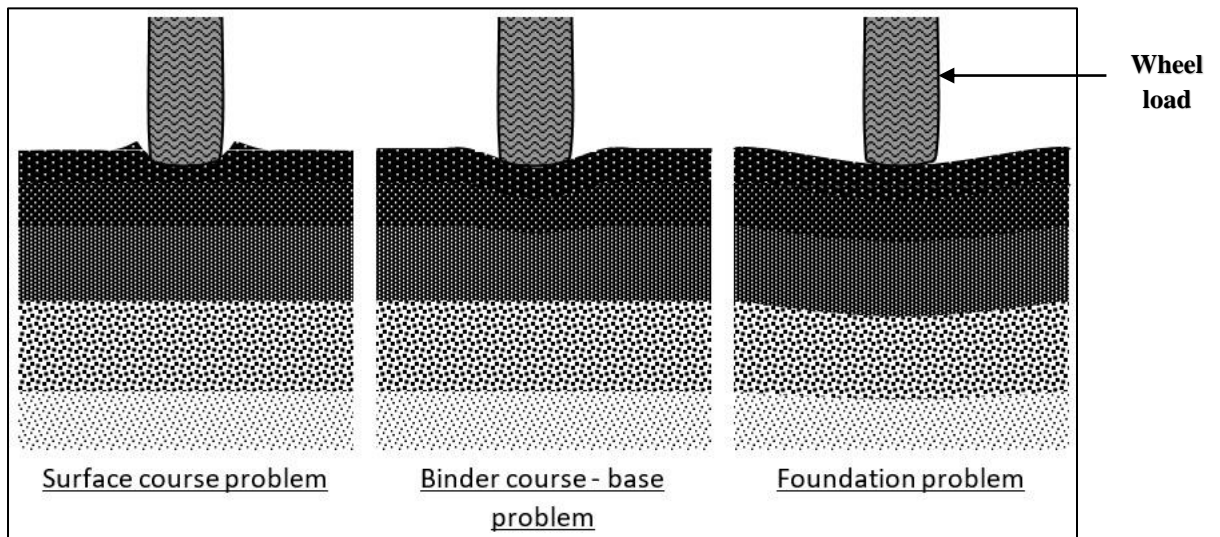


Figure 5-7: Causes of rutting in pavements



Figure 5-8: Rutting in asphalt concrete pavement

5.4 RAVELLING

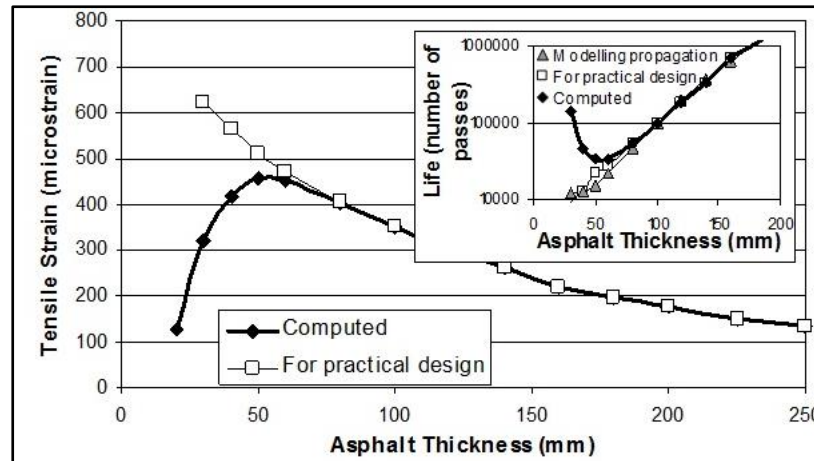
Ravelling (and associated pot holes) occurs when adhesion between binder and aggregate breaks down. Binder hardening and the presence of an excess of filler could be contributory factors. Excess filler can contribute to poor adhesion. Figure 5-9 shows ravelling in the pavement.



Figure 5-9: Ravelling in asphalt concrete pavement

5.5 PERFORMANCE OF THIN ASPHALT LAYERS

Deformation resistance (and therefore curvature) of pavements with thin asphalt layers is affected by the stiffness of underlying support, which means that deformation only increases slightly as asphalt thickness reduces; and strain, which is proportional to curvature but inversely proportional to thickness, actually reduces at low thickness (Thom, 2013). Although calculated strain may reduce as asphalt thickness reduces, experience shows that pavement life does not start increasing (Thom, 2013). Graph 5-1 shows the relationship between tensile strain versus asphalt thickness and deformation versus asphalt thickness.



Graph 5-1: Tensile strain and deformation versus asphalt thickness (Thom, 2013)

5.6 DISTRESSES IN MICROASPHALT ROAD SURFACING

For many years, reflective cracking and rutting have been a problem in microasphalt road surfacing. Various options have been tried in the past as discussed in section 4.8 above. However, these systems have necessitated other ancillary works.

The simplicity of a cold applied microasphalt system is an attraction itself especially to the experienced contractor. The surfacing provides the same element of waterproofing and restoration of skid resistance as surface dressing without the need for concern about binder spread rates, chipping size or the adverse effects of temperature and rainfall (Woodside et al., 1993). However, neither surface dressing nor surfacing such as microasphalt offers a satisfactory long-term solution to the problem of reflective cracking and rutting.

To address the above need, the researcher in this project work has developed a composite material consisting of a glass fibre in a microasphalt matrix. A laboratory testing programme and road trials are outlined in the subsequent sections and chapters, indicating how the life of the microasphalt can be enhanced, and reflective cracking and rutting deferred.

The research will discuss the additional advantages of such a system by indicating how this composite material may affect the pavement. The results obtained from the

investigation using fibres to enhance the performance of the microasphalt would indicate that additional tensile strength and enhancement of overall performance could be achieved by the inclusion of such a fibre, and appears to be a step closer to overcoming the problem of reflective cracking and rutting.

5.7 METHODOLOGY

To overcome the problem of cracking and rutting in microasphalt surfacing materials commonly used by the industrial partner, a detailed investigation on the use of novel reinforced fibre was done to produce new super microasphalt with high resistance to cracking and deformation, to enhance its considerable usefulness and durability.

The phase-wise investigation is based on:

- a. Development of curing technology for sample manufacturing and testing procedures.
- b. Laboratory simulation and full-scale testing trials to optimise the ingredients of the new product and demonstrate the material's engineering properties including its long-term durability.
- c. Assessing the ability of the microasphalt to resist cracking parameter due to traffic loadings through standard semi-circular bending test.

This includes:

- i. Control standard microasphalt (CM) i.e. without glass fibres
 - ii. Glass fibre reinforced microasphalt (GFRM)
- d. Evaluating the capability of the microasphalt to resist rutting parameter due to traffic loadings through standard wheel tracking test.

This also includes:

-
-
- i. Control standard microasphalt (CM) i.e. without glass fibres
 - ii. Glass fibre reinforced microasphalt (GFRM)
-
- e. In order to replace OPC with secondary materials, the said material suitability has been checked using XRF and SEM analysis.
 - f. Repeat the same testing on the industrial partner microasphalt using Semi-circular Bending (SCB) and Wheel Tracking (WT) tests.
 - g. Carry out FEM analysis to predict the cracking and deformation properties of mix using optimum content of glass fibres and secondary cementitious filler.
 - h. Then apply on site microasphalt containing the optimum amount of glass fibres which produced the high quality microasphalt revealing the best cracking and deformation properties.

5.8 MATERIAL CHARACTERISATION

The main components used to prepare the control and fibre reinforced microasphalt were aggregates, filler (cement), water, retarder, bitumen emulsion and an additional component of glass fibre.

5.9 AGGREGATE CHARACTERISATION

Key physical characteristics for aggregates, for suitable incorporation into a microasphalt mix are defined by (NHIPP Guide, 2007):

- a) Geology: This determines the aggregate's compatibility with the emulsion along with its adhesive and cohesive properties.
- b) Shape: The aggregates must have fractured faces in order to form the required interlocking matrix (Holleran, 2001). Rounded aggregates will result in poor mix strength.

- c) Texture: Rough surfaces form bonds more easily with emulsions.
- d) Age and Reactivity: Freshly crushed aggregates have a higher surface charge than aged (weathered) aggregates. Surface charge plays a primary role in reaction rates.
- e) Cleanliness: Deleterious materials such as clay, dust, or silt can cause poor cohesion and adversely affect reaction rates.
- f) Soundness and Abrasion Resistance: These features play a particularly important role in areas that experience freeze-thaw cycles or which have a wet climate.

Aggregate physical properties used in the mixes are given below in table 5-1.

Table 5-1: Aggregate physical properties

Material	Property	Value
Coarse aggregate	Bulk particle density, Mg/m ³	2.72
	Apparent particle density, Mg/m ³	2.75
	Water absorption, %	0.2
Fine aggregate	Bulk particle density, Mg/ m ³	2.77
	Apparent particle density, Mg/ m ³	2.82
	Water absorption, %	0.8

Two gradations are specified for microasphalt; namely, Type II and Type III (Caltrans, 2002). The gradation for each type is listed in table 5-2.

Table 5-2: Typical aggregate gradings (Caltrans, 1999)

Sieve size	Percentage passing	
	Type II	Type III
3/8 in (9.5mm)	100	100
No. 4 (4.75 mm)	94-100	70-90
No. 8 (2.36 mm)	65-90	45-70
No. 16 (1.18 mm)	40-70	28-50
No. 30 (600-µm)	25-50	19-34
No. 200 (75-µm)	5-15	5-15

The main difference between Type II and Type III gradations is the aggregate maximum size. This governs the amount of residual binder required by the mix and the purpose for which the microasphalt is to be used on site (Caltrans, 2002). Type II microasphalt is less coarse as compared to the Type III microasphalt and is suggested for urban and residential streets and airport runways (Caltrans, 2002). Type III microasphalts have the coarsest grading and are appropriate for filling minor surface irregularities, correcting ravelling and oxidation, and restoring surface friction. Type III microasphalts are typically used on arterial streets and highways (Caltrans, 2002).

The role of fines (i.e., aggregate particles No. 200 [75 µm] and finer) in a microasphalt mix is to form a mortar with the residual asphalt to cement the larger stones in place. The fines content is essential for creating a cohesive hardwearing mix. Generally, the fines content should be at the midpoint of the grading envelope. Distribution of the sub-No. 200 (75 micron) fraction is critical to control the reaction rate in microasphalt emulsions (Schilling, 2002).

Local aggregates complying with BS EN 13043 (Aggregates for Bituminous Mixtures and Surface Treatments for Roads, Airfields and Other Trafficked Areas) are used. Typical aggregate gradation conforming to Type II microasphalt gradation is used in the mixes and gradation for each type is given below in table 5-3. Figure 5-10 (a) illustrates the sieve shaker used for sieving of aggregates and figure 5-10 (b) shows the aggregates kept in the container in the laboratory after heating in the oven for 24 hours.

Table 5-3: Typical aggregate gradation

Sieve size (mm)	Range (%)
5.00	70-90
2.36	45-70
1.18	28-50
.600	19-34
.300	12-25
.075	5-15

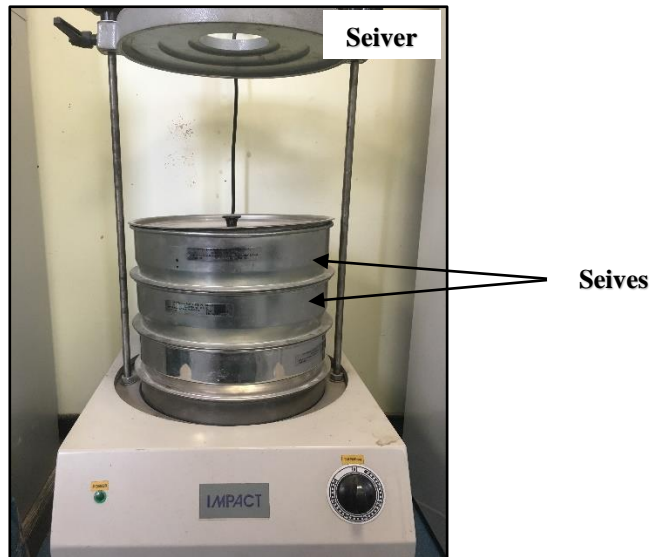


Figure 5-10 (a): Sieve shaker



Figure 5-10 (b): Aggregates in the container

5.10 FILLER CHARACTERISATION

In microasphalt, cement is used as a mixing aid allowing the mixing time to be extended and creating a consistency that is easy to spread. Additionally, hydroxyl ions counteract the emulsifier ions, resulting in a mix that breaks faster with a shorter curing time. Cement is also a fine material and, as such, absorbs water from the emulsion, causing it to break faster after placement. It also promotes cohesion of the mixture by forming a mortar with the residual asphalt. Ordinary Portland cement (OPC) was used as a filler (1% of the total weight of the dry aggregates in the mix).

5.11 BITUMEN EMULSION CHARACTERISATION

Asphalt emulsions are defined in chapter 3 as dispersions of asphalt in water stabilized by a chemical system. Bitumen emulsions are environmentally friendly, the emissions being mainly water vapour. Cutback solvent is usually kerosene (similar to domestic paraffin), one of the hazardous low cost organic solvents. They are quick breaking and most conform to BS 434; these are designated K1-40, K1-60 or K1-70. K1-40 and K1-60 are sprayed at ambient temperature, but K1-70 must be heated to between 80°C and 90°C before it is sufficiently fluid for spraying. They are typically either 60% or 70% binder content emulsions. The binder manufacturer's instructions should be followed for spraying methods but typically the 60% emulsions are sprayed at ambient temperature and the 70% ones are sprayed at between 80°C and 90°C.

In the case of microasphalt surfacing systems, the emulsion may be cationic or anionic; however, cationic emulsions are the most common. British Standard Specifications 13808 (BS EN, 2013) provide specifications for specifying cationic bituminous emulsions.

Bitumen emulsions are specially formulated for compatibility with the aggregate and to meet the appropriate mix design parameters. Emulsion specifications are based on standard emulsion characteristics, such as stability, binder content, and viscosity. In all microasphalt surfacing systems, polymer is added to the emulsion. The polymer enhances stone retention, especially in the early life of the treatment. The added polymer also reduces thermal susceptibility. Polymers also raise softening point and flexibility. Generally, microasphalt surfacing mixtures with a polymer modified emulsion do not impart significant resistance to reflective cracking.

Bitumen emulsion designated as K1-60 was used by total weight of the mix (as detailed in section 5.15 below) to prepare the microasphalt. This is a polymer modified binder which, when mixed with the aggregates and fillers, gives a material with good stability whilst maintaining flexibility (BS EN, 2013). Figure 5-11 shows the bitumen emulsion used to prepare the microasphalt samples in the pavement laboratory. Physical and chemical properties of bitumen emulsion are given in table 5-4.



Figure 5-11: Bitumen emulsion jerrycan

Table 5-4: Properties of bitumen emulsion

Description	Bitumen emulsion
Type	Cationic aqueous emulsion
Physical state	Viscous liquid
Color	Black to brownish black
Bitumen content, (%)	60
Particle surface electric charge	Positive
pH	Acid (1.5 to 3)
Boiling point, (°C)	100
Density at 25 °C, (kg/m ³)	1000+/- 5

Emulsions are usually modified with latex, which is an emulsion of rubber particles. The latex does not mix with the asphalt; rather, the latex and the asphalt particles intermingle to form a 3-D structure. Figure 5-12 shows a bitumen emulsion sample collected in a container. Figure 5-13 shows a bitumen emulsion sample being examined with the help of a high-resolution microscope in the chemical laboratory. Figure 5-14 illustrates the 3-D structure of latex and the bitumen emulsion particles. The latex used is either neoprene or styrene butadiene styrene (SBS) for microasphalt. Microasphalt is modified with either natural latex or SBS latex (Ruggles, 2005).

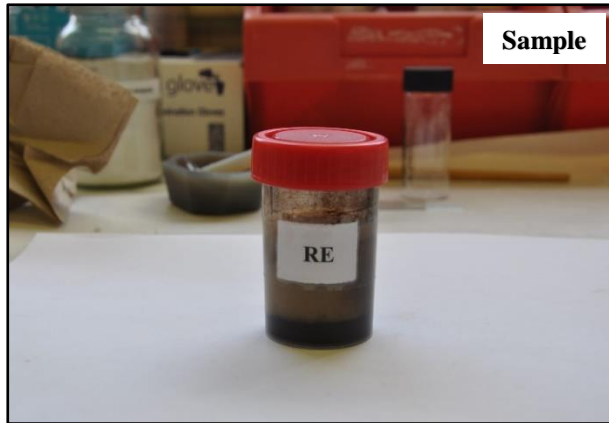


Figure 5-12: Bitumen emulsion sample in the container



Figure 5-13: Bitumen emulsion examined with the help of high resolution microscope

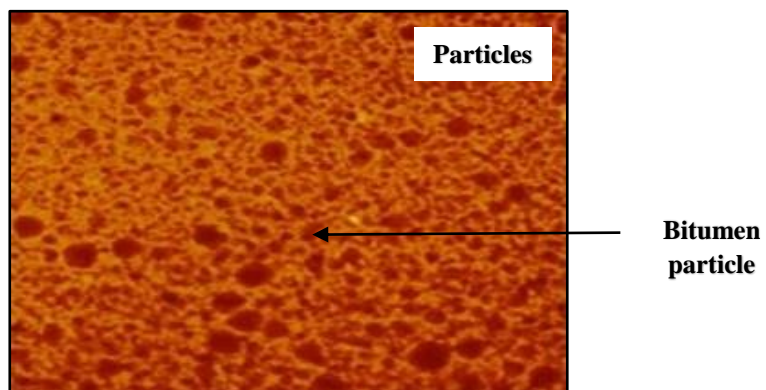


Figure 5-14: Latex and bitumen emulsion particles 3-D structure at magnification level of 100µm

Latex may separate from the emulsion due to the differences in density. If separation occurs, the latex must be remixed into the emulsion by circulation in the tanker before the modified emulsion is transferred to the microasphalt machine for application (Holleran, 2002).

The bitumen emulsion process involves mixing naturally anionic rubber latex (flipped) with cationic surfactants, and emulsifying the resulting liquid with asphalt using a colloid mill (Ruggles, 2005). The natural rubber latex emulsification process is as shown in figure 5-15.

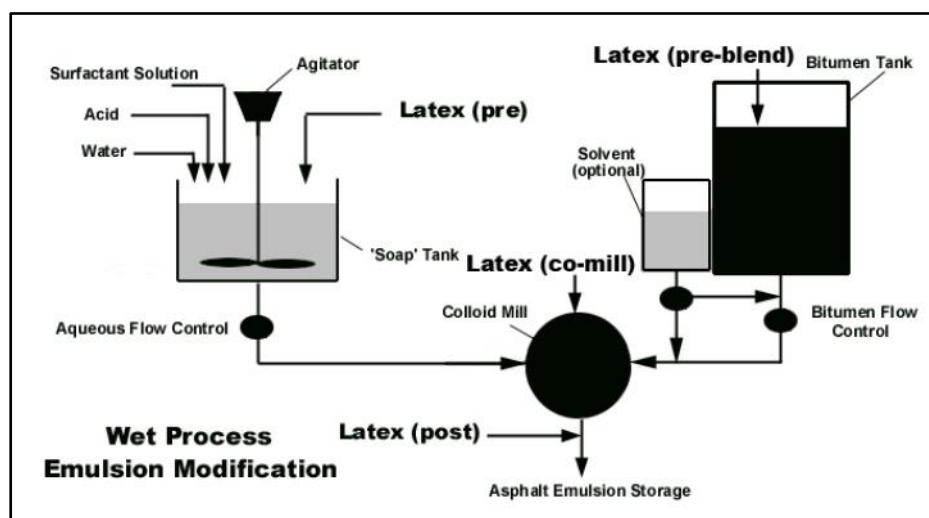


Figure 5-15: Emulsion modification process

The resulting cationic emulsion is attracted to the anionic surfaces of the aggregate, latex, and filler material; thereby increasing oil-wettability and ensuring better adhesion of the coagulated asphalt to the mineral grains once cured (Takamura, 2002). Surfactant action in modified asphalt emulsion is as shown in figure 5-16. This process, referred to as “breaking,” is an essential event in ensuring rapid adhesion and strength development (Takamura, 2002).

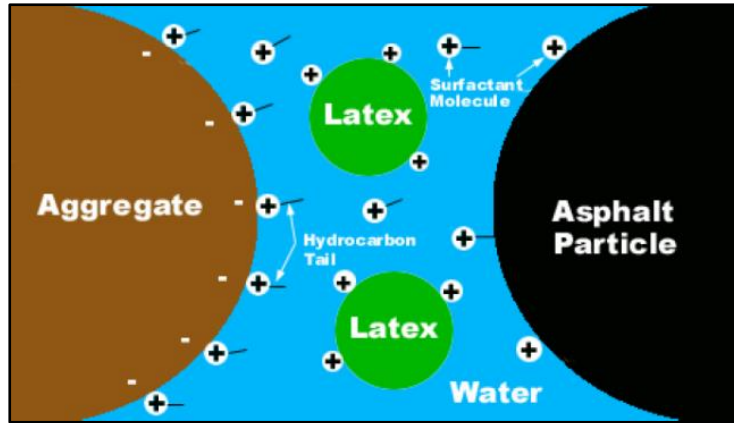


Figure 5-16: Surfactant action in modified asphalt emulsion

Figures 5-17, 5-18, 5-19 & 5-20 show a bitumen emulsion production facility; producing modified bitumen emulsion after the emulsification process.



Figure 5-17: Bitumen emulsion production facility



Figure 5-18: Emulsification of bitumen emulsion in progress



Figure 5-19: Bitumen emulsion production in silos



Figure 5-20: Drums filled with bitumen emulsion

5.12 RETARDER CHARACTERISATION

Additives other than cement vary and are features of particular microasphalt systems. They can act as retardants to the reaction with emulsions, either as a prophylactic, slowing the emulsifier's access to the aggregate surface, or by preferentially reacting with the emulsifier in the system. Additives include emulsifier solutions, aluminum sulfate, aluminum chloride, and borax. Generally, increasing the concentration of an additive slows the breaking and curing times. This is useful when air temperatures increase during the day (Caltrans, 2009).

The chemical used as a retarder in the microasphalt mix is called dope also known as stabiliser. The purpose of the retarder is to extend the workability of the emulsion/aggregate mix so that the bitumen does not flocculate/coalesce before the mix has been applied to the road surface. Physical and chemical properties of retarder (dope) are given in table 5-5.

Table 5-5: Properties of retarder (dope)

Description	Retarder (dope)
Physical state	Liquid
Appearance/color	Yellow
Odour	Faint
Melting Point/Melting Range	-15°C
Flashpoint	100 – 199°C
Flammability	>100°C
Density at 25°C	1070 kg/m ³
pH	6-8 (100 g/l, water)
Viscosity	50 mPa.s (25°C)

5.13 FIBRE CHARACTERISATION

An inorganic (INORG) type of fibre, namely glass fibres, were used in the study to enhance the resistance of microasphalt to fatigue cracking and deformation.

Glass fibre reinforcement (GFR) is made by blending recycled glass materials, melting them in a three-stage furnace, extruding the molten glass, cooling the filaments with water, and then applying a chemical (British Glass, 2014).

Glass fibre is mainly composed of silica and oxygen and consist of strands which are made up of a large number of individual filaments. Glass in molten form is pushed from the furnace tank through a channel known as forehearth to a series of bushings containing accurately dimensioned holes (tips) at the base (British Glass, 2014).

Fine filaments of glass fibres are drawn mechanically downwards from the bushing tips. The glass fibre filament diameter is as small as nine microns. From the bushing the filaments run to a common collecting point, and they are subsequently brought together as bundles or strands (British Glass, 2014). Glass fibre manufacturing process is shown in the figure 5-21.

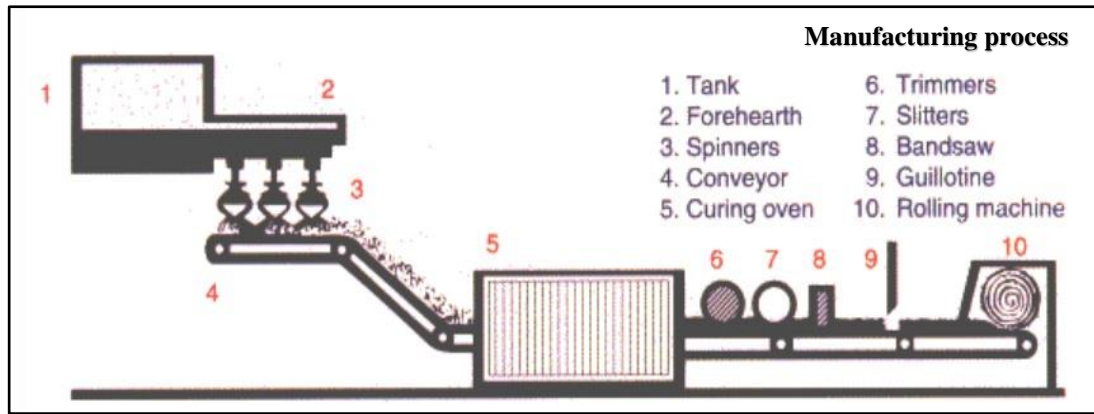


Figure 5-21: Glass fibre manufacturing process (British Glass, 2014)

Figure 5-22 illustrates glass fibre doff, figure 5-23 shows chopped glass fibres and figure 5-24 shows glass fibres in different cut lengths.



Figure 5-22: Glass fibre doff

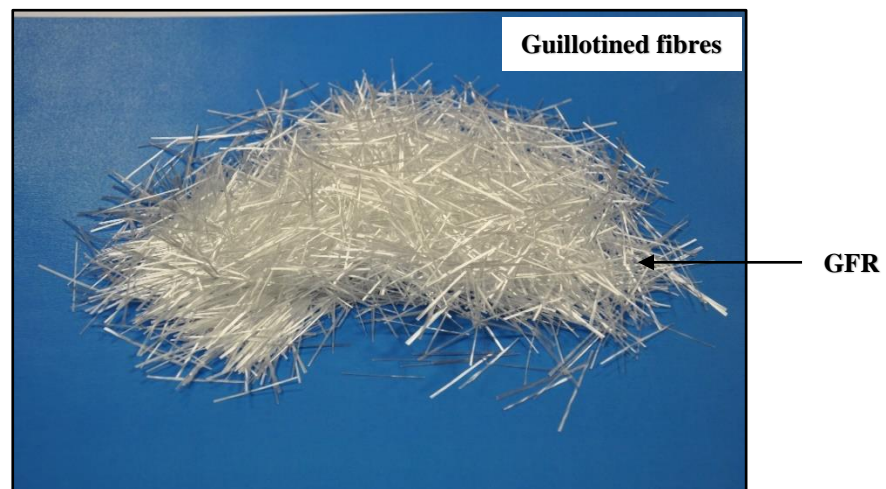


Figure 5-23: Chopped glass fibres

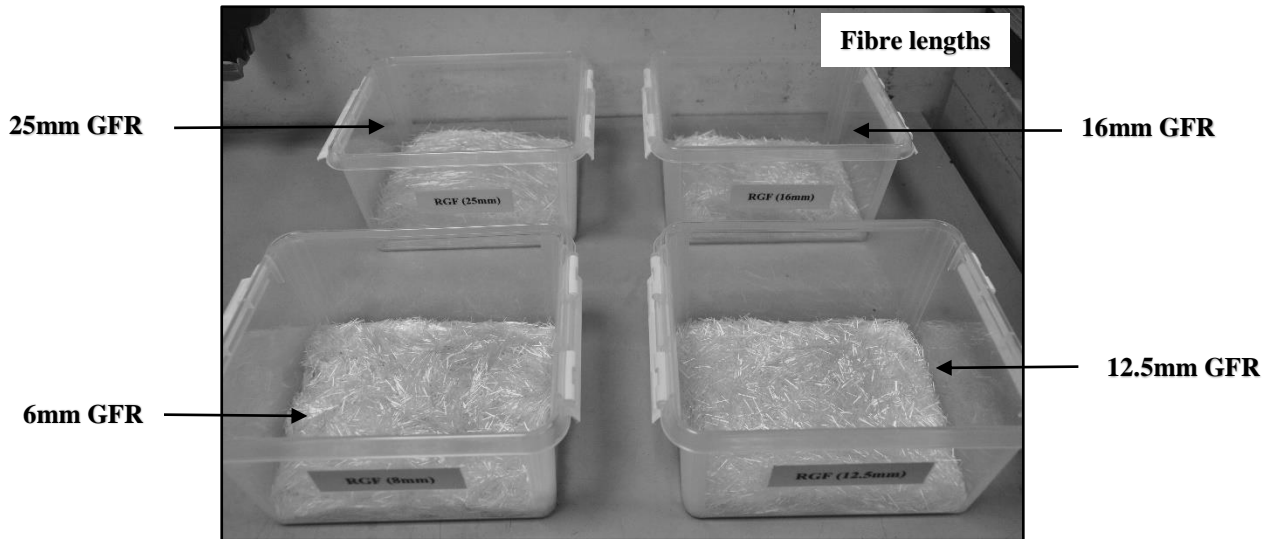


Figure 5-24: Glass fibres in different cut lengths

Figure 5-25 shows the scan electron microscopy (SEM) imagery of the fine needle like structure of glass fibres captured at the magnification level of M:300x, M:1500x and M:2500x. A scanning electron microscope is a type of electron microscope that produces images of a material in test by scanning it with a focused beam of electrons. The electrons interact with atoms in the glass fibres sample, producing various signals that contain information about its surface topography and composition. SEM is discussed in detail in section 5.28.5.

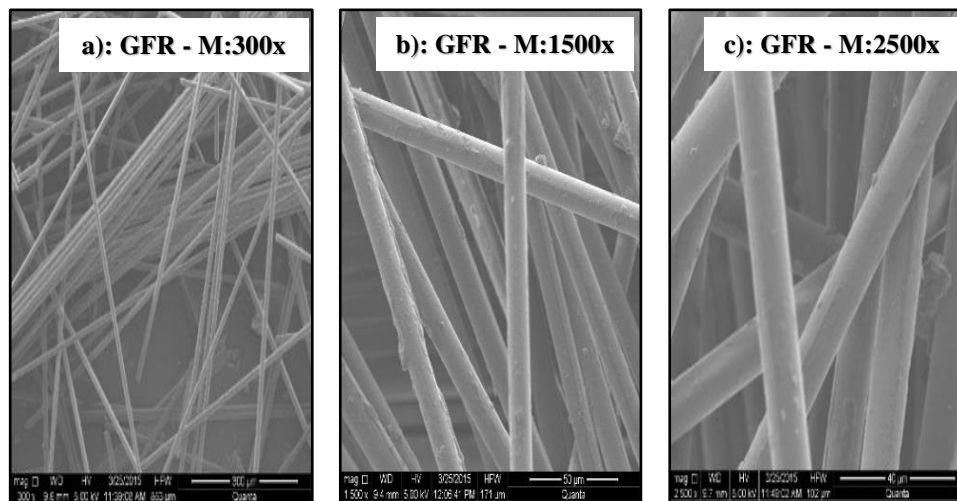


Figure 5-25: SEM images of glass fibres

Specifications of glass fibre are given in table 5-6. X-ray fluorescence (XRF) analysis was also done in the chemical laboratory to determine the chemical composition of glass fibres. X-ray fluorescence is a non-destructive analytical technique used to

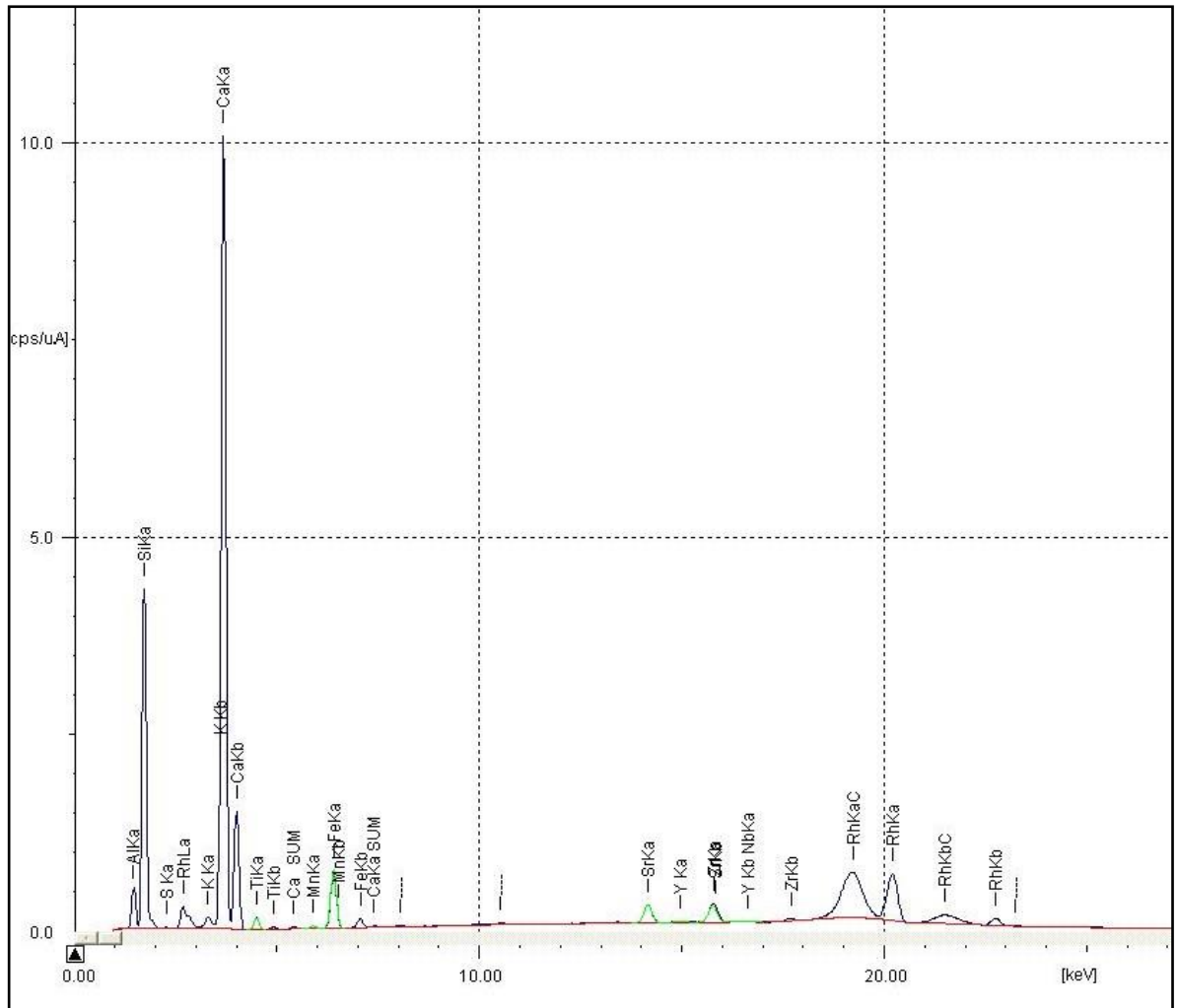
determine the elemental composition of a testing material. The XRF analyser determines the chemistry of a glass fibre by measuring the fluorescent (or secondary) x-ray emitted from a glass fibre sample when it is excited by a primary x-ray source. XRF is discussed at length in section 5.28.2. Graph 5-2 shows the constituent chemical compounds present in the glass fibre structure. Quantitative analysis of chemical compounds for the glass fibre sample is provided in the table 5-7. XRF analysis shows that the glass fibre composition mainly consists of silicon dioxide and calcium oxide.

Glass fibres have the advantage of having CaO and SiO₂ content. CaO (calcium oxide or quicklime), content, is a good measure of the basic (alkalinic) nature of an aggregate, and SiO₂ (silicone dioxide), content gives a good measure of the siliceous (acidic) nature of an aggregate (Vaughan, 1999). Many researchers (Daoud et al., 1980; Jamieson et al., 1993; Brannan et al., 1990; Tolman & Van Gorkum, 1996; Saito & Kawamura, 1986) support the theory that a large surface area and basic nature are very beneficial for a successful aggregate-bitumen bond and that a siliceous nature is not always conducive to a successful bond.

It is important to highlight here that different glass fibres may have different chemical composition (i.e. percentages of constituent chemical compounds in glass fibres may vary depending upon the original source of the material and manufacturing process) and therefore surface of the glass fibres in the long term may react chemically differently with the cement and other ingredients present in the microasphalt mix. This may result in stripping of binder from glass fibres if chemical bonding between the glass fibres and cement is weak.

Table 5-6: Specifications of glass fibre

Description	Glass fibre
Type of glass	E-glass (E)
Type of fibre glass	Assembled roving (R)
Filament diameter	13 microns
Strand diameter	78 microns
Density	2.54 g/cm ³
Moisture content (%)	≤ 0.15 (ISO 3344)
Size content (%)	1.00 ± 0.15 (ISO 1887)



Graph 5-2: XRF analysis of glass fibre

Table 5-7: XRF (quantitative) analysis of glass fibre (GF)

Description (chemical compound)	Percentage (%)
Silicon dioxide SiO ₂	25.11
Calcium oxide CaO	9.63
Aluminum oxide Al ₂ O ₃	7.95
Magnesium oxide MgO	0.37
Iron trioxide Fe ₂ O ₃	0.16
Potassium oxide K ₂ O	0.15

Tensile strength of the glass fibres was examined in the concrete laboratory by using a universal tensile testing machine as per the specifications stipulated in BS EN ISO 6892-1 standards. Glass fibre consist of multiple strands; very minute in thickness in microns which amalgamate together in a helix pattern to form a single glass fibre filament. Figure 5-26 shows the universal testing machine used to test the glass fibre sample. Figure 5-27 depicts the condition of the glass fibre filament after fracture i.e.

upon completion of test. It can be observed from the glass fibre condition that the tiny strands in the filament tend to deform (bulge out) and this results in fracture after reaching the yield point.

In Graph 5-3 below, glass fibre initially shows a linear relationship between the applied force (stress) and the extension (strain). In this linear region of the test, stress is directly proportional to strain and the straight line obeys the relationship that is defined by Hooke's Law where the ratio of stress to strain is constant i.e. up to a force of 18N with an extension of 4.3mm.

Modulus of elasticity is a measure of stiffness, but only of the linear region of the curve. If the glass fibre specimen has loads applied within its linear region, it will return to its same shape and condition when the load is removed. At the point, i.e. after a force of 18N and extension 4.3mm, where the curve no longer shows linearity, therefore deviates from the straight-line relationship, Hooke's Law no longer applies and permanent dimensional deformation occurs in the glass fibre filament. This point is called the elastic or proportional limit. From this point, the glass fibre specimen reacts plastically to any increase in load or stress and the glass fibre filament does not return to its original, un-stressed condition, size or shape, when the load is removed and if load is further applied it results in fracture as shown in the figure 5-27. This plastic region is in the range of 3.8mm to 4.3mm.

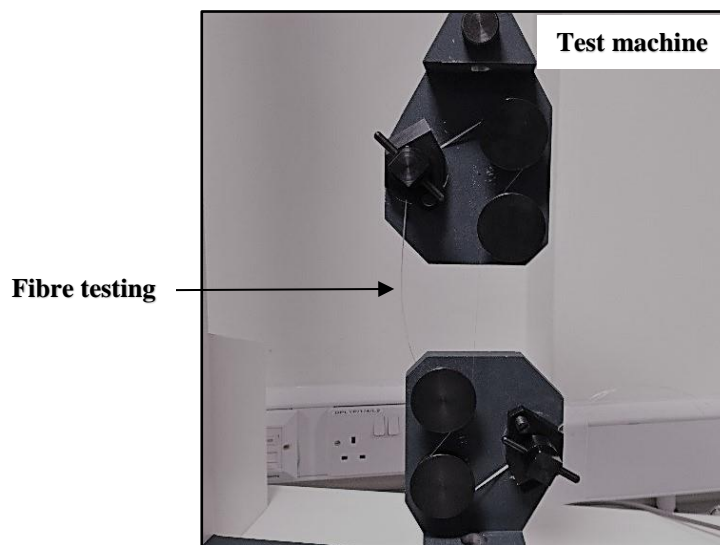


Figure 5-26: Universal tensile testing machine

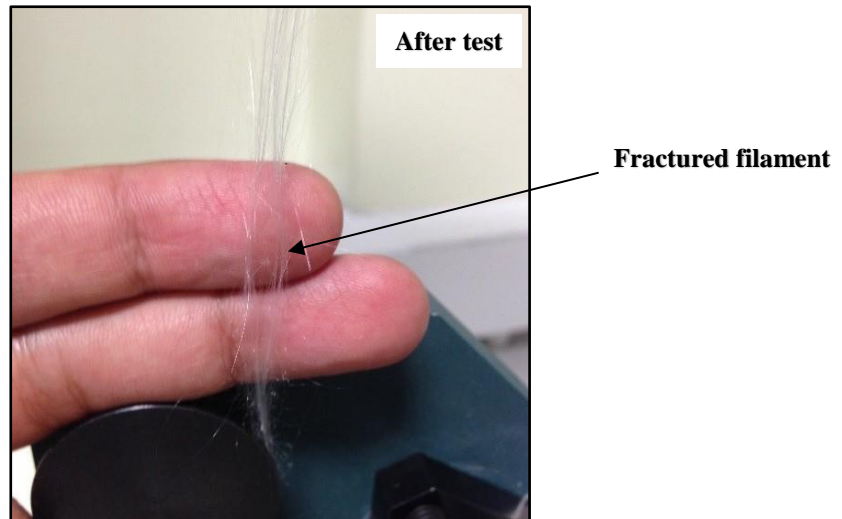
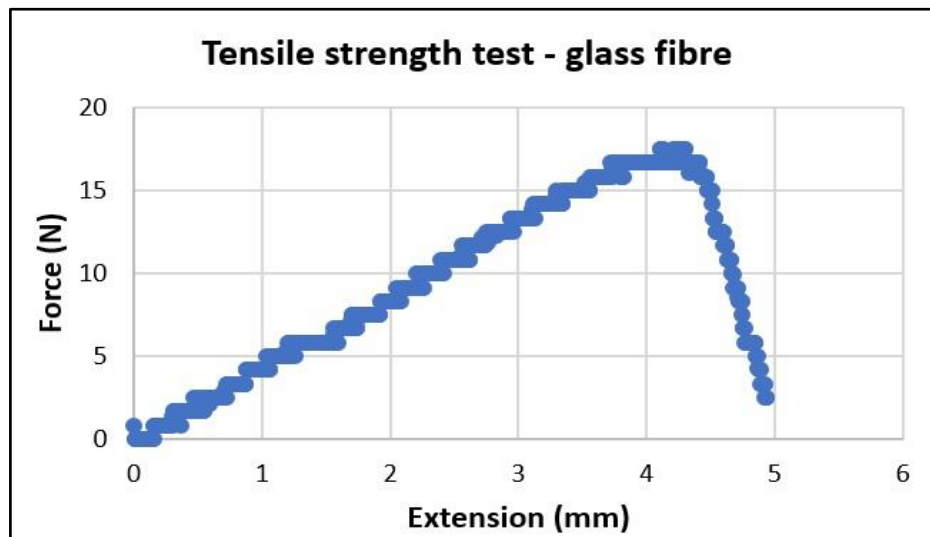


Figure 5-27: Fractured glass fibre filament after the test



Graph 5-3: Tensile strength of a glass fibre filament

5.14 MIX DESIGN

The performance of a microasphalt depends on the quality of the materials and how they interact during curing time and after curing. The mix design procedure looks at:

1. Mixing: questions to be addressed are whether the components mix together and form true, free flowing microasphalt?

-
-
2. Breaking and curing: questions to be addressed are whether the emulsion breaks in a controlled way on the aggregate, coats the aggregate, and forms good bond to the aggregate? Will the emulsion build up cohesion to a level that will resist abrasion due to traffic?
 3. Performance: questions to be addressed are whether the microasphalt resists traffic induced stresses?

The steps in microasphalt design include:

- a) Prescreening of materials
- b) Job mix design
- c) Final testing

At each stage, mixing, breaking, curing, and performance issues are addressed.

5.14.1 PRESCREENING

Prescreening involves testing the physical properties of the raw materials. The emulsion type is selected based on job requirements and is checked against the requirements laid out in the specifications BS EN 13808:2013 and BS 434-2:2006. The aggregate is checked against specification (table 5-2) and a simple mixing test is performed to assess compatibility with the emulsion. When both of these steps are satisfied, the job mix formula is developed.

5.14.2 JOB MIX DESIGN (MIXING PROPORTIONS)

The International Slurry Surfacing Association (ISSA) test method detailed in Technical Bulletin 102 is normally used to determine the approximate proportions of the microasphalt mix components (ISSA, 1990). In this test, which is typically conducted in the lab, a matrix of mix recipes are made up and the manual mixing time is recorded for each mixture. A minimum time is required to ensure that the mixture will be able to mix without breaking in the microasphalt machine. At this stage, phenomena such as foaming and coating

are visually assessed. Also at this stage, the water content and additive content can be determined to produce a composed mixture. Figure 5-28 illustrates a good microasphalt mixture consistency which meets the requirements.



Figure 5-28: Microasphalt mix prepared in the laboratory

The mixing time must be at least 120 seconds for microasphalt at 77°F (25°C) to ensure thorough and uniform mixing. The process may be repeated at elevated or reduced temperatures to simulate expected field conditions at the time of application. The best mix is chosen, based on good coating of mixing times in excess of the minimum required through the entire range of expected application temperatures.

Good coating has been described in BS EN 12697-11 which determines the affinity between aggregate and bitumen. The procedure gives an indirect measure of the binder's ability to adhere to the aggregate. A specified mass of sieved aggregate is mixed with 4% binder by mass of aggregate, if complete coating is not achieved the binder can be increased until complete coating is achieved. Coated particles are placed in a flat container. Sufficient water is added to the container to completely cover the coated particles and allowed to stand for 48 hours at 19°C. The water is decanted from the container and the particles allowed to dry, each particle is inspected for incomplete coating. If more than three particles have incomplete coverage repeat the test on three further samples. A visual estimate can be made of the level of bitumen.

The quantity of aggregate used in the mix is 84% by total weight of the mix, cement is used by 1.0% of the total weight of the dry aggregate in the mix, fibre quantity has been extensively trialled and tested and this is discussed in sections 5.17 and 5.18 respectively. Bitumen emulsion quantity is discussed in section 5.15 below. Water to initiate the hydration process in the mix has been added in the proportion; 5.0% by total weight of the dry aggregate in the mix and dope is used by 2.0% of the total weight of the dry aggregate in the mix. The amount of water and dope was specified by the industrial partner. The optimised proportions of water and dope are based on the extensive research carried out by the chemical scientists of the industrial partner at the in house laboratory facility. However, the amount of each material used within the mix has been discussed in detail in sections 5.17.2 and 5.18.2 respectively.

5.14.3 FINAL TESTING

Once the job mix components have been selected, the mix is tested to determine its properties and ensure compliance with the specifications in BS EN 13808:2013 and BS 434-2:2006 and (table 5-2) listed above. If the mix conforms to the above specifications, the emulsion content and aggregate grading is reported as the job mix formula.

5.15 OPTIMUM BINDER

The optimum percentage emulsion or binder content is found from the Wet Track Test (TB 100) and the Excess Binder Test (TB 109) (ISSA, 2005). In this study, the optimum binder content used is referred in the table 5-8 below:

Table 5-8: Optimum binder content for the microasphalt mixes

Type of mix	Optimum binder content
Control microasphalt	6.0% (by total weight of the mix)
Glass fibre reinforced microasphalt	7.5% (by total weight of the mix)

The optimum binder content for the mixes detailed in the table 5-8 above was determined in-consultation with the industrial partner on the premise that the mixing time of the microasphalt mix is maintained for up to 20 minutes to ensure adequate

workability of the mix so that the newly developed material could be placed on site before breaking i.e. i) the aggregate particles do not coalesce with bitumen droplets instantly and ii) the hydration process between the entrapped water and cement does not make the mix stiff before laying it on site. Further, it has been observed during the preparation of test samples in the laboratory that if the binder content for glass fibre reinforced microasphalt is kept the same as for control microasphalt i.e. 6.0% by total weight of the mix, the addition of glass fibres makes the microasphalt mix dry and most of the glass fibres remain uncoated with the binder. This is because the addition of glass fibres in the microasphalt mix as an additional component increases the total surface area of the material to be coated with the bitumen and at the same time glass fibres may have also absorbed some of the bitumen emulsion thus causing an imbalance in the optimum quantity of bitumen emulsion present in the mix. This entailed further optimisation of bitumen emulsion for the glass fibre reinforced microasphalt i.e. 7.5% by total weight of the mix. Similar binder content for different fibre mixes has been used by researchers in the past (Broughton et al., 2012; Fitzsimons & Gibney, 2003).

5.16 SAMPLE PREPARATION AND CURING TECHNOLOGY

HMA samples are normally demoulded soon after the compaction and are kept in the oven for curing purpose. However, in the case of cold mix microasphalt it was experienced that the samples tend to break if they are demoulded immediately after the compaction because of water entrapped within the mix. Also, the major problem with the CMM application is the long curing time (evaporation of trapped water) required to achieve the required performance and the weak early life strength (because of the existence of water). The full curing in the field of these mixtures may occur between 2 and 24 months depending on the mixture's ingredients and weather conditions (Serfass et al., 2004).

Attempts have been made by the researcher to improve the long curing time for microasphalt mixes by using the microwave technology, but this involves breaking and spreading of mix material on the container and resulted in low early strength of microasphalt. Therefore, a methodical procedure has been adopted to tackle the curing

problem in CMM; based on comprehensive work done by the researchers in the past to address the curing problem in CBEMs (Shakir, 2012).

Evaluating HMA properties normally starts immediately when it cools down after compaction, and reaches its mature stage. This is not correct for CBEMs, as they have evolution characteristics, especially in their early life. Their initial cohesion is low and builds up gradually with time (Serfass et al., 2004). Hence, curing temperature plays a significant role in mixture properties as CBEM strength evolution mainly depends on the removal of the trapped water and the setting of the bitumen emulsion to its origin base bitumen. This is true for CBEM with inert filler, as increasing the curing temperature leads to facilitating the water removal. In the case of active filler, further to that, high early temperature activates the hydration process. Rojas and Cabrera (2002) reported that the curing temperature plays a significant role in the formation of hydrated phases in addition to the amounts normally produced.

Shakir (2012) investigated three curing temperatures for CBEMs, namely 3 days at 20°C, 40°C and 60°C. These were adopted from previous research works (Ruckel et al., 1983; Maccarrone et al., 1994; and Doyle et al., 2010). During the above research the following outcomes were revealed:

- a. At low curing temperature with or without low active filler level, target stiffness modulus was not achievable.
- b. Increasing curing temperature leads to improvement in stiffness modulus in general, for CBEMs with and without active filler.
- c. Improvement in stiffness between 40°C and 60°C for CBEMs with or without low level of active filler is more significant as compared to 20°C; whereas CBEMs with higher levels of active filler showed obvious improvements among all ranges even at 20°C.
- d. With high active filler level, comparative stiffness values to soft and hard HMA are gained by increasing curing temperature.
- e. There were no significant changes in volumetric properties due to the change in curing temperature.

It was observed that the free and trapped water was responsible for inferior CBEM, whereas increasing the temperature led to the increase of the rate of the water evaporation (Shakir, 2012). Consequently, the gain in strength increases. Higher ambient temperature during application is preferable, especially for CBEM without active filler; whereas low temperature causes very limited development in strength (Shakir, 2012). Increasing the curing temperature of CBEM containing inert filler causes increase in the rate of evaporation. Improvement in stiffness started significantly after curing temperature of 40°C (Shakir, 2012). Simultaneously for CBEM with active filler, further to the removal of the trapped water, increasing the curing temperature inspires the hydration process.

Keeping in view the above, the aim was to ensure that the curing protocol selected for CMM is in line with the curing procedure for CBEM mixtures which has been extensively developed in the past by researchers and is compatible with the objective of each test and the evaluation procedure, as cracking and deformation evaluation should be ensured from the early life of the microasphalt material. Therefore, the curing protocol of 3 days at 60°C was adopted to accelerate the representative life of microasphalt mixtures i.e. for the SCB and WT tests. Standard Cooper technology galvanised slotted steel moulds consisting of a base plate and mould body were used to prepare samples. During the compaction, water in the mix drains through slots in the walls of the mould and past the lower platen. This helps in ensuring that no pore water pressure builds up in the specimen and thus avoids any occurrence of deformation in the shape of the sample. Acott (1980) equated the laboratory regime of 3 days of conditioning at 60°C to a very broad span of 23-200 days of field curing whereas Maccarrone et. al., (1994) estimated that this simulates an equivalent of 1 year of field curing. Health and safety aspects were taken into consideration and samples were prepared in the fume cupboard to safely capture and remove the air-borne hazardous substances (gases, vapours and particulates/dust) generated in the laboratory during the chemical reaction occurrence within the CMM. The fume cupboard was used only for preparation of microasphalt samples and not as storage areas as use for storage will interfere with the air flow within the cupboard and will increase the likelihood of harmful substances being released from the cupboard into the laboratory. Subsequently, microasphalt samples were cured in the oven.

Further, CMM specimens were also kept in the open air in the laboratory for 1 day at room temperature i.e. after mould extraction, for more understanding of the strength evolution at ambient conditions. The humidity was controlled during the open air curing process and the specimen's sides were sealed with plastic adhesive tape to prevent them being influenced by humidity and also to ensure that the volatiles evaporate through the surface of the mixture as recommended by Thanaya (2003). The objective of this treatment was to simulate realistic site curing conditions where the evaporation of water will predominantly occur through the surface of the microasphalt.

During the entire process, care has been taken in adopting the curing protocol to make the evaluation of the CMM as representative and close to the on-site conditions as possible. This enabled the researcher to successfully develop the curing regime for CMM and helped in removing the entrapped water in the microasphalt and thus aided in eliminating the issue of breaking of the mix, experienced initially during the preparation of test samples.

5.17 LABORATORY TESTING

This presents a laboratory study in which the semi-circular bending test (SCBT) was evaluated for its suitability to characterise the tensile strength, fracture toughness and fatigue life of microasphalt. Numerical analyses indicate a good correlation and therefore agreement between the results of the tensile strength and fracture toughness obtained from the SCBT. It was found that the SCBT is very promising for determination of microasphalt characteristics, mainly tensile and fracture resistance, while it clearly shows the emulsion-aggregate-fibres interaction in the mechanical behaviour of the microasphalt mix.

5.17.1 SEMI-CIRCULAR (THREE POINT) BENDING TEST PROTOCOL

This presents a method to characterise the crack resistance of the control mix and the fibre containing microasphalt using a semi-circular bending (SCB) fracture test according to the standards prescribed in BS EN 12697-44.

The principle of the semi-circular bending test to determine the tensile strength is shown in Figure 5-29. Monotonic load was applied to a semi-circular specimen until failure. The load and vertical deformation was recorded continuously. The loading rate was 5 mm/min. Two roller supports, and a loading roller were used for loading conditions (Schapery, 1975). The distances between the supports in different researches were about $2s = 0.8D$; where “s” is the distance from centre of the roller support to the centre of the crack notch in the specimen and “D” is the diameter of the specimen (Krans et al., 1996; Molenaar, et al., 2002; Huang et al., 2004). The horizontal length of the loading strip was 9.4 mm and the horizontal length of the support strip was 6.25 mm (Molenaar et al., 2002; Huang et al., 2004). The specimens’ diameters were 150 mm, resulting in a span length of $2s = 120$ mm. The specimens’ thicknesses were selected to be 50 mm.

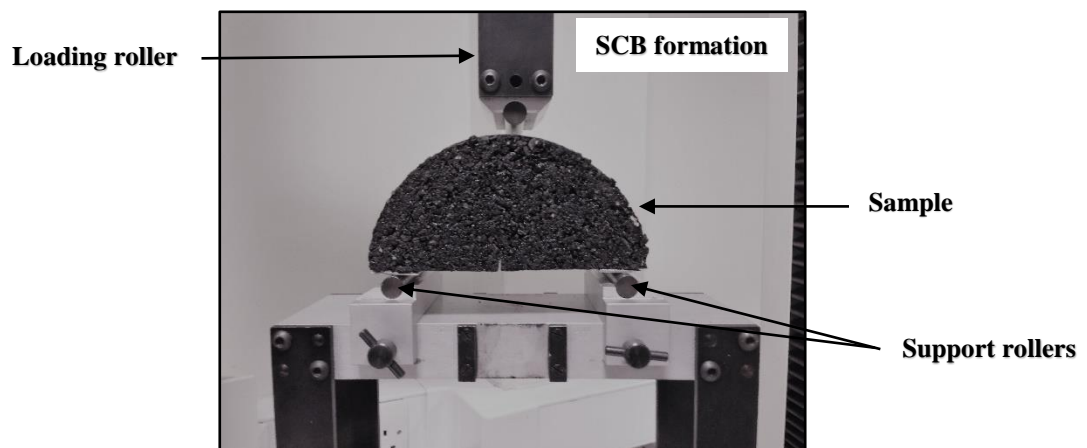


Figure 5-29: Principles of SCBT

Figure 5-30 shows the schematic view of the fracture toughness test using SCB specimens. Parameter (a_0) is the length of the notch crack which was about 10 mm for the prepared specimens. The other geometric parameters are diameter ($D = 2r$) and thickness (t). The fracture toughness SCB test is developed to measure the cracking susceptibility of asphalt (Schapery, 1975). The static SCBT on notched specimens used for determining the fracture toughness of the asphalt has already been used in various research (Molenaar & Molenaar, 2000; Krans et al., 1996; Molenaar, et al., 2002; Hofman et al., 2003;

Mohammad et al., 2004). With this material property, it is possible to calculate the critical load at which a construction with a certain crack length fails. With this parameter, it is also possible to predict the critical crack length at which a construction fails when a specific axle load passes. All static SCB experiments for finding the fracture toughness value were conducted on halved microasphalt core at 5°C. The samples were subjected to a compression load with continuous strain rate of 0.085 mm/s.

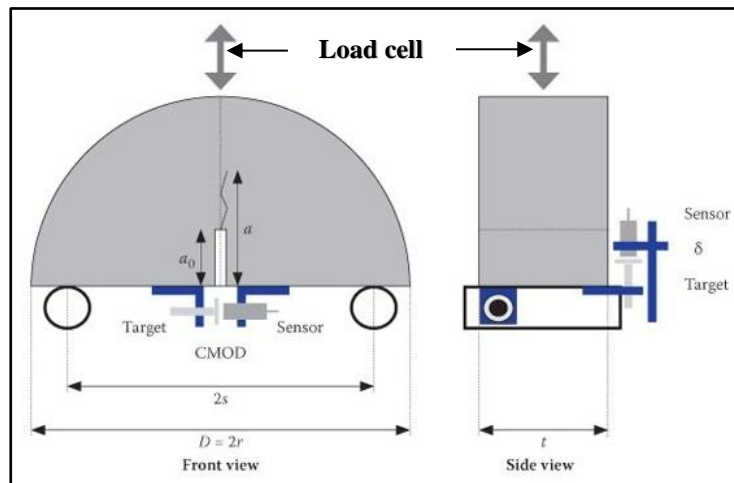


Figure 5-30: Schematic of the experimental setup for SCBT

5.17.2 SAMPLE PREPARATION

Control microasphalt CM mixes were prepared by mixing the Type II gradation aggregates with K1 grade bitumen emulsion. The dry blending method was used in which aggregate and the filler were blended before the emulsion was added. The filler content (OPC) is 1% by total weight of the aggregates in the mix. The optimum bitumen emulsion content (EC) for the control microasphalt was 6.0% by total weight of the mix as explained above in section 5.15. Figure 5-a below (flow chart) illustrates the process for preparation of a sample to testing of a specimen.

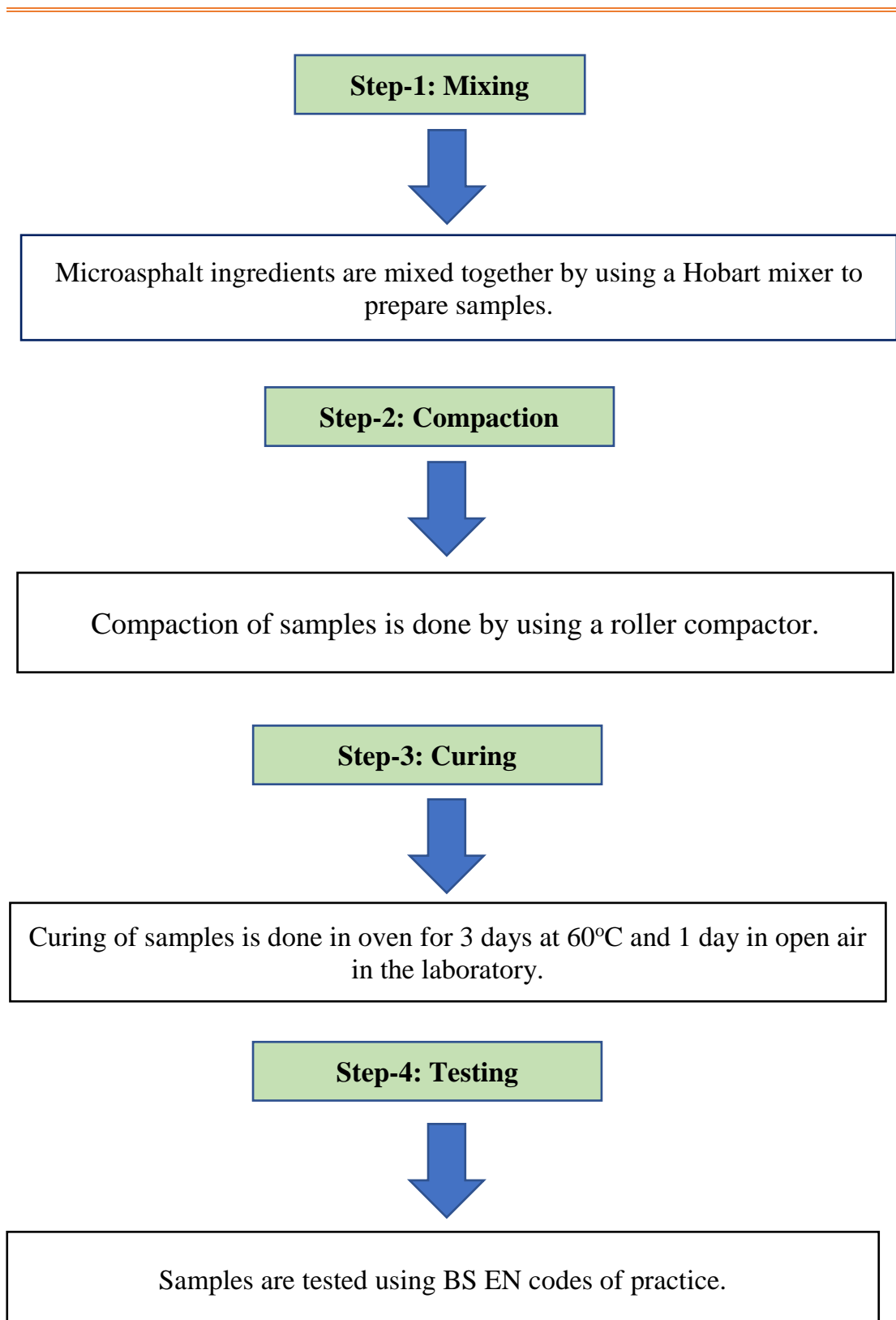


Figure 5-FC: Process for preparation of a sample to testing of a specimen

Glass fibre reinforced microasphalt (GFRM) mixes were prepared by mixing the Type II gradation aggregates with K1 grade bitumen emulsion and glass fibres. The dry blending method was used in which the glass fibres were blended with aggregate and the filler before the binder was added. The filler content (OPC) was 1% by total weight of the aggregates in the mix. The glass fibre content was varied between 0.1%, 0.2%, 0.3%, and 0.4% by total weight of aggregates in the mix. Volume fraction of glass fibres was also taken into consideration. Volume fraction (ϕ_i) is the percentage volume of glass fibres (V_i) divided by the volume of all constituents of the microasphalt in the mix (V_f) prior to mixing and is given by Equation 5-1 (McNaught and Wilkinson, 1997). The glass fibre volume fractions corresponding to the above percentages (0.1%, 0.2%, 0.3%, and 0.4% by total weight of aggregates) were 0.04%, 0.09%, 0.14% and 0.19% respectively in the entire volume.

$$\text{Volume fraction } (\phi_i) = \frac{V_i}{\sum V_f} \times 100 \quad (5-1)$$

The glass fibre length was varied between 6mm, 12.5mm, 16mm, 25mm and blend (i.e. 0.25% of each cut lengths). The aspect ratio of glass fibres in the mix was also taken into consideration. The aspect ratio of glass fibre describes the proportional relationship between its length and its diameter. Aspect ratio of glass fibres is represented by the Equation 5-2 (Rouse, 2005). The glass fibre aspect ratios corresponding to the above lengths (6mm, 12.5mm, 16mm, 25mm and blend) are 75, 156, 200, 312 and 187 respectively in the mix.

$$\text{Aspect ratio (AR)} = \frac{\text{length}}{\text{diameter}} \quad (5-2)$$

The optimum bitumen emulsion content (EC) for the glass fibre reinforced microasphalt mixtures was 7.5% by total weight of the mix as explained above in section 5.15.

Initially, the fibre quantity in the mixture was preserved as a constant parameter with a value equal to 0.2% and iterations made for fibre length

varied between 6mm, 12.5mm, 16mm, 25mm and blend (i.e. 0.25% of each cut lengths) to optimise the fibre length in the GFRM mix. Subsequently, the optimised fibre length in the mixture was preserved as a constant parameter and iterations made for fibre quantities varied between 0.1%, 0.2%, 0.3% and 0.4% to optimise the fibre quantity in the GFRM mix.

CM and GFRM cylindrical samples of nominal 150mm diameter and 100mm thickness were prepared in standard Cooper technology galvanised slotted steel moulds and compacted in the laboratory using hydraulic and roller compactors (see figure 5-31) according to the standards defined in BS EN 12697-33. Specifications of hydraulic standard roller compactor (CRT-RC-H2) are given in table 5-9.

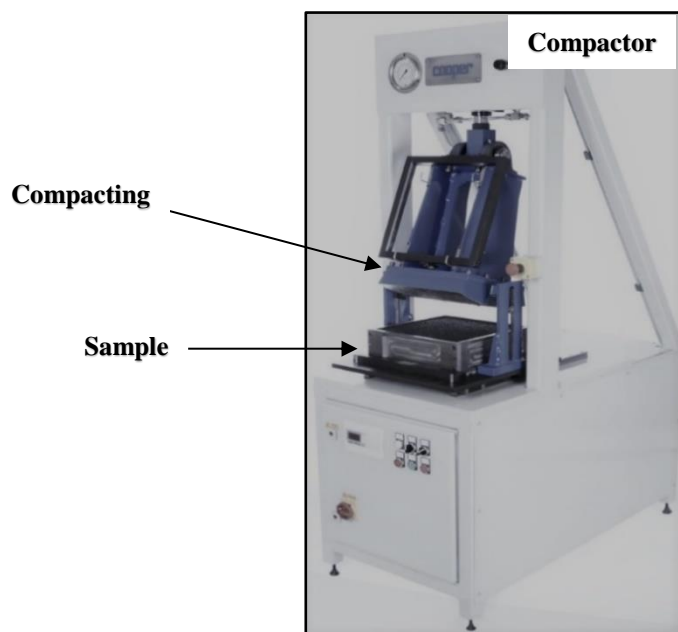


Figure 5-31: Hydraulic standard roller compactor (CRT-RC-H2)

Table 5-9: Specifications of hydraulic standard roller compactor (CRT-RC-H2)

Description	Roller compactor (CRT-RC-H2)
Maximum roller load	30kN over 305 mm roll width
Trolley travel	± 150 mm or ± 200 mm
Speed	Variable up to 10 cycles per minute
Mould thickness	40-135 mm
Electric supply	220-240 volts 50 Hz @ 16A
Working space required mm (WxDxH)	1600 x 1700 x 2000
Estimated weight	270 kg

Each cylinder was then cured in the oven for 3 days at 60°C and 1 day in the open air in the laboratory based on the sample preparation and curing technology described in section 5.16, before cutting it from diametric surface to 150mm to obtain semi-circular samples using a diamond-tip tile cutter (see figure 5-32). Specifications of core and beam saw (CRT-SAW150) are given in table 5-10. These were then smoothly notched at mid-point in the direction of the load again using the diamond-tip tile cutter. The notch length was 10mm to produce a notch to a radius ratio of 0.2 (Molenaar et al., 2002; Huang et al., 2004). Samples were then stored in an incubator at 5°C until test commencement. For each type of mix four samples were prepared for testing.

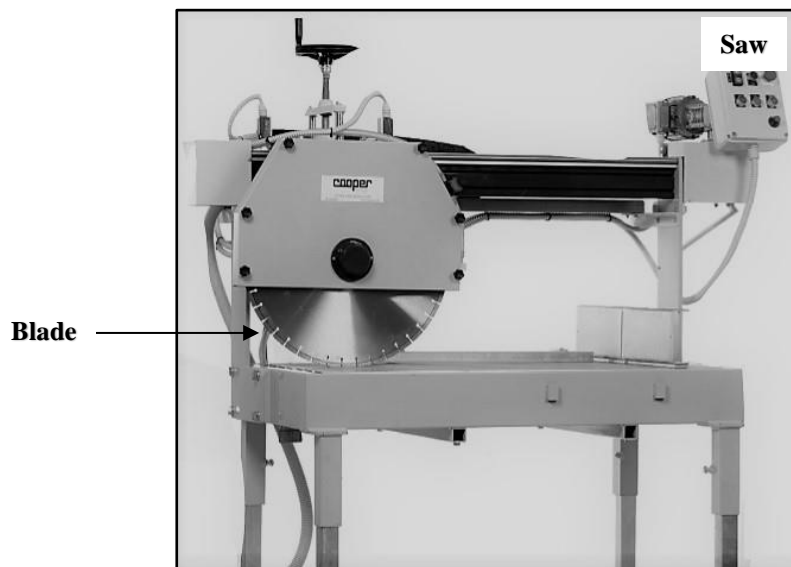


Figure 5-32: Core and beam saw (CRT-SAW150)

Table 5-10: Specifications of Core and beam saw (CRT-SAW150)

Description	Core and beam saw (CRT-SAW150)
Diamond disk	250-350 mm
Depth of cut	150mm max with 450mm blade
Cutting length	750 mm
Water cooled cutting	Yes
Cores up to	150 mm
Speed	2800 rpm
Estimated weight	150 kg
Power	3.75kW

5.17.3 TESTING

SCBT samples were tested for determination of crack propagation using the three-point bending test assembly shown in figure 5-29 above. Samples were tested with fibre lengths of 6.0mm, 12.5mm, 16.0mm, 25mm & blend (i.e. 0.25% of each cut lengths) to investigate optimisation of the length of glass fibre in the mix i.e. to investigate the effect of fibre length in microasphalt mix to resist reflective cracking. Further, fibre quantities of 0.1%, 0.2%, 0.3% & 0.4% by total weight of the dry aggregates in the mix were tested to optimise the quantity of glass fibre in the mix i.e. to probe the effect of fibre quantity in microasphalt to retard fatigue cracking. A core sample for SCB test is shown in figure 5-33 and the test conditions are summarised in table 5-11. Figure 5-34 (a) illustrates the test assembly with a test in progress (notch was set up exactly in line with the loading roller) and figure 5-34 (b) displays the condition of the sample after the test. SCB test results are discussed in chapter 7.

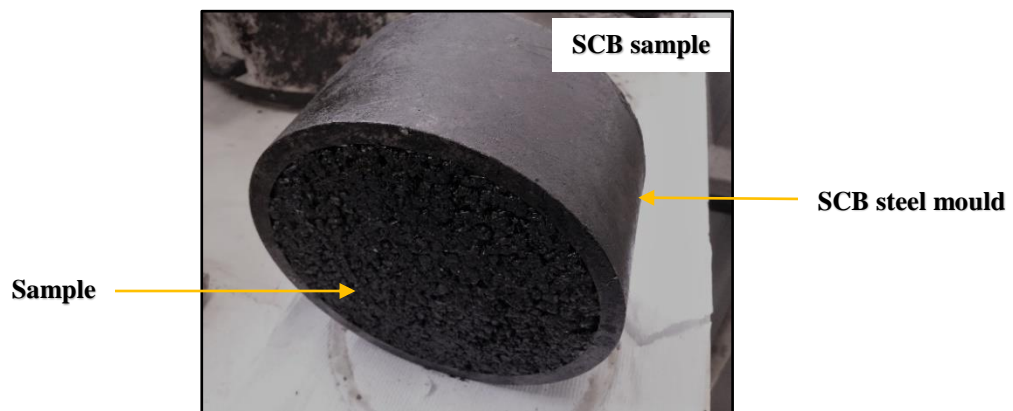


Figure 5-33: Compressed sample for SCB test

Table 5-11: Semi-circular bending test conditions

Item	Range
Sample diameter, (mm)	150
Sample thickness, (mm)	50
Notch length, (mm)	10
Constant load application rate	5 (mm/min)
Test temperature, (°C)	5
Compaction	Hydraulic / roller compactor
Specimen temperature conditioning	4hr before testing

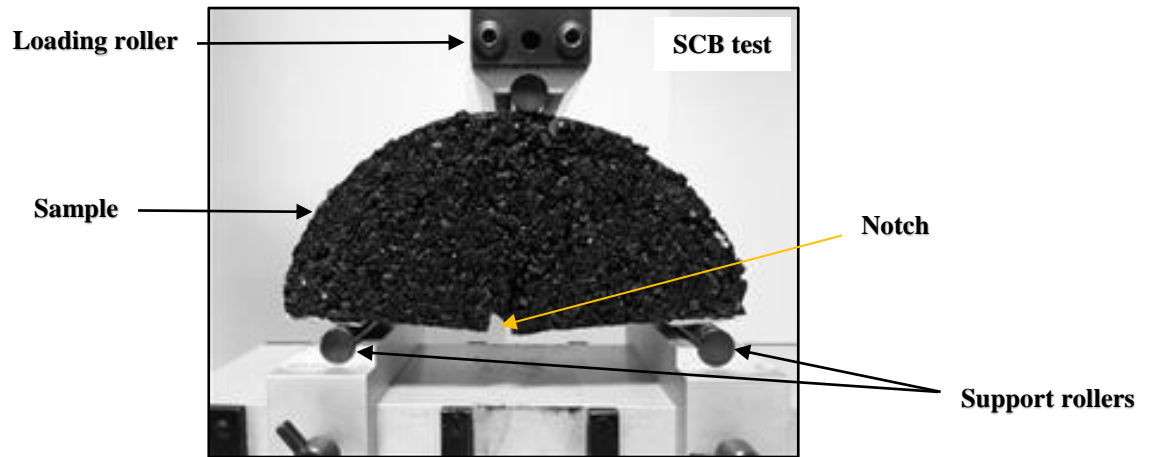


Figure 5-34 (a): SCB test assembly with sample under test

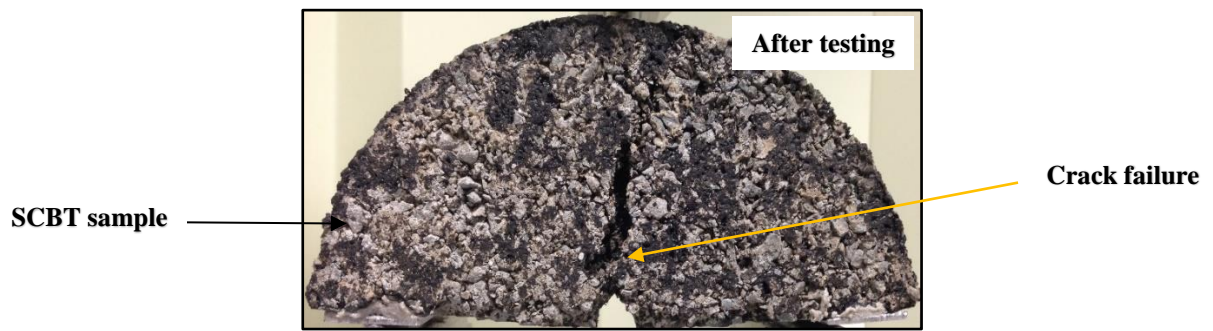


Figure 5-34 (b): Condition of the sample after the test

5.18 LABORATORY TESTING

This presents a laboratory study in which the wheel tracking is used to assess the resistance to rutting of microasphalt under conditions which simulate the effect of traffic. In this test machine, specimens are tested by tracking with a wheel fitted with a pneumatic tyre under specified conditions of load, speed and temperature while the development of the rut profile is monitored at specified intervals during the test. The moulded specimens are inserted and removed from the wheel tracker using an easy-load system.

5.18.1 WHEEL TRACKING TEST PROTOCOL

The rate of rutting of a particular wearing course depends on the temperature of the surface as well as the traffic loading, speed and material properties (Highway Agency, 1999). There has been a significant increase in tyre

pressure in the last 20 years which concentrates the load on the road, and there has been a considerable increase in the use of tri-axle trailers with “super single” tyres, which concentrate the rutting forces into a narrower track (Highway Agency, 1999). A more stringent requirement has become necessary for the design of wearing courses. For this reason, the WTT has been introduced as a requirement for surface courses generally, and for microasphalt in particular (IAN 154, 2012).

The WTT measures the rut potential (RP) by tracking a loaded rubber wheel back and forth across an asphalt sample. By repeating this for thousands of cycles, it simulates the effect of traffic loading on the pavement over time. The device measures the rut depth in the sample continuously during the test according to the standards enshrined in BS EN 12697-22. The principle of the wheel tracking test is to determine the deformation resistance of asphalt samples, as shown in figure 5-35.

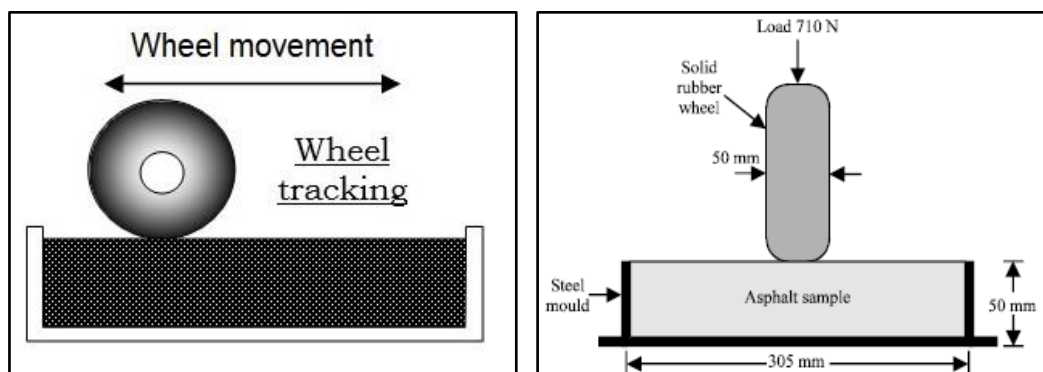


Figure 5-35: Principle of WTT

Rutting of pavements is caused by the passage of heavy or slow-moving vehicles, where after each wheel pass the pavement deflects downwards and then rebounds leaving an irrecoverable downwards deformation, this accumulates and after millions of passes, or sometimes less, a significant rut forms (i.e. >20mm) and the pavement requires rehabilitation (Arnold, 2004).

5.18.2 SAMPLE PREPARATION

CM samples were prepared by mixing the Type II gradation aggregates with K1 grade bitumen emulsion. The dry blending method was used in which aggregate and the filler were blended before the emulsion was added. The filler content (OPC) is 1% by total weight of the aggregates in the mix. The optimum bitumen emulsion content (EC) for control microasphalt was 6.0% by total weight of the mix as explained above in section 5.15.

GFRM samples were prepared by mixing the Type II gradation aggregates with K1 grade bitumen emulsion and glass fibres. The dry blending method was used in which the glass fibres were blended with aggregate and the filler before the binder was added. The filler content (OPC) was 1% by total weight of the aggregates in the mix. The glass fibre content used was 0.2% by total dry weight of aggregates in the mix i.e. the optimised quantity of glass fibres determined from SCB test, while the glass fibre blend (i.e. 0.25% of each cut lengths) i.e. the optimised glass fibre length determined from SCB test was used.

Control microasphalt (CM) and optimised glass fibre reinforced microasphalt (GFRM) slabs of dimensions 400 x 305 x 50mm were prepared in standard Cooper technology galvanised slotted steel moulds using a Hobart mixer; to ensure uniform mixing of microasphalt ingredients (see figures 5-36-1 & 5-36-2) and were subsequently compacted in the laboratory using a roller compactor. The Roller compactor details and specifications have been provided above in the figure 5-30 and in table 5-8. Slabs in moulds were later cured at 60°C in the oven for 3 days and 1 day in the open air based on the sample preparation and curing technology discussed above in this chapter at section 5.16. For each type of mix three samples were prepared for testing.

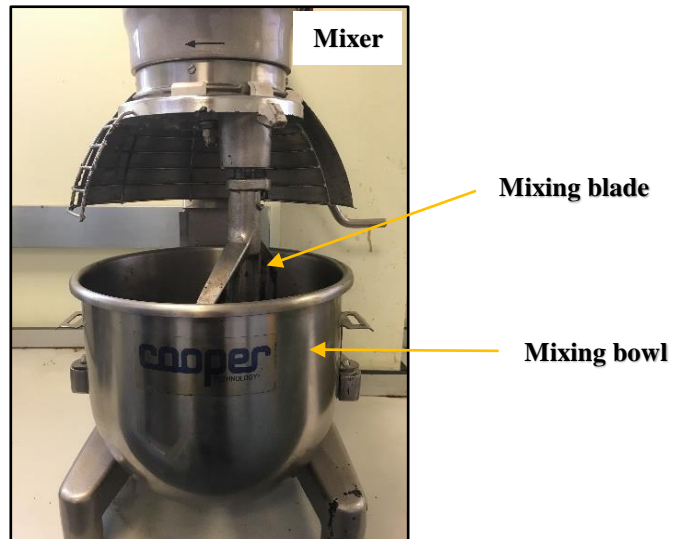


Figure 5-36-1: Hobart mixer

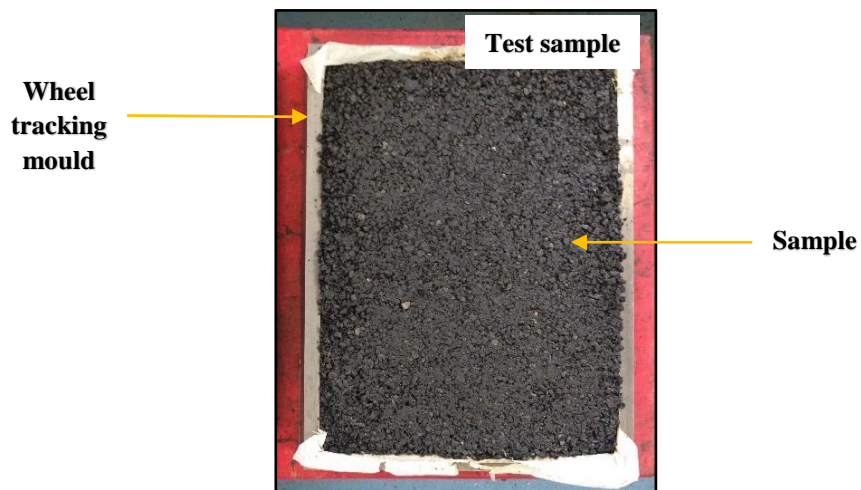


Figure 5-36-2: Wheel tracking test sample

5.18.3 TESTING

WTT samples were tested for deformation using the automatic wheel tracking tester (HYCZ-5) machine shown in figure 5-37. Sample to be tested was placed in the test chamber and wheel load was applied to ensure that the tyre makes full contact with the specimen. Temperature in the incubator was maintained at 45°C and the displacement sensor was adjusted so that the displacement value displayed is within 3mm - 5mm range and sensor was accordingly locked.

The WT operation mechanism is shown in schematic figure 5-38 (BACTIA, HYCZ-5, Operation Manual, 2013). The test conditions for wheel tracking sample testing are given in table 5-12. The photograph in figure 5-39 shows a wheel tracking sample testing during test, and figure 5-40 displays the condition of the sample after the completion of the WT test.

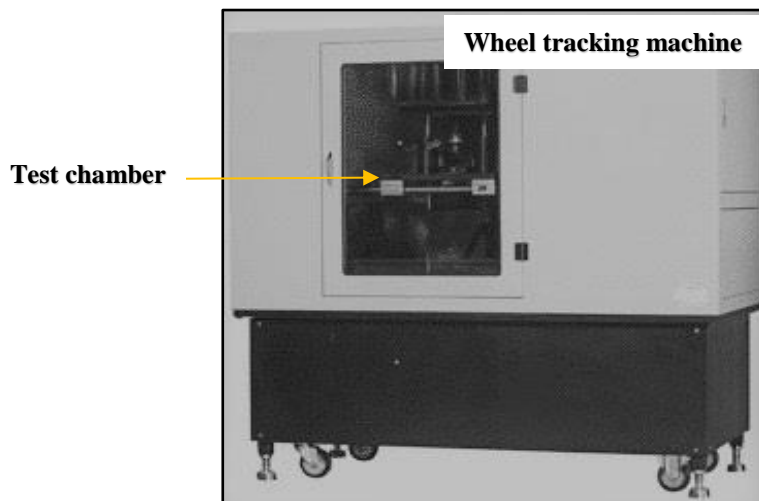


Figure 5-37: Automatic wheel tracking tester (HYCZ-5)

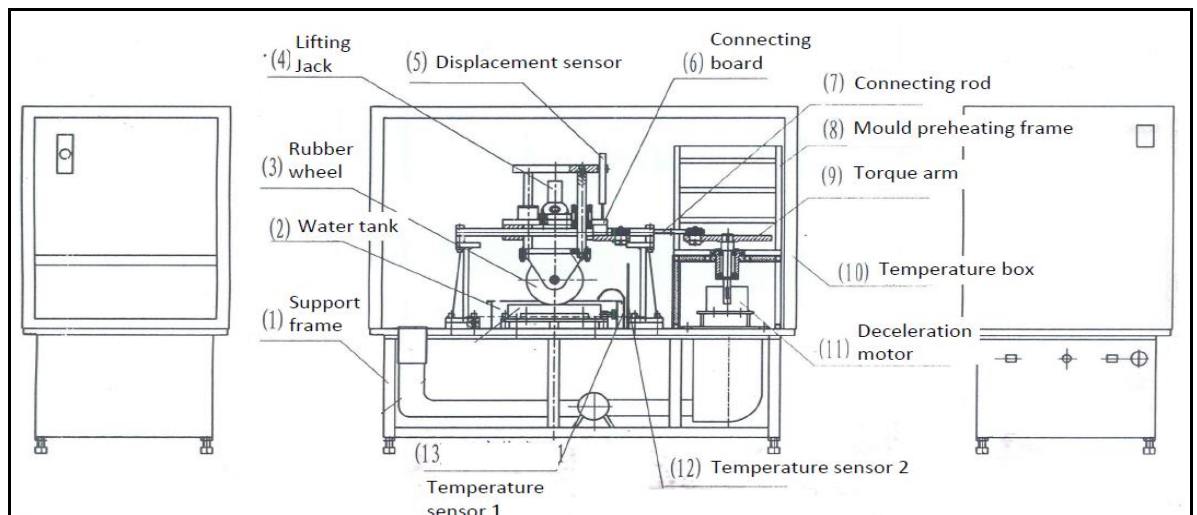


Figure 5-38: Schematic of the experimental setup for wheel tracking test (BACTIA, HYCZ-5, Operation Manual, 2013)

Table 5-12: Wheel tracking test conditions

Item	Range
Tire of outside diameter, (mm)	200-205
Tire width, (mm)	50 ± 5
Trolley travel distance, (mm)	230 ± 10
Trolley travel speed, (s/min)	42 ± 1
Wheel load	710 N
No. of conditioning cycles	5
No. of test passes	10,000
Test temperature, (°C)	45
Compaction	Roller compactor
Specimen temperature conditioning	4hr before testing

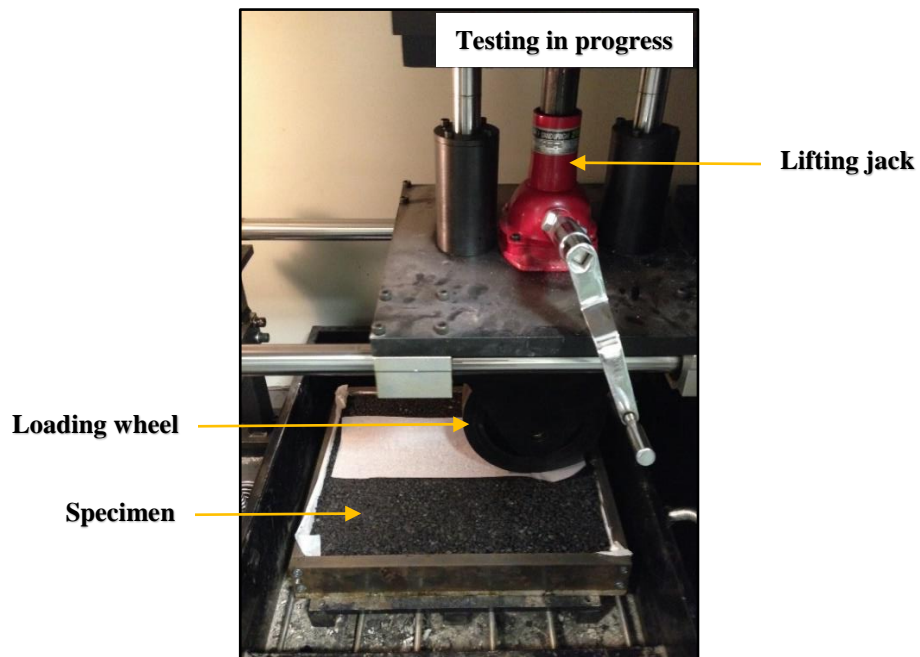


Figure 5-39: Wheel tracking test in progress

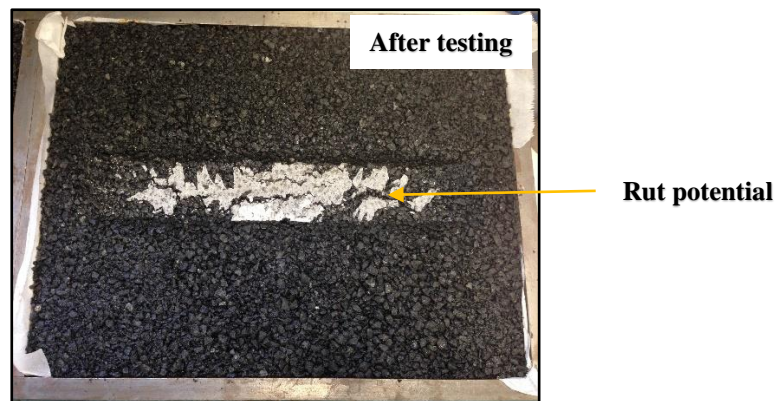


Figure 5-40: Condition of the sample after the test

5.19 REPLACEMENT OF A CONVENTIONAL FILLER

OPC has been used extensively in improving the mechanical properties of CBEM. A significant improvement was reported by several researchers when extra OPC was added and the CBEMs were in full curing. But a question arises: has all OPC potential for improving CBEMs' performance been explored in previous research works, or is there any possibility to develop further the current practice of using supplementary cementitious materials (SCMs) in microasphalt? This section presents a new novel technique to incorporate by-product material for further development in cement modified microasphalt.

Currently in the production of OPC the limestone and clay are heated to an elevated temperature of 1,100-1,700°C and with each tonne producing a similar amount of CO₂ with global emissions of 1800 Mt CO₂ per annum (Andrew, 2017). Cement produced worldwide at a volume of 6,000 Mm³ annually with a value in the order of \$450,000M employs more than 100 million people. Therefore, its environmental impact is a matter of huge concern to scientists at a global level and cannot be ignored.

5.20 FILLER AND FILLER SUPPLEMENTARY APPROACH TO ENHANCE MICROASPHALT

Waste or by-product materials have been widely used as supplementary cementitious materials SCMs, as a partial replacement for OPC in concrete and CMA construction materials (Al-Nageim et al., 2012; Shakir, 2012; Abbas, 2014). Some of them have proven successful up to a certain percentage of replacement. In this section, selected waste or by-product materials are investigated as an alternative to OPC.

Although OPC alone or with an activator has proven successful in improving curing time and mechanical properties of cold mix asphalt, the successful use of waste or by-product alternatives could represent a unique environmental and economic achievement. Thus, for the first time, these materials were selected exclusively as a supplementary cementitious material for improving the curing and strength of microasphalt.

Filler is defined as an aggregate, most of which passes a 0.063 mm sieve, which can be added to construction materials to provide certain properties (BSI, 2002). Filler can be active or inert. Active filler is filler that produces hydration in the presence of water, while inert filler does not. Inert filler is added to bituminous mixture to complete the mixture skeleton and finalise aggregate gradation requirements, while active filler addition is for further roles such as enhancing moisture sensitivity of the mix. Incorporating active fillers in CBEM has shown a highly significant improvement in the mechanical properties of CBEM. OPC has been used widely, and has proved its validity among other active fillers such as lime and calcium chloride (Needham, 1996). On the other hand, efforts were recently made to investigate the suitability of incorporating waste or by-product materials as SCM for OPC. Incorporating such materials could gain environmental benefits in term of reducing CO₂ emission, minimizing the impact on landfills, enhancing mechanical and durability properties of concrete products, and of course providing economic benefits (Khatri et al., 1995; Papadakis and Tsimas, 2002; Lothenbach et al., 2011). Recently, a wide range of materials have been proven to be successful SCMs, such as pulverised fuel ash (PFA) (combustion residue of coal), granulated ground blast furnace slag (GGBFS) (by-product of steel industry) and silica fume (SF) (by-product of silicon metal or ferrosilicon alloys production). However, SF has been proven to be the most suitable SCM amongst this group (Khatri et al., 1995; Papadakis and Tsimas, 2002; Lothenbach et al., 2011).

According to SCMs' reactivity properties, they can be classified in to two groups:

- a) Pozzolanic: materials that gain no strength when blended alone with water, such as SF, and low calcium PFA.
- b) Cementitious: materials that gain strength when blended alone with water, such as GGBFS, and high calcium PFA.

In this section, the suitability of incorporating waste filler in the microasphalt mix was investigated. The premise was to produce a high performance microasphalt by

incorporating by-product material, and to introduce further development to cement modified microasphalt.

5.21 ALTERNATIVES: WASTE AND BY-PRODUCT ACTIVE FILLERS

As mentioned previously, replacing filler in CBEMs approach was adopted in this section to upgrade microasphalt. The developed cement-modified microasphalt offered a reasonable reduction in environmental and economic impact in contrast to control microasphalt. However, OPC production always seems to be associated with significant CO₂ emission. For this reason, the author decided to study the potential of using waste and by-product materials as a replacement for OPC in microasphalt. Waste and by-product materials, which initiate massive impact on landfills, are available in huge quantities and their uses provide social, economic, and environment benefits.

The use of waste and by-product materials as replacements for OPC in microasphalt start with finding the answer to the question “What is unique in OPC to enhance microasphalt and is it available in waste and by-product materials with or without some sort of upgrading to their chemical and physical properties?”. Of course, the cementitious characteristics is the main answer, but not the unique answer; because the improvement in curing time and strength depends on removing trapped water besides creating secondary binders. Thus, both the cementitious and absorption characteristics are essential properties to enhance microasphalt.

Filler materials can be pozzolanic or cementitious as mentioned above, and can have various characteristics. Thus, waste or by-product filler were selected to examine their validity for improving microasphalt. Their selection was dependent on their cementitious and other characteristics, plus of course their availability in the UK and worldwide.

Therefore, the central theme here concerns the use of a novel filler to reduce CO₂ emissions. The new filler to be used is ash residue resulting from the waste fly ash (FA). Annually, millions of tons of such waste filler are generated in the United Kingdom and worldwide. Approximately, 70% of this waste type is used in

construction and agricultural sectors, while the remainder is sent to landfill (Shakir, 2012 and Monower, 2012). Incorporation of the said waste product in the highways pavement industry can minimize the impact to landfill because it can accommodate all the quantities currently produced. Also, an economic benefit can be gained from this material because hitherto it has been regarded as waste.

The cementitious filler to be produced is a green cement that can be used in cold mix microasphalt. Its main candidate ingredients are namely;

1. Paper sludge ash (PSA)
2. Cement kiln dust (CKD)
3. Rice husk ash (RHA)

These materials were previously sent to the landfill as a waste material but are now treated and converted into a raw material i.e. ground to a fine, dry powder form. Figure 5-41 shows samples of candidate fillers.

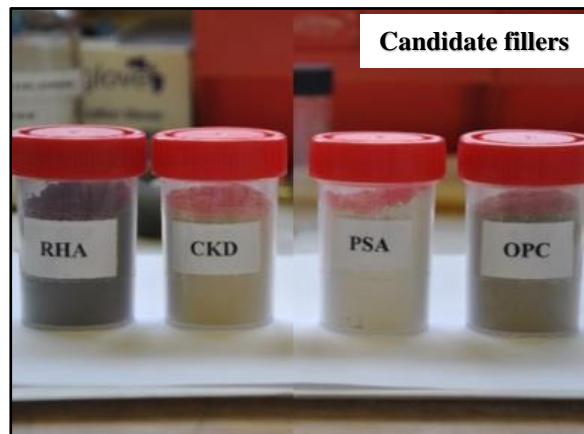


Figure 5-41: Conventional filler OPC and new candidate fillers PSA, CKD & RHA

Thus, this section primarily seeks to open a new development on replacement of conventional filler i.e. OPC by using waste raw material in a useful cementitious material for producing cement namely; (GCF) with zero CO₂ emission to combat the contribution of cement to adverse global emissions.

5.22 BENEFITS OF CEMENTITIOUS FILLER

The new secondary filler (SF) namely; green cement filler (GCF) has the following benefits:

- a) Initial direct savings on the cost of the recycled waste filler. It is available almost free of cost in the market i.e. it has a zero cost as compared to the conventional OPC filler. Secondary filler is all available from the paper and construction industry and agricultural sites. However, cost may rise when the waste product is found to be useful.
- b) The avoidance of landfill tax on the waste material of new filler. Currently it is £3 per tonne for inert materials and £86 per tonne for non-inert materials (LFT, 2017).
- c) The avoidance of the climate change levy (CCL) applied to the production of primary filler (PF) OPC due to CO₂ emissions while GCF has zero CO₂ emission. The use of new zero CO₂ emission filler also complies with the government strategy for sustainable construction (SSC, 2008).

The construction of our built environment has important economic effects, on the rate at which we use resources. Roads and buildings are responsible for almost half of the country's carbon emissions, half of our water consumption, about one third of landfill waste and one quarter of all raw materials used in the economy therefore, construction plays a central role in our drive to promote sustainable growth and development.

5.23 CHARACTERISATION OF OPC

Cement is any material which, if added in a suitable form to a non-coherent assemblage of particles, will subsequently harden by physical or chemical means and bind the particles into a coherent mass (O'Flaherty, 2007). Although bitumen, tar and lime can be defined as "cements", this term is almost always associated with Portland and such kind of fine powder cements, which, in the presence of water process a "hydration". Hydration generally produces hydration products which, after setting and

hardening, are very strong and durable binders. The most well-known type of cement is Ordinary Portland cement, which provides 95% of cement used in construction (Domone and Illston, 2010).

OPC is manufactured by heating a mixture of limestone and clay, or other materials of similar bulk constitution and appropriate reactivity, to nearly 1450°C, where materials are partially fused and result in clinker. Finally, the clinker is mixed with 3-5% of gypsum and finely ground (Taylor, 1997). The produced powder is typically grey, with a relative density of about 3.14 kg/m³; particle sizes between 2-80µm, and specific surface area of 300-500m²/kg.

OPC is formed from a number of oxides produced due to high temperature in the burning zone. Among these oxides, the four listed in table 5-13 are the most important in characterising the cement properties. These components or “Phases” are hydrated with time in the presence of water. C₃S or “Alite” constitutes 50-70% of the OPC. It reacts very quickly compared to other phases, whereas most of the development in early strength is a result of C₃S hydration. C₂S or “Belite” forms 15-30% of the OPC; its reactivity is slow, but most of the strength after 28 days results from its hydration. C₃A constitutes 5-10% of the OPC, and it reacts very quickly, so gypsum is added to control C₃A rapid setting. Finally, C₄AF represents 5-15% of the OPC; its reactivity is variable, but generally it is initially high, then releases with age. OPC for this study was supplied by Lafarge, UK.

Table 5-13: Most important oxides of cement (Domone and Illston, 2010)

Oxide name	Chemical composition	Abbreviation
Tricalcium silicate	3CaO.SiO ₂	C ₃ S
Dicalcium silicate	2CaO.SiO ₂	C ₂ S
Tricalcium aluminate	3CaO.Al ₂ O ₃	C ₃ A
Tetracalcium aluminoferrite	4CaO.Al ₂ O ₃ .Fe ₂ O ₃	C ₄ AF

5.24 CHARACTERISATION OF PSA

PSA is a residue which results from the incineration of paper sludge and other input materials during the recycling of newspaper and similar products. The incineration is a unique process to minimize the volume of landfill materials (normally it reaches 13% of the original volume); simultaneously energy recovery is effected to produce

electricity or heat (Koshikawa and Isogai, 2004). Paper sludge comprises organic fibres, inorganic clay-sized materials, and about 60% water; after incineration at 800°-1150°C, fusion occurs between the calcium, aluminium and silicon components, accordingly mullite ($\text{Al}_2\text{O}_3 \cdot 4/3\text{SiO}_2$), cristobalite (SiO_2), or calcium silicate (CaSiO_3) are formed, depending on the incineration temperature (Koshikawa and Isogai, 2004). Annually, 8 and 2 million tonnes of paper sludge result as waste in the USA and the UK, respectively (Wajima et al., 2006). Paper sludge has limited uses mainly due to high moisture content, but conversion to PSA allows multi uses in construction materials and agriculture. In the UK, 70% is utilised, while 30% is landfilled (Environment Agency, 2008). It is recommended that PSA should not replace more than 10% of OPC (Fava et al., 2011); this is due to the high fineness and high water absorption properties of PSA, resulting in the requirement for a high water cement ratio. PSA for this study was supplied by Aylesford Newsprint Mill Limited, UK where the paper sludge is burned to generate heat to produce energy. The PSA is collected from the incinerator flue (Environmental Agency, 2008).

5.25 CHARACTERISATION OF CKD

Cement kiln dust (CKD) is a by-product of the cement manufacturing process and is a fine, powdery material, portions of which contain some reactive calcium oxide, depending on the location within the dust collection system, the type of operation, the dust collection facility, and the type of fuel used (Konsta-Gdoutos & Shah, 2003). CKD consists of four major components: unreacted raw feed, partially calcined feed and clinker dust, free lime, and enriched salts of alkali sulfates, halides, and other volatile compounds (Detwiler et al., 1996).

The relatively high alkaline content of CKD is the predominant factor preventing its recycling in cement manufacturing. One effective way to utilize CKD is to use it in the production of blended cements (Konsta-Gdoutos & Shah, 2003). However, research has been sporadic regarding the applicability of CKD as such an activator in CMA. Past research of blended cements containing CKD as a partial replacement of cement and ground granulated blast-furnace slag and/or fly ash has produced results that are variable (Konsta-Gdoutos & Shah, 2003).

CKD can be used with fly ash and ground granulated blast furnace slag up to 15% by mass of cementitious material and in ground granulated blast furnace slag cements up to 10% by mass of cementitious material (Detwiler et al., 1996).

The following advantages are realized resulting from the addition of CKD along with fly ash and blast furnace slag to Portland cement:

- a. Decreased initial and final setting times
- b. Increased strengths
- c. Pore refinement

CKD, when used alone as a secondary cementitious material, may result in decreased workability, setting times, and strength due to high alkali content. When using CKD with high alkali content, fly ash or blast furnace slag should be incorporated to prevent alkali-silica reaction problems (Walters & Jones, 1991; and Kelham et al., 1995). CKD can be used as the alkali activator with silicon rich material, to produce a cement replacement. CKD for this study was supplied by Cemex, UK.

5.26 CHARACTERISATION OF RHA

The rice milling industry generates a lot of rice husk during the milling of paddy which comes from the fields. This rice husk is mostly used as a fuel in the boilers for processing of paddy. Rice husk is also used as a fuel for power generation. Rice husk ash (RHA) is about 25% by weight of rice husk when burnt in boilers (Siddique, 2008). It is estimated that about 70 million tons of RHA is produced annually worldwide. This RHA is a great environment threat causing damage to the land and the surrounding area in which it is dumped.

During milling of paddy about 78% of weight is received as rice, broken rice and bran. The remainder, approximately 22% of the weight of paddy, is received as husk. This husk is used as fuel in the rice mills to generate steam for the parboiling process. This husk contains about 75% organic volatile matter and the balance of the weight of this husk is converted into ash during the firing process, is known as rice husk ash. This

RHA in turn contains high volumes of amorphous silica (Sivakumar & Manikandan, 2014).

RHA is a carbon neutral green product. Many potential economic and commercial uses are being investigated. RHA is a good super-pozzolan. This super-pozzolan can be used to make special concrete mixes. There is a growing demand for fine amorphous silica in the production of special cement and concrete mixes, high performance concrete, high strength, low permeability concrete, for use in bridges, marine environments, nuclear power plants etc. The market is currently filled by silica fume or micro silica, being imported from Norway, China and from Myanmar. Due to limited supply of silica fumes and the demand being high the price of silica fume has risen to as much as \$500/ton approximately (Hasan et al., 2016).

Research on ash from burning of rice husks has already demonstrated that it is one of the most promising supplementary cementing materials (SCM), given its high specific surface and great amount of silica soluble in alkaline conditions. Most of the published work has exploited the effectiveness of RHA of very high specific surface and reactive silica, without really investigating the effect of these factors with respect to mechanical and durability characteristics of the derived cement and concrete (Antiohos et al., 2014). RHA is a material which is extremely “sensitive” to fineness changes; the higher the fineness the more positive is the effect of RHA inclusion in CMA. Not surprisingly, active silica holds a key role especially for later-age strength gain, indicating that pozzolanic effect takes over from the “physical” effect of the pozzolan as hydration evolves (Antiohos et al., 2014). Pozzolanic potential, strength development of mortars and concrete and resistance against chloride penetration reveal the importance of the secondary action of RHA in producing competitive blended cement (Antiohos et al., 2014). This can resist the chloride action by reducing the rate of transfer and thus increases the quality of the cement making it competitive in the market.

Rice husk (RH) is an agricultural waste and abundantly available in rice producing countries like China, India, Bangladesh, Brazil, US, Cambodia, Vietnam, Myanmar, and South-East Asia. Despite the massive amount of annual production worldwide, so

far RHs have been recycled only for low-value applications. In recent years, many rice mills in rice producing countries have started using RH for the energy production for mill operations as well as household lighting in rural regions. Burning of RHs produces the rice husk ash. The disposal in landfills or open fields can be problematic and may cause a serious environmental and human health related problems due to the low bulk density of RHA. Rice husk ash for this study was supplied by Singhania Enterprises, India.

5.27 MICROSTRUCTURE CHARACTERISATION OF ACTIVE FILLERS

Detailed investigation was achieved to characterise the chemical and physical properties of the selected waste active fillers by adopting the test methods below. The main aim was to identify the similarity to OPC, and to investigate their behaviour in microasphalt.

5.28 EXPERIMENTAL SETUP

The following test methods were used to characterise the selected waste active filler:

5.28.1 PH

The pH of the fillers was measured using a Beckman Coulter pH meter model P/N 123141. A suspension of water with 3% filler content was prepared and tested at lab temperature, i.e. 20°C. A buffer solution was used for calibration before the measurement. The results obtained are presented in section 6.6, subsection 6.6.7, table 6-5 (chemical and physical characteristics of selected fillers) in chapter 6.

5.28.2 XRF ANALYSIS OF NEW CEMENTITIOUS FILLER

In section 5.13, x-ray fluorescence (XRF) and its use within the context of this research has been explained. In this section, the procedure for XRF analysis is

discussed in detail. XRF analysis was done to probe the chemical composition of candidate fillers as per the specifications stipulated in BS ISO 29581-2:2010 standards.

The elemental composition of materials (major oxides and trace elements) were analysed using a Shimadzu EDX 720, energy dispersive x-ray fluorescence spectrometer. This apparatus performs qualitative and quantitative elemental analysis and is ideal for non-destructive applications. Chemical composition by XRF analysis, with calculation of Ca/Si oxides ratio, and sum of Al, Fe and Si oxides were determined.

During the x-ray fluorescence (XRF) test, the waste sample fillers are excited by bombarding with high energy x-rays and thus characteristic fluorescent x-rays are emitted by them. This phenomenon is widely used for elemental analysis and chemical analysis of materials for research into pavement materials geochemistry.

Figure 5-42 shows the XRF machine (a), candidate sample pellets placed in the XRF chamber (b).

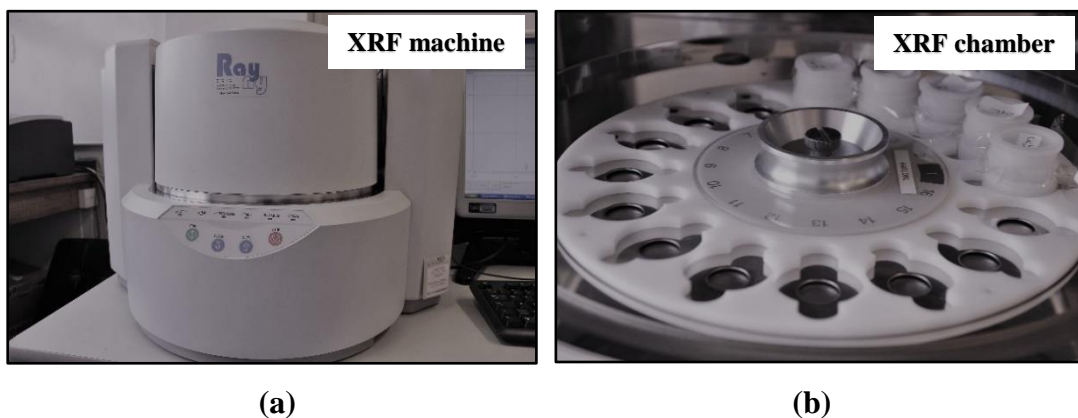


Figure 5-42: XRF analysis of candidate fillers

Each of the elements present in the sample fillers produces a set of characteristic fluorescent x-rays (a fingerprint) that is unique for that specific element. This technology enables the XRF spectroscopy to carry out the

qualitative and quantitative analysis for the fillers i.e. to determine its chemical composition. The results obtained are presented and discussed in section 6.6, sub-section 6.6.1-4, sub-section 6.6.7, and table 6-5 (chemical and physical characteristics of selected fillers) in chapter 6.

5.28.3 SPECIFIC SURFACE AREA

The specific surface area of the fillers was determined following the model of Brunauer, Emmett and Teller (BET) method (BS ISO 9277, 2010). The specific surface area is estimated from the quantity of nitrogen adsorbed in relation to pressure, at the boiling temperature of liquid nitrogen under normal atmospheric pressure. The test was conducted using the NOVA 2000 model equipment, figure 5-43 (a). To perform the test, candidate samples were collected in test tubes as shown in figure 5-43 (b). Results have been provided in section 6.6, sub-section 6.6.7, and table 6-5 (chemical and physical characteristics of selected fillers) in chapter 6.



Figure 5-43 (a): Surface area apparatus



Figure 5-43 (b): Samples in the test tubes

5.28.4 PARTICLE SIZE CHARACTERISTICS

The Beckmen Coulter laser diffraction particle size analyser, figure 5-44, was used to determine the grain size distribution of filler materials. Beckmen Coulter LS 13 320 utilizes reverse Fourier optics incorporated in a patented fibre optic spatial filter system and a binocular lens system. Results are discussed in section 6.6, sub-section 6.6.7, and table 6-5 (chemical and physical characteristics of selected fillers) in chapter 6.

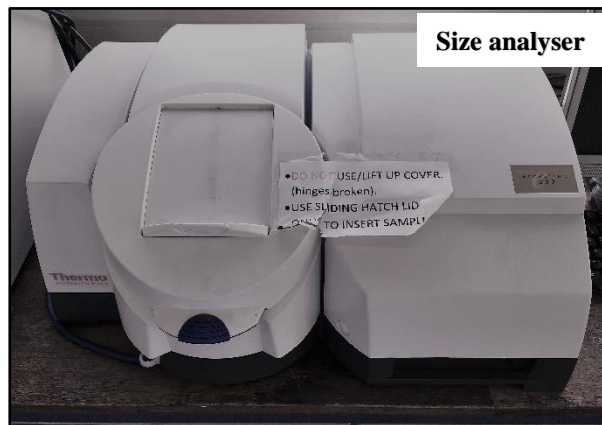


Figure 5-44: Particle size analyser

5.28.5 SEM ANALYSIS OF NEW CEMENTITIOUS FILLER

In continuation of the SEM definition explained in section 5.13, a detailed and encompassing procedure for SEM analysis is explained in this section. SEM

analysis was done to examine the surface topography and characteristics of candidate fillers according to the specifications enshrined in BS ISO 16700: 2016 standards.

In morphological analysis, SEM applies a focused beam of high-energy electrons to create a variety of signals at the surface of solid test specimens. The signals that arise from electron-sample interactions disclose information about the sample, including external morphology (texture), chemical composition, crystalline structure and orientation of materials making up the sample. SEM analysis was operated under the following conditions: resolution of 3-4 nm; high vacuum and test voltage 12.5-20 kV. The SEM was also equipped with an energy-dispersive spectroscopy (EDS) containing Oxford Inca x-act detector with a probe current 45nA and counting time of 100 sec.

During the scan electron microscopy (SEM) test, characteristic x-rays are produced for each element in the waste filler that is excited by the electron beam. Principally, electrons are either reflected (scattered) or absorbed. In fact secondary electrons (SE), backscattered electrons (BSE), x-rays (X), auger electrons (AE) and other responses are produced (Ramachandran and Beaudoin, 2001). These allow various modes of observation and microanalysis of new cementitious fillers. Figure 5-45-1 below illustrates the SEM principle. SEM is the most common observation mode, which includes the capture of secondary and backscattered electrons. SEM analysis is non-destructive, and x-rays generated by electron interactions do not lead to volume loss of the sample. It is also possible to analyse the same sample repeatedly.

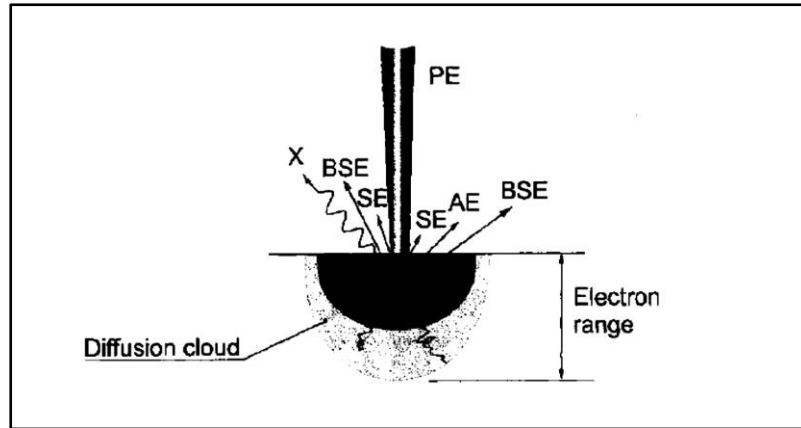


Figure 5-45-1: Different interactions of an electron beam with a solid target (Ramachandran and Beaudoin, 2001)

Figure 5-45-2 shows the SEM machine (a), test samples mounted on the stubs (b), high vacuum chamber (c) to coat the samples with gold to protect them from moisture contact and ensure they are dry before being placed in the SEM compartment (d) for the test.

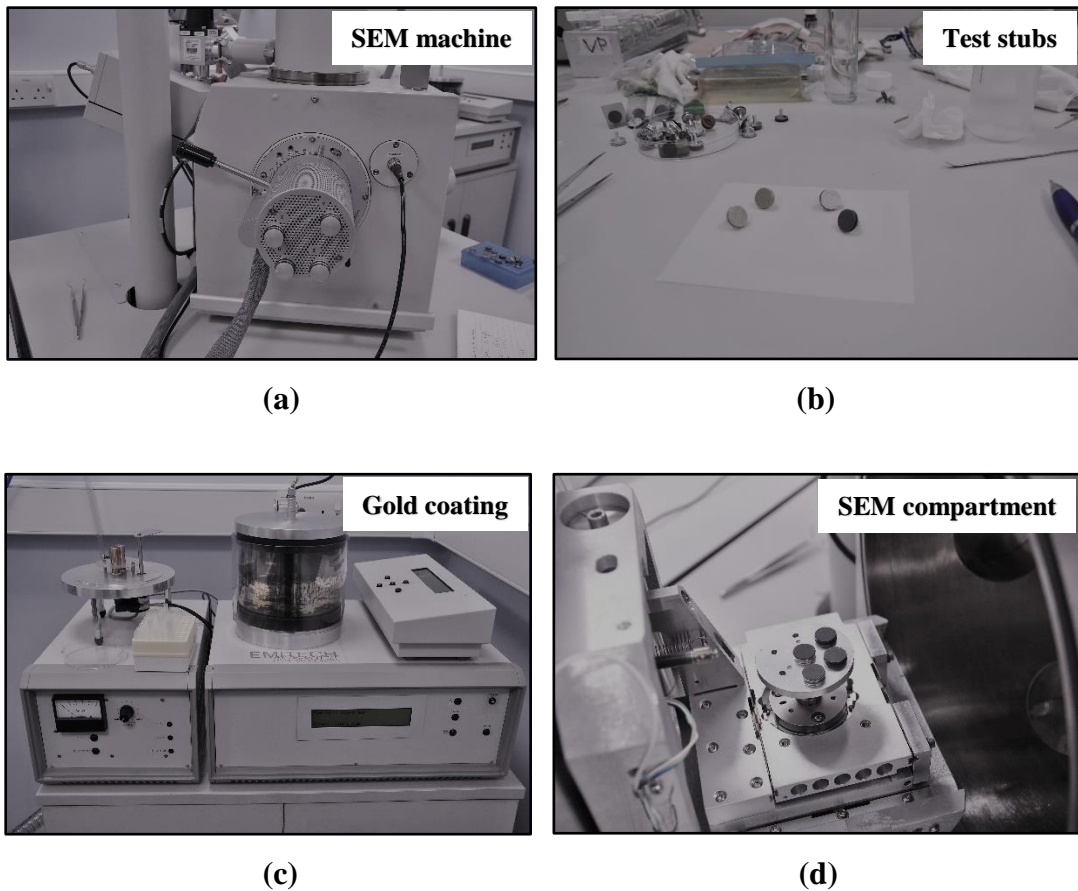


Figure 5-45-2: SEM analysis of candidate fillers

Data is collected over a selected area of the surface of the candidate samples and a 2-dimensional image is generated that displays spatial variations in these properties. Areas ranging from approximately 1 cm to 5 microns in width can be imaged in a scanning mode with magnification ranging from 20x to approximately 30000x, and spatial resolution of 50 to 100 nm. Test results have been analysed in section 6.6, and sub-sections 6.6.8-12 in the succeeding chapter 6.

5.28.6 DENSITY

Density of the fillers was evaluated according to BS EN 1097-7 (BSI, 2008) by means of a pycnometer. Density is calculated as the volume of irregularly formed samples (determined by replacing a certain amount of liquid of known density with the test portion) over a known sample mass. Density is required for volumetric analysis of mixes. Test results are presented in section 6.6, sub-section 6.6.7, and table 6-5 (chemical and physical characteristics of selected fillers) in chapter 6.

5.29 EVALUATION OF SCB AND WT TESTS USING FINITE ELEMENT MODELLING

In this section, an experimental evaluation of the SCB test and WT test is conducted using computer aided engineering (CAE) tool; i) to identify the main failure mechanisms during the SCB testing process; ii) to study the damage propagation in the SCB test for the CM, 0.2% GFRM blend and GCF - 0.2% GFRM blend mixes and iii) to study the deformation distress during the WT test process for the CM, 0.2% GFRM blend and GCF - 0.2% GFRM blend mixes and validated by the laboratory findings achieved in the SCBT and WTT. An elementary finite element (FE) modelling approach has been used to simulate the SCB and WT tests process.

Three CMM mixtures were tested for FE modelling, CM, 0.2% GFRM blend and GCF - 0.2% GFRM blend with the parameter i.e. Poisson's ratio (ν) of 0.38, 0.34 and 0.27 respectively. The value of (ν) reduces with the addition of glass fibres and with the replacement of OPC with GCF correspondingly for the 0.2% GFRM blend and GCF

- 0.2% GFRM blends. This is due to the fact that the glass fibres and GCF enhance the strength of the microasphalt mix enhancing the strain resistance of the 0.2% GFRM blend and GCF - 0.2% GFRM blend as compared to the CM. Thus, the more strength the microasphalt has, thenmore it will withstand the applied force, i.e. it will deform less and this would result in less lateral strain and therefore, the value of (ν) will reduce.

5.29.1 DETERMINATION OF PARAMETER FOR FINITE ELEMENT MODELLING

Based on the work of Islam et al. (2015), the author calculated the Poisson's ratio (ν) for the CM, 0.2% GFRM blend and GCF - 0.2% GFRM blend mixes based on the results of a relaxation test. The procedure for preparation of the test samples and setup for the relaxation test is discussed in detail below. Poisson's ratio is a measure of the Poisson effect, the phenomenon in which a material tends to expand in directions perpendicular to the direction of compression (Greaves et al., 2011). The lateral and longitudinal strain principle is illustrated in figure 5-46 and Poisson's ratio is determined with the help of an Equation 5-3 given below.

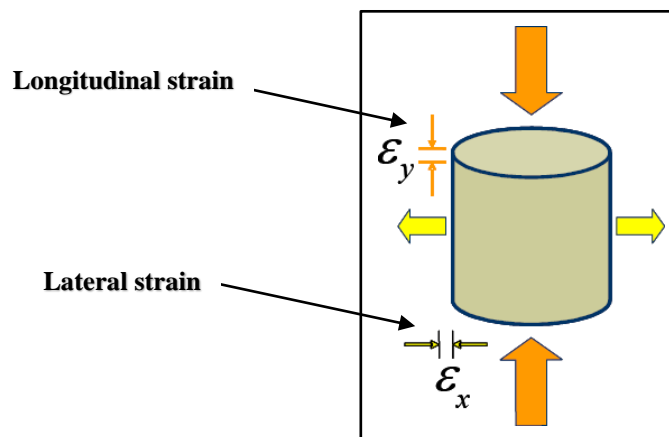


Figure 5-46: Principle of Poisson's ratio (Greaves et al., 2011)

$$\nu = \frac{\text{lateral strain}}{\text{longitudinal strain}} = \frac{\epsilon_x}{\epsilon_y} \quad (5-3)$$

To determine the Poisson's ratio for the CM, 0.2% GFRM blend and GCF - 0.2% GFRM blend mixtures, Marshall samples were prepared in the laboratory according to the Marshall method (MS-15, 1989). The design mix i.e. ingredients for the Marshall samples were the same for the CM, 0.2% GFRM blend and GCF - 0.2% GFRM blend mixtures as in the SCBT and WTT but were used in different quantities based on volumetric size of the Marshall mould. Figure 5-47 shows the Marshall test mould and the base plate.

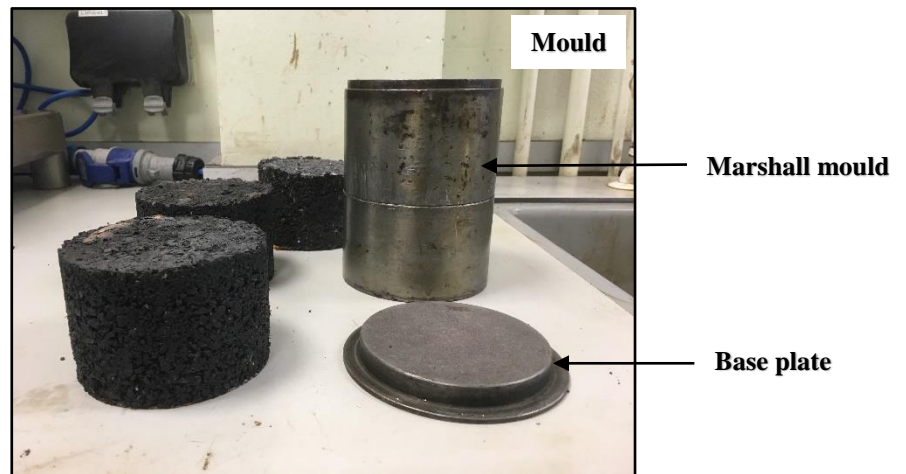


Figure 5-47: Marshall sample mould and base plate

The Marshall hammer was used to compact the specimens by giving 50 blows on each face of the samples. The mass of the sliding tamping hammer is 4.53kg. Figure 5-48 below shows the Marshall compactor and figure 5-49 displays the Marshall samples.

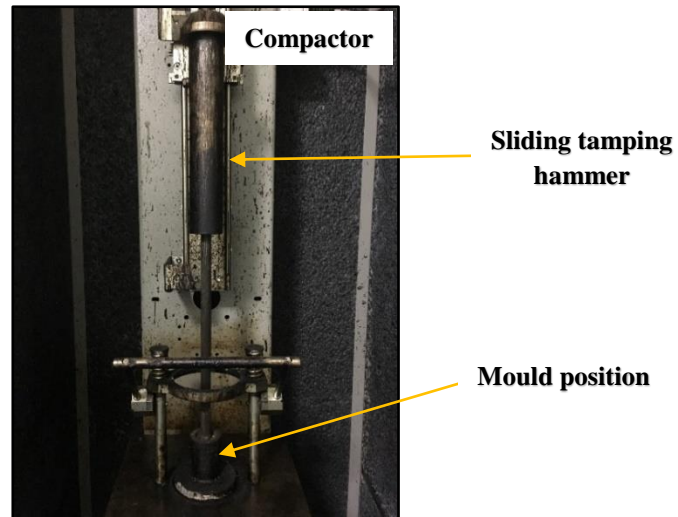


Figure 5-48: Marshall hammer

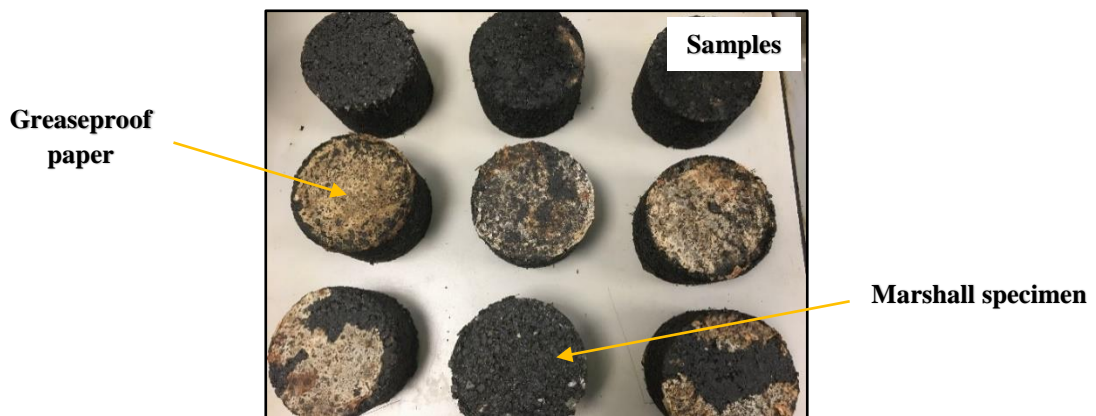


Figure 5-49: Marshall samples

After the preparation of samples, the air voids content for the CM, 0.2% GFRM blend and GCF - 0.2% GFRM blend mixtures was calculated by determining the dry weight, the weight of the sample submerged in water and the saturated surface dry weight of the samples. The air voids content for the CM, 0.2% GFRM blend and GCF - 0.2% GFRM blend was calculated as 5.53%, 4.94% and 3.61% respectively. This air voids content is consistent with the Highway Authority and Utility Committee document (HAUC, 2010), which requires that the air voids after compaction of cold mixes used for carriageways is between 2 and 10%. It can be evidenced from the decrease in the air voids content for the GCF - 0.2% GFRM blend mix that the use of the CKD has resulted in further pore refinement of the CMM as discussed and concluded in

sections 5.25, 6.6.3 and 6.16.12. Subsequently, the relaxation test was conducted by applying vertical strain at 5°C of 200µε for up to 240s (Islam et al., 2015). The test time is sufficient to examine the relaxation behaviour of CMM. The test is conducted in accordance with BS EN 12697-26 (BSI, 2012). The servo-pneumatic universal testing machine was used, figure 5-50 with the test conditions as indicated in table 5-14.

Table 5-14: Relaxation test conditions

Item	Range
Sample diameter, (mm)	100
Sample thickness, (mm)	50
Vertical strain, (µε)	200
Frequency, (Hz)	0.5
Loading time (s)	240
Test temperature (°C)	5
Compaction	Marshall hammer (50 x 2)
Specimen temperature conditioning	4hr before testing

Figure 5-50 below shows the test setup in the temperature controlled chamber. Two linear variable displacement transducers (LVDT's) were clamped. The gauge length of the LVDT was 50mm. After the test, indentation measurements for the samples were taken to determine the lateral strain and longitudinal strain. The Poisson's ratio for the CM, 0.2% GFRM blend and GCF - 0.2% GFRM blend mixtures were calculated as 0.38, 0.34 and 0.27 respectively. This is consistent with the Poisson's ratio for asphaltic materials which generally range between 0.27 & 0.35.

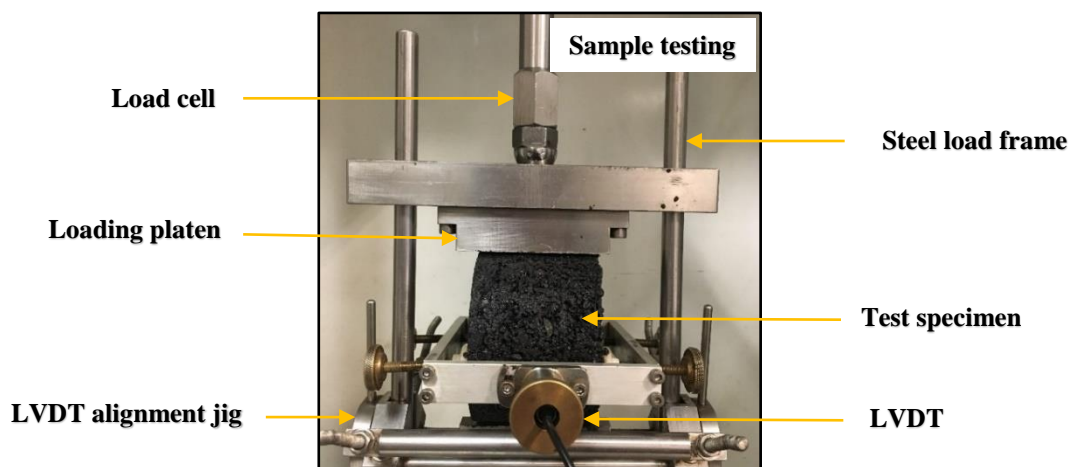


Figure 5-50: Poisson's ratio test setup

5.29.2 FEM FOR THE SCB TEST

Molenaar et al., (2002) studied the effectiveness of SCB to characterise asphalt mixtures, using an FE model that was developed to calculate tensile and compression stresses developing in SCB samples during testing. Computer aided pavement analysis three-dimensional FE software (CAPA-3D) was used to run the simulations. The analysis revealed that the dominant failure mode in the SCB test is cracking due to tension stresses. Thus, the SCBT gives relevant information on the tensile characteristics of the CMM mixes tested (Molenaar, 2000). Most previous models adopted the classical FEM approach to depict cracking in asphalt. Ozer et al., (2011) used the generalised finite element modelling (GFEM) to investigate crack development under repeated wheel loading. The capability of FEM to allow the crack to propagate in the specimen makes the GFEM approach efficient for asphalt crack modelling (Sallam & Abd-Elhady, 2012).

Commercially available software Abaqus version 6-16-3 was used for FE modelling of the SCB test utilising the software built-in functions (Abaqus, 2016). The model geometry corresponds to the laboratory prepared SCB samples; dimensions of the model are consistent with the laboratory experiment as described previously in section 5.17, and sub-section 5.17.1. The free medial axis quadratic elements meshing algorithm was used to generate the model. It is found suitable because the medial axis algorithm first decomposes the region (SCB specimen geometry) to be meshed into a group of simpler regions. The algorithm then fills each simple region with elements. If the region being meshed is relatively simple and contains a large number of elements, the medial axis algorithm generates a mesh faster. Boundary conditions are created in Abaqus/CAE in order to control the response of meshes (elements) when loading is applied to the SCB model. The boundary conditions in both 2D and 3D FE models are imposed such that the vertical direction on the opposite side of the symmetric boundary is fixed (i.e. sideways movement in the sample is restricted), whereas the bottom of the SCB specimen is fixed in the horizontal direction (i.e. movement on the edges of the

sample is restricted). The element types used in the 2D FE simulations in Abaqus are plane strain four-node element with full integration, first-order interpolation (CPE4) for plane strain analysis, whereas 3D eight-node elements with full integration, second-order interpolation (C3D8) were used for conducting 3D FE simulations. An element's number of nodes (interpolation) determines how the nodal degrees of freedom will be interpolated over the domain of the element. Abaqus includes elements with both first and second-order interpolation. Figure 5-51 (a-c) illustrates the cohesive element shapes and FE mesh model for the SCB test specimen with a notch depth of 10mm.

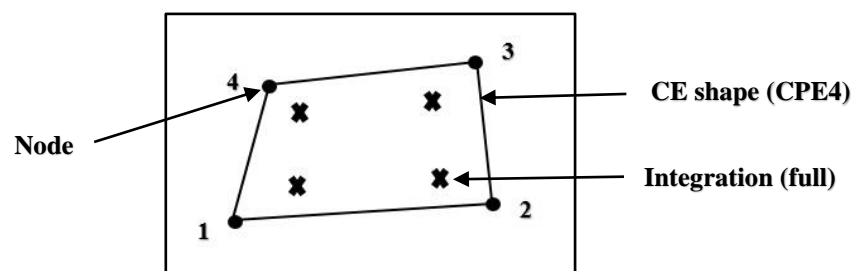


Figure 5-51 (a): Shape of cohesive element CPE4 (first-order interpolation)

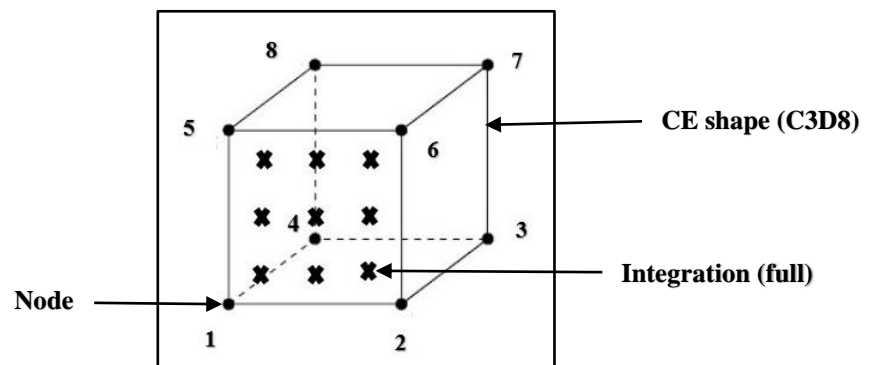


Figure 5-51 (b): Shape of cohesive element C3D8 (second-order interpolation)

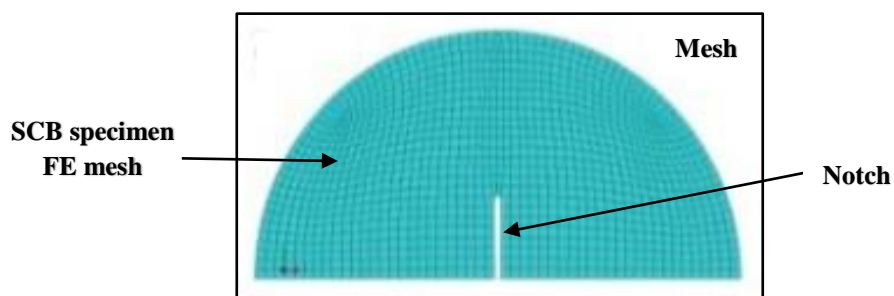


Figure 5-51 (c): Abaqus FE mesh for the SCB test specimen

Results of the experimental program were investigated using a 3D FE approach. The 3D FE model was used to achieve two objectives: i) to identify the main failure mechanisms during the SCB testing process; and ii) to study the damage propagation in the SCB test for the CM, 0.2% GFRM blend and GCF - 0.2% GFRM blend mixes. Figure 5-52 illustrates the general layout of the FE model.

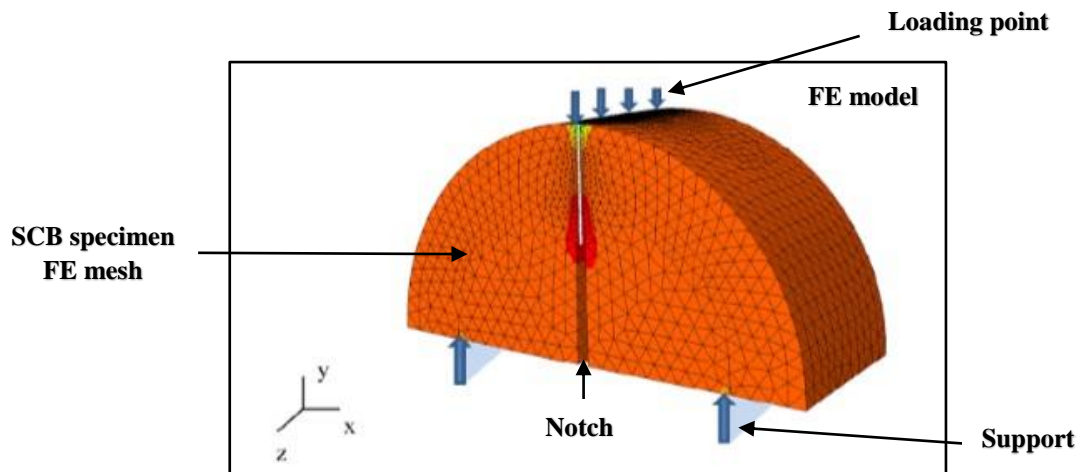


Figure 5-52: Layout of the FE model

Crack propagation during the test was investigated using the FE model results. Figure 5-53 illustrates crack evolution in the SCB test as predicted by the FE model for the CM, 0.2% GFRM blend and GCF - 0.2% GFRM blend mixtures. To study crack propagation in the fracture process zone (FPZ) located above the notch tip, three points for each CM, 0.2% GFRM blend and GCF - 0.2% GFRM blend mixtures were selected: A, crack initiation point; B, peak force point; C, failure point i.e. point A: just above the notch tip, points B and C from the graph 6-11 in section 6.9 in chapter 6. Crack propagation status at each loading point is shown in figure 5-53 (a-c) for points A, B and C, respectively for the CM, 0.2% GFRM blend and GCF - 0.2% GFRM blend mixtures. Due to stress concentration, a crack is initiated in the vicinity of the notch tip; when the loading magnitude reaches point A, the damage evolution process starts for the element at the notch tip, and the element will crack, splitting into two elements.

The stress concentration will then transfer to the next element. This element will crack as the load increases. As the loading continues to increase, the crack will continue to propagate. As the crack propagates through, the CM, 0.2% GFRM blend and GCF - 0.2% GFRM blend mixtures are enduring damage up until point B, at which point the damage level in each mix has progressed to the extent that less load is required for the crack to advance. As the displacement loading continues, the crack gradually progresses until the failure point C is reached. From the FE analysis, it was observed that the CM, 0.2% GFRM blend and GCF - 0.2% GFRM blend mixtures undergo similar fracture patterns as depicted in figure 5-53 below. However, the tendency of the CM, 0.2% GFRM blend and GCF - 0.2% GFRM blend mixtures to resist the cracking varies depending upon the strength of each mix, as evaluated in sections 6.1, and 6.9 respectively.

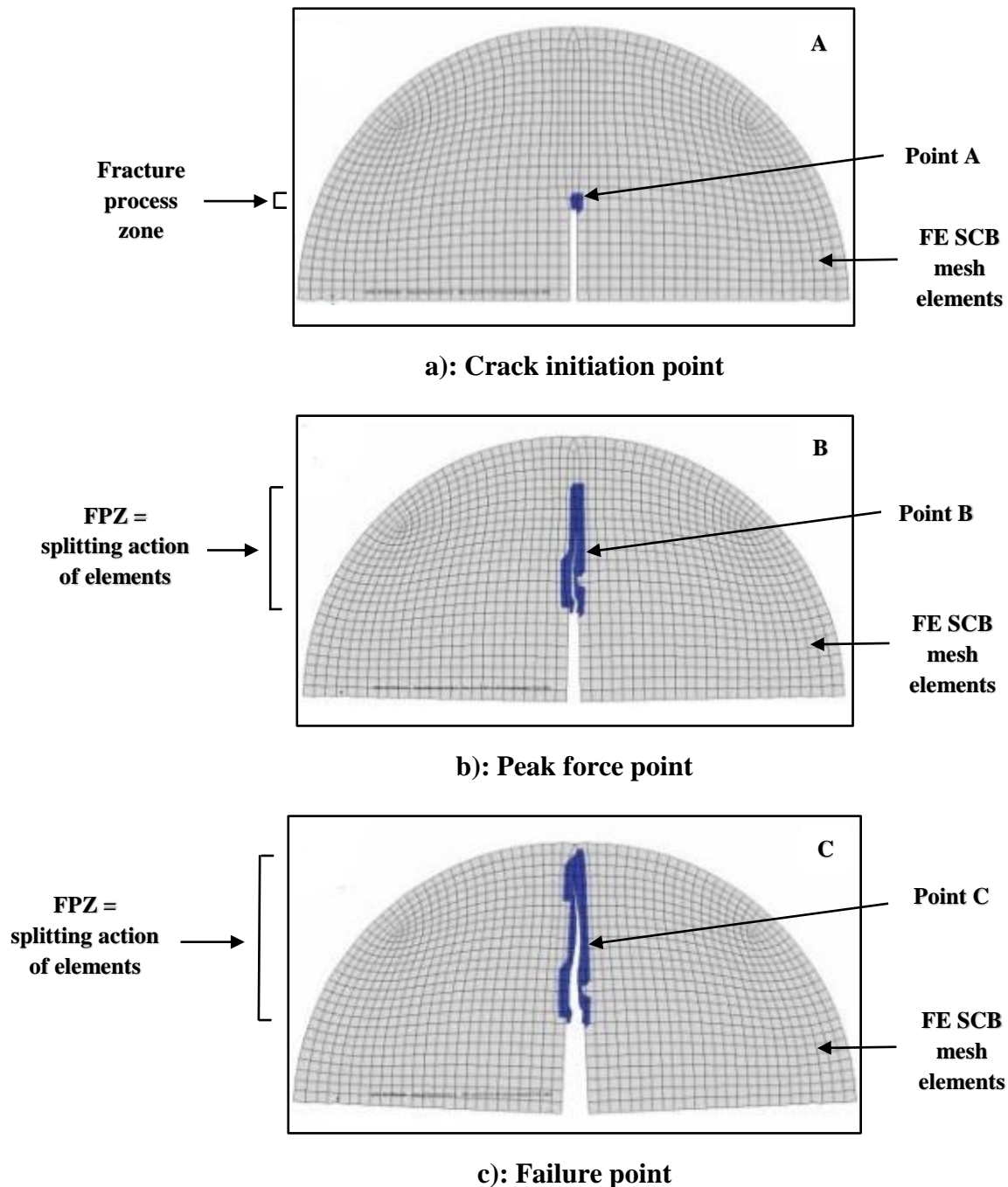


Figure 5-53: Crack evolution process in the SCBT

The crack plane is perpendicular to the maximum principal stress (MAXPS). The MAXPS is parallel to the horizontal axis i.e. along the diameter of the specimen and stresses are acting on the face of the sample due to the applied load on it as described in section 6.2, and illustrated in figure 6-2 below. A vertical crack propagation line indicates that the failure is attributed to tensile stresses. Figure 5-54 clearly indicates that the crack propagation occurs in the

central strip of the specimen, and even though it is not perfectly vertical, it is obvious that the most significant component of the MAXPS is due to tensile stresses. The lack of a perfectly vertical crack propagation through a symmetrical SCB; CM, 0.2% GFRM blend and GCF - 0.2% GFRM blend samples could be attributed to the free medial axis quadratic element meshing algorithm, which in essence introduced a heterogeneity to the model. The vertical crack propagation observed in the FEM for SCB below also coincides with the conclusion highlighted during the experimental analysis of crack propagation rate in section 6.3 below which showed that the crack propagation rate in the CMM mixes is linear. Therefore, an agreement exists between the experimental and numerical modelling finding.

Corresponding evolution of damage (ED) to the failure mechanism in the figure 5-53 above for CM, 0.2% GFRM blend and GCF - 0.2% GFRM blend mixtures was further investigated using the cross-sections obtained from the results of the FE model in figure 5-54. Figure 5-54 below illustrates the damage propagation during the test as predicted by the FE model for the CM, 0.2% GFRM blend and GCF - 0.2% GFRM blend specimens. Damage describes the degradation of material stiffness of CM, 0.2% GFRM blend and GCF - 0.2% GFRM blend through the testing process. The crack evolution damage pattern in the CM, 0.2% GFRM blend and GCF - 0.2% GFRM blend mixes is found to be the same i.e. during the crack initiation, maximum load point and failure point stages. However, it is important to mention that the ability of CM, 0.2% GFRM blend and GCF - 0.2% GFRM blend to retard the cracking process varies due to the different types of CMM under testing. As shown in the figure 6-54 (b-d) below, damage starts to propagate locally at the notch tip, stage 1. Once the total damage of the cohesive element (CE) is reached in the vicinity of the notch tip, the damaged element is removed from the simulation and damage progresses upward, stage 2. As the applied displacement is increased, damage gradually progresses upward until total failure is reached, stage 3.

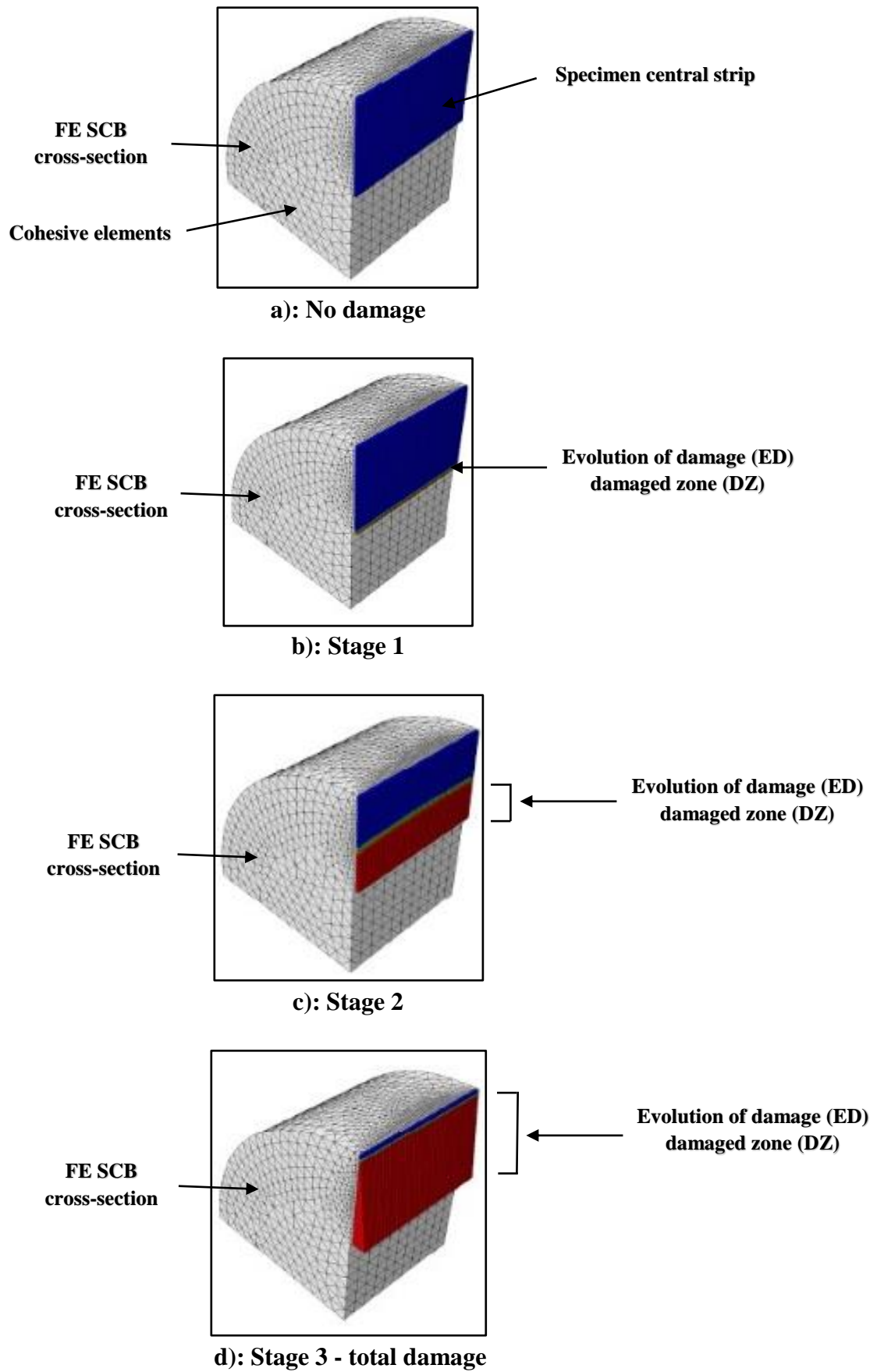


Figure 5-54: Crack evolution damage in the SCBT

5.29.3 FEM FOR THE WT TEST

Abaqus software, version 6-16-3 was used for FE modelling of the WT test utilising the software built-in functions (Abaqus, 2016). The model geometry corresponds to the laboratory prepared wheel tracking samples; the dimensions of the model are consistent with the laboratory experiment as explained previously in section 5.18, and sub-section 5.18.1. The influence of the fibres on resisting the deformation is represented by stress and strain variables associated with the material properties i.e. Poisson's ratio (ν) and Young Modulus (E) for the 0.2% GFRM blend and GCF - 0.2% GFRM blend mixes. The free medial axis quadratic elements meshing algorithm was used to generate the model.

The results of the experimental program were investigated using a 3D FE model approach. The 3D FE model was used to study the deformation distress during the WT test process for the CM, 0.2% GFRM blend and GCF - 0.2% GFRM blend mixes. Figure 5-55 illustrates the general layout of the FE model.

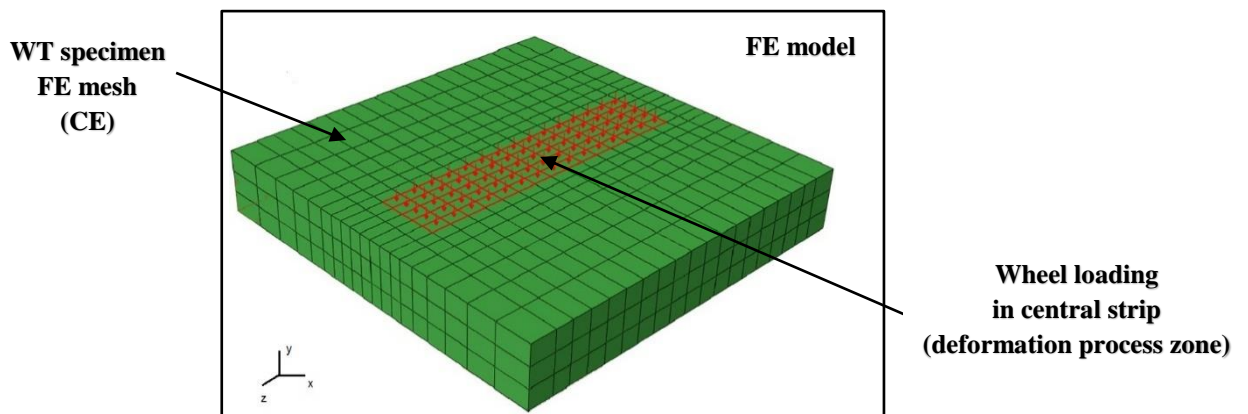


Figure 5-55: Layout of the FE model

The rut potential during the test was investigated using the FE model results. Figure 6-11 in chapter 6 illustrates deformation evolution in the WT test as predicted by the FE model for the CM, 0.2% GFRM blend and GCF - 0.2% GFRM blend mixtures. Rutting was primarily examined in the deformation process zone (DPZ) located in the central median of the specimen under the

tracked wheel load for each of the CM, 0.2% GFRM blend and GCF - 0.2% GFRM blend mixtures. During the FE modelling the deformation concentration propagates from one cohesive element to the next element. The CE will deform as the number of wheel passes increases up to 10,000. As the wheel loading continues to increase, the deformation will continue to propagate.

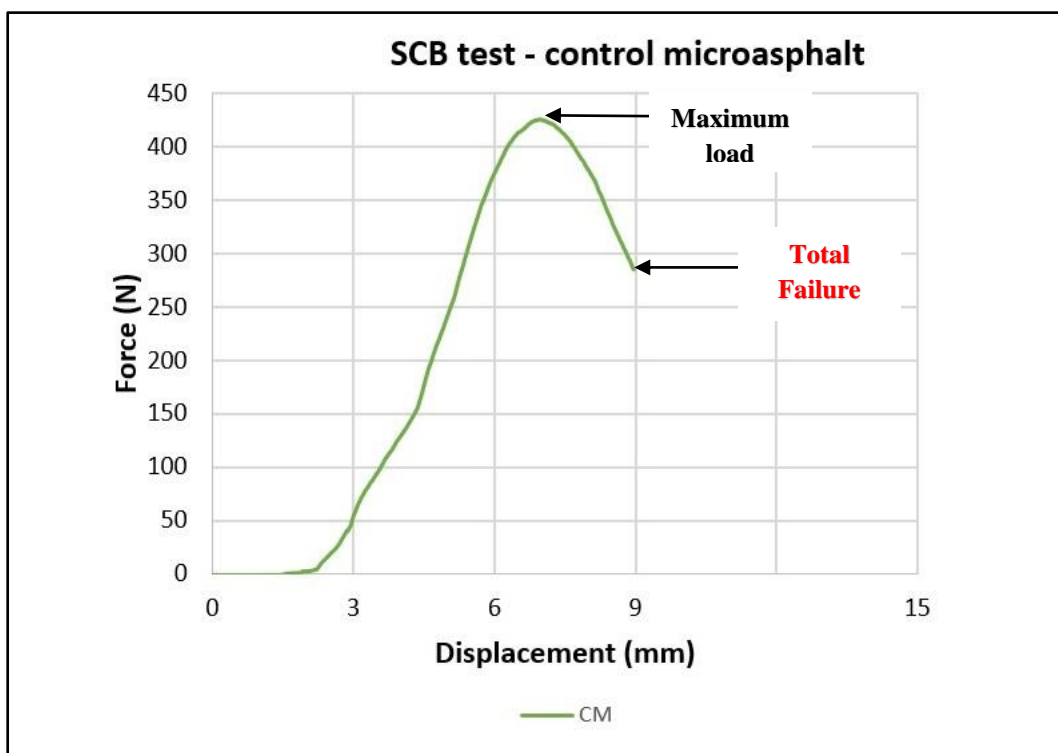
Chapter

6

Critical Analysis of Test Results

6.1 SEMI-CIRCULAR BENDING TEST RESULTS

A force-displacement graph was plotted (graph 6-1 below) for the semi-circular bending test on the control microasphalt (CM) samples (averaged for four samples). It is seen from the graph that the CM takes a peak load of 425N. The vertical displacement at the maximum load is 7mm. Subsequently there is a sharp drop in the curve and the sample then fails completely. The area under the curve indicates the energy absorbed by the CM mixes and thus designates the potential to retard reflective cracking.



Graph 6-1: Flexural load as function of vertical displacement

To analyse the effect of the addition of glass fibres in the microasphalt, the SCB test graph was plotted between the flexural load versus vertical displacement below (graph 6-2) to optimise the length of glass fibre in the mix. The data points (averaged for four samples for each type) show the behaviour of GFRM for each of the fibre lengths used in the mix i.e. 6mm, 12.5mm, 16mm and 25mm. During this test, the fibre quantity in the mix was kept as a constant parameter; a value equal to 0.2%. The samples containing 6mm and 12.5mm glass fibre lengths reveals that they can be subjected to

a compressional force of 405N and 400N respectively with a displacement equivalent to 8.2mm and 8.7mm respectively. The best performing sample was the one which had contained glass fibre of 16mm length in the mix. The sample withstood a peak flexural load of 450N approximately with a displacement of 8.2mm compared with a peak load of 425N and a vertical displacement of 7mm for control microasphalt mixture. This resulted in improvement of up to 5.5% in load bearing capacity and 33% in resistance to cracking of GFRM samples at ultimate failure compared with CM mixture above. Microasphalt with 25mm of glass fibres length was the least performing sample. The peak load for the mix was 325N while the displacement was recorded at 9.2mm. Though in case of 25mm glass fibre length mix, displacement was logged slightly higher as compared to the 16mm glass fibre length mix at the peak flexural load, the overall displacement at the ultimate fracture point i.e. where the sample ceased to take further load, was observed at 13.5mm and was nearly the same as of 16mm glass fibre length. The glass fibre length of 16mm exhibited improvement in the flexural load property of microasphalt up to 28% as compared to 25mm glass fibre length, 10% and 11% as compared to 6mm and 12.5mm glass fibre lengths respectively.

During the laboratory testing, it was observed that the glass fibres having 25mm of length in the sample started to tangle thus forming a “balling”. The sharp drop of curve exhibited by the 25mm glass fibre length sample reasonably advocated the argument that the glass fibres had not dispersed uniformly in the mix; and due to excessive length, they had tangled at one area and therefore, did not withstand the load to which they were intended to resist the cracking. This phenomenon also limits the use of glass fibre in excessive lengths i.e. greater than 25mm in the microasphalt. The test results aided in determining the optimised length of glass fibre as 16mm in the microasphalt mix.

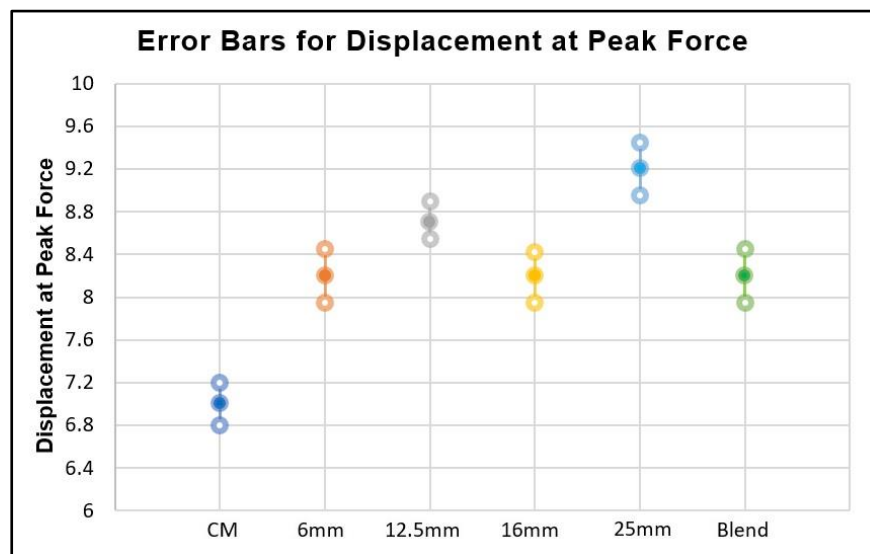
Subsequent to optimisation of glass fibre length in the microasphalt mix an effort was made to probe the effect of using a blend of glass fibre lengths in the microasphalt mix i.e. 0.25% of each cut lengths 6mm, 12.5mm, 16mm and 25mm of 0.2% fibre quantity (of total dry weight of the aggregates in the mix) a parameter which was kept previously as a constant to optimise the glass fibre lengths in the mix. Data points for

GFRM blend were plotted (see graph 6-2) which gives an interesting insight. It shows that the GFRM blend had marginally performed better than the optimised glass fibre length of 16mm. The area under the curve was somewhat more i.e. it had absorbed more energy and had slightly enhanced the ability of microasphalt to resist the cracking further.

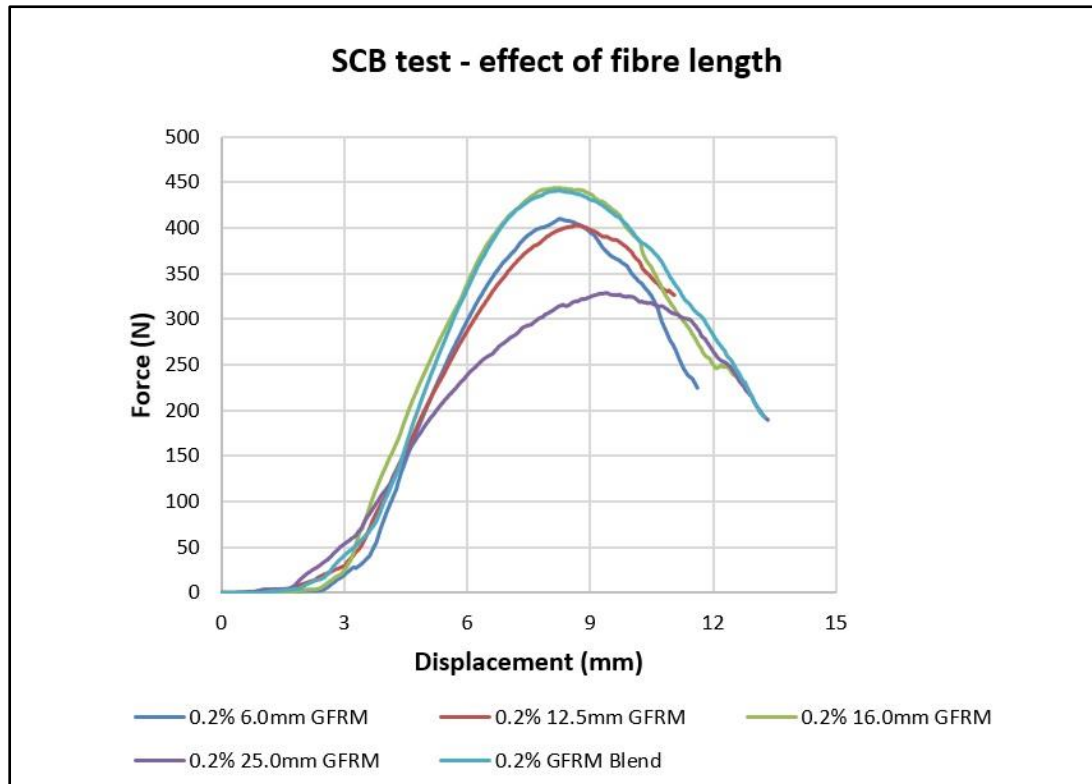
The potential reason for this could be the uniform but varying dispersion of glass fibre lengths in the mix which when cracking triggers in the test sample, more effectively resists the cracks due to the complex state of stresses found within the specimen body as analysed and explained in section 6.1 above. GFRM blend was used to determine the effect of quantity of glass fibre in the microasphalt however, for practical purposes optimised glass fibre length of 16mm was used for the field trial because of the cutting of glass fibres in varying lengths on site using a chopper was not feasible.

Table 6-a: Effect of fibre length

Mix type	Avg. no. of samples	Glass fibre length	Glass fibre quantity	Peak force	Displacement at peak load	Displacement at ultimate failure
CM	4	-	-	425N	7mm	9mm
GFRM	4	6 mm	0.2%	405N	8.2mm	11.7mm
GFRM	4	12.5 mm	0.2%	400N	8.7mm	11mm
GFRM	4	16 mm	0.2%	450N	8.2mm	12.8mm
GFRM	4	25 mm	0.2%	325N	9.2mm	13.5mm
GFRM	4	Blend	0.2%	450N	8.2mm	13.5mm



Graph 6-a: Error bars for displacement at peak force



Graph 6-2: Effect of fibre length in microasphalt

In graph 6-3 below, the effect of varying quantities of glass fibre in the microasphalt was investigated with the help of the SCBT and a graph was plotted between the force and displacement to optimise the quantity of glass fibre in the mix.

The data points show the behaviour of the GFRM blend for each of the fibre quantities used in the mix i.e. 0.1%, 0.2%, 0.3% and 0.4% (by total dry weight of the aggregates in the mix). During this test, the blend of lengths in the mix was kept as a constant parameter; a value equal to the optimised length of fibre determined above in graph 6-2; GFRM blend i.e. 0.25% of each cut lengths 6mm, 12.5mm, 16mm and 25mm.

The best performing sample was the one containing a glass fibre quantity of 0.2% blend by total dry weight of the aggregates in the mix. The sample withstood a peak flexural load of 450N approximately with a displacement of 8.2mm. Microasphalt with 0.3% glass fibre quantity in the mix was the least performing sample (i.e. area under the curve). The peak load for the 0.3% GFRM blend mix was 225N while the displacement recorded was 5.2mm.

The glass fibre in a quantity of 0.2% exhibited improvement in the flexural load property of microasphalt up to 50% as compared to the 0.3% glass fibre quantity in the mix, 29% and 28% as compared to 0.1% and 0.4% glass fibre quantities in the mixes respectively. The glass fibre in 0.2% quantity has also shown improvement in the displacement property up to 37.5% and 8.5% as compared to 0.3% and 0.4% glass fibre quantities in the microasphalt samples respectively at the peak load. However, there was only a marginal difference in the displacement property of 0.2% glass fibre quantity as compared to the 0.1% glass fibre quantity in the microasphalt mixes at the peak load.

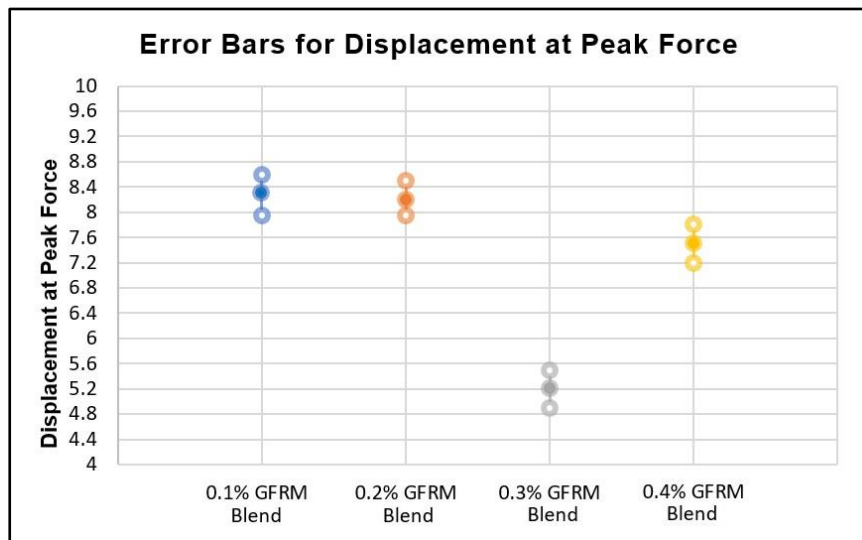
During the laboratory testing, it was observed that the microasphalt containing 0.3% and 0.4% quantities of glass fibre (by total dry weight of the aggregates in the mix) in the samples started to tangle thus forming a “balling (see figure 6-1)”. The sharp decrease in the slope of the curve shown by 0.3% and 0.4% glass fibre quantities samples rationally supports the argument that the glass fibres had not dispersed uniformly in the mix and due to the excessive quantity present it has tangled at one area and therefore, could not withstand the loading or retard cracking. This phenomenon precludes the use of glass fibre in excessive quantities i.e. greater than 0.2% in the microasphalt. The glass fibres strands are very light in weight and if the quantity exceeds 0.2% in the microasphalt it gains a lot of volume in the mix and thus tends to tangle (gathers at one place to form a “balling”) upon addition of bitumen emulsion and mixing of ingredients during the preparation of samples. The test results assisted in determining the optimised quantity of glass fibre as 0.2% by total dry weight of the aggregates in the microasphalt mix.



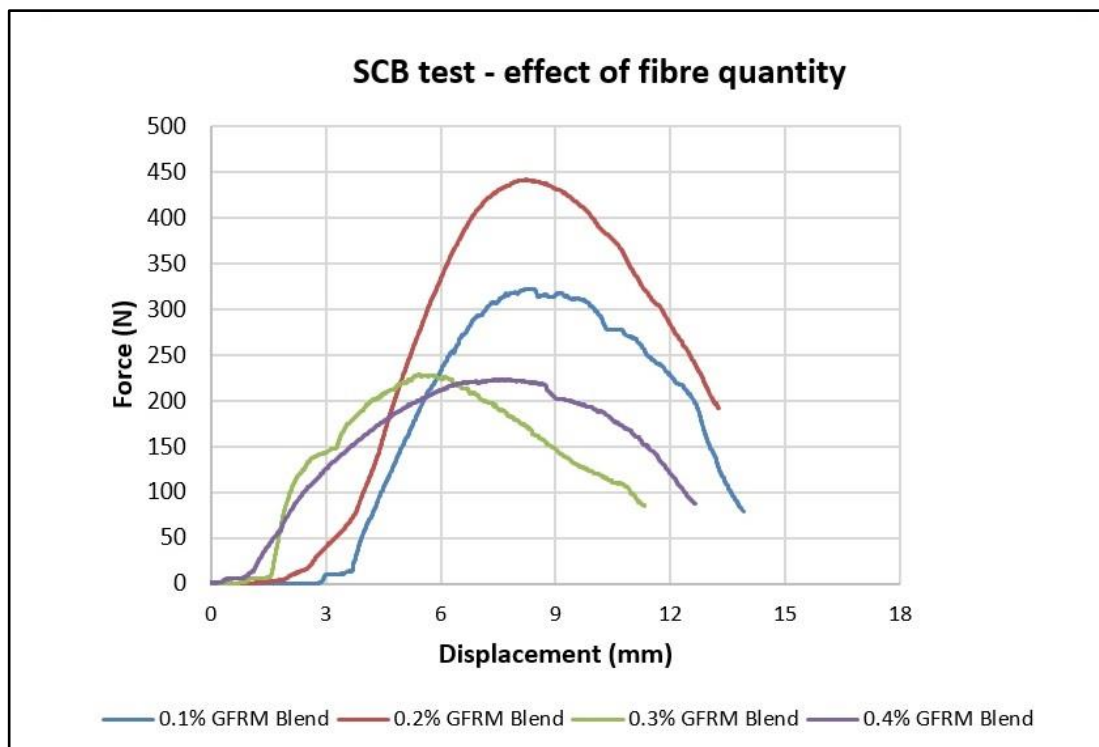
Figure 6-1: Balling phenomenon in microasphalt

Table 6-b: Effect of fibre quantity

Mix type	Avg. no. of samples	Glass fibre length	Glass fibre quantity	Peak force	Displacement at peak load	Displacement at ultimate failure
GFRM	4	Blend	0.1%	325N	8.3mm	14mm
GFRM	4	Blend	0.2%	450N	8.2mm	13.5mm
GFRM	4	Blend	0.3%	225N	5.2mm	11.2mm
GFRM	4	Blend	0.4%	225N	7.5mm	12.8mm



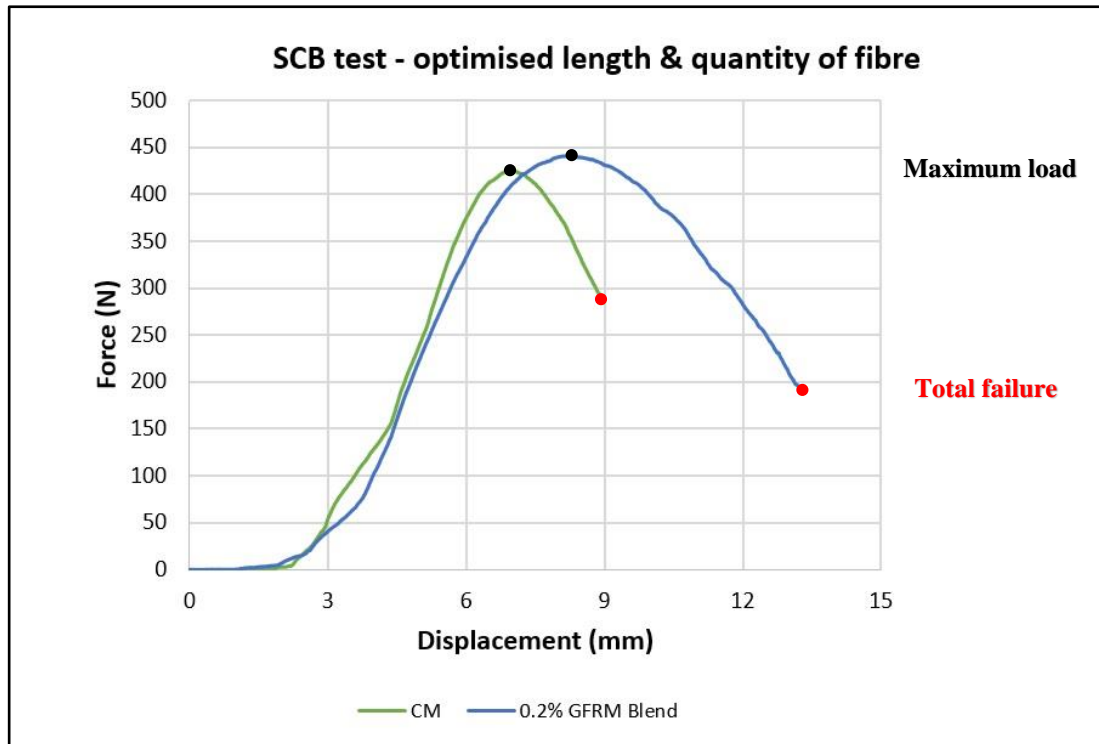
Graph 6-b: Error bars for displacement at peak force



Graph 6-3: Effect of fibre quantity in microasphalt

A graphical representation of the flexural load (force) as a function of displacement is offered in Graph 6-4 below. The data sets for the fibreless and optimised fiberized microasphalt were selected to be plotted as an indication of the typical behaviour for each type of mix. It can be seen from the graph that for a given set of conditions detailed in table 5-11, the effect of the fibre is driven by a change in the area under the curve as an indication of the energy absorbed. The samples containing fibre experienced greater softening behaviour i.e. the slope of the force-displacement graph following the peak load is significantly lower than the fibreless samples. The peak flexural load for the GFRM is 450N approximately while for CM it is 425N; demonstrating that the fibres have enhanced the load bearing strength of microasphalt up to 5.5% allowing the mix to absorb more energy as compared to the fibreless mix.

The initial response of both types of mixes is the same but when the peak load is approached the fibre component comes into play and thus augments the mixture strength and ductility. Further, the SCBT results suggest that the energy absorbed by the optimised GFRM test samples is sustained for a longer duration (in terms of displacement) and thus has offered 15% more ductility in comparison to CM mixes until maximum load failure of the sample and 33% more ductility in comparison to CM mixes until ultimate failure of the sample. The GFRM samples have complemented both parameters; force and displacement i.e. it has more strength to take the flexural load and absorb energy for a longer period. The cracking phenomenon in the optimised GFRM mix is not as abrupt as in CM mixes and it takes ample time (gives an ample warning) before failing completely i.e. GFRM has enhanced the ductility of the mix. This means that the GFRM can take more traffic load and will offer more resistance to reflective cracking for a longer duration and would fail in a smooth ductile manner in contrast to the CM. The importance of displacement can be well understood from the fact that the GFRM mixtures offering more displacement values at a given load can absorb more fracture energy for a longer duration within the viscoelastic-plastic region as compared to the CM mixtures. Thus, GFRM mixtures have the potential to resist reflective cracking (both longitudinal and transverse) showing enhanced performance in comparison with the CM mixtures. This phenomenon will be simulated and validated on-site during the trial section explained in the succeeding chapter 7.



Graph 6-4: Optimised length and quantity of glass fibre in microasphalt versus control microasphalt

6.2 SEMI-CIRCULAR BENDING TEST ANALYSIS

During the test performance, micro-cracking damage is initiated within the area of highest bending moment across the diameter of the specimen and in the area above the support. It gradually extends diametrically and then coalesces near the centreline of the specimen. Due to this significant coalescing of tension damage in time, intense localization of cracking along the diameter of the specimen occurs in the final stages of the test. Some distributed compressive damage can also be observed near the edge of the loading strip and near the support rollers also, but it is negligible compared to the tensile damage (Molenaar & Molenaar, 2000).

Stress analysis in the specimen of the SCB test (figure 6-2) shows the large tensile stresses occurring at the bottom of the specimen and a compressive arch develops and pure tension always occurs at the mid-point of the specimen across the diameter. The way in which the SCB specimens fail indicates that tension might be the dominant failure mode.

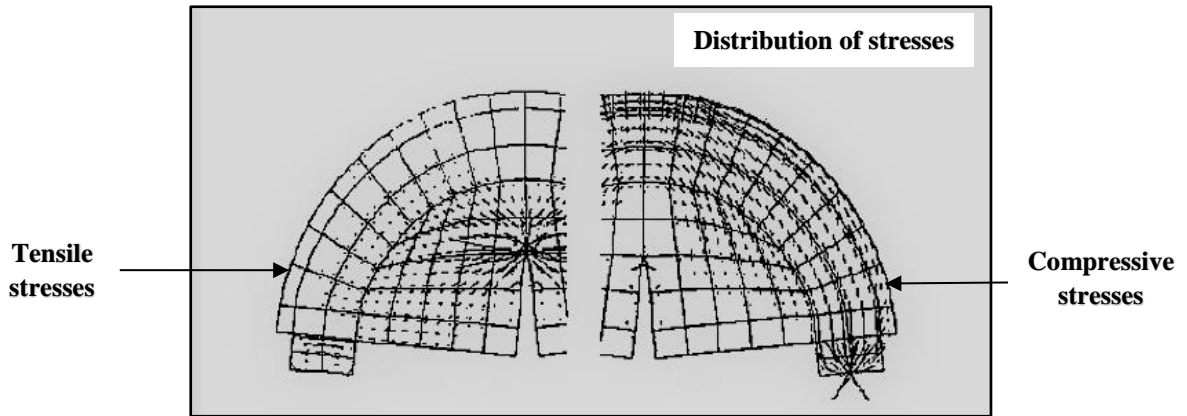


Figure 6-2: Left FEA diagram shows the distribution of tensile stresses and right one shows the distribution of compressive stresses (Molenaar & Molenaar, 2000)

The above figure 6-2 shows the tensile and compressive stresses by means of a finite element model assuming that the material behaves in a linear elastic manner. The figure 6-2 referred to above shows that indeed large tensile stresses occur at the bottom of the specimen but also that a compressive arch develops. Figure 6-3 below shows a simulation of a semi-circular bending (SCB) test, modelled using an advanced viscoelastic cohesive zone model, using computer-aided engineering (CAE) virtual testing software (MultiMechanics, 2014) for advanced composite analysis of materials.

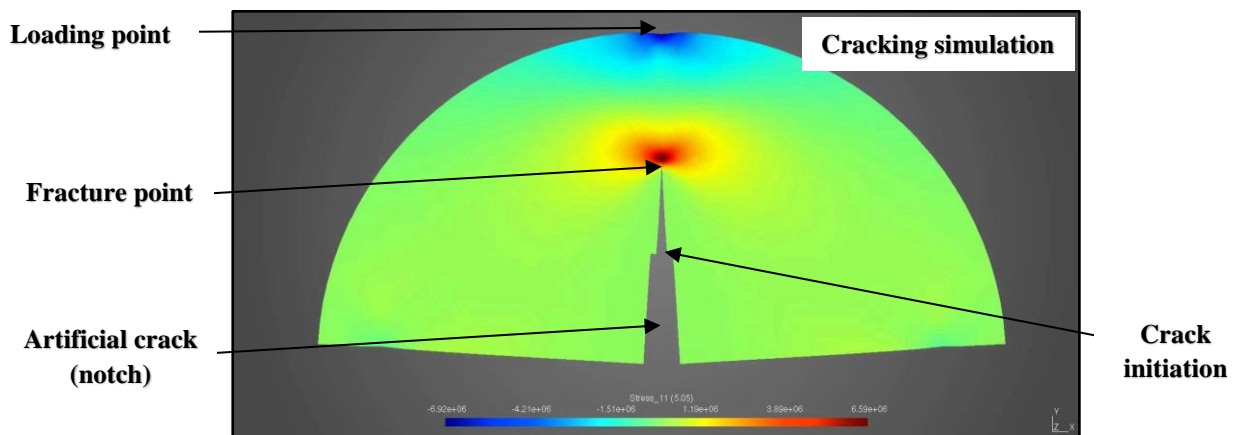


Figure 6-3: Graphic illustration of cracking phenomena in 3D space for SCB test and stress concentration within the SCB specimen

In the SCBT, the specimen starts with a pure tensile flexural failure, which reflects a relatively “true” tensile strength of the mixture (Louay et al., 2004; Molenaar, 2000). From the stress analyses, it appeared that significant compressive stress concentration occurs under the loading strips and/or rollers. Although asphalt mixtures normally have much higher compressive strength than tensile strength, excessive compressive stress concentration can still cause localized punching failure which in turn could affect the stress distributions and cause test errors.

6.3 CRACK PROPAGATION RATE

In graph 6-5 below, the crack behaviour is modelled using The Paris Law (2010). The Paris Law is visualized as a graph on a log-log plot, where the x-axis represents the stress intensity factor and the y-axis represents the crack growth rate. The term crack growth rate, denotes the crack length growth per increasing number of load cycles for the tested microasphalt, and the stress intensity factor is defined as a uniform tensile stress perpendicular to the crack plane.

The two parameters used to determine the crack propagation rate are ΔK and da/dN where (a) is the crack length and (N) is the number of load cycles. ΔK is the stress intensity factor and is determined using the Equation 6-1 & 6-2 and da/dN is the crack growth rate and is obtained from Equation 6-3 both from Paris Law (2010).

Stress intensity factor: ΔK (N/mm^{3/2})

$$\sigma = \frac{4.263 \times F}{D \times t} \text{ (N/mm}^2\text{)} \quad (6-1)$$

where F is the applied force (at each point along the load deflection curve until maximum point), D is the specimen diameter, t is the specimen thickness and W is the height of the specimen before the test

$$\Delta K = \sigma \times f\left(\frac{a}{W}\right) \text{ N/mm}^{3/2} \quad (6-2)$$

since $9 < a < 11$ and $70 < W < 75$, then;

$$f\left(\frac{a}{W}\right) = 5.956 \text{ (where “a” here is the notch depth)}$$

Crack growth rate: da/dN (mm/cycle)

$$\frac{da}{dN} = A \Delta K^n \quad (6-3)$$

where A and n are material parameters; for cold mixtures A = 0.00011 and n = 0.82

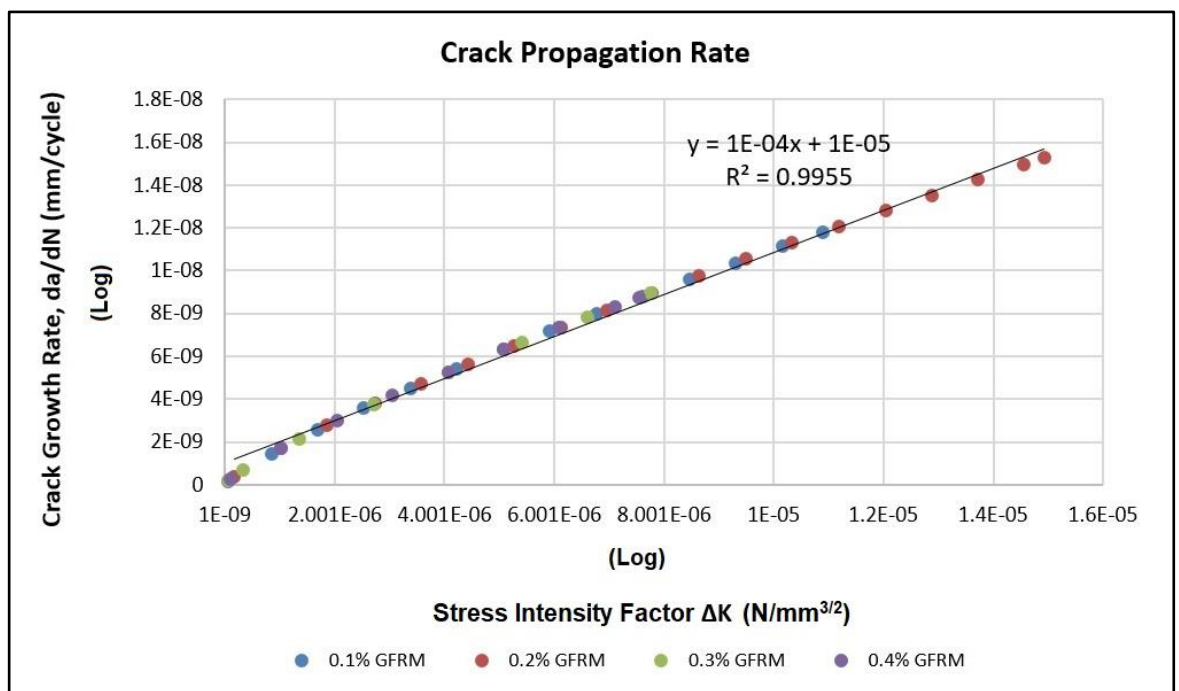
Data points for different quantities of glass fibres were plotted from loading start point until yield point (where the equipment is reading displacement and load just before failure). These are the top points in blue, red, green and purple colours. It is observed that the relationship between crack growth rate and stress intensity factor is linear i.e. the increase in stress intensity factor results in an increase in the material visco-elasto-plastic behaviour and indirectly suggests an increase in resistance to crack propagation phenomena in microasphalt and is higher at 0.1% and 0.2% GFRM, where 0.2% shows the highest results.

The crack growth rate (CGR) at 0.2% GFRM is maximum, whereas the crack CGR at 0.1% GFRM is lower in comparison to 0.2% GFRM, and the CGR at 0.3% GFRM, and 0.4% GFRM are the lowest among all the fibre quantities used in the microasphalt. Thus, we will have a higher CGR, a higher loading cycle and a higher stress intensity factor for the microasphalt with 0.2% quantity of glass fibres until it fails. Similarly, the 0.2% GFRM has a higher stress intensity factor range. This illustrates visco-elasto-plastic behaviour and the material visco-elasto-plastic behaviour is improved by 94% when comparing the 0.2% GFRM to the 0.3% and the 0.4 % GFRM mixes.

The graph 6-5 indicates, if the crack growth is high, the resistance of the microasphalt to cracking is high i.e. glass fibres matrix to failure at the 0.2% GFRM amount of fibre percentages. The higher the number of load cycles to failure, the more the resistance to deformation and material failure that occurs at 0.2% GFRM. In other words, the crack growth rate represents a value and the higher the value the more resistance of material to deformation i.e. the more the stress intensity factor the material can sustain.

The graph 6-5 depicts the correlation between the cracking rates and the ΔK values. The solid line through the measured data points is an exponential regression model on a semi-log plot of cracking rate versus the SCB ΔK . A strong upward trend of the

regression line was observed as the ΔK values increase, which indicates that the cracking rate of microasphalt increases as the fracture resistance of microasphalt mixtures decreases. The coefficient of determination (R^2) of the regression was 0.995, which means that approximately 99% of the variability in the cracking rates observed from those four different GFRM mixes can be explained by the sole independent variable, SCB ΔK value. It is noted that other influencing factors on the cracking performance of microasphalt, such as the structural and environmental aspects, were not taken into account. These results support the suitability of the SCB test method for estimating the fatigue cracking performance of microasphalt in the field.



Graph 6-5: Crack growth rate in microasphalt with varying quantity of glass fibre

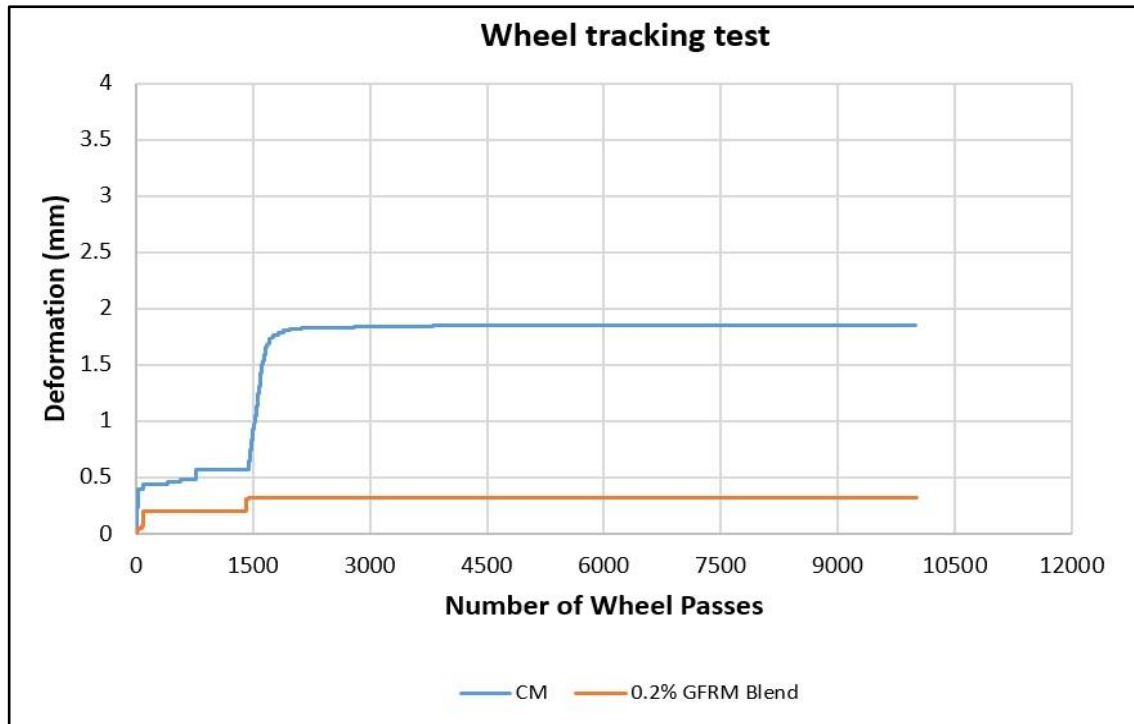
6.4 WHEEL TRACKING TEST RESULTS

A graphical representation of the deformation as a function of the number of wheel passes is presented in Graph 6-6 below. The data points for the fibreless and optimised fiberized microasphalt (averaged for three samples of each mix) were plotted to reflect the distinctive behaviour for each type of mix. It can be seen from the graph that for a given set of conditions described in table 5-12, the effect of the fibre is driven by difference in the area between the two deformation curves as an indication of

resistance to rutting due to the traffic loading. The control microasphalt samples initially exhibited greater softening behaviour under the wheel load and were more prone to deformation which also endorses the conclusion derived from the literature review that cold mix microasphalt is more susceptible to rutting in its early life when it is opened to traffic but later, it tends to gain strength and stabilise which is precisely evidenced from the test results. In the start, i.e. up to 1,600 wheel passes there is a sudden and sharp rise in the deformation curve noted up to 1.8mm and after that the deformation in the control microasphalt mix remains constant at 1.9mm until the completion of the test.

On the contrary, the optimised GFRM experienced lesser softening behaviour under the wheel load and was less prone to deformation which reinforces the positive effect of addition of glass fibres in the microasphalt as observed in the SCB tests. The test results show that the cold mix glass fibre reinforced microasphalt is less susceptible to rutting in its early life, as compared to the control microasphalt when subjected to the traffic loading and further, tends to gain more strength and consolidates with the time. The addition of glass fibres in the mix reduces the softening behaviour of microasphalt and thus contributes to arrest the rutting initiation process in the early life of the microasphalt i.e. when it is more vulnerable to deformation. In the early stages of the WTT i.e. up to 1,500 wheel passes there is a rise in the deformation curve recorded up to 0.33mm but during this transition stage (early life of microasphalt); i.e. when microasphalt start to acquire strength, the slope of the curve is not as steep as the CM mixes and deformation in the fiberized mix from then onward remained steady until the completion of 10,000 wheel passes.

The glass fibre reinforced mix exhibited reduction in deformation of microasphalt up to 83% as compared to the CM mixes after 10,000 wheel passes and during the transition period explained above, deformation i.e. after 1,500 wheel passes GFRM mixes showed an improvement in the deformation up to 67% as compared to the control microasphalt.



Graph 6-6: Wheel tracking test for control and glass fibre reinforced microasphalt

6.5 DISCUSSION

From the above semi-circular bending and wheel tracking tests, it is observed that the 16mm fibre length and blend (glass fibre of selected cut lengths) performed well to retard the reflective cracking. However, the testing undertaken did not examine reflective cracking directly. In graph 6-2, the area under the curve is more for this combination. This means the capability of 16mm and blend glass fibres to take force is more, thus has the good strength to resist cracking. Further, in graph 6-3, the use of fibre quantity of 0.2% by total weight of the dry aggregate in the mix depicted more tensile strength to retard the cracking phenomena in microasphalt.

During the laboratory tests, it is seen that if the quantity of glass fibre in the mix is increased from 0.2% to 0.4% the fibres are tangled, and the mix gets drier and reduces the strength of the material. In glass fibre reinforced microasphalt, the emulsion content (EC) has been increased from 6.0% to 7.5% residual binder by total weight of the mix to address the workability issue. The addition of glass fibre makes the mix dry

therefore, to ensure uniform coating of fibres in the emulsion and workability, the bitumen emulsion content has been optimised to give 7.5% residual binder.

Graph 6-4 shows the comparison between the control microasphalt and the optimised glass fibre reinforced microasphalt. The optimised glass fibre reinforced microasphalt is more elastic and tends to take more load i.e. up to 450N with an extension of 8.2mm and overall extension of 13.5mm before the ultimate fracture. This means that the addition of glass fibres has reinforced (enhanced) the tensile strength of microasphalt up to 33% (at ultimate failure) as compared to the control microasphalt.

In graph 6-6, the control microasphalt has deformation up to 1.9mm after 10,000 wheel passes while the glass fibre reinforced microasphalt has deformation of up to 0.33mm after 10,000 loading cycles. The glass fibre reinforced microasphalt has an increased improvement of 83% in deformation.

The anionic i.e. negatively charged aggregate particles have coalesced with the cationic i.e. positively charged bitumen emulsion molecules in the microasphalt mix and the addition of silicon rich glass fibres (chemical composition of which has been explained at section 5.13) has further increased the adhesion strength between the glass fibres and the other ingredients of microasphalt (Vaughan, 1999). This has improved the bonding between the glass fibres, aggregates and bitumen emulsion in the microstructure of the GFRM and therefore, is responsible for a significant increase in crack resistance and deformation of GFRM mixes as seen from the SCB and WT test results above.

6.6 CHEMICAL AND PHYSICAL TEST RESULTS FOR THE ACTIVE FILLERS

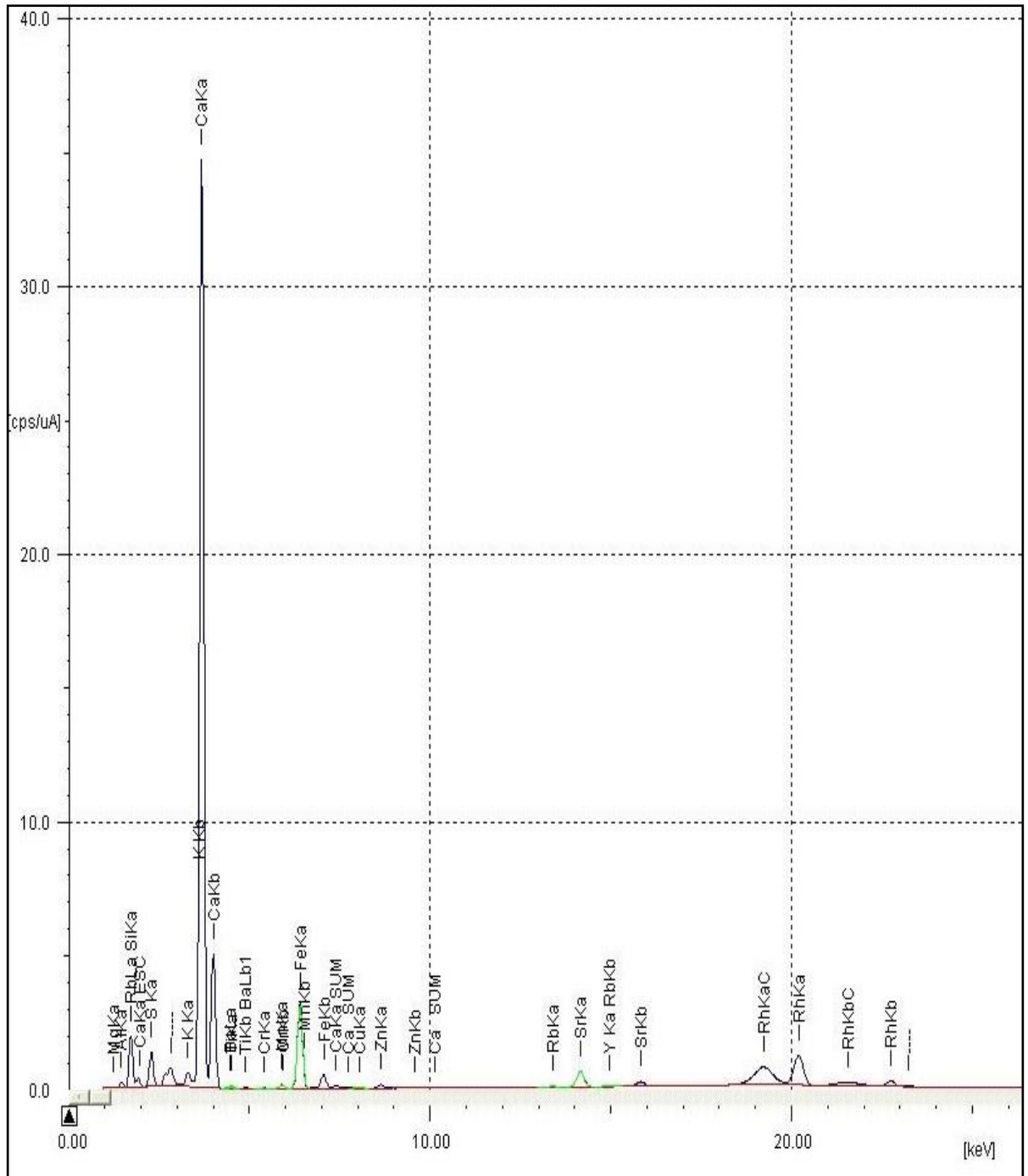
Results of the mentioned test methods in chapter 5 for the selected active fillers are discussed below:

- a. Tables 6-1, 6-2, 6-3 and 6-4 illustrates the chemical compositions of potential fillers.

-
-
- b. Figure 6-4 presents the particle size distributions of selected fillers.
 - c. Figure 6-5 shows the percentages of the main oxides for the selected fillers.
 - d. Table 6-5 illustrates the specific surface area, density and filler particles' characteristics.
 - e. Figures 6-6, 6-7, 6-8, 6-9, and 6-10 display the morphology of the selected fillers and mastics at different ages of 3, 7, 14, 28 and 180 days.

6.6.1 XRF ANALYSIS FOR OPC

Graph 6-7 shows the constituent chemical compounds present in the OPC structure. Quantitative analysis of chemical compounds for the OPC filler sample is provided in table 6-1. XRF analysis confirms that the OPC filler composition mainly consists of calcium oxide, silicon dioxide, aluminium oxide and sulphur trioxide in the quantity of 38.57%, 11.17%, 3.02% and 2.53% as indicated in the above referred table. The presence of these chemical compounds in the OPC results in reactivity with the water in CMM and produces hydration products namely; ettringite (hydrous calcium aluminium sulphate), portlandite (calcium hydroxide) and calcium silicate hydrate (C-S-H) gel, contributing to further strength improvement of CMM and reducing the curing time (Domone and Illston, 2010). This is confirmed during the SEM analysis done for OPC, duly discussed in section 6.6.8 below.



Graph 6-7: XRF analysis of OPC

Table 6-1: XRF (quantitative) analysis of OPC

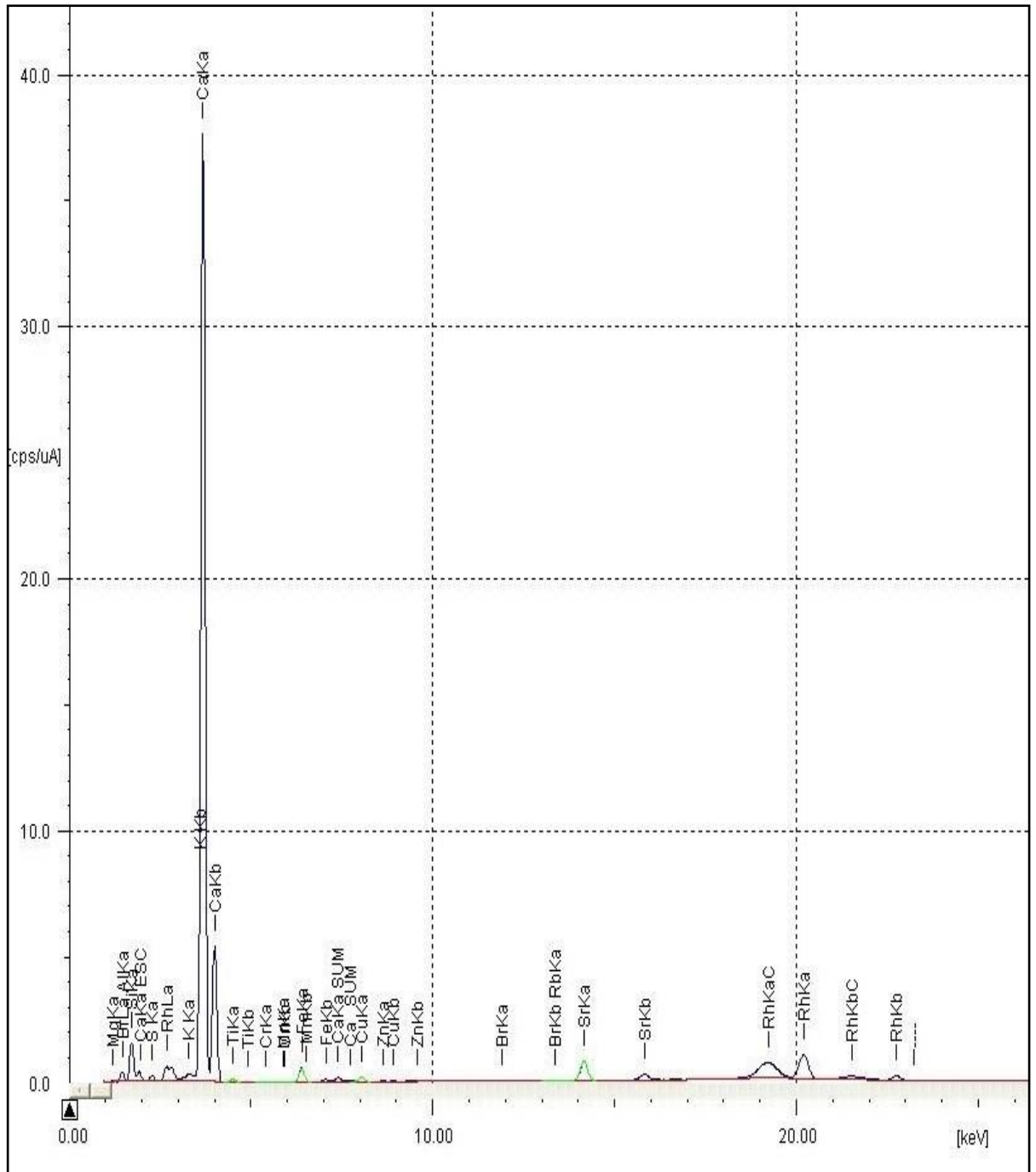
Description (chemical compound)	Percentage (%)
Calcium oxide CaO	38.57
Silicon dioxide SiO ₂	11.17
Aluminum oxide Al ₂ O ₃	3.02
Sulfur trioxide SO ₃	2.53
Iron trioxide Fe ₂ O ₃	1.44
Magnesium oxide MgO	1.39
Potassium oxide K ₂ O	0.54

6.6.2 XRF ANALYSIS FOR PSA

The constituent chemical compounds present in the PSA structure are shown in graph 6-8. Quantitative analysis of chemical compounds for the PSA filler sample is detailed in the table 6-2 below. XRF analysis reveals that the PSA filler is mainly composed of calcium oxide (40.42%), silicon dioxide (9.38%), and aluminium oxide (5.87%) as indicated in the table referred above.

This shows that the PSA possesses chemical compounds very similar to the OPC and thus, makes it a strong candidate for replacement of OPC in the microasphalt mix as a green filler i.e. it contains calcium oxide and silicon dioxide enriched compounds; mainly required for the hydration process to act as a cementitious material.

The presence of these chemical compounds in the PSA will result in reactivity with the water in CMM and would produce hydration products namely; portlandite (calcium hydroxide), hydrotalcite (double hydroxide) and calcium silicate hydrate (C-S-H) gel, contributing to further strength development in CMM and reducing the curing time (Shakir, 2012). This has been discussed in section 6.6.9 under SEM analysis for PSA.



Graph 6-8: XRF analysis of PSA

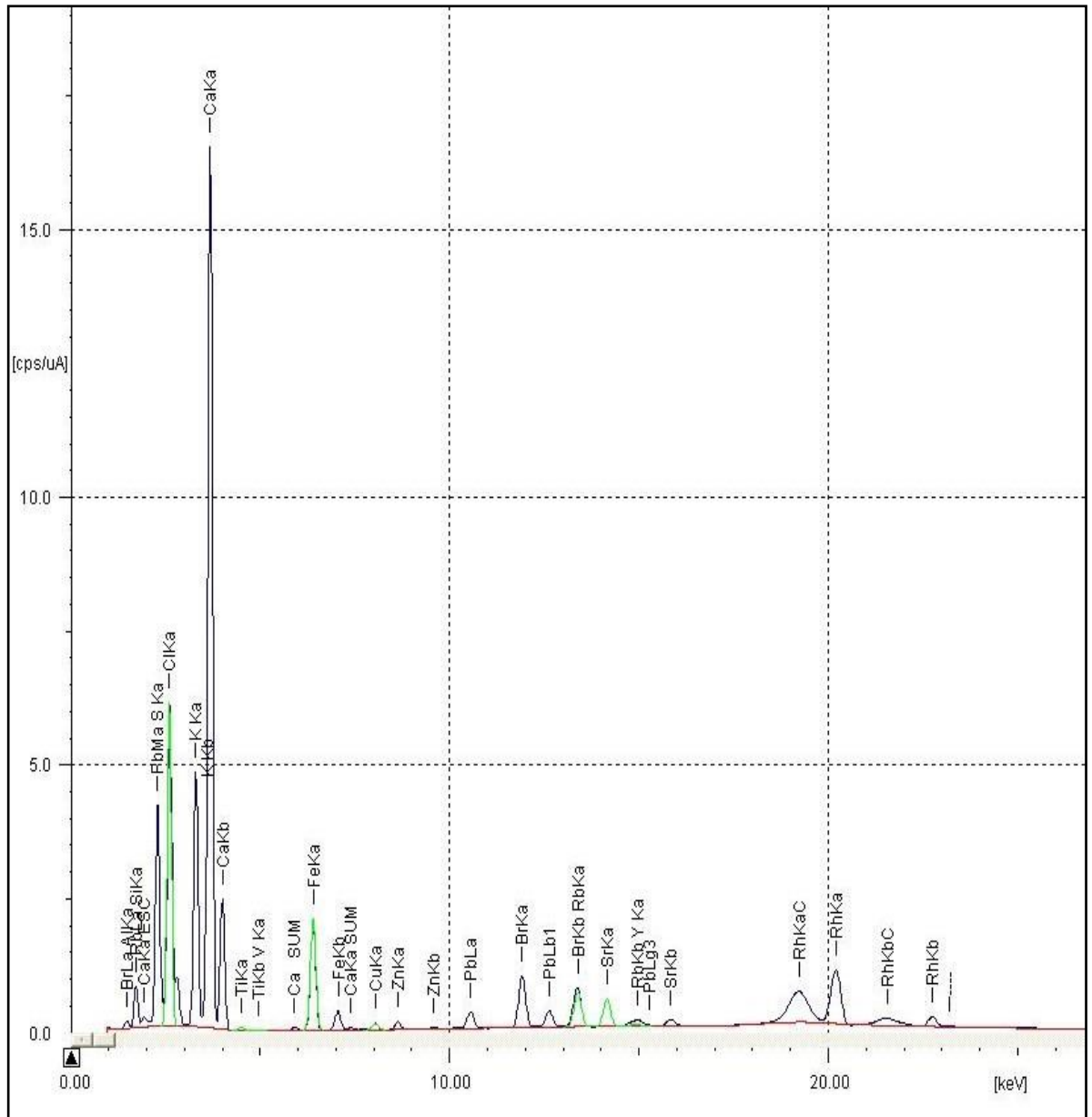
Table 6-2: XRF (quantitative) analysis of PSA

Description (chemical compound)	Percentage (%)
Calcium oxide CaO	40.42
Silicon dioxide SiO ₂	9.38
Aluminum oxide Al ₂ O ₃	5.87
Magnesium oxide MgO	1.37
Sulfur trioxide SO ₃	0.41
Iron trioxide Fe ₂ O ₃	0.26

6.6.3 XRF ANALYSIS FOR CKD

Graph 6-9 below shows the chemical compounds present in the CKD. Quantitative analysis for the CKD filler sample has been provided in table 6-3. The analysis reveals that the CKD filler is primarily composed of calcium oxide (27.43%), potassium oxide (8.22%), and sulphur trioxide (7.48%), chlorine (6.51%), silicon dioxide (3.91%) and aluminium oxide (2.01%) chemical compounds and element as indicated in the table referred above.

This shows that the CKD filler is also enriched with calcium oxide however, it is pozzolanic in nature therefore, it should be blended with a silicon rich material to be used as an alkali activator to further accelerate the hydration process which will help in pore refinement and would contribute to the strength improvement of CMM as discussed above in section 5.25.



Graph 6-9: XRF analysis of CKD

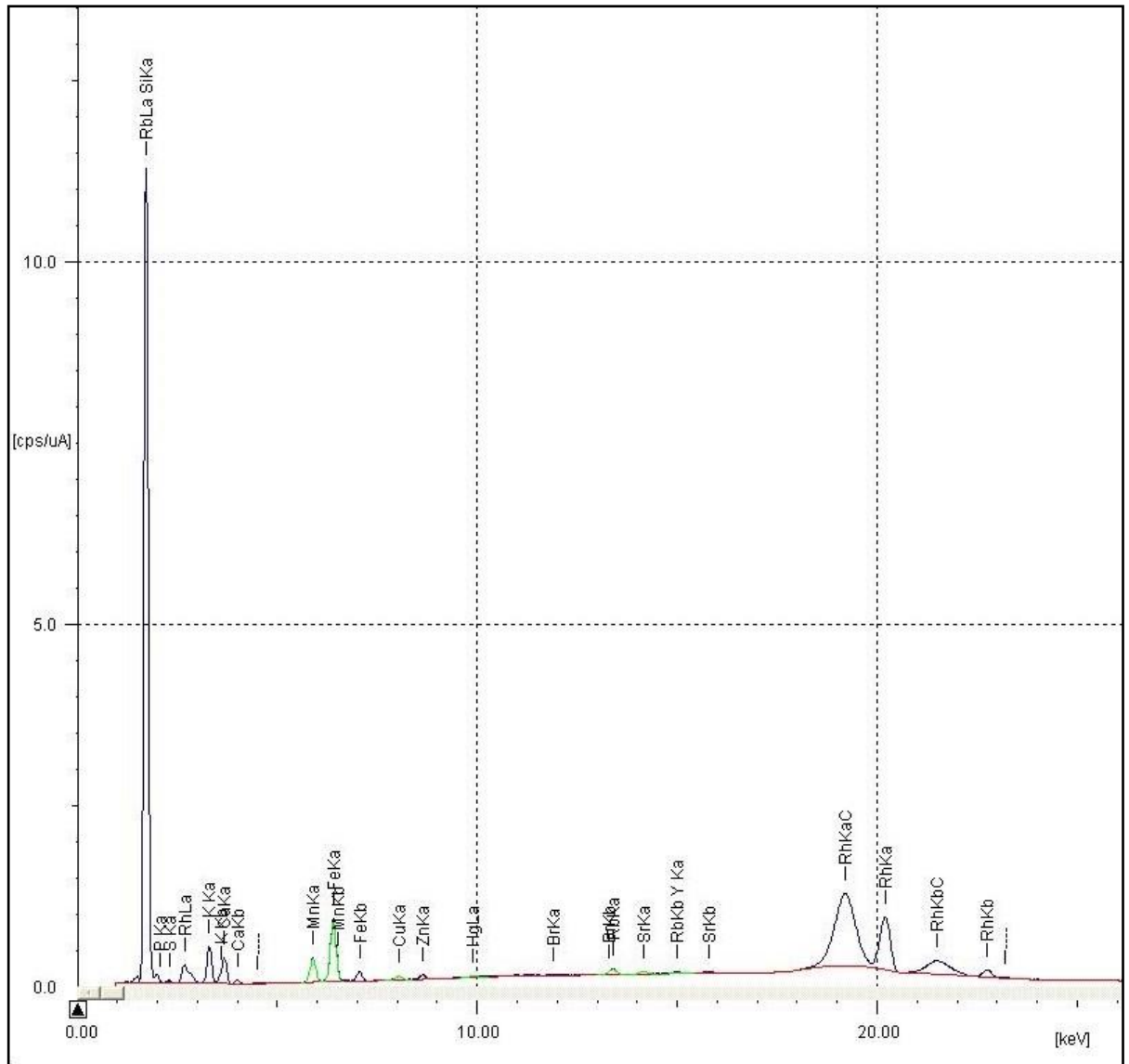
Table 6-3: XRF (quantitative) analysis of CKD

Description (chemical compound/element)	Percentage (%)
Calcium oxide CaO	27.43
Potassium oxide K ₂ O	8.22
Sulfur trioxide SO ₃	7.48
Chlorine Cl	6.51
Silicon dioxide SiO ₂	3.91
Aluminum oxide Al ₂ O ₃	2.01
Iron trioxide Fe ₂ O ₃	1.00

6.6.4 XRF ANALYSIS FOR RHA

Graph 6-10 shows the chemical compounds present in the RHA. Detailed quantitative analysis for chemical compounds in the RHA filler sample is given in the table 6-4 below. The analysis reveals that the RHA filler is composed of silicon dioxide (68.31%), aluminium oxide (1.59%) and potassium oxide (1.15%).

The PSA and CKD fillers are deficient of silicon dioxide content when compared to OPC however, the RHA filler has the advantage of being rich in silicon dioxide content. Fine RHA filler particles when mixed with the CKD in the cold mix microasphalt will enable both fillers i.e. CKD and RHA to serve as a good replacement for existing cement (OPC) and would further augment the bonding between the aggregates and bitumen as earlier discussed in section 5.25. Thus, consolidation of all the potential fillers will contribute to the development of a new and resilient green cement filler.



Graph 6-10: XRF analysis of RHA

Table 6-4: XRF (quantitative) analysis of RHA

Description (chemical compound)	Percentage (%)
Silicon dioxide SiO ₂	68.31
Aluminum oxide Al ₂ O ₃	1.59
Potassium oxide K ₂ O	1.15
Phosphorus pentoxide P ₂ O ₅	0.85
Calcium oxide CaO	0.50
Magnesium oxide MgO	0.27
Iron trioxide Fe ₂ O ₃	0.19

6.6.5 PARTICLE SIZE DISTRIBUTION OF FILLERS

Figure 6-4 illustrates the particle size distribution of OPC, PSA, CKD and RHA measured by laser diffraction particle size analyser (LDPZA). The mean

particle size of OPC, PSA, CKD and RHA were found to be 19.49, 15.17, 14.90 and 13.60 μm respectively. It is observed that the OPC has the largest size of filler particles and the RHA has the finest size of filler particles. Further, the particle size of PSA filler is finer as compared to the OPC filler particle size. It is germane to mention here that the particle size of filler materials has an energetic effect on the properties of CBEM in two terms: physically and chemically (Shakir, 2012). The finer particle materials lead to more pore refinement and a denser skeleton of mix is produced. Moreover, the fine particles also increase the reactive surface and therefore more hydration is expected. It can be seen that the selected fillers have particles size finer than the OPC filler particles size, this will result in more hydration thus contributing more to the CMM strength.

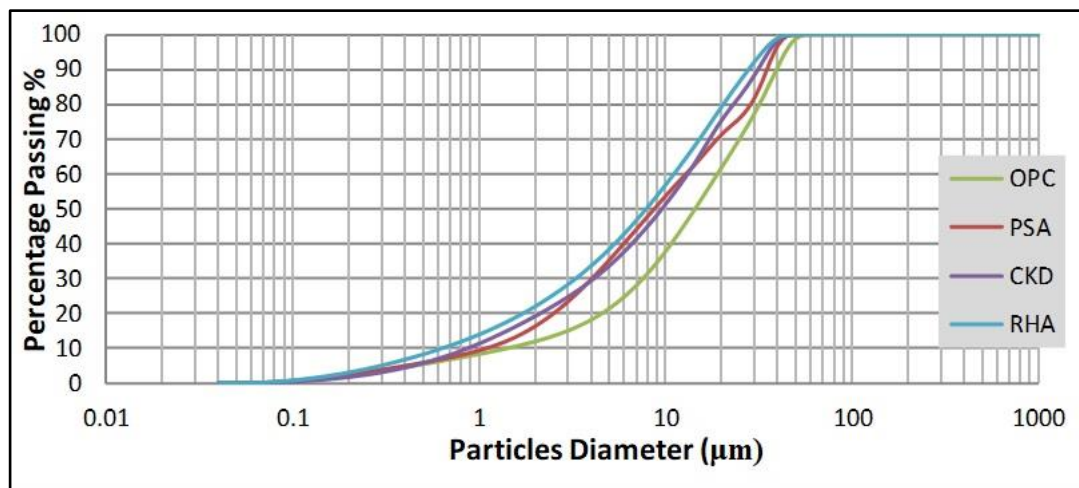


Figure 6-4: Particle size distributions for the selected fillers

6.6.6 MAIN OXIDES PERCENTAGES FOR FILLERS

Figure 6-5 represents the percentages of the main oxides for the selected fillers. It can be seen from the figure that the OPC is rich in calcium oxide with a reasonable percentage of silicon dioxide and aluminium oxide. On the other hand, the PSA is also primarily composed of calcium oxide with a small percentage of other contents i.e. silicon dioxide and aluminium oxide. The comparison below shows that the PSA possesses chemical compounds very similar to OPC and therefore, makes it a strong candidate for replacement of

OPC in the microasphalt mix i.e. it contains the oxide mainly required for the hydration process to act as a cementitious material. In addition, CKD is also rich in calcium oxide and acts as an alkali activator when mixed with silicon enriched material to further accelerate the hydration process and to enhance pore refinement in CMM as earlier explained in section 5.25. Moreover, PSA and CKD are deficient of silicon oxide content but on the other hand, the RHA filler possesses a significant quantity of silicon dioxide (68.31%). The presence of fine particles of silicon oxide rich RHA, when used with CKD in the mix, serves as a good replacement for existing cement (OPC) and enhances the bonding between the aggregates and bitumen as earlier discussed in section 5.25. Thus, amalgamation of all the potential fillers contributes to the development of a new and robust green cement filler.

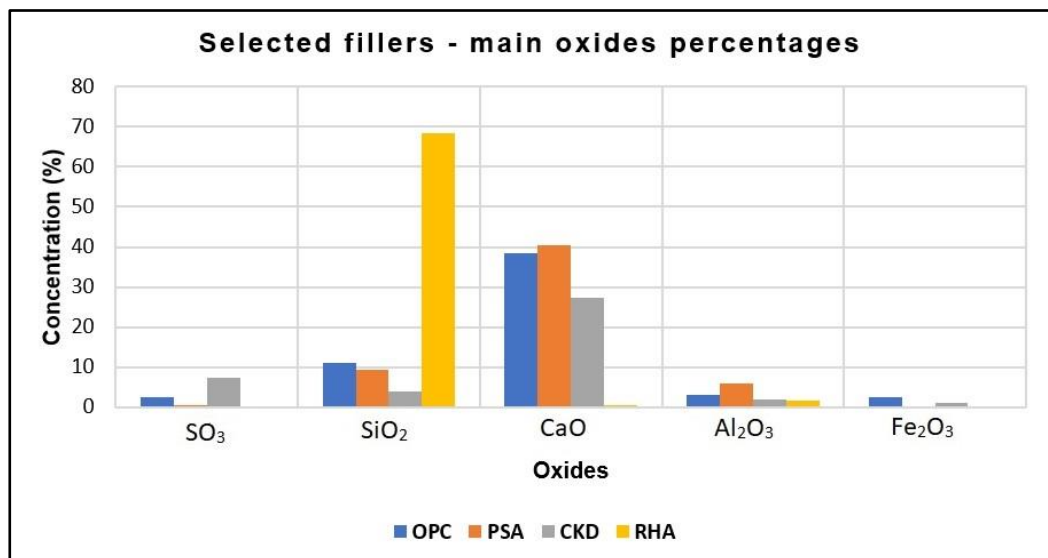


Figure 6-5: Main oxides percentages for the selected fillers

6.6.7 CHEMICAL & PHYSICAL CHARACTERISTICS OF FILLERS

Table 6-5 below provides the chemical and physical characteristics of the fillers investigated, including pH, oxides ratio, oxides content, specific surface area, density and particles size duly obtained from the test methods explained above in section 5.28.

Table 6-5: Chemical and physical characteristics of selected fillers

Properties	OPC	PSA	CKD	RHA
(Ca/Si) oxides	3.45	4.30	7.01	0.007
(Si+Al+Fe) oxides	15.63%	15.51%	6.02%	70.09%
pH	12.1	12.65	12.62	8.03
Specific surface area, BET (m ² /kg)	431	460	487	498
Density (kg/m ³)	2.956	2.422	2.41	2.90
Mean partial size (μm)	19.49	15.17	14.90	13.60

6.6.8 SEM ANALYSIS OF OPC POWDER & MASTIC

Figures 6-6 below display the morphology of the OPC powder and mastic at different ages. Dry OPC particles are irregular in shape and evenly distributed. OPC mastic forms an agglomerating structure, where OPC particles are distributed finely. Also, the density of the mix increased with time. Continuous micro-structure changes occurred with time for the hydrated OPC mastic, with new forms of micro-structure growing from OPC particles. SEM for OPC mastic provides the evidence of the hydration process, where the hydration products are easily observed. The ettringite, portlandite and calcium silicate hydrate (C-S-H) gel were observed and it continuously grew in volume to fill the free spaces to ultimately penetrate in bitumen gel as discussed in section 6.6.1 above.

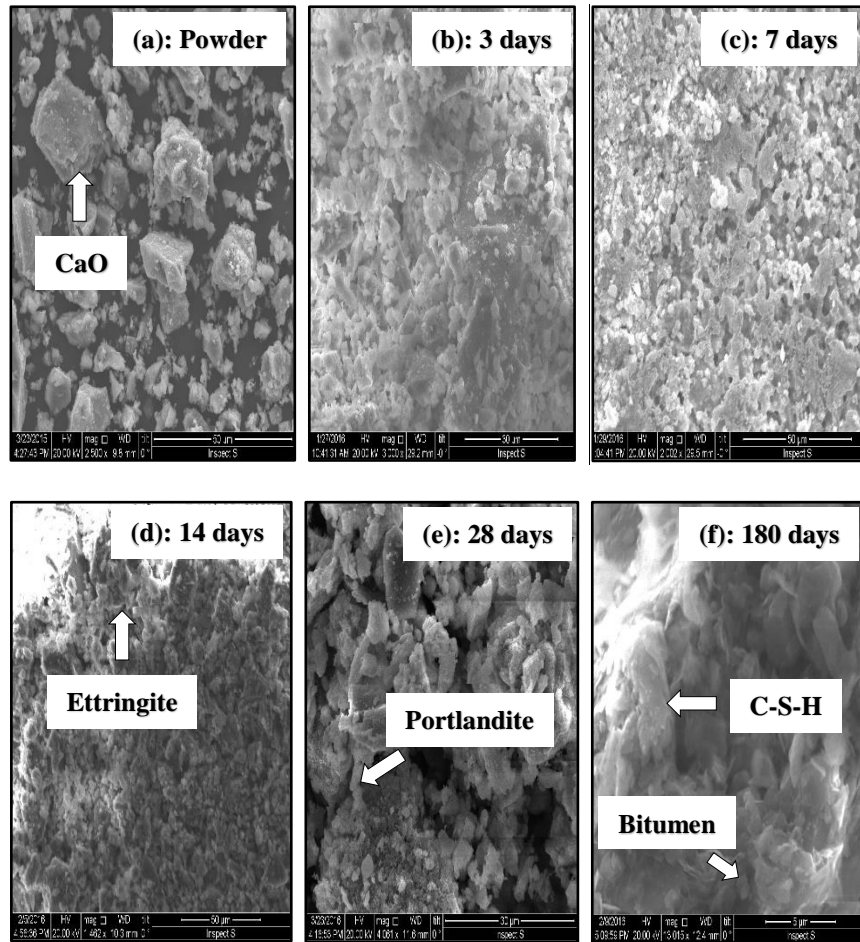


Figure 6-6: SEM analysis of OPC powder & mastic

6.6.9 SEM ANALYSIS OF PSA POWDER & MASTIC

SEM observations for PSA powder are presented in figure 6-7, together with PSA mastic observations after curing for 3, 7, 14, 28 and 180 days in figures (6-7: b, c, d, e and f), respectively. The morphology of the PSA powder indicates that PSA has generally agglomerated irregular particles and therefore, produces agglomerating mastic when mixed with water. Generally, PSA particles were distributed finely, and the structure is denser than OPC mastics. Also, the density of the mix increased with time. PSA mastics showed continuous morphological changes with time, with new forms growing from PSA particles. SEM confirmed the well observed hydration process. The portlandite, hydrotalcite and calcium silicate hydrate (C-S-H) gel were observed at the early stage, and then they kept growing to fill the free spaces and penetrate the bitumen gel. However, the hydration products are the main

reason responsible for microasphalt strength improvement, in similar mechanisms mentioned for OPC mastic and earlier explained in section 6.6.2 above.

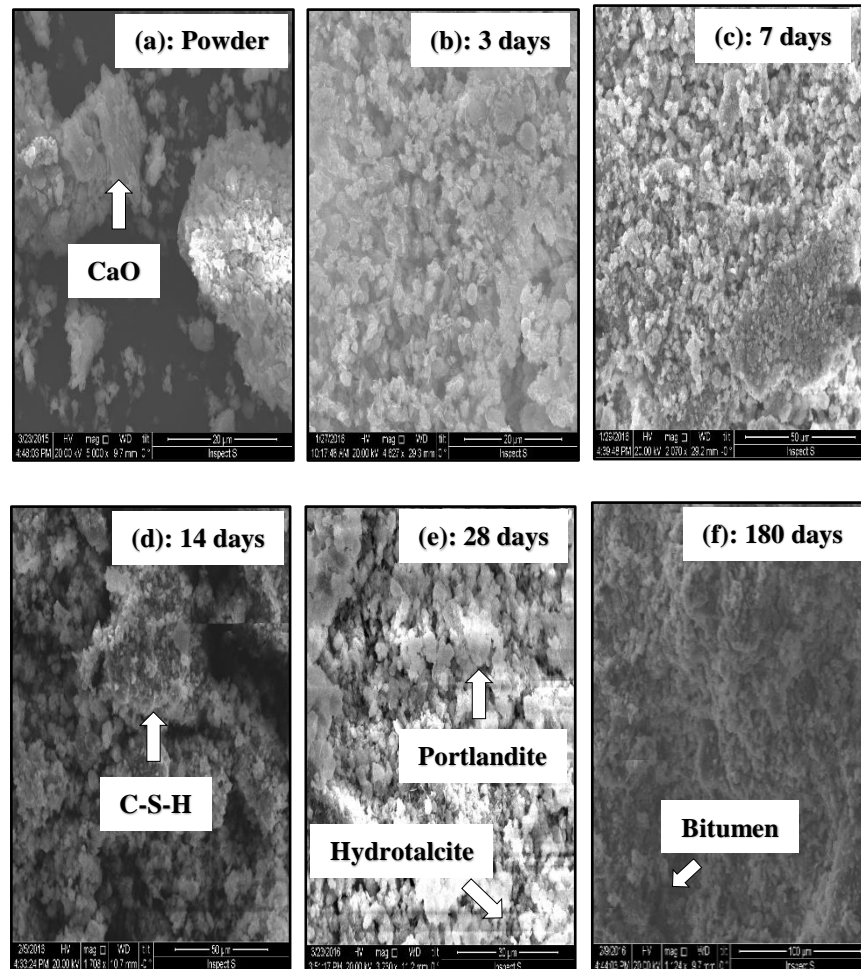


Figure 6-7: SEM analysis of PSA powder & mastic

6.6.10 SEM ANALYSIS OF CKD POWDER & MASTIC

Figures 6-8 illustrates the morphology of the CKD filler and hydrated mastic at different ages. The morphology of the CKD powder indicates that the CKD has generally agglomerated irregular particles. However, when CKD is blended alone with water, the CKD mastic does not produce any significant hydration products due to its pozzolanic nature. Description of pozzolanic materials and their reactivity property has been discussed in section 5.20 above i.e. they do not gain strength when blended alone with water. Further, balling or agglomerating of fine filler particles with emulsion occurs due to their high

specific surface area. They tend to absorb the emulsion and leave the aggregate particles uncoated. Thus, the CKD mastic, i.e. when CKD is used alone with water as a secondary cementitious filler, does not contribute to the strength of the microasphalt.

CKD particles due to the balling effect, were found randomly distributed and the structure was observed to be less dense than OPC and PSA mastics. SEM confirmed the formation of partial and weak calcium silicate hydrate (C-S-H) gel only which did not grow to fill the free spaces and penetrate the bitumen gel. Hence, the strength of the microasphalt was not enhanced. CKD is mainly enriched with the chemical compound calcium oxide (as discussed during the XRF analysis in section 6.6.3 above) and is classified as a pozzolanic material (as revealed during the discussion in section 5.25 above). The SEM observations further ratify the above findings. The CKD filler is a “silicon-loving” material and thus entails its blending with a silicon rich material. This will enable the CKD to further accelerate the hydration process and achieve pore refinement in microasphalt and to contribute to the strength improvement of CMM as discussed in sections 5.25 and 6.6, sub-section 6.6.3 above.

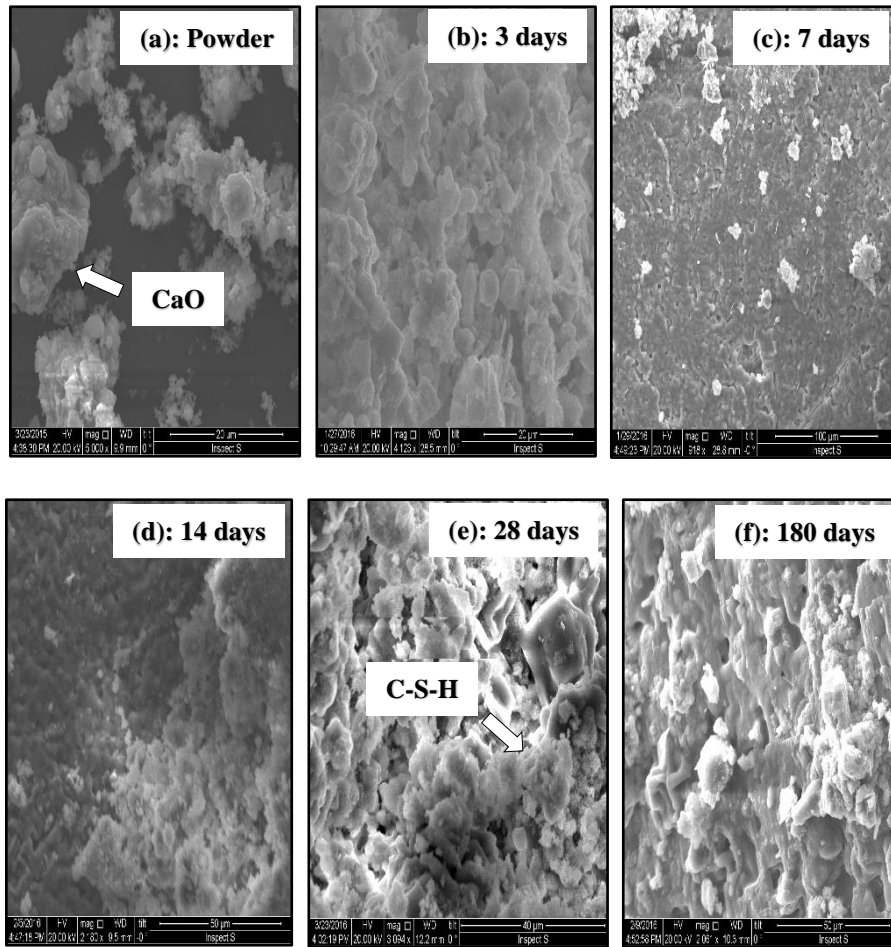


Figure 6-8: SEM analysis of CKD powder & mastic

6.6.11 SEM ANALYSIS OF RHA POWDER & MASTIC

Figures 6-9 shows the morphology of the RHA filler and mastic at different ages. The morphology of the RHA powder indicates that the RHA has mostly agglomerated irregular particles. However, when RHA is blended with water, the RHA mastic produces partial hydration products. Further, trivial balling effect or agglomerating of very fine filler particles with emulsion occurs due to their high specific surface area compared with OPC, PSA and CKD fillers (as indicated in section 6.6, sub-section 6.6.7, and table 6-5 during the chemical and physical characterisation of selected fillers). They tend to absorb less emulsion and do not leave the aggregate particles uncoated. Thus, the RHA mastic partially contributes to the strength of the microasphalt.

RHA particles, due to a fractional balling effect were found randomly distributed, and the structure was observed to be less dense than OPC and PSA mastics. SEM confirmed the formation of moderate calcium silicate hydrate (C-S-H) gel which partly grew to fill the free spaces and penetrate the bitumen gel, hence being responsible for partial strength gain in the microasphalt.

The PSA and CKD fillers are deficient of silicon dioxide content as witnessed during the XRF analysis of PSA and CKD in section 6.6, sub-section 6.6.2, section 6.6, and sub-section 6.6.3 respectively. However, the RHA filler has the advantage of being rich in silicon dioxide content as discussed in section 6.6, and sub-section 6.6.4. Fine RHA filler particles when mixed with the CKD in the cold mix microasphalt will enable both fillers, i.e. CKD and RHA, to further augment the bonding between the aggregates and bitumen as earlier discussed in section 5.25.

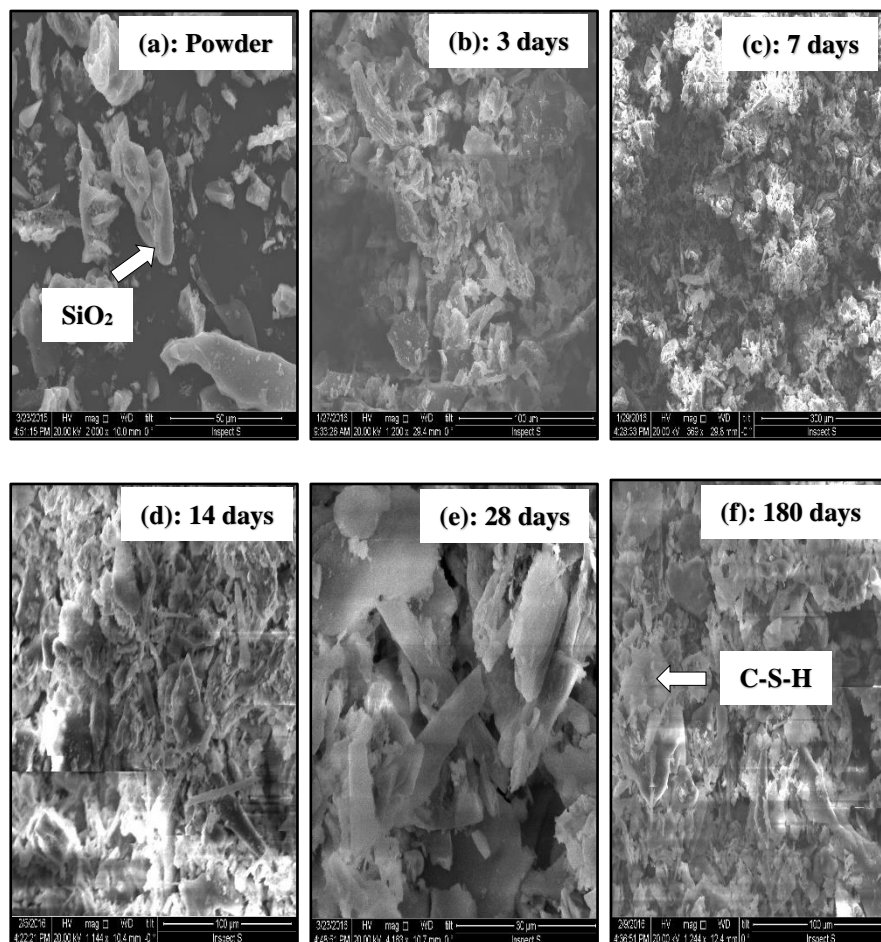


Figure 6-9: SEM analysis of RHA powder & mastic

6.6.12 SEM ANALYSIS OF BLEND (PSA, CKD & RHA) MASTIC

Comprehensive work has been done on optimising the proportion of PSA, CKD and RHA to develop the new and effective green cement filler blend. The blend is based on the compressive strength of PSA, CKD and RHA cube mortars at 28 days (Shakir, 2012; Abbas, 2014) and the following optimised values for the ingredients were obtained and used 0.76%PSA + 0.16%CKD + 0.08%RHA to prepare the blend mastic. The quantity of PSA is more in the blend mastic because PSA possesses very good absorption power due to high and active calcium oxide content in it, as learnt from the section 6.6.2 above and thus tends to absorb the entrapped water quickly within the mastic structure. Alongside this the chemical composition of the above-mentioned optimised ingredients imparts a synergistic effect and this results in the improvement of CMM strength which has been duly discussed in section 6.9 below. During the preparation of blend mastic, it was also observed that if the PSA, CKD or RHA quantities are further increased it tends to make the blend mastic stiffer and thus reduces the workability considerably.

SEM observations for the blend mastic after curing for 3, 7, 14, 28 and 180 days are presented in figures (6-10: a, b, c, d and e), respectively. From the physical characterisation of fillers (i.e. specific surface area of PSA, CKD and RHA fillers determined in section 6.6, sub-section 6.6.7, and table 6-5) and the SEM observations in figures 6-7-a, 6-8-a, and 6-9-a, it has been established that the morphology of the powders; PSA, CKD and RHA are generally agglomerated irregular particles.

The blend produces agglomerating mastic when mixed with water. Generally, the PSA, CKD and RHA particles were observed to be distributed finely and the structure deemed denser than OPC mastics. The density of the mix was observed to increase with time. Blended mastics showed continuous morphological changes with time, with new forms growing from blended particles. SEM confirmed the well observed hydration process. The ettringite, portlandite, hydrotalcite and calcium silicate hydrate (C-S-H) gel were

observed at early stages of curing. These continued to grow and increased in numbers to fill the free spaces and penetrate the bitumen gel. The hydration products developed from the fusion of blended filler ingredients are the main reason for the microasphalt strength improvement, in similar mechanisms mentioned for OPC mastic and during the XRF and SEM analysis of individual fillers vis-à-vis their role in the development of a new green cement filler in 6.6.2 - 6.6.4 and 6.6.9 - 6.6.11. above.

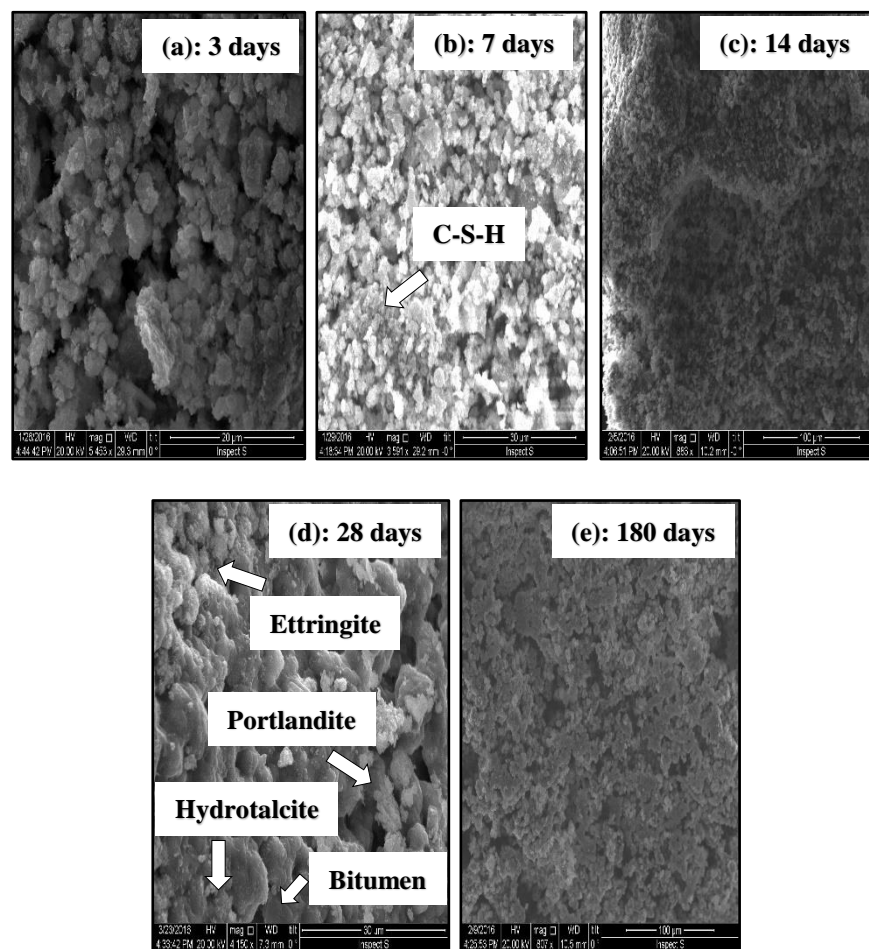


Figure 6-10: SEM analysis of blend (PSA, CKD & RHA) mastic

6.7 DISCUSSION

Filler plays significant physical and chemical roles in controlling the properties of microasphalt. Its physical and chemical characteristics could influence all preparations and service life stages. Thus, in this study, fundamental test methods were used to characterise selected fillers' properties. This helped in identifying the candidate waste

filler which could potentially replace the OPC in microasphalt. In contrast to OPC, the selected fillers were exposed to alkalinity, specific surface area and morphology:

6.7.1 ALKALINE NATURE

The alkaline nature of the filler compositions increases the alkalinity in the pores. Consequently, it activates the pozzolanic materials in the hydration process (Shakir, 2012). Increasing the alkalinity will increase the coalescence of the bitumen emulsion, which results in faster setting and strength gain (Shakir, 2012). Lime is mainly responsible for alkalinity (Lampris et al., 2008). None of the waste fillers tested exceeded the lime content of OPC, but the lime content of PSA was found to be similar, while the levels of lime in the RHA was found to be the lowest, as can be seen in table 6-1, 6-2, 6-3 and 6-4. Also, CKD and RHA exceed the OPC in terms of sodium and potassium content, respectively. Thus, with regards to high lime content, PSA impacts the alkalinity more than the other fillers under review.

The pH value of alkaline filler ranges between 8 to 14; 8 being the lowest and 14 being the highest. Strength achieved from the hydraulic cement is a direct result of the hydration process, and if less alkaline filler is used as a cementitious material in replacement of OPC filler, it may decrease the hydration process thus influencing the microstructure in CMM resulting in lower early strength. On the contrary, if more alkaline filler is used it will increase the hydration process resulting in a denser microstructure in CMM thus leading to higher earlier strength.

It can be seen from table 6-5 in section 6.6.7 above that the PSA filler has a pH value of 12.65 and is more alkaline in nature as compared to the OPC filler with a pH value of 12.10. Thus, PSA further enhances the hydration process as depicted in section 6.6.9 above with potential to increase the early strength of CMM. This initial hydration process will reduce the alkalinity of the filler in the microstructure of CMM and therefore, will reduce the hydration process at later stages which means that the PSA will not be able to actively contribute further to the hydration process in the long-term strength of the CMM.

The addition of CKD filler, which has a pH value of 12.62 and is also alkaline in nature, reacts with the by-products of the hydration reaction as indicated in section 6.6.12 above. Thus, long-term strength can be achieved using the pozzolans - CKD and RHA - which react more slowly but more thoroughly with the by-products of the hydration reaction to continue the strengthening process and thus enhance the pore refinement.

6.7.2 CEMENTITIOUS ACTION

Introducing filler material having cementitious properties namely; i) PSA, ii) CKD and iii) RHA to microasphalt possesses three advantages. Firstly, the hydration products offer secondary binding material. Secondly, secondary binding material reinforces the bitumen binder; and thirdly, the hydration process increases coalescence of bitumen emulsion by absorbing the water. In fact, the absorption is continued after coalescence by absorbing trapped water between the bitumen and aggregate. The critical components of OPC are calcium silicates as hitherto discussed in section 5.23, but also other oxides are very significant to the cement phases, and consequently its properties (Domone and Illston, 2010). These other main oxides are the aluminium and iron oxides, and the lesser ones are magnesium, sodium and potassium. However, the selected waste fillers showed variation in content of these oxides. In contrast to OPC, PSA showed close values of Ca/Si ratio and the sum of Si, Fe and Al, table 6-5. It can be seen from figure 6-5 that the PSA has almost identical oxide content to OPC. Other waste fillers showed less similarity in their oxide content. Thus, PSA when blended with CKD and RHA provides a better hydration process, when used as a replacement to the filler in microasphalt.

6.7.3 SPECIFIC SURFACE AREA AND PARTICLE SIZE

Particle size and fineness of filler materials have a “synergistic” effect on properties of microasphalt, both physically and chemically. The finer particle materials lead to a reduction in the pore and a denser skeleton is produced. Also, the fineness of filler increases the reactive surface and more hydration is

expected. Furthermore, increasing the specific surface area will increase the water absorption, which can affect the workability of the mix after a certain value. Table 6-5 shows that all fillers have specific surface area more than OPC, which is a positive indication that the fillers' surfaces will show activity in the present of water, consequently more hydration is expected. From the same table and from figure 6-4, the particle size properties showed that all fillers are fine and well graded, which is another positive indication in terms of mix backing properties. Waste fillers have shown encouraging properties in terms of particle size and specific surface area (refer to table 6-5) as compared to the OPC.

6.7.4 MORPHOLOGY

The morphology of a filler significantly influences the properties of the fresh microasphalt in terms of the workability and total water absorption. A highly porous filler with agglomerated particles will absorb more water into its pores (Shakir, 2012). Sharp irregularly shaped particles reduce the mix workability. From figures 6-6, 6-7, 6-8, 6-9, and 6-10 above it is clear that OPC has sharp and irregularly shaped particles; PSA, CKD and RHA have agglomerated irregular particles, especially PSA. Accordingly, PSA, CKD and RHA absorb more water with a significant impact on the workability.

6.8 SUMMARY ON FILLER DEVELOPMENT

The following key points are drawn from the work undertaken:

- a. Replacing OPC with PSA exclusively and then collectively in the blend introduces significant improvement in the hydration process in CMM as evidenced during the SEM analysis in section 6.6, sub-section 6.6.9, section 6.6, and sub-section 6.6.12 respectively. This is due to; (i) the high alkaline properties of PSA and CKD collectively as accentuated in section 6.7, and sub-section 6.7.1, (ii) the cementitious properties as discussed in section 6.7, and sub-section 6.7.2; which is identical to OPC, (iii) the high specific surface area as indicated in section 6.6, sub-section 6.6.7, and in table 6-5; duly discussed

in section 6.7, sub-section 6.7.3, and (iv) the agglomerated and porous mineral morphology coherent with discussion in section 6.7, and sub-section 6.7.4.

- b. Coalescence of bitumen emulsion increased as evidenced during the SEM analysis of GCF in section 6.6, sub-section 6.6.9 and section 6.6, sub-section 6.6.12 respectively; due to the rise in pH, where the pH in the mixture's pores changes from around 6 to about 12.65 as indicated in section 6.6, sub-section 6.6.7, and in table 6-5 duly discussed in section 6.7, and sub-section 6.7.1.
- c. Hydration products improved due to the addition of hydraulic ingredients supplied by the GCF blend. These products lead to initiate secondary binding material, and simultaneously strengthen and reinforce the primary bitumen binder.
- d. Absorption of water improved as a result of the hydration process as evidenced during the SEM analysis of the GCF paste in section 6.6, and sub-section 6.6.12. The high absorbability of PSA resulted from its morphology, high specific surface area and chemical phases as outlined in section 6.7, sub-sections 6.7.1, 6.7.2, 6.7.3 and 6.7.4 respectively.
- e. Characterising the filler offers a tool to predict its potential to improve the mechanical and durability properties of microasphalt. This characterisation includes chemical composition, pH value, specific surface area and particle morphology.
- f. The successful candidate filler to improve microasphalt should possess a combination of high pH, specific surface area, and cementitious chemical phases further to agglomerating morphology.

6.9 NEW CEMENTITIOUS FILLER TEST RESULT ANALYSIS

The SCBT was carried out on samples prepared by replacing the OPC filler used earlier in the study in the glass fibre reinforced microasphalt mix with an equivalent

quantity of green cement filler GCF blend containing PSA, CKD and RHA. The GCF blend was optimised in the laboratory by using varied percentages of 1%, 1.5%, 2.0 and 2.5% by total weight of the dry aggregates in the mix. It was observed, during the preparation of samples, that if the quantity of the new GCF is increased more than 1% in the mix then the mixing time reduces drastically, and the material tends to get dry more quickly by absorbing the bitumen emulsion and water content in the mix. The mixing time for the primary filler OPC and the secondary filler GCF is recorded as 20 minutes if they are used at 1% of the total weight of the dry aggregates in the mix but if the percentage of GCF is exceeded up to the above-mentioned trial percentages it reduces the mixing time up to 5 minutes. For practical reasons, this reduction in the mixing time was not deemed suitable for placing the microasphalt material on site due to workability issues and thus the substituted quantity of OPC filler with GCF blend was restricted to 1% by total weight of the dry aggregates in the mix. Comprehensive work has been done on finding the proportion of ingredients: PSA, CKD and RHA to make the new green cement filler blend. The optimised ingredients of GCF blend amounting to 1% by total weight of the dry aggregates in the mix was used in the proportion 0.76%PSA + 0.16%CKD + 0.08%RHA. The GCF blend is based on the compressive strength of PSA, CKD and RHA cube mortars at 28 days and the above optimised values were obtained (Shakir, 2012; and Abbas, 2014) as also explained in section 6.6, and sub-section 6.6.12 above.

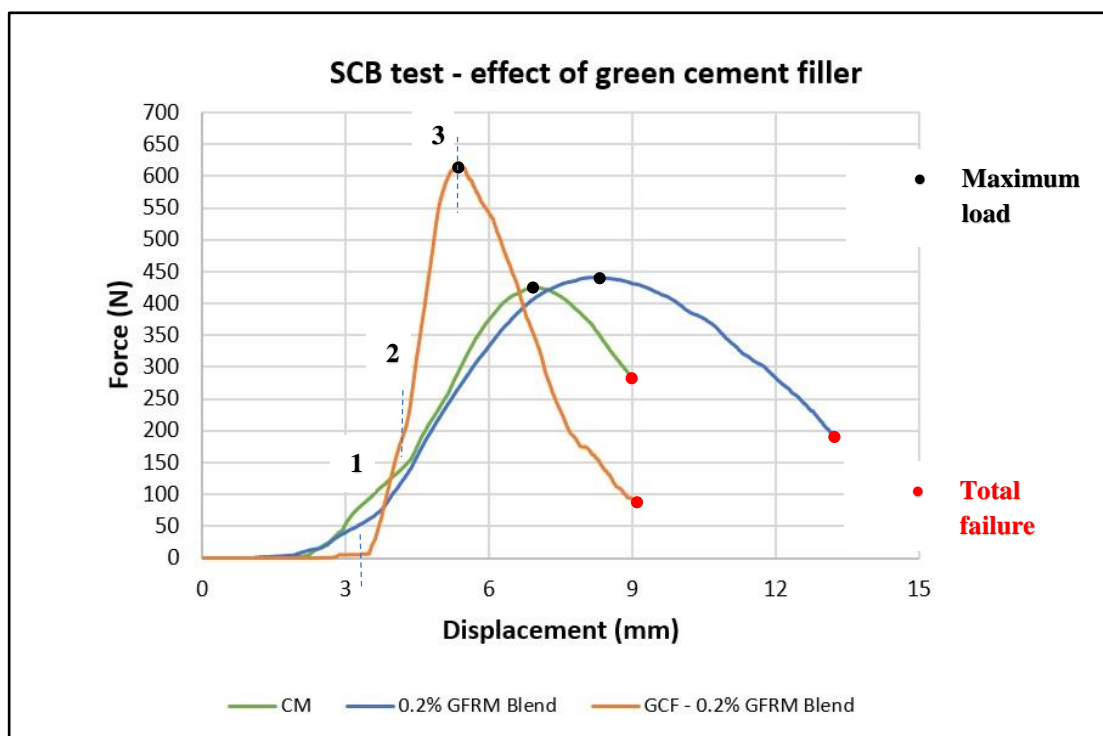
The data points for the GCF fiberized microasphalt (averaged for four samples) were plotted in graph 6-11 below. The effect of replacement of OPC with GCF is driven by a change in the area under the curve as an indication of the energy absorbed. The GCF fiberized microasphalt experienced lesser softening behaviour i.e. quick drop in load value after reaching the peak load than the GFRM samples with OPC. The peak flexural load for the GCF fiberized microasphalt is 620N while for GFRM with OPC filler the peak flexural load is 450N which means the secondary green cement filler has considerably improved the resistance of fiberized microasphalt to cracking by 27%. Similarly, GCF fiberized microasphalt has offered an improvement of up to 31% to resist the cracks compared with control microasphalt with OPC filler (as evaluated by the area under the load deflection curve).

The displacement for GCF fiberized microasphalt is recorded as 5mm at the peak load, and for the GFRM samples with OPC filler the displacement value is 8.2mm. This means the replacement of GCF has compromised the ductility of fiberized microasphalt by 39% compared with GFRM samples with OPC filler.

The plastic region for GCF fiberized microasphalt comprises of three phases. In the first phase, there is no cracking, in the second phase, cracking initiates and in the third phase maximum cracking occurs at the peak load. If the SCB curve for GCF fiberized microasphalt is divided into small fragments within the phases above i.e. in between the plastic region where the displacement ranges from 4mm to 5.2mm, it is observed that the slope of the GCF fiberized microasphalt curve is steep as compared to the CM and GFRM curves. The force at 5mm of displacement is recorded as 550N for the GCF fiberized microasphalt but the force at 5mm of displacement in the CM and GFRM corresponds to approximately 225N. This shows significant enhancement in the load bearing capacity of the GCF fiberized microasphalt i.e. up to 59% higher as compared to the CM and GFRM and thus suggests substantial improvement in resistance to cracking for the GCF fiberized microasphalt. Further, when the force increases from 550N to 620N the corresponding displacement is recorded as 5mm and 5.2mm. This shows that the fractional displacement of 0.2mm is able to sustain a significant amount of force i.e. up to 70N. Moreover, a displacement of 1.2mm in GCF fiberized microasphalt i.e. from 4mm to 5.2mm is important in crack prevention. However, further investigation may be needed to confirm the importance of displacement.

The GCF fiberized mixes have more resistance to cracking but on the contrary, it has been observed that the samples after attaining the peak load value do not fail in a smooth manner i.e. these samples do not provide ample warning and thus reach ultimate failure point swiftly after the peak flexural load. This implies that the new cementitious filler has marginalised the advantage of smooth failure achieved in the GFRM samples containing the primary OPC filler. This is due to the fact that the secondary GC filler has absorbed the entrapped water in the mix and a chemical reaction has taken place which results in the formation of a cementitious material i.e. cement within the microasphalt structure. A major component of the load is taken by

the cement composition and the glass fibre present in the microasphalt does not fully play its role to ensure smooth failure in the GCF fiberized microasphalt samples because the new cement has more strength as compared to the fibres in the mix and that is why the failure in GCF fiberized microasphalt offers elasticity i.e. it is less ductile. The GCF fiberized microasphalt has perceived advantages and disadvantages. The ductility of the GCF fiberized microasphalt can further be improved by carrying out a further research. However, the major contribution of the newly developed material is that it does not involve any carbon emissions and has offered more resistance to cracking.



Graph 6-11: Effect of green cement filler in microasphalt (SCBT)

WTT was conducted by replacing the OPC filler earlier used by 1% of the total weight of the dry aggregates in the glass fibre reinforced microasphalt mix with an equivalent quantity of the GCF blend i.e. 1% by total weight of the dry aggregates in the mix. Ingredients proportion i.e. for PSA, CKD and RHA in the green cement filler were kept as optimised and indicated in the SCB test above for the GCF - 0.2% GFRM blend. The data points for the GCF fiberized microasphalt were plotted in graph 6-12 below. The effect of replacement of OPC with GCF is driven by change in the area between the 0.2% GFRM and GCF - 0.2% GFRM blend deformation curves as an

indication of further improvement in resistance to rutting due to the simulated traffic loading.

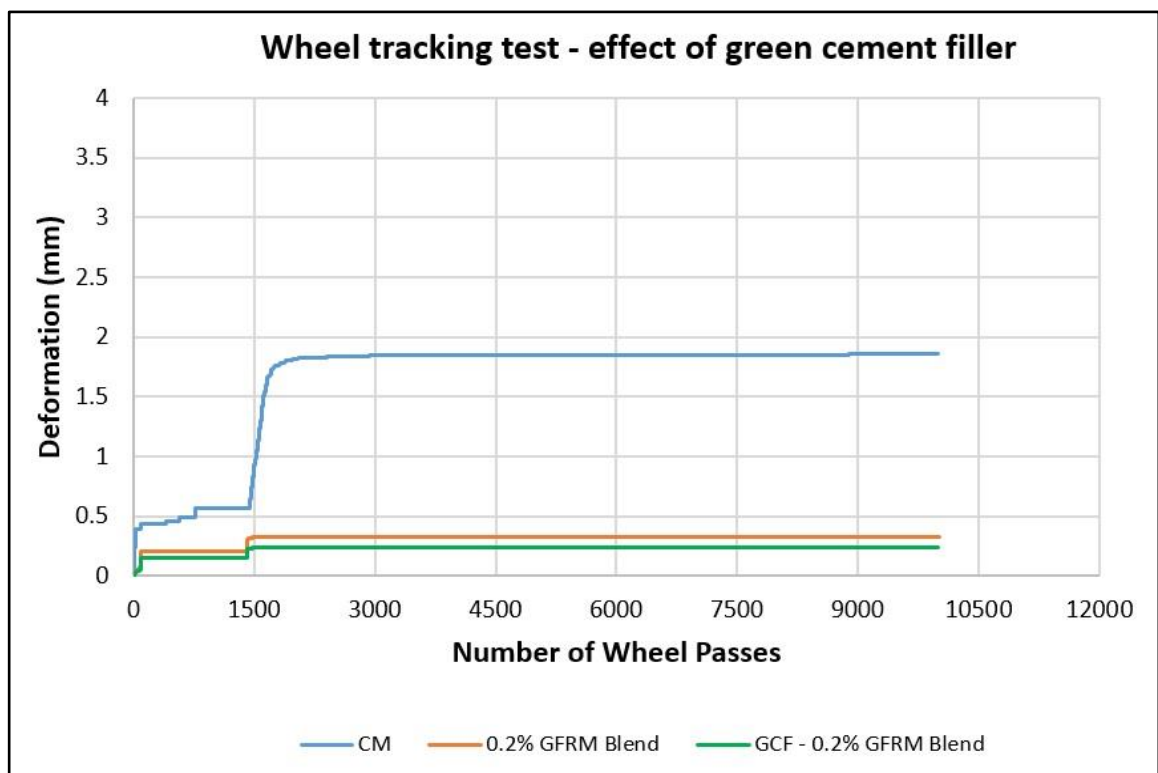
The control microasphalt deformation was earlier more susceptible to rutting in its early life when opened to traffic as concluded from the literature review and during the previous series of deformation testing has been outperformed by the GCF - 0.2% GFRM blend. The GCF - 0.2% GFRM blend has improved the rut potential (RT) by reducing the softening behaviour of CM and 0.2% GFRM under the wheel load and is less prone to deformation distress, which shows the positive effect of replacement of OPC with GCF in the microasphalt derived from the WTT.

The test results show that the GCF - 0.2% GFRM blend tends to gain more strength during the early life of the microasphalt, and further consolidates with the time as compared to both the control and the glass fibre reinforced microasphalt with conventional cement filler. This underpins the conclusion derived in the characterisation of green cement filler in sections 6.6 and 6.7 correspondingly above, that the GCF tends to gain early and long-term strength due to the evolution of the hydration process that takes place within the microstructure of the microasphalt. Thus, resulting in significant improvement in the deformation property of the microasphalt.

The addition of GCF in the glass fibre reinforced mix reduces the softening behaviour of microasphalt and thus plays its intended resilience function to arrest the rutting initiation process in the early life of the microasphalt i.e. when it is more vulnerable to deformation either due to the cold mix material in question or the underlying (existing) structural and functional condition of the pavement. For GCF - 0.2% GFRM blend, in the start, i.e. up to 1,500 wheel passes, there is a partial rise in the deformation curve recorded up to 0.22mm but during this transition phase when the microasphalt starts to gain strength, the gradient of the curve is not as steep as that observed in the CM mix, and deformation in the GCF - 0.2% GFRM blend from then onward remains steady until the completion of 10,000 wheel passes.

The GCF - 0.2% GFRM blend exhibited improvement in the deformation property of the microasphalt, up to 15%, as compared to the 0.2% GFRM blend after 10,000 wheel

passes. Similarly, the GCF fiberized microasphalt has offered an improvement of up to 85% in deformation resistance compared with the control microasphalt with OPC filler. During the transition period explained above, deformation i.e. after 1,500 wheel passes the GCF - 0.2% GFRM blend mixes showed an improvement in the deformation up to 78% as compared to the control microasphalt. Hence, the GCF - 0.2% GFRM blend essentially does not allow excessive deformation to accumulate within the microasphalt as compared to CM under the repeated traffic loading, since it is a potential source of wheel path rutting at the pavement surface as explained in section 5.3 in chapter 5 above.



Graph 6-12: Effect of green cement filler in microasphalt (WTT)

In summary, the GCF offered strength enhancement to the mix in comparison to the OPC in addition to improving the cracking and deformation resistance of the microasphalt, based on the SCB and WT test results discussed above; mainly due to the reasons explicated in section 6.8 above i.e. the high PSA absorption which facilitates the gain in strength, as it removes the trapped water (the main cause of inferior microasphalt strength).

6.10 TEST RESULTS FOR THE FEM

Experimental results for the composite CM, 0.2% GFRM blend and GCF - 0.2% GFRM blend mixtures have been simulated in the Abaqus software. Figure 6-11 (a-f) below shows the stress concentration zone (SCZ) in the CM, 0.2% GFRM blend and GCF - 0.2% GFRM blend specimens. The extent and severity of damage due to the tracked wheel load results in rutting phenomena in CMM and has been modelled with the help of loaded wheel distribution contours (LWDC) within the embodied specimens. The colour coding legend shows the stress induced concentration areas (SICA) areas in the specimen. Red depicts the highest SCZ in the WTT and blue shows the lowest extent of SCZ. The 3D FE simulations in figure 6-11 (a-f) illustrate the LWDC in the CM, 0.2% GFRM blend and GCF - 0.2% GFRM blend specimens. Under the tracked wheel load application i.e. in the central median of the specimen the deformation level is high, and the deformation level tends to dissipate from top to bottom within the sample. From figure 6-11 (a-f), it can be seen that the cumulative values for the SCZ with severe deformation (red, orange, mustard and yellow) are high in the CM mix as compared with the 0.2% GFRM blend and GCF - 0.2% GFRM blend mixes. This underpins the fact that the CM mix is experiencing more deformation within the specimen and is more prone to rutting damage as earlier evidenced during the experimental results duly explained in section 6.4, and illustrated in graph 6-6. The CM FE model clearly suggests that due to high LWDC values the deformation resistance of CM mix reduces therefore, the rut potential accelerates in the CM specimen and thus is the cause of early rutting in the CM mix. Consequently, the deformation of the CM mix due to high SCZ values causes the specimen to deform and re-meshing of cohesive elements in the CM FE model takes place as illustrated in figure 6-11 (a-b). The two figures are the same; figure 6-11 (a) shows the top view and figure 6-11 (b) shows the bottom view of the same model.

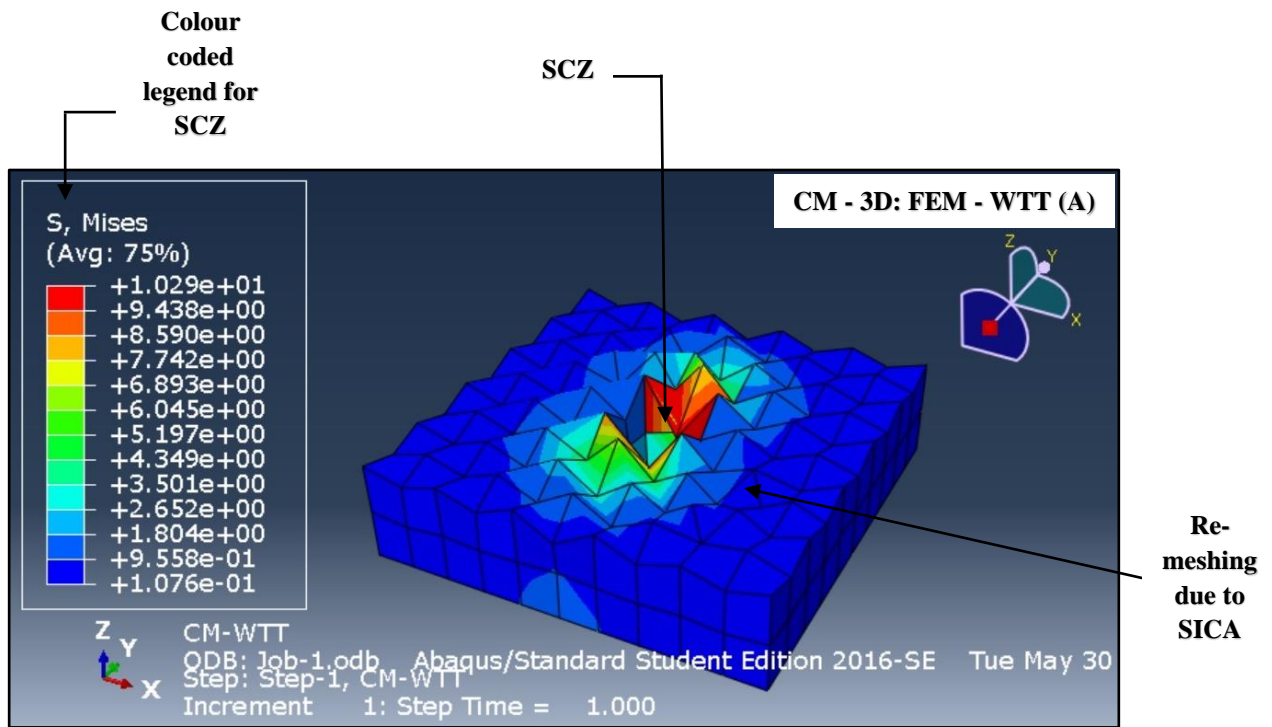


Figure 6-11 (a): Stress concentration zone 3D FE modelling for the CM - WTT (A)

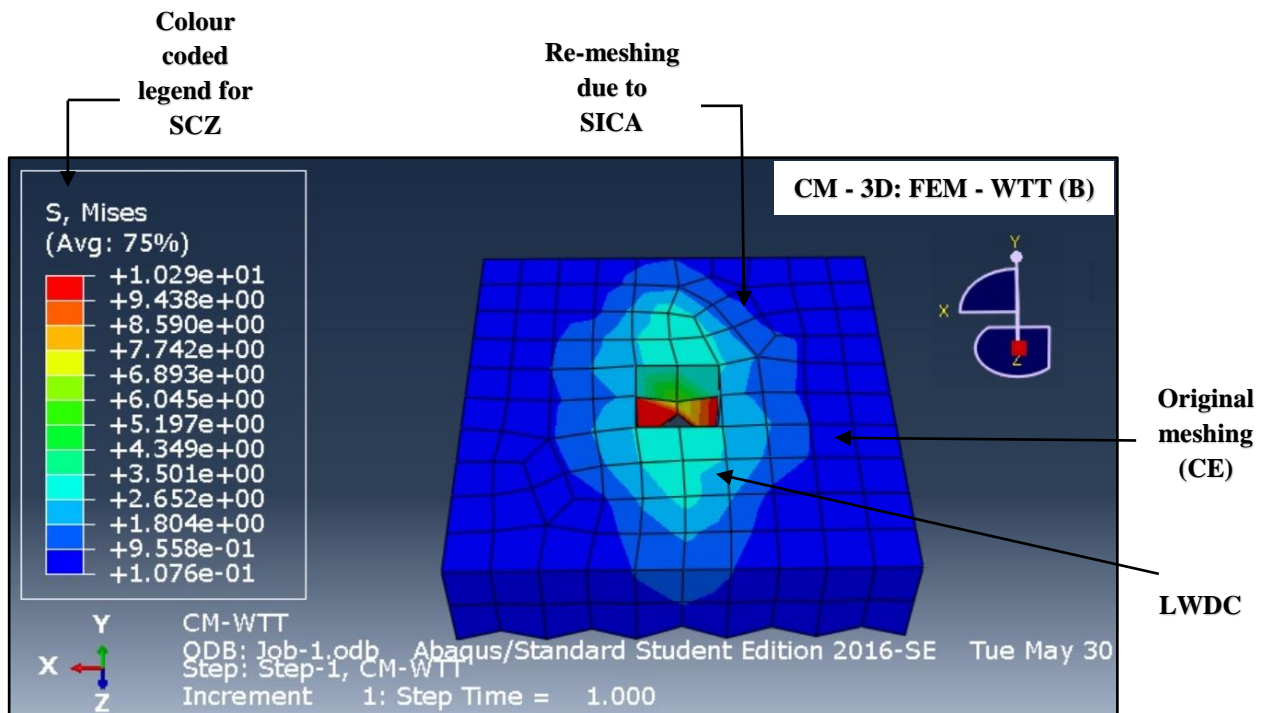


Figure 6-11 (b): Stress concentration zone 3D FE modelling for the CM - WTT (B)

Similarly, in figure 6-11 (c-d) below, the 0.2% GFRM blend FE model suggests that the SCZ cumulative values (red, orange, mustard and yellow) have more severity and the extent of deformation has reduced considerably as compared to the SCZ values in the CM FE model. From the colour coded SCZ legend, in figure 6-11 (c-d), it can be seen that the values of colour codes (red, orange, mustard and yellow) depicting severe SCZ has decreased and the values of colour codes (dark blue, medium blue and light blue) showing the lowest extent of SCZ has also decreased as compared with the SCZ values in figure 6-11 (a-b) above for the CM FE model thus the 0.2% GFRM blend has more resistance to deformation when a tracked wheel load is simulated. This improvement, observed in the 0.2% GFRM blend mix is associated with the addition of glass fibre reinforcement (GFR) in the microasphalt which has enhanced the deformation endurance strength of the 0.2% GFRM blend mix and therefore, is contributing significantly in retarding the rut potential, and hence controls the rutting phenomena in the 0.2% GFRM blend samples. The 0.2% GFRM blend FE model reinforces the significance of the addition of GFR in the microasphalt, as evaluated during the experimental results achieved in the laboratory duly discussed in section 6.4, and graph 6-6 above. This clearly shows that a consensus exists between the 0.2% GFRM blend FE model and the experimental findings.

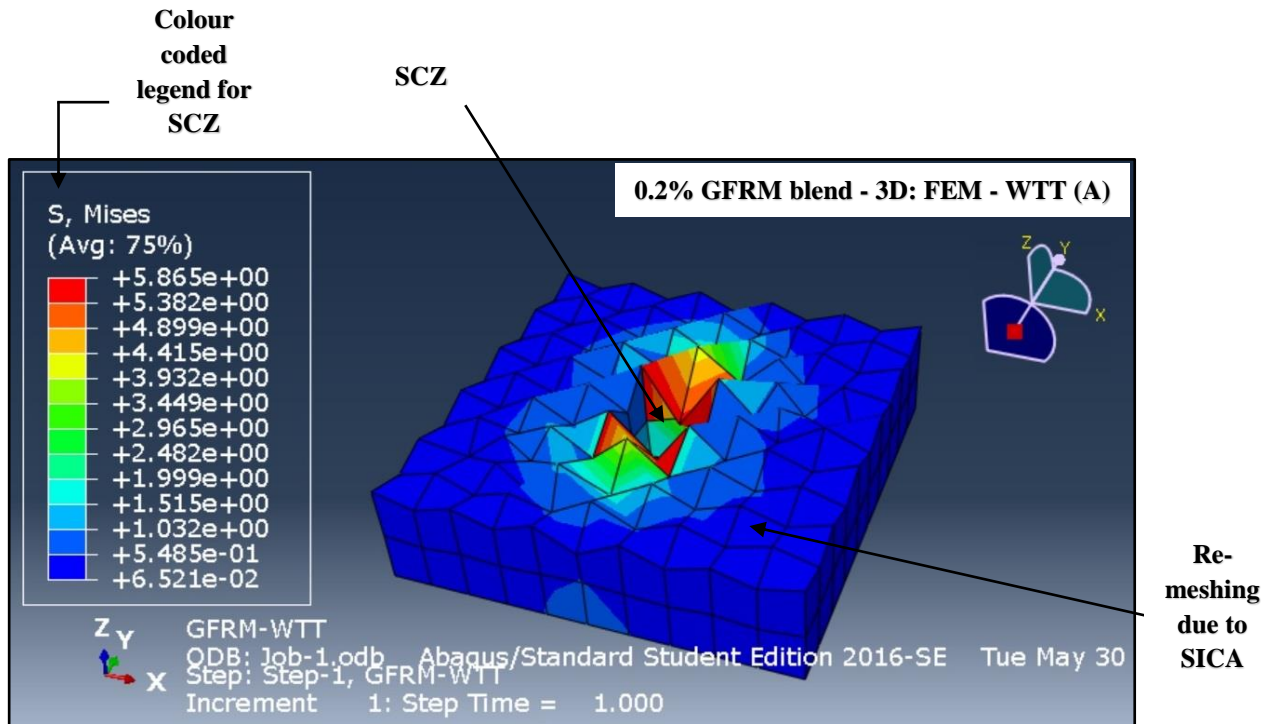


Figure 6-11 (c): Stress concentration zone 3D FE modelling for the 0.2% GFRM blend - WTT (A)

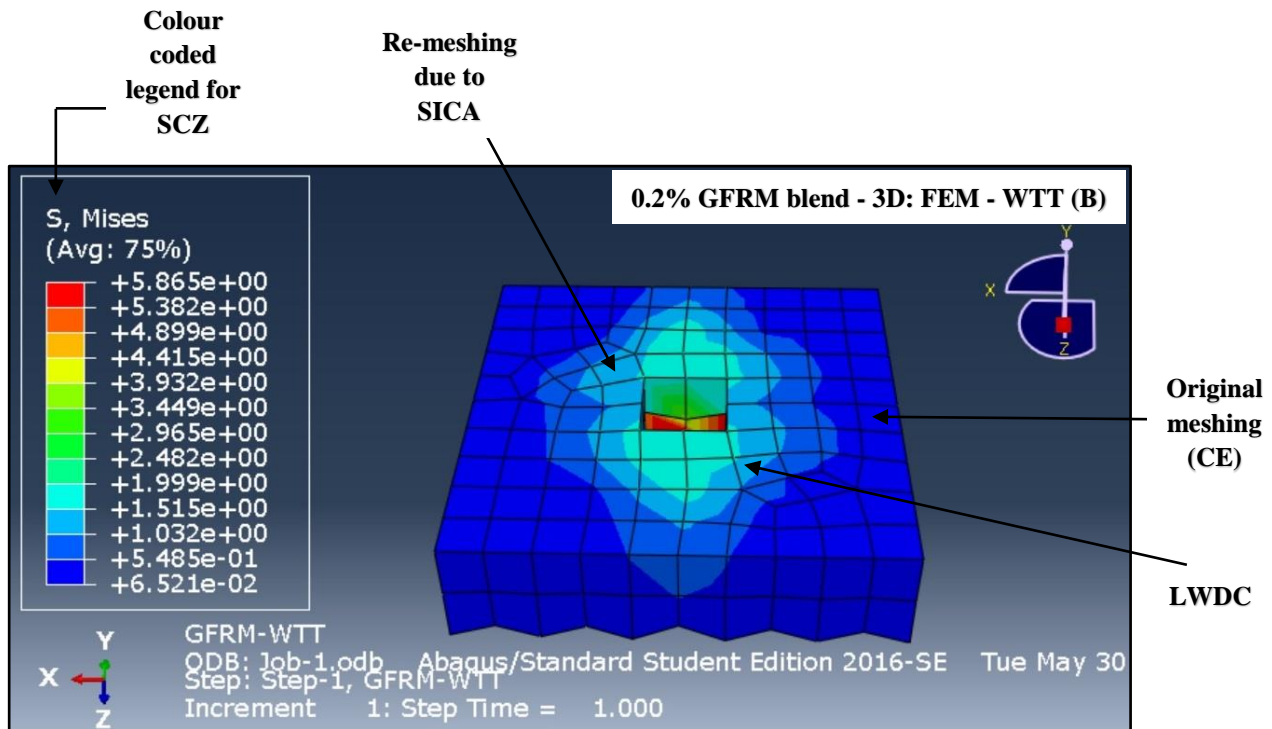


Figure 6-11 (d): Stress concentration zone 3D FE modelling for the 0.2% GFRM blend - WTT (B)

Figure 6-11 (e-f) below, illustrates the simulated GCF - 0.2% GFRM blend FE model. It has been observed that the SCZ cumulative values (red, orange, mustard and yellow) representing more severity and extent of deformation have further meaningfully reduced as compared to the SCZ values in the CM FE model and 0.2% GFRM blend FE model respectively. From the colour coded SCZ legend, in figure 6-11 (e-f), it is evident that the values of colour codes (red, orange, mustard and yellow) showing severe SCZ has substantially decreased and the value of colour codes (dark blue, medium blue and light blue) depicting the lowest extent of SCZ has also significantly decreased as compared with the SCZ values in figure 6-11 (a-b) and figure 6-11 (c-d) above for the CM FE and 0.2% GFRM blend models thus the GCF - 0.2% GFRM blend is resisting more deformation within the embodied specimen when a tracked wheel load is applied. This improvement in the 0.2% GFRM blend mix is attributed to the replacement of OPC with the newly developed GCF in the microasphalt which has further enhanced the deformation resilience of GCF - 0.2% GFRM blend mix and therefore, is playing an important role in retarding the rut potential and hence is more effective in controlling the rutting phenomena in the GCF - 0.2% GFRM blend samples. The GCF - 0.2% GFRM blend FE model ratifies the positive implication of replacement of OPC with the GCF in the microasphalt as assessed during the experimental results attained in the laboratory and accordingly discussed in section 6.9, and graph 6-12 above. This confirms that the GCF - 0.2% GFRM blend FE model and the experimental findings articulate with each other.

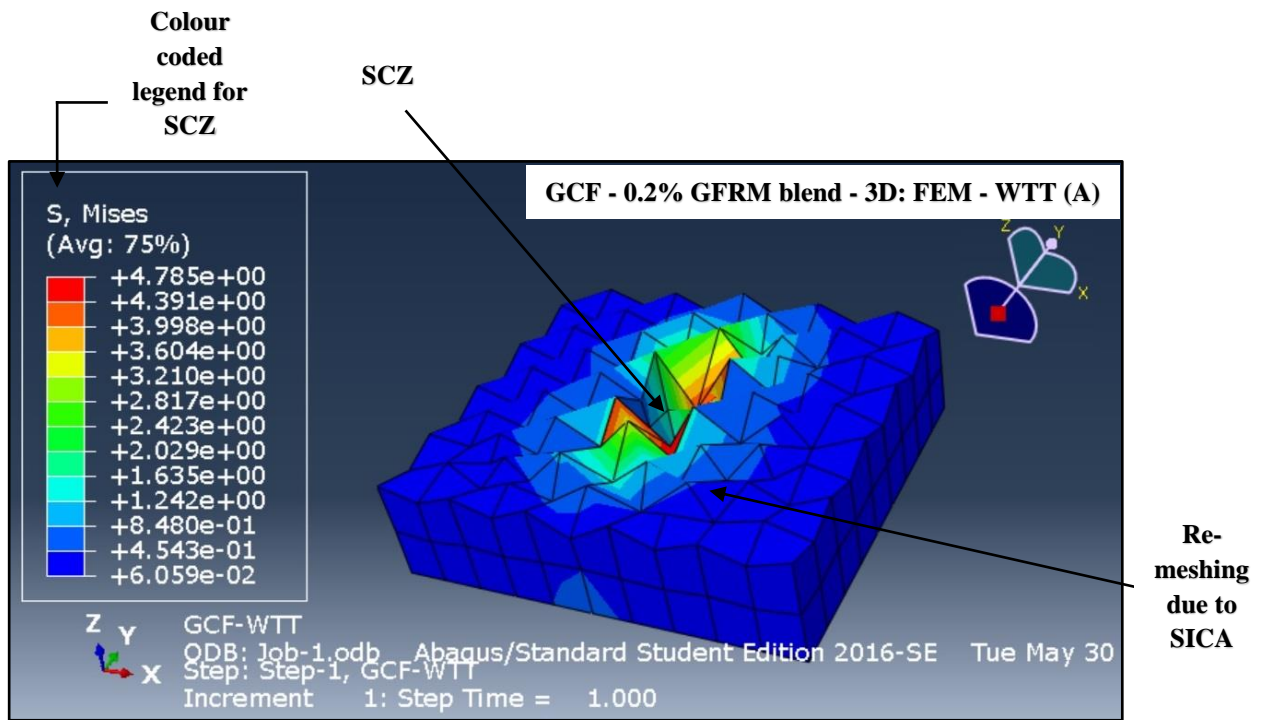


Figure 6-11 (e): Stress concentration zone 3D FE modelling for the GCF - 0.2% GFRM blend - WTT (A)

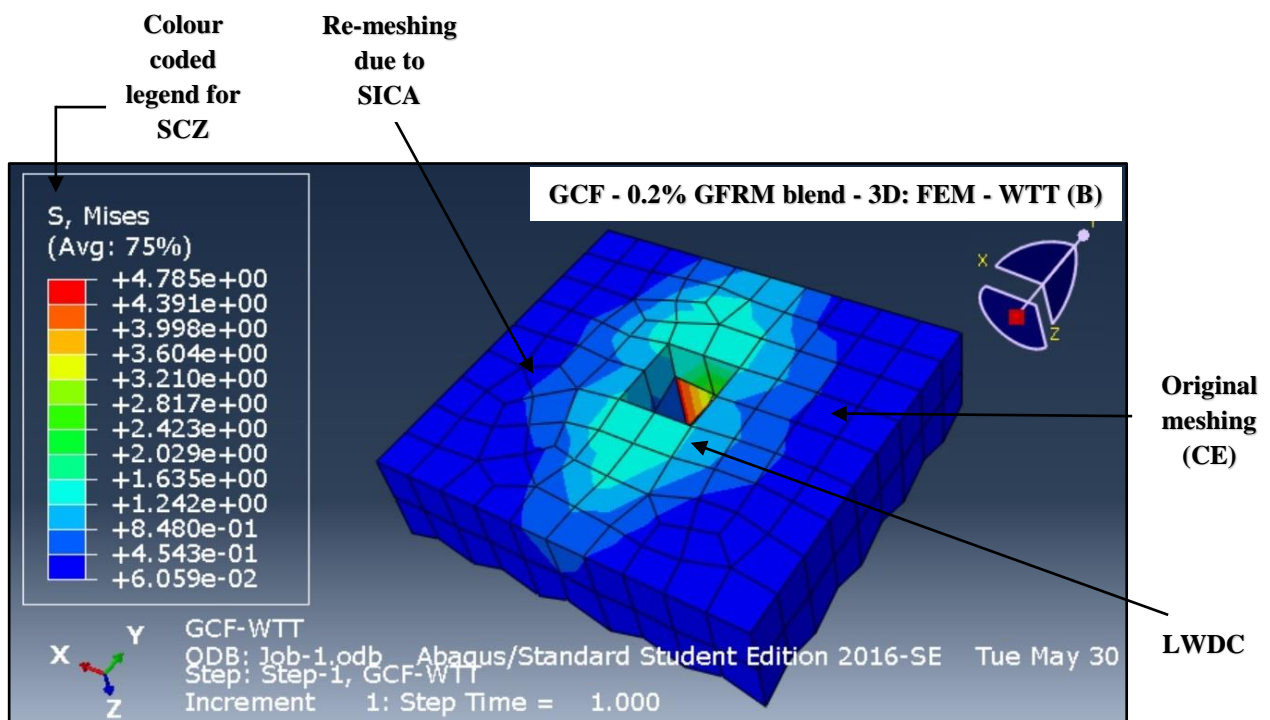
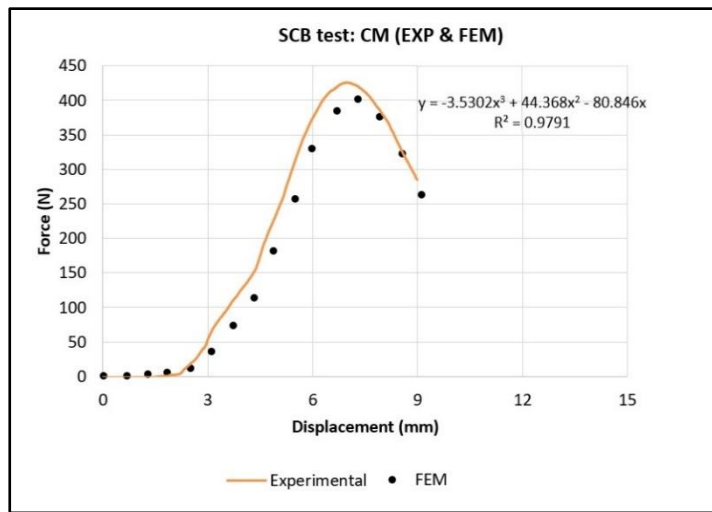


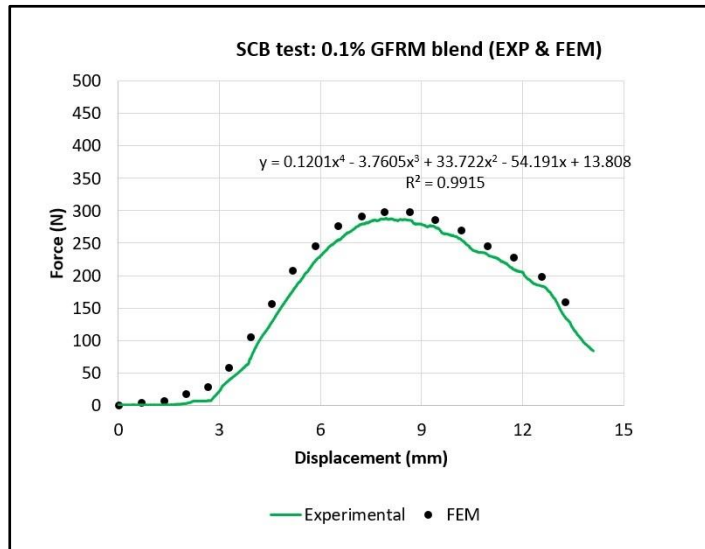
Figure 6-11 (f): Stress concentration zone 3D FE modelling for the GCF - 0.2% GFRM blend - WTT (B)

6.11 EXPERIMENTAL AND FEM RESULTS FOR THE SCBT

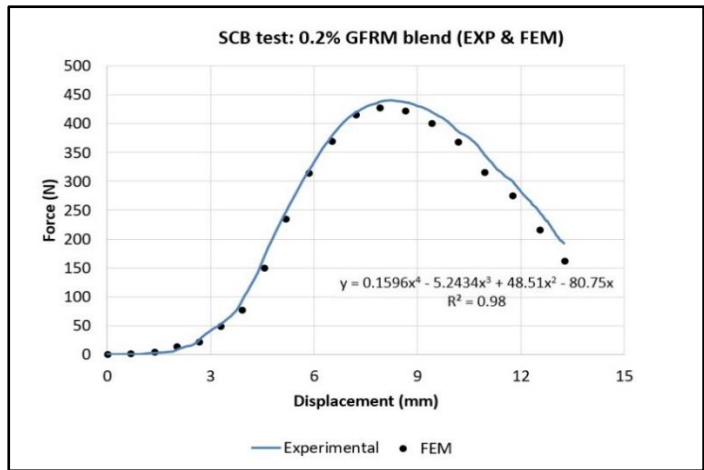
Data points obtained for the CM, 0.2% GFRM blend and GCF - 0.2% GFRM mixtures from the experimental test results and the finite element modelling (FEM) results based on the SCBT were plotted. The experimental and FEM models are compared and contrasted in graphs 6-13, 6-14, and 6-15 below. The results clearly show that the FE models had a very good agreement with the experimental test results for the CM, 0.2% GFRM blend and GCF - 0.2% GFRM mixtures and the FEM model provides a suitable numerical tool to represent SCB testing.



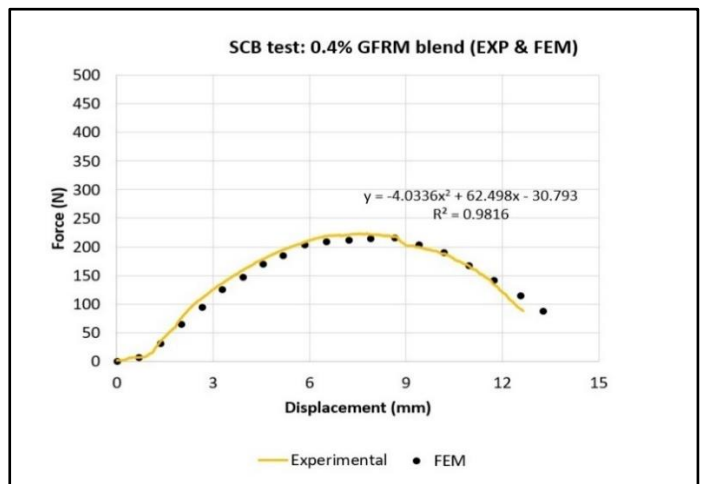
Graph 6-13: Experimental and FEM results for the CM - SCBT



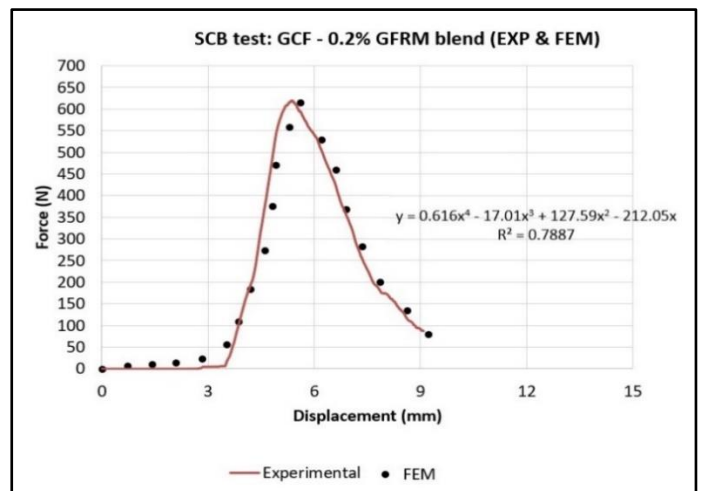
Graph 6-14 (a): Experimental and FEM results for the 0.1 % GFRM blend - SCBT



Graph 6-14 (b): Experimental and FEM results for the 0.2 % GFRM blend - SCBT



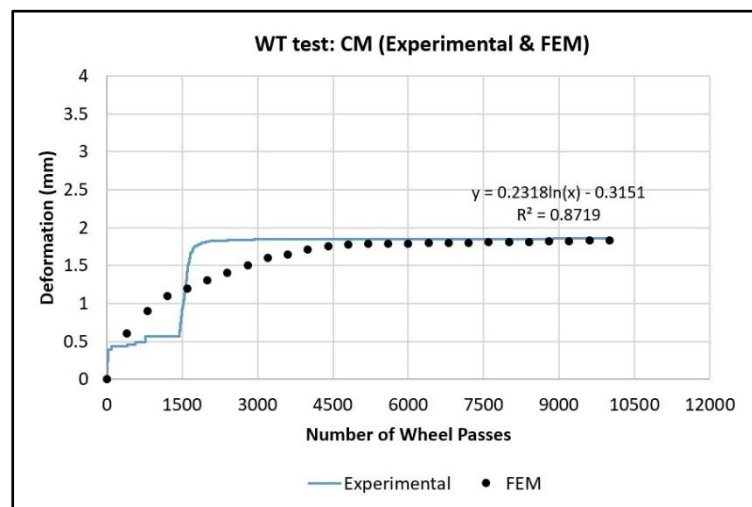
Graph 6-14 (c): Experimental and FEM results for the 0.4 % GFRM blend - SCBT



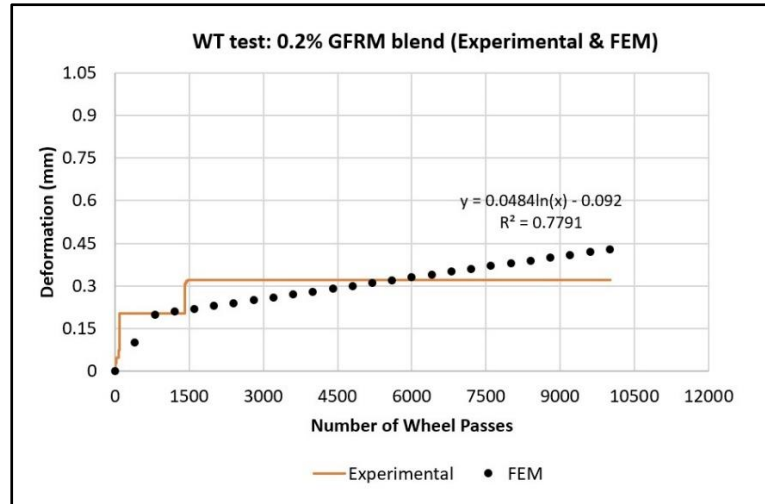
Graph 6-15: Experimental and FEM results for the GCF - 0.2 % GFRM blend - SCBT

6.12 EXPERIMENTAL AND FEM RESULTS FOR THE WTT

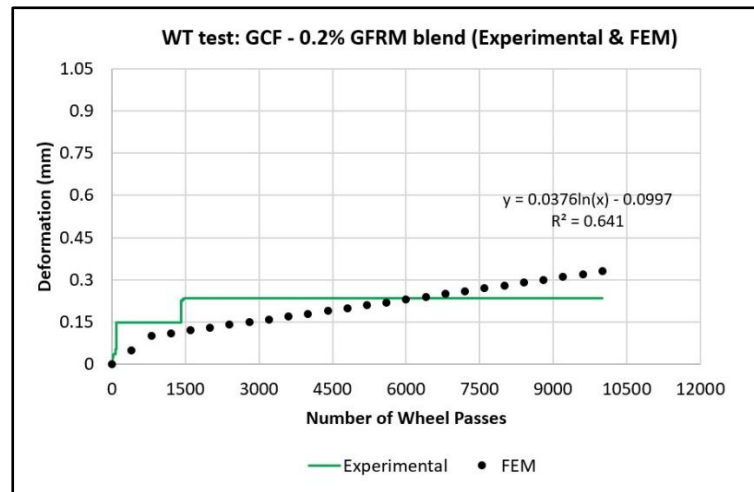
The experimental test results and the FEM model results for the WTT were compared and contrasted in graphs 6-16, 6-17 and 6-18 below. The results clearly indicate that the FE model has good agreement with the experimental test results for the CM, 0.2% GFRM blend and GCF - 0.2% GFRM mixtures and the FEM model provides a harmonised numerical tool to represent WT testing. The results show that in the start, i.e. up to 1,500 wheel passes; there is a sudden rise in the deformation curve up to 1.20mm for the CM, a partial rise in the deformation curve of 0.33mm due to the addition of glass fibres in the microasphalt for the 0.2% GFRM blend followed by an insignificant rise in the deformation of 0.22mm due to replacement of OPC with GCF and the addition of glass fibres in the microasphalt for the GCF - 0.2% GFRM blend. During the transition stage, i.e. the microasphalt in its early life tends to develop strength and is prone to deformation however, the deformation onwards tends to remain steady by achieving substantial strength until the completion of 10,000 wheel passes.



Graph 6-16: Experimental and FEM results for the CM - WTT



Graph 6-17: Experimental and FEM results for the 0.2 % GFRM blend - WTT



Graph 6-18: Experimental and FEM results for the GCF - 0.2 % GFRM blend - WTT

6.13 SUMMARY OF FINDINGS ON FEM

Experimental test results were used to validate a 3D FE model, which was used to interpret and to analyse the failure and deformation mechanism in the SCB and WT tests. Based on the results above, the following summary findings are drawn:

- a. SCB and WT tests results predicted that the CM mix is more brittle as compared to the 0.2% GFRM blend mix which provides high cracking and deformation characteristics. The GCF - 0.2% GFRM mix provides higher

resistance to the applied force at the same displacement and further, helps in retarding the crack propagation rate as well as an additional resistance to deformation as compared to the CM and 0.2% GFRM blend mixes. The FE models successfully describe the fracture performance of the evaluated mixes and were able to differentiate between them in terms of cracking resistance against fracture and rutting resistance against deformation.

- b. The SCB test process, and propagation of damage were successfully simulated using 3D FE and cohesive elements. The presented modelling was in good agreement with the measured experimental test results for all the CM, 0.2% GFRM blend and GCF - 0.2% GFRM mixes.
- c. Also, the WT test process, and deformation development were successfully simulated using 3D FE and cohesive elements. The presented modelling was in good agreement with the measured experimental test results for all the CM, 0.2% GFRM blend and GCF - 0.2% GFRM mixes.
- d. Based on the SCB results from the FE model, it can be deduced that damage propagates in the vicinity of the notch and is mainly caused by a combination of vertical and horizontal stresses in the specimen.
- e. Based on the WT results from the FE model, deformation occurs in the propinquity of the central median (strip) of the specimen and is mainly caused by stresses accumulated due to a loaded wheel movement.

However, more detailed FEM analysis is recommended for further work to be carried out by using extended finite element modelling coupled with the cohesive zone modelling approach to model the fracture and rutting in the CMM. This will enable further examination of the heterogenous quasi-brittle visco-elastic behaviour of the CMM and a relatively large FPZ for cracking and rutting can be simulated without re-meshing of cohesive elements in the FE model.

Chapter

7

Site Trial for Control and Glass Fibre Reinforced Cold Mix Microasphalt

7.1 INTRODUCTION

Microasphalt may be used for a range of applications, but job selection is critical and often pre-treatments such as pothole patching, crack sealing, and dig outs are required. Keeping in mind these actualities, the newly developed material was applied on site in Talbot Road, Leeds on 24th September 2014 incorporating glass fibre as part of the research for real world verification of laboratory findings.

7.2 FIELD TRIAL

The site trial was carried out on the southern end of the installation of microasphalt in Talbot Road, Leeds. The area incorporating glass fibre is from the junction with Lidgett Park Avenue south to the end of Talbot Road and the junction with North Park Avenue. Figure 7-1 shows the site trial location on Talbot Road, Leeds.



Figure 7-1: Site trial location on Talbot Road, Leeds

The map (figure 7-2) below gives a good representation of the site location and topography.

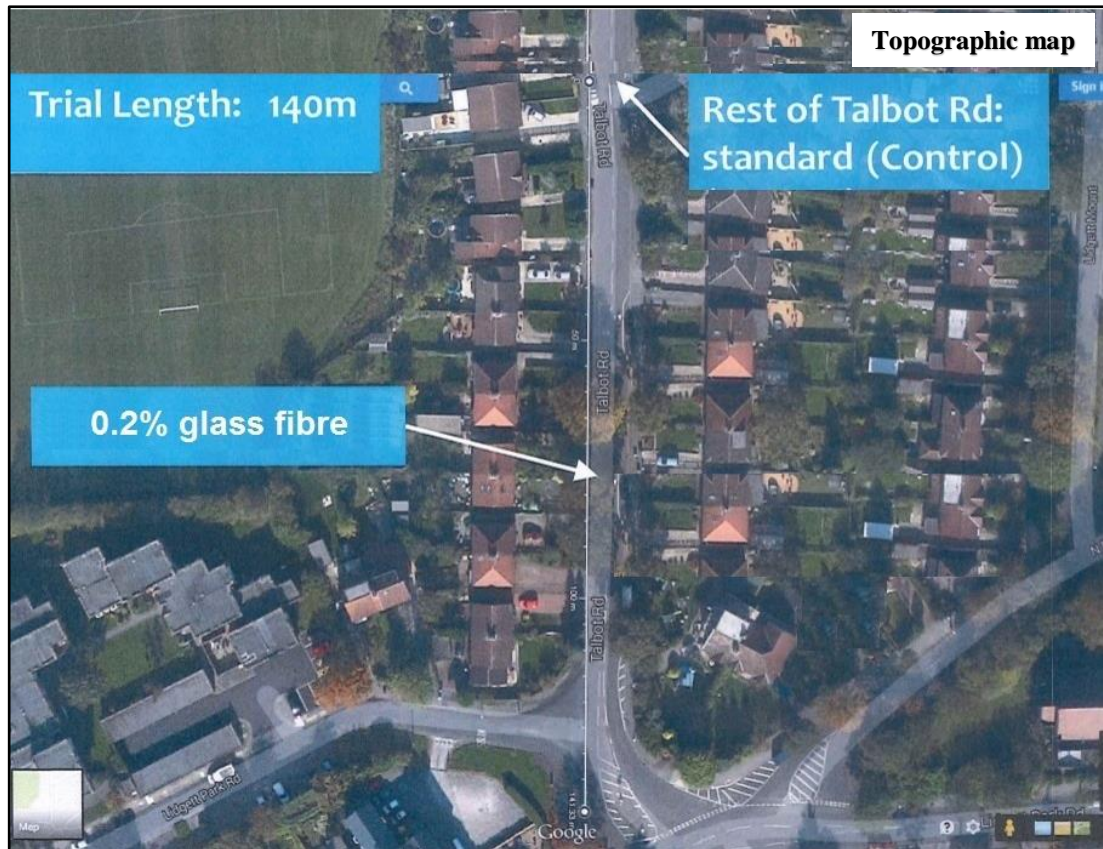


Figure 7-2: Location map of site trial section on Talbot Road, Leeds

The trial has a slight slope from Lidgett Park Avenue down to North Park Avenue. There is a speed hump about 50m south of Lidgett Park Avenue and a 30-degree bend as Talbot Road joins North Park Avenue. At the south end, Talbot Road widens to allow the junction with Lidgett Park Road to join and there is a hatched area containing traffic islands at the junction with North Park Road.

The original surface is hot laid mix with a myriad of cracks; hence its choice as a trial site. The number, size and position of all the cracks are too numerous to record. There are 10 small reinstatements with cracks around their perimeter and cracks propagating into the original hot mix. The four largest reinstatements are about 1x1 m² and positioned just south of the speed hump and located in the outer wheel tracks of each carriageway. There are two reinstated trenches across the road roughly just outside the lines of the brick pillars for the double gates for a house just north of the traffic islands. The photo (figure 7-3) shows the myriad of extensive cracks.



Figure 7-3: Myriad of extensive cracks

The glass fibre trial site is about 140m long and 7m wide, which gives an area of about 980m². There are several large trees giving shade, and with roots causing deformation of the road surface, along the pavement on the west side of the trial site. Figure 7-4 shows the condition of Talbot road before application of control and fibre reinforced microasphalt for preventive maintenance.

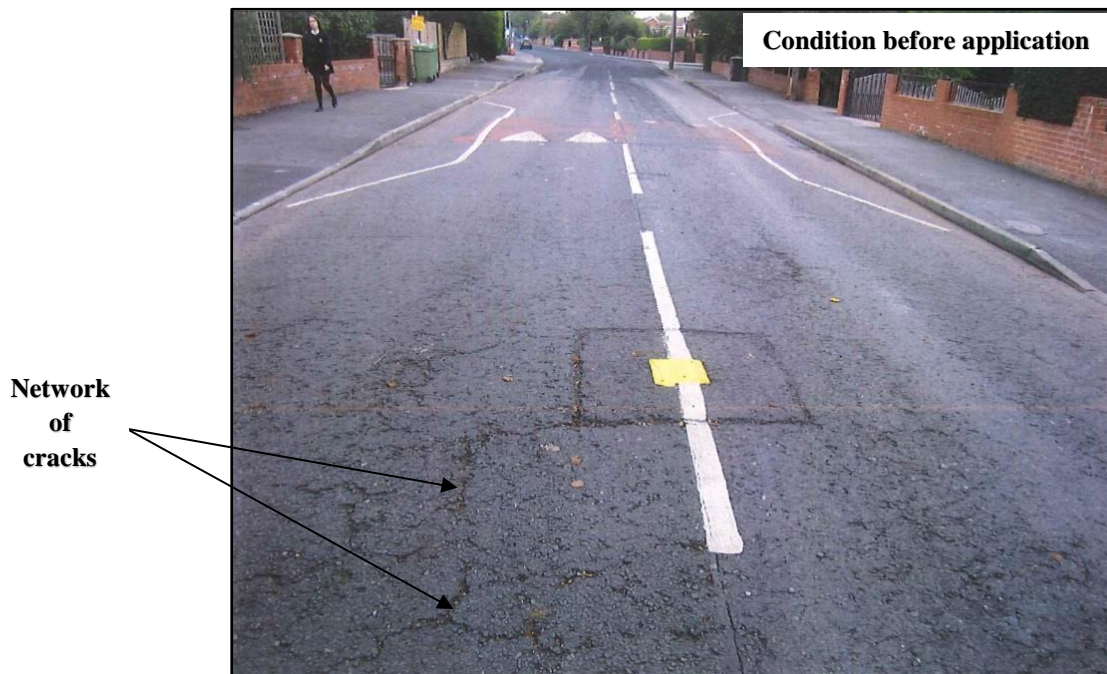


Figure 7-4: Condition of Talbot road before application of control and fibre reinforced microasphalt

7.3 INGREDIENTS

The ingredients used for the trial site:

- i. Bitumen emulsion (6.0% for CM section and 7.5% for GFRM section)
- ii. Aggregates with size ranging from 6mm to of 0.075mm
- iii. Glass fibres with length: 16mm and quantity: 0.2% by total weight of the aggregates
- iv. Site control agent - retarder
- v. Cement (OPC)

7.4 APPLICATION

The material was applied using a rigid applicator. The procedure for on-site application of glass fibre reinforced microasphalt is illustrated in figure 7-5.

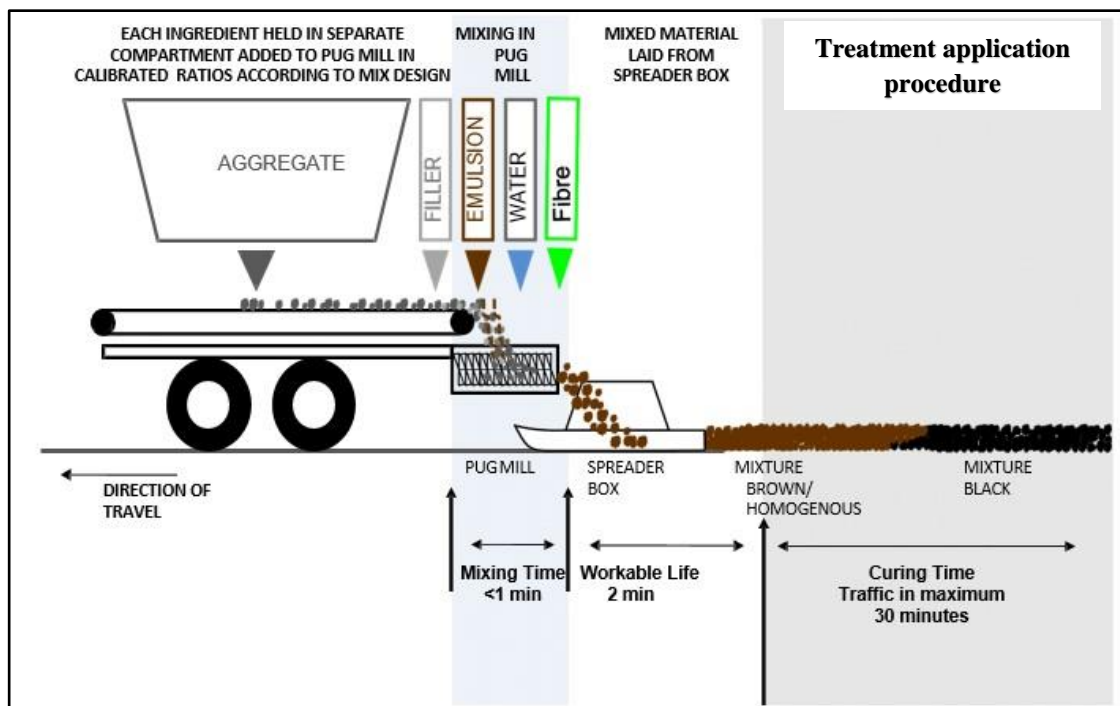


Figure 7-5: Schematic for application of glass fibre reinforced microasphalt

The applicator has a single chopper for the glass fibre stand that can be fed from two reels of glass fibre. The chopper cover was left off to ensure no blocking occurred, also permitting the glass fibre to be seen in the photograph (figure 7-6).



Figure 7-6: Two reels of glass fibre with a chopper (open cover)

The application started at the widened traffic island area at the south end of the site with a couple of short rips and hand work without glass fibre. It was then decided to start the rip up the carriageway with a glass fibre inclusion rate at 0.2%. This level of glass fibre quantity did not affect the mix consistency. Figure 7-7 shows Schematic of glass fibres blended in the mix acting as a stress absorbing membrane interlayer (SAMI), and figure 7-8 illustrates the glass fibres included in the mix.

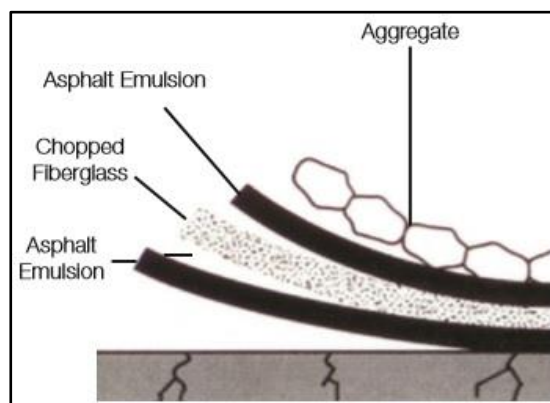


Figure 7-7: Schematic of glass fibres blended in the mix acting as a stress absorbing membrane interlayer (SAMI)

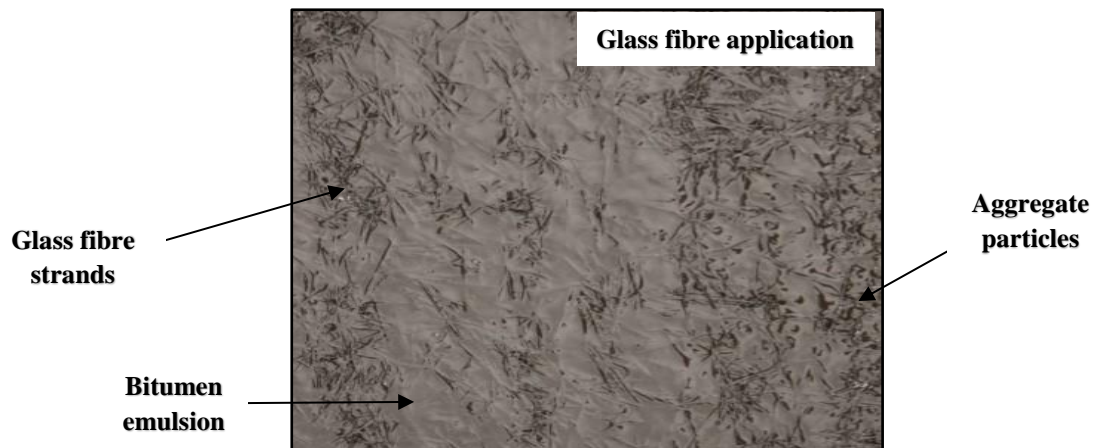


Figure 7-8: On site glass fibres inclusion in the microasphalt

Installation of 0.2% of glass fibre on the carriageway was successfully completed. The visual appearance of the amount of glass fibre dropped onto the aggregate on the belt did not appear excessive for the machine or mix to handle, and the effect on the material consistency in the laying box was not affected. Seven pint pot samples (samples 1 to 7) were taken from the mixing box roughly evenly spaced throughout the rip and a bucket of semi-set material (sample 8) on the road surface was collected from the tape covering the man-holes/drains.

The break time for the 0.2% mix was about 4 minutes, which was similar to the installation of the rest of Talbot Road carried out on the previous day. When semi broken material for 0.2% was removed from the road surface it could easily be seen that the glass fibre had been smashed up into fine filaments from the stiff bundles dropped onto the aggregate on the belt. However, the fibre seen was still about 16mm long; it had not been broken into smaller lengths by the action of mixing. In both cases (i.e. broken/unbroken fibre), there was no sign of glass fibre protruding from the surface of the microasphalt on the road.

After about 30 minutes the surface course was rolled with a Bomag. Specifications for the tandem roller compactor are provided in table 7-1 below. On completion the site had a composed appearance with good uniform texture. The rip lines had been reduced to a minimum by the careful planning.

Table 7-1: Specifications of tandem roller compactor

Description	Technical specification
Working width	1200 mm
Operating weight	2750 kg
Working speed	0-10 km/hr
Driven drum	Front + rear
Engine manufacturer	Kubota
Performance	24.3kW

7.5 APPLICATOR SETTINGS

Throughout the site trial the applicator settings were:

- i. Emulsion = 6.0% (control) & 7.5% (reinforced)
- ii. Water = 4 litre/minute
- iii. Cement = 1.0%
- iv. Site control agent - retarder = 1.8 litre/minute
- v. Glass fibre = 16mm and 0.2%

7.6 WEATHER

Throughout the site trial the weather was:

- i. Cool, damp, breezy
- ii. Ambient = 14⁰C
- iii. Road surface = 12⁰C

7.7 SITE INSPECTION THE NEXT DAY

During the site inspection on the next day the following was observed:

1. The material had not fully dried out due to overnight rain.
2. There was no obvious visual difference between the surface of the control (no glass fibre) and the trial areas containing the 0.2% glass fibre. Some aggregate had been removed from the surface due to vehicles turning out of Talbot Road into North Park Avenue.

3. Edges at the kerbs and junctions were in good condition.
4. There were a few power steering damage marks due to cars turning out of house driveways.
5. The microasphalt remained intact on the speed hump.
6. Lots of 6mm aggregates were held at the surface in the material matrix.
7. Material was still soft and fragile during the inspection as is expected of 'next day' microasphalt.

7.8 SITE SAMPLE TESTING

Samples from the trial were taken from the road surface and in the normal way from the flow out of the mixing box onto the rubber chute:

- i. Sample 1 – taken off road surface before the 0.2% glass fibre rip
- ii. Samples 2 to 7 – Samples from flow out of mixing box during 0.2% glass fibre rip
- iii. Sample 8 – Samples off tape on man-hole/drains of material containing 0.2% glass fibre

The site samples were duly analysed and the results are given in the table 7-2 below (Harrison, 2015):

Table 7-2: Results of site samples

Sample	Binder (%)	Glass fibre added (%)	Glass fibre found (%)	Aggregate grading
1 - Road surface	4.4	0	0	6 - 2 mm
2 - Mixer box	5.9	0.2	0.004	4 - 2 mm
4 - Mixer box	5.7	0.2	0.016	4 - 2 mm
6 - Mixer box	6.3	0.2	0.003	6 - 2 mm
8 - Road surface	5.4	0.2	0.003	6 - 2 mm

The evaluation of the samples taken from the road show they have low binder content and their aggregate grading range from 6 - 2 mm found on all sieves.

It was surprising that the level of glass fibre found in the sample is somewhat low as the amount seen being chopped and going into the mix was rather large. In order, to check that the glass does not get pulverised to a powder at the next trial the glass fibre “balling” will be weighed before and after the trial to measure the weight added to the mix for the whole site (Harrison, 2015). However, see figure 7-9 for observation on glass fibre recovered from site samples. Breaking up the mix samples from the pint pots taken from the flow of material out of the mixing box found glass fibre still in stiff bundles from the chopped strand from the “balling” and some as broken up filaments. Generally, there was more glass fibre as stiff bundles than as fine filaments. This is not the case seen with material taken off the road surface where there are fewer bundles and the glass fibre strands have been broken up into fine filaments spread evenly and uniformly throughout the mix by the action in the laying box of the paddles/augers. This observation was replicated and endorsed during the laboratory testing as well.

The photograph (figure 7-9) below shows a site sample broken open to show the two forms of fibre present; notice the two strands of bundled fibre not broken on the “horizon” and between them a finer filament broken up from a bundle.

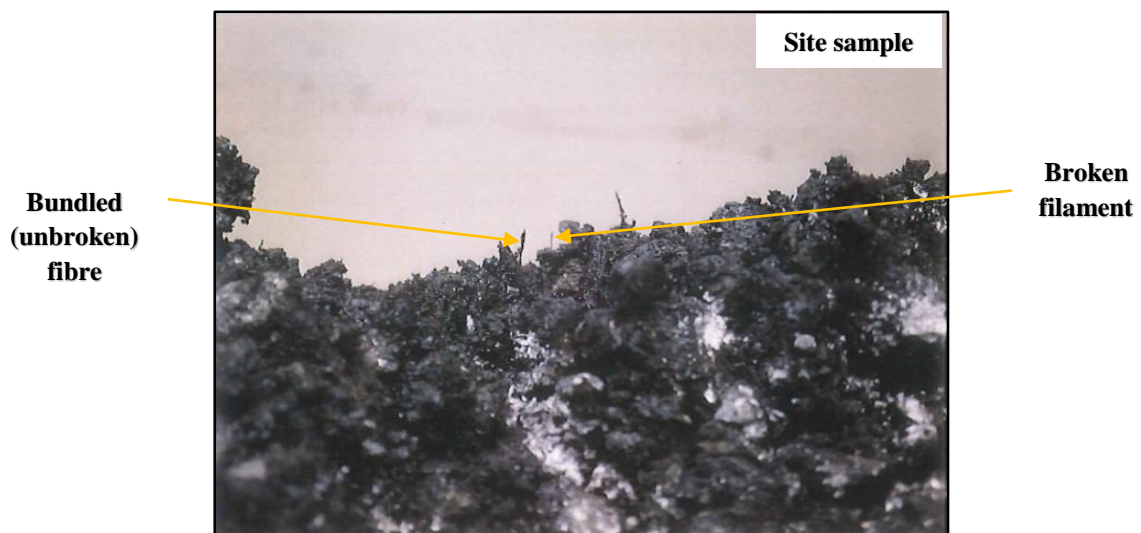


Figure 7-9: Site sample broken open to show the two forms of fibre

The glass fibre found in the samples taken from the microasphalt flow out of the mixing box found the fibre on the 0.25 and 0.063 mm sieves. This is rather strange as the glass fibre is 16 mm long and perhaps would have been expected to collect on the larger sieves. The glass fibre caught on the sieves appears to be about 16 mm long indicating that the glass fibre does not get pulverized to a powder in the mixing action in the mixing and laying boxes. There were two forms of the glass fibre seen recovered from the site samples; straight and rigid unbroken fibre bundles and broken up to fine fibre filaments now agglomerated to form small “cotton wool” type balls. See the two forms of glass fibre and aggregate recovered from a site sample below in figure 7-10.



Figure 7-10: Two forms of glass fibre and aggregates recovered from a site sample

7.9 SUMMARY

Although the site installed was rather small (980m²) it demonstrated that the applicators are capable of adding glass fibre to the microasphalt mix at 0.2%.

The microasphalt mix consistency is not significantly affected by the addition of glass fibre, but it was found that the water level needed to be increased slightly.

The glass fibre could be easily seen in the wet installed material as both filaments and to a lesser extent as bundles/strands.

The analysis of the site samples did not retrieve all the glass fibre added. It was thought that the glass fibre could have been pulverised to powder, but as all the glass fibres retrieved were about 16 mm in length, pulverisation to powder is unlikely. The low level of glass fibre retrieved is strange as the level added looked rather large. It is suggested that the glass fibre reels be weighed before and after the next trial to confirm the amount added because there is a likelihood that some of the fibres during the installation process may have broken down on site and could have been enhancing the performance of test trial section containing glass fibres in it.

7.10 SITE INSPECTION AT 12 MONTHS ON 23RD SEPTEMBER 2015

A site inspection was carried out on 23rd September 2015. The weather was dry and breezy. All three areas on Talbot Road were visually similar; there was no perceivable difference between the areas containing no glass fibre and those containing 0.2% glass fibre. They all had same texture and there were no cracks at the surface.

The upper (North) end of Talbot Road had a higher texture with a more open surface, but this was due to the lower level of traffic, especially in the early life of the material, rather than an effect of having no glass fibre. In the area below the school (South) end the two areas (0 & 0.2% glass fibre) had a similar, good texture.

The edge step next to the tress (in figure 7-11 below) shows a sign of storm water accumulation. Potentially the storm water could have infiltrated through the cracks should there have been any and would have resulted in an increase in pore water pressure within the subgrade and subbase structure of the microasphalt pavement causing failure. But on inspection, it was noted that there were no cracks at this location due to storm water accumulation during the rainfall. Also, the roots of the big trees growing right at the carriageway edge had not caused any cracks in the road surface. The adjacent road surface has 0.2% glass fibre. The photo (figure 7-11) below shows the appearance of roughly the same area as the initial photo (figure 7-1) before the application given in section 7.2 above, albeit from a different angle. The original photo is of an area where the silver car is now parked. The three large trees are just

out of shot to the left. Figure 7-12 below shows the on-site conditions at one year inspection.



Figure 7-11: Appearance of roughly the same area as the initial photo before application given in section 7.2 above



Figure 7-12: Condition of Talbot Road on inspection at 12 months, fibreless section on left and a closer look at the surface texture of fibre reinforced section on right

As the photo shows, the trial area (and the non-trial area) are in excellent condition and have excellent appearance with no cracks at the surface. There were no cracks in the area without fibre to validate the use of glass fibre to obviate cracking and deformation.

Figures 7-13 and 7-14 illustrate the temperature and precipitation variations within the year, 2015, of the site inspection, respectively. The hottest day of 2015 was July 1,

with a high temperature of 29°C. The hottest month of 2015 was August with an average daily high temperature of 18°C. The coldest day of 2015 was February 2, with a low temperature of -3°C. The coldest month of 2015 was February with an average daily low temperature of 1°C.

The daily low and high temperature during 2015 are shown in blue and red respectively while the area between them is shaded in grey and superimposed over them are the corresponding averages (solid trend lines). The bar at the top of the graph is red where both the daily high and low are above average and blue where they are both below average. The data is from Leeds Bradford International Airport records (WeatherSpark, 2015).

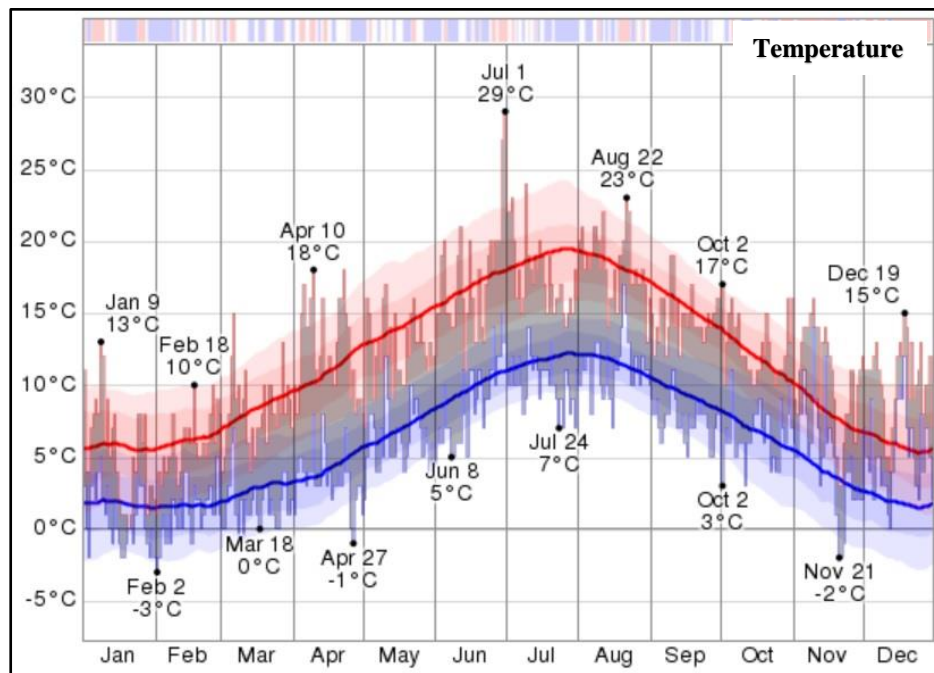


Figure 7-13: Temperature for Leeds, UK (WeatherSpark, 2015)

The day in 2015 with the most precipitation observations was January 21. As determined by the weather reports, the longest dry spell was from June 3 to June 13. The daily number of hourly observed precipitation (i.e. precipitation recorded on daily basis after every hour each month) during 2015 are colour coded according to precipitation type and stacked in order of severity. From the bottom up, the categories are thunderstorms (orange); heavy, moderate, and light snow (dark to light blue); heavy, moderate and light rain (dark to light green); and drizzle (lightest green).

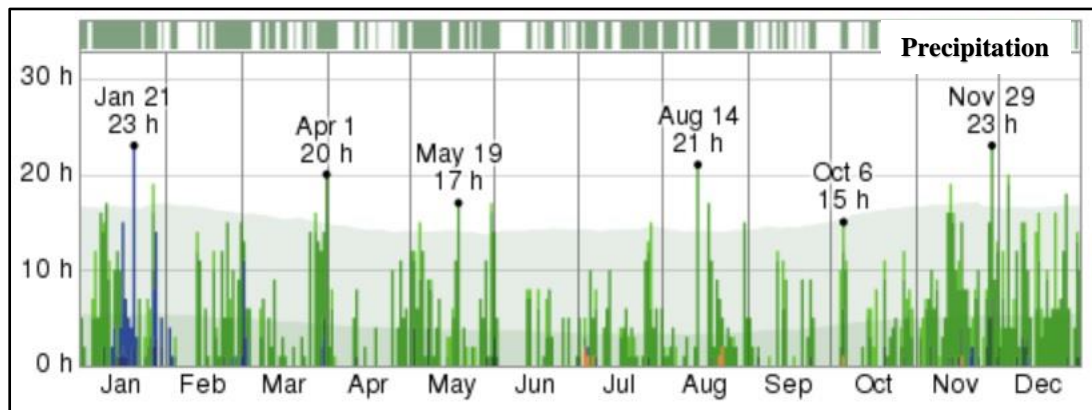


Figure 7-14: Precipitation for Leeds, UK (WeatherSpark, 2015)

7.11 SITE INSPECTION AT 25 MONTHS ON 24TH OCTOBER 2016

Two years after the placement of the microasphalt, a field performance evaluation was conducted, on 24th October 2016 to compare the sections with and without fibre over an existing pavement that had reflective cracks. The weather was dry, partially cloudy and breezy. During the site inspection it was observed that cracks has started to appear at a few places in the fibreless section versus no cracks in the fibre reinforced section.

The cracks could not be stopped in the non-fibre section and reflective cracking had started to develop (see figure 7-15 & 7-16) whereas, the fibre reinforced section showed resistance to the reflective cracking. The fibre reinforced section showed good performance after 25 months. It can be said that the addition of fibre resulted in an improvement in terms of cracking resistance compared to the control microasphalt.

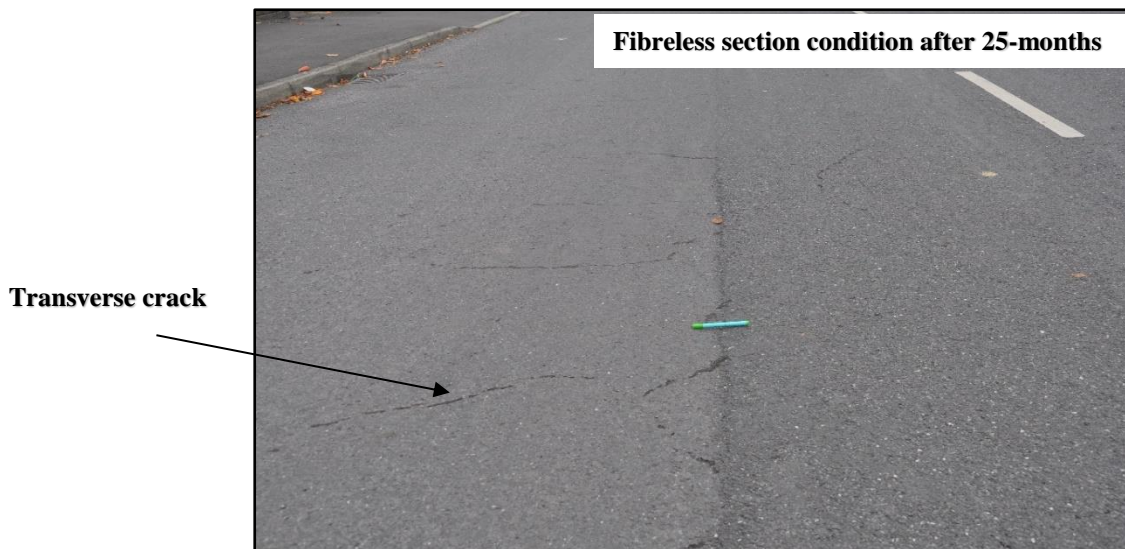


Figure 7-15: Reflective cracking (transverse) in fibreless section

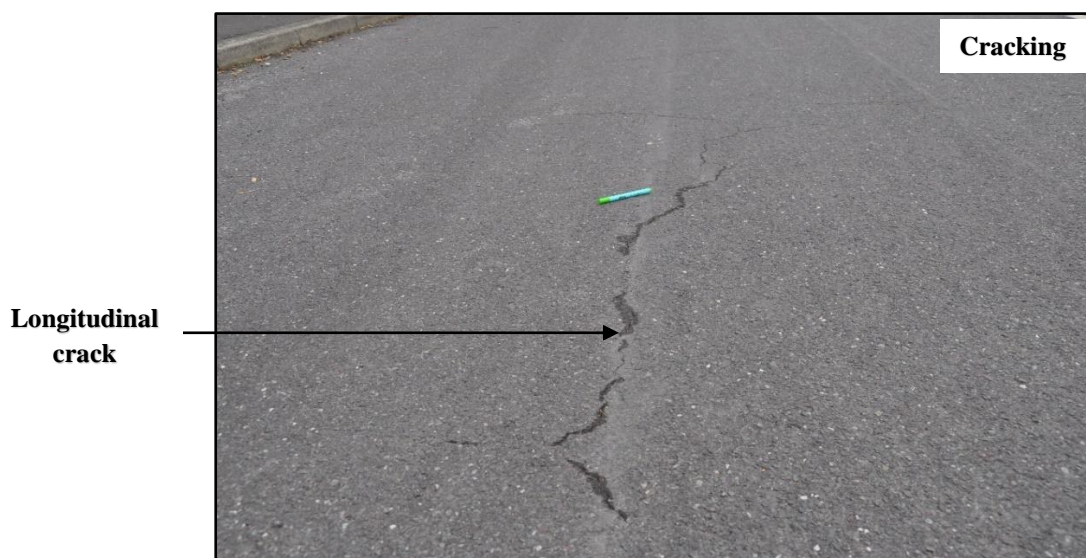


Figure 7-16: Reflective cracking (longitudinal) in fibreless section

Further, the non-fibre section showed a few signs of ravelling i.e. dislodging of aggregate particles on the road surface (see figure 7-17). No ravelling was witnessed in the fibre reinforced section. It was evident that both sections had withstood deformation distress. The reason for ravelling in the control microasphalt section could be due to the phenomenon of oxidation of bitumen emulsion that has occurred in the control microasphalt section which made it brittle earlier than the fibre reinforced section; possibly due to the lower bitumen emulsion content (6%) as compared to (7.5%) in the fibre reinforced section i.e. the bitumen emulsion coating bond with the

aggregate particles starts to get weak under repeated traffic loading. Technical reasoning suggests that the area near the hump with no fibre in the section will develop rutting earlier, due to the braking action of vehicle wheels as compared to the fibre reinforced section.



Figure 7-17: Minor ravelling in fibreless section

There were no cracks, ravelling and deformation distresses in the fibre reinforced section which validates the laboratory findings i.e. it is in agreement with the premise elucidated during the critical analysis in chapter 6. Thus, the fibre reinforced section showed an overall good performance on inspection at 25 months. It can be said with confidence that the addition of fibre resulted in an improvement in terms of cracking, ravelling and deformation resistance as compared to the control microasphalt. The photos (figure 7-18 & 7-19) below show the trial area on-site inspection at 25 months.



Figure 7-18: Glass fibre reinforced section



Figure 7-19: Glass fibre reinforced section near hump

Figures 7-20 and 7-21 illustrates the temperature and precipitation variations within the year, 2016, of the site inspection, respectively. The hottest day of 2016 was July 19, with a high temperature of 28°C. The hottest month of 2016 was July with an average daily high temperature of 19°C. The coldest day of 2016 was February 24,

with a low temperature of -4°C . The coldest month of 2016 was February with an average daily low temperature of 1°C . The longest cold spell was from April 19 to May 2.

The daily low and high temperatures during 2016 are shown in blue and red respectively while the area between them is shaded in grey and superimposed over them are the corresponding average high and low temperatures (thick lines). The bar at the top of the graph is red where both the daily high and low are above average and blue where they are both below average. The data are from Leeds Bradford International Airport records (WeatherSpark, 2016).

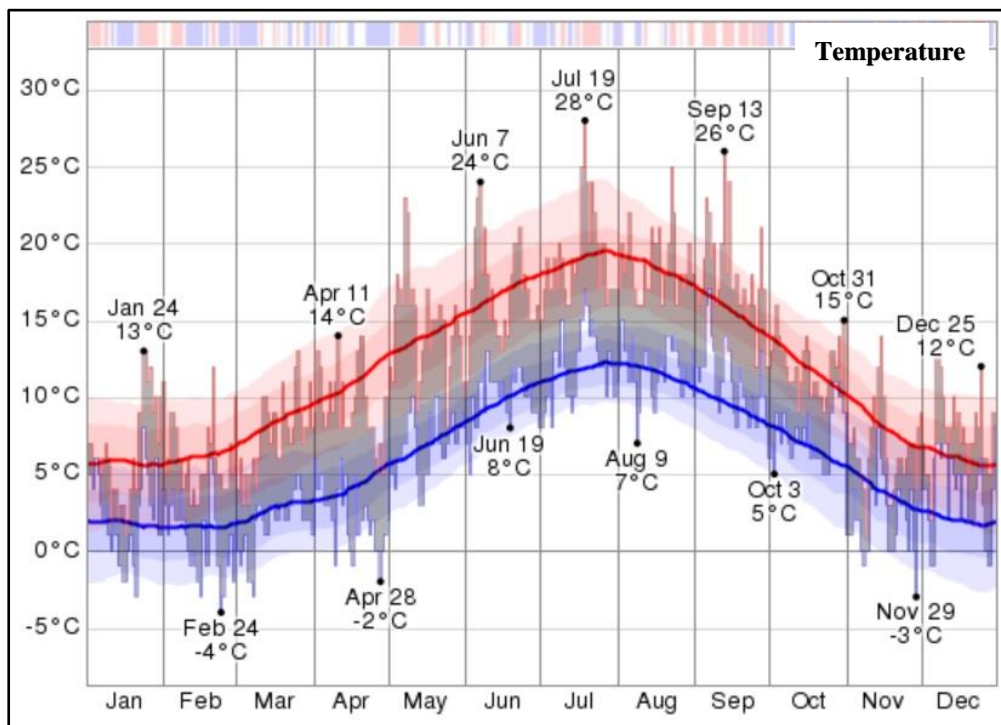


Figure 7-20: Temperature for Leeds, UK (WeatherSpark, 2016)

The day in 2016 with the most precipitation observations was January 2. The month with the most precipitation observations was January. As determined by the present weather reports, the longest dry spell was from May 4 to May 10. The daily number of hourly observed precipitation (i.e. precipitation recorded on daily basis after every hour each month) during 2016 is colour coded according to precipitation type, and stacked in order of severity. From the bottom up, the categories are thunderstorms

(orange); heavy, moderate, and light snow (dark to light blue); heavy, moderate, and light rain (dark to light green); and drizzle (lightest green).

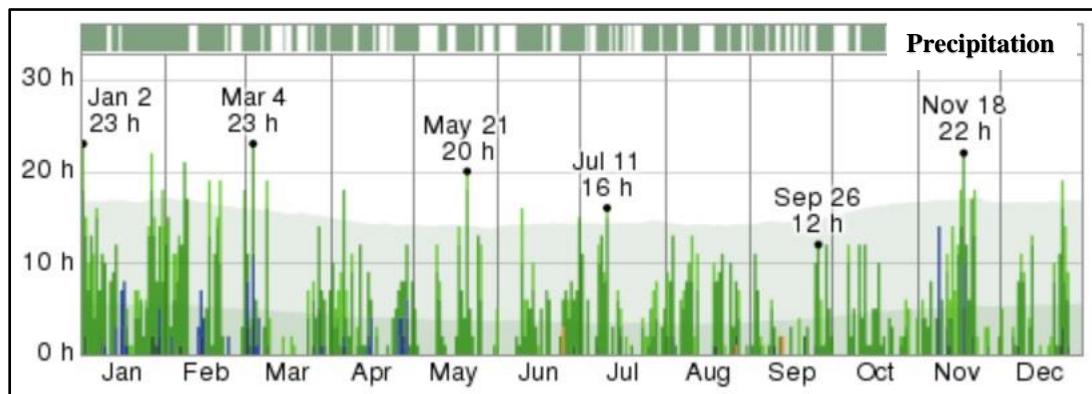


Figure 7-21: Precipitation for Leeds, UK (WeatherSpark, 2016)

With the foregoing in mind, the road trial carried out on a residential road shows that the laboratory findings are in agreement with the field performance of glass fibre reinforced microasphalt. Areas were selected which displayed signs of reflective cracking. A small section of these areas was reinforced using glass fibres, while adjacent areas were surfaced in the normal manner with the control microasphalt. After two years reflective cracking has partially reappeared in the surrounding areas adjacent to the reinforced areas. Thus, the life of the reinforced overlay appears to be greater than that of the unreinforced control microasphalt.

The temperature data for the year 2015 and 2016 above shows that the test trial sections were subject to varied climatic conditions i.e. from hot weather to cold weather including rainfalls throughout the year and the on-site performance of the microasphalt demonstrated that the newly developed microasphalt is resilient to cracking and deformation in extreme weather conditions. Further, the triangulation between the laboratory testing, FEM and site trial test also suggest that there exists a complete harmony between the experimental findings, FEM simulation and on-site test trial sections of microasphalt and the results obtained from these evaluation methods superimpose each other.

Chapter

8

Conclusions & Recommendations

8.1 CONCLUSIONS

The research presented in this thesis is aimed at developing a reinforced cold mix microasphalt for road surfacing with a high resistance to cracking and deformation. Based on the literature review and communication with the industrial partner, the CMMs are observed to be associated mainly with high porosity, long curing time, very low early strength and high sensitivity to water damage. Although substantial beneficial characteristics can be achieved by using reinforced CMM in the pavement industry, many studies have resulted in the development of either high cost CMMs or environmentally unfriendly solutions.

In this study, the development is based on adopting both environmentally friendly and sustainable approaches, where novel glass fibres and novel waste, by-product materials (PSA, CKD and RHA) were used to achieve the main research aim. The validity of the new and resilient CMMs developments has been investigated through specifying cracking and deformation mechanical properties of CMMs' variation using up-to-date fundamental test procedures and FEM. It is pertinent to mention that wearing, cohesion and surface friction tests were carried out by the industrial partner scientists at their research laboratory and are as such not part of this thesis. Also, microanalysis has been used to explain these developments. As a result of this work the following global conclusions can be justified:

1. **Effect of novel glass fibre length (aspect ratio):** Microasphalt containing 16mm length of glass fibres, showed highest performance for semi-circular bending test. The glass fibre corresponding aspect ratio to the above length is 200 in the mix as mentioned in section 5.17.2.
2. **Effect of novel glass fibre blend (aspect ratio):** Also, the blend of different length of glass fibres (i.e. 6mm, 12.5mm, 16mm and 25mm) added in the same proportion (i.e. 0.05% each length) in the microasphalt mix showed slightly more strength for the SCB test as compared to the 16 mm glass fibre lengths in (2) above. The corresponding glass fibre aspect ratio to the blend is 187 in the mix as discussed in section 5.17.2.

-
-
3. **Effect of novel glass fibre content (volume fraction):** Glass fibres in a quantity of 0.2% of total weight of the aggregates in the mix exhibited high resistance to reflective cracking and deformation pavement distresses in the microasphalt. The glass fibre corresponding volume fraction to the above percentage was 0.09% in the entire volume.
 4. **Emulsion content:** Initially, the emulsion content of 6.0% residual binder by total weight of the mix used in glass fibre reinforced microasphalt resulted in a “dry” mix. This resulted in the breaking of the mix very quickly during the mixing and preparation of sample. Therefore, as a result of communication with the industrial partner a bitumen emulsion content of 7.5% by total weight of the mix was used in the glass fibre reinforced microasphalt to achieve better workability.
 5. **Tensile strength:** The addition of glass fibres has reinforced/enhanced the tensile strength of microasphalt up to 15% and 33% at maximum load failure and ultimate failure respectively as compared to the control microasphalt based on the results of the three point bending test (graph 6-4).
 6. **Deformation:** The glass fibre reinforced microasphalt has an improvement of 83% in deformation from the wheel track test as compared to the control microasphalt (graph 6-6).
 7. **Visco-elasto-plastic behaviour:** Interestingly the findings from 6 and 7 above coincide with the following: the use of the optimum amount of glass fibre (0.2% of total aggregates) provides higher visco-elasto-plastic behaviour characteristics to the microasphalt, where the results of the three point bending tests indicate that the material visco-elasto-plastic behaviour is improved by 94% when 0.2% GFRM replaces 0.3% and or 0.4 % GFRM (graph 6-5). Further laboratory work and new site trial are necessary to support this finding, as it indicates that the use of fibres at this quantity produces a high quality microasphalt.

-
-
8. **Resistance to cracking & rutting:** The tests results indicated that the fibre has the potential to improve structural resistance to distress that occurs in microasphalt as a result of increased traffic loading. The addition of fibre improves the fatigue life of the microasphalt by increasing its resistance to cracking and permanent deformation.

 9. **Glass fibre content limit:** It was noticed that the fibre content of 0.2% by weight of the total aggregates in the mix resulted in the highest performance in terms of resistance to cracking and permanent deformation as compared to the control microasphalt. There was a slight deterioration in these properties when the fibre content exceeded 0.2% (graph 6-3). On the whole, the results showed that the addition of glass fibre will be beneficial in improving some of the main properties of the flexible microasphalt pavement.

 10. **Effect of exceeding the glass fibre content limit:** During the laboratory testing, it was observed that if glass fibre length and quantity is exceeded exceptionally i.e. beyond 25 mm and 0.4% respectively, this resulted in tangling of glass fibres during the mixing of material for preparation of samples (graph 6-3). It takes the form of a “balling” which perhaps defeats the purpose of adding glass fibres in the microasphalt due to a non-uniform dispersion of the fibres in the mix.

 11. **SCB test:** The research evaluates the SCB test for determining tensile and fracture resistance of microasphalt mixtures and it can be drawn from the investigation that the SCB test could be used to characterize the tensile strength of microasphalt mixtures with good repeatability, which makes it a potentially simple performance test for microasphalt.

 12. **Low carbon emission:** The newly developed microasphalt material containing the new cementitious materials from waste is based on cold mix technology which essentially means no heating is involved to make the aggregates and bitumen ready in the laboratory and on site as compared to hot mix and thus significantly reduces greenhouse gas and CO₂ emissions and

helps in lowering the carbon footprint. This means reduced energy consumption, in the total construction cycle of cold mix microasphalt when compared to conventional road surfacing treatments. However, still CO₂ is produced during the production of glass fibres in the industry.

13. **Field trial:** For all practical purposes, glass fibre of 16mm length was only used for the trial road section because cutting of glass fibres of various lengths to be used as a blend was not possible on site for the choppers. The fiberized cold mix asphalt overlay was placed using normal paving equipment with multiple systems and operations in place i.e. pugmill, chopper, spreader box and roller compactor. No additional manpower was required and placement was achieved without noticeable difficulty or delay.

14. **Site inspection:** During the site inspection at 25 months, it was observed that the number of transverse cracks developed in the road covered by conventional microasphalt was essentially more as compared to longitudinal cracking.

15. **Validation of laboratory findings:** Up-to-date field trial visual inspection results for fibreless and fiberized sections validates the laboratory findings with confidence on the usefulness of adding glass fibres to retard the cracking and deformation distresses in microasphalt.

16. **Use of novel secondary binder:** One of the sustainable approaches which can be applied without making a significant environmental and economic impact is the incorporation of hydraulic filler materials into CMMs. Use of novel hydraulic filler material has absorbed the trapped water between bitumen film and aggregate and besides has provided further reinforcement to the primary bituminous binder as a secondary binder in the microasphalt.

17. **Characteristics of novel waste materials:** The specific characteristics of novel waste or by-product materials that made them useful in upgrading conventional CMMs include; chemical compositions, specific surface area, particle morphology and alkalinity. Accordingly, novel waste or by-product material such as PSA, CKD and RHA showed significant improvement to the

cracking and rutting properties of CMMs developed. However, the approach of filler characteristics is significantly valid to predict the worth of such novel fillers to improve CMMs.

18. Use of microanalysis techniques and benefits of novel waste materials:

Microanalysis techniques, namely XRD and SEM, have provided understanding of the role of the hydraulic filler in the CMMs, ensuring that the hydration process is continuous even in the presence of bitumen emulsion. Microanalysis techniques supplied the evidence of secondary binding initiation, removal of trapped water and reinforcement of the primary binder. Further, PSA has been proven as a superior alternative to OPC for producing CMMs and improve their durability properties. This research and for the first time shows that PSA-waste material has introduced outstanding properties to CMM. Furthermore, adding CKD and RHA to CMMs containing PSA has shown significant improvement in the mixture's mechanical and durability properties. Also, it also stated that the mechanical and durability properties of CMM containing PSA could be affected by application conditions, thus optimisation is required to ensure best application.

19. Research limitations:

Practical lengths (aspect ratios) and quantities (volume fractions) of glass fibres have been probed in the research as it was witnessed that if aspect ratio and volume fraction of glass fibre is increased substantially it causes the balling phenomenon in microasphalt. Further, on site the ability of the chopper to cut varied lengths of glass fibres for the mix is limited due to the constraint of the blade teeth's and the chopper cannot cut glass fibres of too many different lengths at the same time for incorporation in the microasphalt pavement. Also, the results obtained during the research shows indicative behaviour of the newly developed microasphalt and are valid for the materials (aggregates, bitumen emulsion, glass fibres, retarder, primary and secondary cementitious fillers) acquired from specific source, grade and type and procedures adopted for compaction and curing technology only. If the source and/or the production batch of these materials are differed or compaction and curing technology vary, the performance of the microasphalt will vary. Even if there is a slight interruption (surge) in the voltage of power

supply from the main grid station or power house; feeding electricity to the industry producing these materials especially waste cementitious filler, it will have an impact on the calcination and incineration processes involved in the production of waste fillers material and would change the percentages of chemical composition in the filler material and thus the performance of the microasphalt will change. Hobart mixer has been used to prepare the samples in the laboratory and it is generally assumed that uniform mixing of microasphalt ingredients takes place. Moreover, it is stated that though the newly developed microasphalt material is environmentally friendly, and no CO₂ is evolved during the production of secondary cementitious material and/or during the preparation of cold mix microasphalt itself, but still some CO₂ is produced during the manufacturing of glass fibres in the industry and it will be useful to carry out a full life CO₂ analysis for the microasphalt.

8.2 RECOMMENDATIONS

The development achieved in this research study opens up a new generation of CMMs, in terms of environmental, economic, safety and mechanical and durability characteristics. Further research on this new generation of CMMs would help us to establish a great degree of understanding of the mix design and properties. With the foregoing in mind, the following recommendations are made for implementation and further research.

8.2.1 RECOMMENDATIONS FOR IMPLEMENTATION

1. **Quantification of distresses:** Distresses in test trial sections should be quantified in technical terms i.e. criteria shall be devised to formulate an index or legend such as pavement condition index (PCI) or remaining service life (RSL) to examine the deterioration process in microasphalt. This can be achieved with the help of pavement condition data which shall be collected on site.
2. **Pavement condition data:** Pavement condition data should be collected through visual condition survey and mechanical laser profilometer to

determine pavement distresses in microasphalt which includes cracking, rutting and international roughness index (IRI) to calculate the remaining service life (RSL) of the pavement.

3. **Remaining service life:** Pavement condition data for the test trial section will help to quantify the actual useful service life of the control and glass fibre reinforced microasphalt treatments in terms of remaining service life (RSL) i.e. in years and will enable the local highway authorities to prepare the next maintenance strategy.
4. **Microasphalt treatment:** Use of glass fibre reinforced microasphalt treatment to retard the reflective cracking and deformation is not recommended merely on the basis of life-cycle cost analysis but the decision to apply newly developed glass fibre reinforced microasphalt should be made based on the structural condition assessment of the existing pavement.
5. **Best material application:** It is recommended that the newly developed best material and best mix which is ready to go to the market for test trial purposes shall be applied under site conditions.

8.2.2 RECOMMENDATIONS FOR FURTHER RESEARCH

1. **Life-cycle cost analysis:** Life-cycle cost analysis (LCCA) shall be done for the test trial sections. Further, in the future, life-cycle cost analysis should also be taken into account before applying microasphalt on site as a preventive maintenance tool.
2. **Deterioration modelling:** Monitoring (inspection) of test trial sections should be done in the subsequent years with the help of pavement condition survey as explained in section 8.2.1, sub-point (2) above i.e. to assess the behaviour of control microasphalt and glass fibre reinforced microasphalt test sections in more depth and subsequently to carry out deterioration modelling for such pavements for further research.

-
-
3. **Ductility:** Ductility of GCF fiberized microasphalt could be improved by carrying out further research on the use of different waste filler material available in the market, as an integral ingredient of the potential green cement.
 4. **Curing protocol:** Curing protocol of CMMs comprising inert filler has been studied by various researchers, however there is a gap in the literature in respect of the curing protocols for CMMs comprising hydraulic material. Thus, it is recommended that the curing protocol for the said mixtures be investigated to simulate relationship between on-site curing and laboratory curing.
 5. **Publication:** Currently, the publication has been constrained by the need for industrial confidentiality however, when this technology dies down publication with prior approval of industrial partner is recommended.
 6. **Mix design:** Currently, the mix design for CMMs containing OPC is in high demand therefore, a more detailed study is recommended to optimise the OPC by using different grades of bitumen emulsion available in the open market, as the current or other procedures did not accommodate these variations within the required properties. Further research can also be carried out to investigate different types of aggregates with different gradations acquired from various quarry sites and their effect on the microasphalt.

REFERENCES

Abaqus Theory Manual, Version 6-16-3. Habbitt, Karlsson & Sorenson, Inc., Pawtucket RI, 2016.

Abbas, A. H., “High Strength Cold Rolled Asphalt Surface Course Mixtures.” Ph.D. thesis, Liverpool John Moores University, Liverpool, UK, 2014.

Acott, S. M., “The stabilization of Sand by a Foamed Bitumen: A Laboratory and Field Performance Study”. Department of Civil Engineering, Univ. of Natal, Durban, South Africa, Dissertation, 1980.

Adams, T. M., and Kang, M., Considerations for Establishing a Pavement Preservation Program. *85th Annual Meeting of the Transportation Research Board* Washington, D.C., 2006.

AEMA, “A basic asphalt emulsion manual”, American Emulsion Manufacturers Association, 2nd Edition, 1979.

Allan, G., “History of slurry and the international slurry surfacing association,” in *Proceedings of the International Slurry Surfacing Association’s 5th World Congress*, Berlin, Germany, March 2002.

Al-Nageim, H., Busaltan, S. A., Atherton, W., and Sharples, G., A comparative study for improving the mechanical properties of cold bituminous emulsion mixtures with cement and waste materials’ *Construction and Building Materials*-36, pp. 743–748, 2012.

Anderson, H., “Slurry seal vs. micro-surfacing,” in *Proceedings of the 34th Annual Utah Asphalt Conference*, South Towne Exposition Center, Sandy, Utah, USA, April 2009, <http://www.pavementpreservation.org/toolbox/guidelines.html>.

Andrew, M. R., *Global CO₂ Emissions from Cement Production*, Centre for International Climate Research (CICERO), Norway, 2017.

Antiohos, S. K., Papadakis, V. G., and Tsimas. Rice Husk Ash (RHA) effectiveness in cement and concrete as a function of reactive silica and fineness, *Cement and Concrete Research*, 61-62, pp. 20-27, 2014.

Anurag, K., Xiao, F. and Amir Khanian, S. N., Laboratory investigation of indirect tensile strength using roofing polyester waste fibers in hot mix asphalt. *Construction and Building Materials*, 23, 2035-2040, 2009.

Aravind, K. and Das, A., Pavement design with central plant hot-mix recycled asphalt mixes. *Construction and Building Materials*, 21, pp. 928-936, 2007.

Arnold, G. K., Rutting of Granular Pavements. PhD Thesis, University of Nottingham, UK, 2004.

Asphalt Institute, Asphalt Cold Mix Manual, Series No.14 (MS-14), Maryland, USA, 1989.

Asphalt Institute, Basic Asphalt Emulsion Manual, Series No.19 (MS-19), Maryland, USA, 1979.

Asphalt Institute, "Energy Requirements for Road Pavements", Asphalt Institute Report (AIR) - Misc-75-3, 1993.

Asphalt Institute, Thickness Design of Asphalt Pavement for Highways and Street, Manual Series No. 1 (MS-1), Maryland, USA, 1991.

ASTM C 78., Standard Test Method for Flexural Strength of Concrete (Using Simple Beam with Third-Point Loading), 1987.

ASTM C 1018., Standard Test Method for Flexural Toughness and First-Crack Strength of Fibre-Reinforced Concrete (Using Beam with Third-Point Loading), 1997.

ASTM D 6372., Standard Practice for Design, Testing, and Construction of Micro-Surfacing, 2005.

Baladi, G. Y., Svasdisant, T., Van, T., Buch, N., and Chatti, K., Cost-effective preventive maintenance: Case studies. In *Transportation Research Record: Journal of the Transportation Research Board*, No. 1795, TRB, National Research Council, Washington, D.C., pp. 17-26, 2002.

Baladi G. Y., Chatti K., and Buch, N., An Excellent Asset Management Tool The Remaining Service Life, 6th International Conference on Managing Pavements (2004), TRB Committee AFD on Pavement Management Systems.

Beijing Aerospace Control Technology Institute of Aerospace (BACTIA), Wheel Tracking Tester, HYCZ-5, Operation Manual, 2013.

Bergeron, G., The Performance of Full-Depth Reclamation and Cold In-Place Recycling Techniques in Quebec. Annual Conference of the Transportation Association of Canada. Calgary, Canada, 2005.

Bindu, C. S., Influence of Additives on the Characteristics of Stone Matrix Asphalt. PhD Thesis, University of Science and Technology, Kochi, India, 2012.

Bonaquist, R., Mix Design Practices for Warm Mix Asphalt. In: REPORT:691, N. (ed.) Project 09-43. Transportation Research Board, 2011.

Bouteiller, E. L., Asphalt Emulsion for Sustainable pavements. First International Conference on Pavement Preservation. Newport Beach, California, USA, 2010.

Brannan, C. J., Jeon, Y. W., Perry, L. M., and Curtis, C. W., Adsorption Behaviour of Asphalt Models and Asphalts on Siliceous and Calcareous Aggregates, Transportation Research Record 1323, pp. 10-21, 1990.

Brandt, H. C. A., Beverwijk, C. D. M., Harrison, T., "Health Aspects of Hot Bitumen Application", Eurobitume, Sweden, 1993, pp 437-442.

Broughton, B., Lee, S. J., and Kim, Y. J., "30 Years of Microsurfacing: A Review," International Scholarly Research Network (ISRN), Civil Engineering Volume, Article ID 279643, 7-pages, 2012.

Brown, S. F., Rowlett, R. D., and Boucher, J. L., Asphalt Modification. Proceedings of the Conference on the United States Strategic Highway Research Program: Sharing the Benefits. London, Thomas Telford (pub). pp. 181-203, 1990.

British Glass, Glass Fibre Manufacturing Process, [Online]. Available: <http://www.britglass.org.uk/glass-fibre-manufacture> [Accessed 16/07/2014].

British Standards Institute, BS 4987: Part 1 "Coated macadam for roads and other paved areas", HMSO, 1988.

British Standards Institution, BS EN 13043 "Aggregates for bituminous mixtures and surface treatments for roads, airfields and other trafficked areas". London: British Standards Institution (BSI), 2002.

British Standards Institution, Guidance on the use BS EN 12697-22 "Bituminous mixtures. Test methods for hot mix asphalt. Wheel tracking test". London: British Standards Institution (BSI), 2003.

British Standards Institution, BS EN 12697-33 "Bituminous mixtures. Test methods for hot mix asphalt. Specimen prepared by roller compactor". London: British Standards Institution (BSI), 2003.

British Standards Institution, BS 434-2 “Bitumen road emulsions. Code of practice for the use of cationic bitumen emulsions on roads and other paved areas”. London: British Standards Institution (BSI), 2006.

British Standards Institution, BS EN 1097-7 “Tests for mechanical and physical properties of aggregates”. Determination of the particle density of filler. Pycnometer method”. British Standards Institution (BSI), London, UK, 2008.

British Standards Institution, PD 6682-2: Aggregates Part 2: Aggregates for bituminous mixtures and surface treatments for roads, airfields and other trafficked areas – Guidance on the use of BS EN 13043. British Standards Institution (BSI), London, UK, 2009.

British Standards Institution, Guidance on the use BS ISO 29581-2 “Cement. Test methods. Chemical analysis by X-ray fluorescence”. British Standards Institution (BSI), London, UK, 2010.

British Standards Institution, Guidance on the use BS ISO 9277 “Determination of the specific surface area of solids by gas adsorption - BET method”. British Standards Institution (BSI), London, UK, 2010.

British Standards Institution, Guidance on the use BS EN 12697-44 “Bituminous Mixtures – Test methods for hot mix asphalt. Crack propagation by semi-circular bending test”. London: British Standards Institution (BSI), 2010.

British Standards Institution, BS EN 12697-11 “Bituminous mixtures. Test methods for hot mix asphalt. Determination of the affinity between aggregate and bitumen”. London: British Standards Institution (BSI), 2012.

British Standards Institution, BS EN 12697-26 “Bituminous mixtures. Test methods for hot mix asphalt. Stiffness”. London: British Standards Institution (BSI), 2012.

British Standards Institution, BS EN 13043 “Aggregates for Bituminous Mixtures and Surface Treatments for Roads, Airfields and Other Trafficked Areas”. London: British Standards Institution (BSI), 2013.

British Standards Institution, BS EN 13808 “Bitumen and bituminous binders. Framework for specifying cationic bituminous emulsions”. British Standards Institution (BSI), 2013.

British Standards Institution, BS EN ISO 6892-1 “Metallic materials. Tensile testing. Method of test at room temperature”. British Standards Institution (BSI), 2016.

British Standards Institution, Guidance on the use BS ISO 16700 “Microbeam analysis. Scanning electron microscopy. Guidelines for calibrating image magnification”. British Standards Institution (BSI), London, UK, 2016.

Bushing, H. W., and Antrim, J. D., Fibre Reinforcement of Bituminous Mixtures. Proceedings of the Association of Asphalt Paving Technologists. Vol. 37. pp. 629-659, 1968.

Button, J. W., and Lytton, R. L., Evaluation of Fabrics, Fibres and Grids in Overlays. Sixth International Conference on the Structural Design of Asphalt Pavements. Ann Arbor, Michigan, 1987.

Button, J. W., Estakhri, C., and Wimsatt, A., A Synthesis of Warm-Mix Asphalt. Report No. 0-5597-1. College Station, Texas, USA: Texas Transportation Institute, 2007.

California Department of Transportation, Caltrans Code of Safe Operating Practices, Chapter 12, Sacramento, California, 1999.

California Department of Transportation, Caltrans Micro-Surfacing Pilot Study 2001, Final Report, Sacramento, California, June 2002.

California Department of Transportation, Caltrans MTAG, Volume I, Flexible Pavement Preservation 2nd Edition, Chapter 9 – Micro-surfacing, June 2009.

Campbell, R., “Asphalt in pavement maintenance,” in *The Asphalt Handbook*, B. Boyer, Ed., pp. 569–616, Asphalt Institute, College Park, Md, US, 2007.

Capitao, S. D., Picado-Santos, L. G., and Martinho, F., Pavement engineering materials: Review on the use of warm-mix asphalt. *Construction and Building Materials* 36, pp. 1016-1024, 2012.

Chan, A., Keoleian, G., and Gabler, E., “Evaluation of lifecycle cost analysis practices used by the Michigan department of transportation,” *Journal of Transportation Engineering*, vol. 134, no. 6, pp. 236–245, 2008.

Chasey, A. D., Using Simulation to Understand the Impact of Deferred Maintenance. *Journal of Computer-Aided Civil and Infrastructure Engineering*, Vol. 17, 2002.

Chauhan, S. K., Sharma, S., Shukla, A. & Gangopadhyay, S., Recent Trends of the Emission Characteristics from the Road Construction Industry. *International Journal of Environmental Science and Pollution Research*, 17, 1493–1501, 2010.

Chowdhury, A. & Button, J. W., A Review of Warm Mix Asphalt. College Station, Texas, USA: Texas Transportation Institute, 2008.

Chevron. Bitumuls Mix Manual Chevron, Asphalt Division, California, USA, 1977.
Csanyi, L. H., Foamed Asphalt in Bituminous Paving Mixes Highway Research Board Bulletin, Vol. 10, pp. 108-122, 1957.

Daoud, O. E. K., Guirguis, H. R., and Hamdani, S. K., Factors Effecting the Coating of Aggregates with Portland Cement, Ministry of Public Works, Kuwait, Internal Report 80/4, 1980.

D'Angelo, J., Harm, E., Bartoszek, J., Baumgardner, G., Corrigan, M., Cowsert, J., Harman, T., Jamshidi, M., Jones, W., Newcomb, D., Prowell, B., Sines, R. & Yeaton, B., Warm-Mix Asphalt: European Practice. In: FHWA-PL-08-007 (Ed.), 2008.

Deborah A. C, Robert J. E., Gruszczynski, L., Marlowe, J., Roohanirad, A., and Titi, H. Capital Preventive Maintenance. Midwest Regional University Transportation Center, Madison, 2004.

Detwiler, R. J., Bhatta, J. I., and Sankar B., Supplementary Cementing Materials for Use in Blended Cements, Research and Development Bulletin RD112T, Portland Cement Association, Skokie, Illinois, 1996.

Di, J. & Liu, Z., Influence of Fly Ash Substitution for Mineral Powder on High Temperature Stability of Bituminous Mixture. Energy Procedia, 16, Part A, 91-96, 2012.

Domone, P. & Illston, J. Construction Materials Their nature and behaviour, Spon Press, 2010.

Doyle, T., Gibney, A., McNally, C. & Tabakovic, A., Development of Maturity Methods for Predicting Performance of Cold-Mix Pavement Materials. Asphalt Professional the Journal of the Institute of Asphalt Technology, 44, pp. 26-31, 2010.

Earl, J. Paying for Deferred Maintenance, *Buildings Magazine*, June 2006 Issue, Stamats Business Media, Cedar Rapids, IA, 2009.

Environmental Agency, Paper sludge ash A technical report on the production and use of paper sludge ash, Banbury, Oxon, UK, Environmental Agency, 2008.

Erwin, T., and Tighe, S. L., "Safety effect of preventive maintenance: a case study of microsurfacing," *Transportation Research Record*, no. 2044, pp. 79–85, 2008.

European Asphalt Pavement Association (EAPA), Asphalt in Figures, Brussels – Belgium, 2010.

Fava, G., Ruello, M. L. & Corinaldesi, V., Paper Mill Sludge Ash as Supplementary Cementitious Material. *Journal of Materials in Civil Engineering*, 23, 772-776, 2011.

Federal Highway Administration (FHWA), Pavement Condition Index Distress Identification Manual for Asphalt and Surface Treatment Pavements. Federal Highway Administration, United States Department of Transportation, 1998.

Federal Highway Administration (FHWA), Construction and Maintenance Fact Sheets, *Optimizing Highway Performance: Pavement Preservation*. FHWA-IF-00-013, September, 2000.

Federal Highway Administration (FHWA), Pavement Preservation: A Road Map for the future. Publication FHWA-SA-99-015. FHWA, U.S. Department of Transportation, 1999.

Fitzsimons, L., and Gibney, A., “Recycled Glass in Hot Rolled Asphalt Wearing Course Mix”, *Proceedings of the International Conference by the Concrete and Masonry Research Group*, Kingston University, London, 2004.

Foundation for Pavement Preservation (FPP), 2012. <http://www.fp2.org/2012/01/05/microsurfacing/>.

Freeman, T., Pinchett, D., Haobo, R., and Spiegelman, C., *Analysis and Treatment Recommendations from the Supplemental Maintenance Effectiveness Research Program (SMERP)*, Texas Transportation Institute, College Station, Tex, USA, 2002.

Galehouse, L. Strategic planning for pavement preventive maintenance: Michigan Department of Transportation's "mix of fixes" program. *TR News*, Vol. 219, pp. 3-8, 2002.

Galehouse, L., Moulthrop, J.S., Hicks, R.G. Principles of Pavement Preservation. In *TR News, September/October. Issue*, 2003.

Geiger, D. R., Office of Asset Management. Pavement Preservation Definitions. FHWA, September 2005.

Geoffroy, D. N., Cost-effective Preventative Maintenance. National Cooperative Highway Research Program Synthesis of Highway Practice 223, Transportation Research Board, National Research Council, Washington, DC, USA, 1996.

Gorkem, C. and Sengoz, B., Predicting stripping and moisture induced damage of asphalt concrete prepared with polymer modified bitumen and hydrated lime. *Construction and Building Materials*, 23, 2227-2236, 2009.

Greaves, G. N., Greer, A. L., Lakes, R. S., and Rouxel, T., "Poisson's Ratio and Modern Materials", *Nature Materials*, 10, 823-837 Nov, 2011.

Haider, S. W., & Dwaikat, M. B., "Estimating optimum timing for preventive maintenance treatment to mitigate pavement roughness". *Transportation Research Record*, (2235), pp. 43-53, 2011.

Hasan, M. A., Islam, M. A., Ahmed, Z., and Ahmad, I., Compressive Strength Behaviour of Concrete using Rice Husk Ash as Supplementary to Cement. *Proceedings of 3rd International Conference on Advances in Civil Engineering*, pp. 327-330, December 2016.

Harrison, M., Laboratory Report LR 2206 MH - Liverpool John Moores University, Effect of Glass Fibre in Microasphalt, September 2015.

Harrison, T. and Christodulaki, L., "Innovative Processes in Asphalt Production and Application-Strengthening Asphalt's Position in Helping to Build a Better World,". *Proceedings, First International Conference, World of Asphalt Pavements*, Australian. Kew, Victoria, Australia: Asphalt Pavement Association, 2000.

Hein, D., Olidis, C., Darter, M., and Quintus, H. V., "Impact of recent technology advancements on pavement life," in *Proceedings of the Annual Conference of the Transportation Association of Canada*, St. John's, 2003.

Heukelom, W., "A Bitumen Test Data Chart for Showing the Effect of Temperature on the Mechanical Behaviour of Asphaltic Bitumens". *Journal of Institute of Petroleum*, Vol 55, No. 546, pp. 404-417, Fig-13, Tab-2, 1969.

Hicks, R. G., Dunn, K., and Moulthrop, J., "Framework for selecting effective preventive maintenance treatments for flexible pavements," *Transportation Research Record*, no. 1597, pp. 1-10, 1997.

Highway Agency, Design Manual for Roads and Bridges (DMRB), Volume 7: Pavement Design and Maintenance, section 1: Preamble, PART 1: HD 23/99 general information, London, UK, 1999.

Highway Authority and Utilities Committee (HAUC), "New Roads and Streetworks Act 1991 - Specification for the Reinstatement of Opening in Highways", - HMSO, 1992.

Highway Authority and Utilities Committee (HAUC), New Roads and Street Works Act 1991 Specification for the Reinstatement of Openings in Highways. London, UK: Department for Transport, 2010.

Hixon, C. D., and Ooten, D. A., “Nine years of micro-surfacing in Oklahoma,” *Transportation Research Record*, no. 1392, pp. 13–19, 1993.

Hofman, R., Oosterbaan, B., Erkens, S.M.J.G. and Kooji, J., “Semi-Circular Bending Test to Assess the Resistance Against Crack Growth”, 6th Rilem Symposium PTEBM’03, Zurich, Switzerland, (2003), 257-269.

Holleran, G., ABC’s of Slurry Surfacing, Asphalt Contractor Magazine, 2001.

Holleran, G., Slurry Surfacing Workshop - The Benefits of Polymer Modification in Slurry Surfacing, International Slurry Surfacing Association, Las Vegas, Nevada, January, 2002.

Huang, B., Xiang, S. and Zuo, G., “Laboratory Evaluation of Semi-Circular Bending Tensile Strength Test for HMA Mixtures”, AMEC Earth and Environment Congress, U.S.A., 231-245, 2004.

Ibrahim, H. E. & Thom, N. H., The Effect of Emulsion Aggregate Mixture Stiffness on Both Mixture and Pavement Design. Proceeding of the second European symposium on Performance and Durability of Bituminous Materials. University of Leeds, 1997.

Interim Advice Note (IAN) 154/12, Revision of Specification for Highway Works (SHW) Clause 903, Clause 921 and Clause 942, Design Manual for Roads and Bridges and the Manual of Contract Documents for Highway Works, 2012.

International Organization of Motor Vehicle Manufacturers (IOMVMS), Production statistics [Online]. Available: <http://oica.net/category/production-statistics/> 2016.

International Slurry Surfacing Association (ISSA), Flexural Tension Test Method for Determination of Cracking Resistance of Slurry Mixes at Ambient and 40C. Technical Bulletin No 146, Washington, D.C., 1989.

International Slurry Surfacing Association (ISSA), Design Technical Bulletins 102, 1990.

International Slurry Surfacing Association (ISSA), Test Method for Wet Track Abrasion of Slurry Surfaces. Design Technical Bulletins, 100. Annapolis (Md.): International Slurry Surfacing Association, May, 2005.

International Slurry Surfacing Association (ISSA), Test Method for Measurement of Excess Binder in Bituminous Mixtures by Use of a Loaded Wheel Tester and Sand Adhesion. Design Technical Bulletins, 100. Annapolis (Md.): International Slurry Surfacing Association, May, 2005.

International Slurry Surfacing Association (ISSA), Recommended Performance Guidelines for Micro-Surfacing A143, Annapolis, MD, May 2005.

International Slurry Surfacing Association (ISSA), *Recommended Performance Guidelines for Micro-Surfacing A143*, Annapolis, Md, USA, 2010.

International Slurry Surfacing Association (ISSA), 2012. <http://www.slurry.org/index.php/education/issa-disciplines-guidelines/what-is-micro-surfacing>.

Irfan, M., Khurshid, M. B., Labi, S., and Flora W., Evaluating the Cost-effectiveness of Flexible Rehabilitation Treatments using Different Performance Criteria, *ASCE Journal of Transportation Engineering*, Vol. 135 (10), pp. 753-763, 2009.

Islam, R. M., Faisal, M. H., and Tarefder A. R., “Determining temperature and time dependent Poisson’s ratio of asphalt concrete using indirect tension test”, *The Science and Technology of Fuel and Energy Journal*, pp. 119-124, 2015.

Islam, S. T., Study of Some Parameters Affecting the Measured Flexural Toughness of Fibre Reinforced Concrete. Master of Applied Science. The University of British Columbia, 2012.

James, A. D., and Stewart, D. “The Use of Fatty Amine Derivatives to Slow Down the Age-hardening Process in Bitumen”, *International Symposium - Chemistry of Bitumens*, Rome, 1991.

Jamieson, I. L., Jones, D. R., & Moulthrop, J. S. Advances in the Understanding of Binder-Aggregate Adhesion and Resistance to Stripping, *Highways and Transportation Journal*, pp. 6-19, 1993.

Jenkins, K. J., De Groot, J., Van De Ven, M., and Molenaar, A. Half-Warm Foamed Bitumen Treatment, A New Process. 7th Conference on Asphalt Pavements for Southern Africa, 1999.

Jiang, Y., and McDaniel, R. S., Application of Cracking and Sealing and Use of Fibres to Control Reflection Cracking. *Transportation Research Record No. 1388*, pp. 150-159, 1993.

Jenq, Y.S., Chwen-Jang, L., and Pei, L., 'analysis of crack resistance of asphalt concrete overlays. a fracture mechanics approach', *Transportation Research Record*, 1388, 160–166, 1993.

Jorgensen, T., Jebens, A., and Ruud O. E., "Emission Monitoring from Two Types of Drum Mix Plants", *Eurobitume*, Sweden, pp. 453-456, 1993.

Kargah-Ostadi N., Stoffels S. M., and Tabatabaee N., "Network-Level Pavement Roughness Prediction Model for Rehabilitation Recommendations". *Transportation Research Record: Journal of the Transportation Research Board*, Vol. 2155, Washington, D.C., pp. 124-133, 2010.

Karlsson, R., and Isacson, U., Material-Related Aspects of Asphalt Recycling: State of the Art. *Journal of Materials in Civil Engineering*, 18, pp. 81-92, 2006.

Kazmierowski, T. J., and Bradbury, A., "Micro-surfacing: solution for deteriorated freeway surfaces," *Transportation Research Record*, no. 1473, pp. 120–130, 1995.

Kelham, S., Damtoft, J. S., and Talling, B. L. O., "The Influence of High Early-Strength (HES) Mineralized Clinker on the Strength Development of Blended Cements Containing Fly Ash, Slag, or Ground Limestone," *Proc. of Fly Ash, Silica Fume, Slag and Natural Pozzolans in Concrete*, ACI SP 153, 1995.

Kendrick, P., Copson, M., Beresford, S., and McCormick, P., *Roadwork Theory and Practice*, Elsevier Butterworth Heinemann, 2004.

Khatri, R. P., Sirivivatnanon, V., and Gross, W., Effect of different supplementary cementitious materials on mechanical properties of high performance concrete. *Cement and Concrete Research*, 25, 209-220, 1995.

Khurshid, M. B., *A Framework for Establishing Optimal Performance Thresholds for Highway Asset Interventions*. PhD Dissertation. Purdue University, W. Lafayette, IN., 2010.

Khurshid, M. B., Irfan, M., and Labi, S., Comparing the Methods for Evaluating Pavement Interventions – Evaluation and Case Study. In *Transportation Research Record* No. 2108, Transportation Research Board, Washington, D.C., pp. 25-36, 2009.

Khurshid, M. B., Irfan, M., and Labi, S., Optimal Performance Threshold Determination for Highway Asset Interventions - An Analytical Framework and Application, *ASCE Journal of Transportation Engineering*, 2010.

Kietzman, J. H., The Effect of Short Asbestos Fibres on Basic Physical Properties of Asphalt Pavement Mixes. Highway Research Board. Bulletin No. 270. pp. 1 - 19, 1960.

Kim, Y., and Lee, H. D., Development of Mix Design Procedure for Cold In-Place Recycling with Foamed Asphalt. *Journal of Materials in Civil Engineering*, 18, pp. 116-124, 2006.

Konsta-Gdoutos, M. S., & Shah, S. P. Cement Kiln Dust (CKD): Characterisation and utilisation in cement and concrete. Proceedings of the International Symposium dedicated to Professor Fred Glasser, University of Aberdeen, Scotland (pp. 59-70), 2003.

Koshikawa, M., and Isogai, A., Analyses of incinerated ash of paper sludge: comparison with incinerated ash of municipal solid waste. *Material Cycles Waste Management* 6, 64-72, 2004.

Krans, R. L., Tolman, F., and Van De Ven, M. F. C., "Semi-Circular Bending Test: Practical Crack Growth Test Using Asphalt Concrete Cores", Third International RILEM Conference, Reflecting Cracking in Pavements, Spon Press, U.K., 123-133, 1996.

Kristjansdottir, O., Warm Mix Asphalt for Cold Weather Paving. PhD Thesis, University of Washington, Seattle, USA, 2006.

Kuennen, T., Making High-Volume Roads Last Longer. *Better Roads, April Issue*, 2005.

Labi, S., Lamptey, G., and Kong, S. H., "Effectiveness of micro-surfacing treatments," *Journal of Transportation Engineering*, Vol. 133, no. 5, pp. 298–307, 2007.

Labi, S., Mahmodi, M. I., Fang, C., and Nunoo, C., Cost Effectiveness of Microsurfacing and Thin HMA Overlays – A Comparative Analysis. Transportation Research Board of the National Academies, Washington, D.C., Annual Meeting CD-ROM, 2007.

Lampris, C., Stegemann, J. A., and Cheeseman, C. R., Chloride leaching from air pollution control residues solidified using ground granulated blast furnace slag. *Chemosphere*, 73, 1544-1549, 2008.

Landfill Tax (LFT), Excise Notice LFT1: A general guide to Landfill Tax, 2017.

Lee, D., "Fundamentals of Life-Cycle Cost Analysis." *Transportation Research Record: Journal of the Transportation Research Board*, 1812(-1), pp. 203-210, 2002.

Lee, S. J., Akisetty, C. K., and Amirghanian, S. N., The effect of crumb rubber modifier (CRM) on the performance properties of rubberized binders in HMA pavements. *Construction and Building Materials*, 22, pp. 1368-1376, 2008.

Leech, D., *Cold Bituminous Materials for Use in the Structural Layers of roads*. Transportation Research Laboratory, Project Report 75, UK, 1994.

Li, Z., and Madanu, S., "Highway project level life-cycle benefit/cost analysis under certainty, risk, and uncertainty: methodology with case study," *Journal of Transportation Engineering*, Vol. 135, no. 8, pp. 516-526, 2009.

Lien, J. E., "Survey of Occupational Exposures of Asphalt Workers", *Eurobitume*, Sweden, pp. 457-461, 1993.

Lothenbach, B., Scrivener, K., and Hooton, R. D., Supplementary cementitious materials. *Cement and Concrete Research*, 41, 1244-1256, 2011.

Louay, N. M., Wu, Z., Zhang, C., Mohammad, J. K., Chris, A., and John, W. H., "Variability of Air Voids and Mechanistic Properties of Plant Produced Asphalt Mixtures", 83th Transportation Research Board Annual Meeting, 85-102, 2004.

Maccarrone, S., Holleran, G., and Ky, A., *Cold Asphalt Systems as an Alternative to Hot Mix*. 9th Australian Asphalt Pavement Association International Asphalt Conference. Australian, 1994.

Mallick, R. B., Kandhal, P. S., and Bradbury, R. L., Using Warm-Mix Asphalt Technology to Incorporate High Percentage of Reclaimed Asphalt Pavement Material in Asphalt Mixtures *Transportation Research Record: Journal of the Transportation Research Board*, 2051, 2008.

Marais, C. P., *The Use of Asbestos in Trial Sections of Cap-Graded Asphalt and Slurry seals*. Proceedings of the Third Conference on Asphalt Pavements for South Africa. Durban. pp. 172-175, 1979.

Marquis, B., "The use of micro-surfacing for pavement preservation", Tech. Rep. 02-3, Transportation Research Division, Maine Department of Transportation, 2004.

Maurer, D. A., and Malasheskie, G., Field performance of fabrics and fibres to retard reflective cracking *Transportation Research Record No. 1248*, pp. 13-23, 1989.

McDaniel, R., Soleymani, H., and Shah, A., Use of Reclaimed Asphalt Pavement (RAP) under Superpave Specifications: A Regional Pooled Fund Project. Purdue University, West Lafayette, 2002.

McNaught, A. D., and Wilkinson, A., Compendium of Chemical Terminology, 2nd Ed. (the "Gold Book"), Blackwell Scientific Publications, Oxford, 1997.

Michigan Department of Transportation (MDOT), "Capital Preventive Maintenance Manual", Edition, 2003.

Mills, D. R., and Keller Jr., T., The Effectiveness of Synthetic Fibre – Reinforced Asphaltic Concrete Overlays in Delaware. Delaware Department of Transportation. Dover, November, 1982.

Minnesota Department of Transportation (MnDOT), "Pavement Condition Annual Report", 2003.

Minnesota Department of Transportation (MnDOT), "Flexible Microsurfacing Research Report", 2005.

Mohammad, L. N., Wu, Z., and Aglan, M. A., "Characterization of Fracture and Fatigue Resistance on Recycled Polymer-Modified Asphalt Pavements", 6th Rilem Symposium PTEBM'03, Zurich, Switzerland, 375-387, 2004.

Molenaar, A. A. A., "Are There Any Lessons to be Learned from Pavement Research", Report, Delft University of Technology, Netherlands, 2000.

Molenaar, A. A. A., Scarpas, A., and Liu, X., "Semi Circular Bending Test, Simple but Useful", Journal of Association of Asphalt Paving Technologies, Vol. 71, 2002.

Molenaar, J. M. M., and Molenaar, A. A. A., "Fracture Toughness of Asphalt in the Semi-Circular Bend Test", 2nd Euroasphalt and Eurobitume Congress, Barcelona, Spain, 509-517, 2000.

Montestruque, G. E., Rehabilitation of asphaltic pavements using geosynthetics on anti-reflective crack systems. Ph.D. thesis, Technological Institute of Aeronautics, São José dos Campos, Brazil, 2002.

Monower, M., "Development of Low Carbon Cement from Waste Fly Ashes." Ph.D. thesis, Liverpool John Moores University, Liverpool, UK, 2012.

Morgan, P., Mulder, A., "The Shell Bitumen Industrial Handbook", Shell Bitumen, 1995.

Moulthrop, J. S., Day, L., and Ballou, W. R., “Initial improvement in ride quality of jointed, plain concrete pavement with micro-surfacing: case study,” *Transportation Research Record*, no. 1545, pp. 3–10, 1996.

MS-15, Asphalt Institute. Asphalt Cold Mix Manual, manual series No. 14, Maryland, USA, 1989.

MultiMechanics, Computer-Aided Engineering (CAE), Software for Advanced Composite Analysis of Materials, Omaha, USA, 2014.

National Asphalt Pavement Association (NAPA), and European Asphalt Pavement Association (EAPA). The Asphalt Paving Industry a Global Perspective. Global Series 101, 3rd Edition, 2011.

National Cooperative Highway Research Program (NCHRP), *Synthesis of Highway Practice 58*. Consequences of Deferred Maintenance. Transportation Research Board, Washington, D.C., 1979.

National Highway Institute’s Pavement Preservation Treatment Construction Guide on Characteristics of Aggregates, Missouri, Department of Transport, 2007.

Nasseri S., Gunaratne M., Yang J., and Nazef A., Application of an Improved Crack Prediction Methodology in Florida’s Highway Network. *Journal of the Transportation Research Board* 2093, pp. 67-75, 2009.

Needham, D., “Developments in bitumen emulsion mixtures for roads”. PhD thesis, University of Nottingham, 1996.

Nikolaides, A. F., Design of dense graded cold bituminous emulsion mixtures and evaluation of their engineering properties. PhD thesis, The University of Leeds, 1983.

O'Brien, L. G., Evolution and Benefits of Preventive Maintenance Strategies. *National Cooperative Highway Research Program Synthesis of Highway Practice 153*, Washington D.C., 1989.

OECD, “Road Binders and Energy Savings”, 1984.

O’Flaherty, C. A., *Highways the Location, Design, Construction and Maintenance of Road Pavements*, Butterworth Heinemann, 2007.

Ozer, H., Al-Qadi, I. L., and Duarte, C. A., Effects of nonuniform and three-dimensional contact stresses on near-surface cracking. *Transp Res Rec, J Transp Res Board*; 2210:97-105, 2011.

Papadakis, V. G., and Tsimas, S., Supplementary cementing materials in concrete: Part I: efficiency and design. *Cement and Concrete Research*, 32, 1525-1532, 2002.

Pasetto, M., and Baldo, N., Experimental evaluation of high performance base course and road base asphalt concrete with electric arc furnace steel slags. *Journal of Hazardous Materials*, 181, pp. 938-948, 2010.

Pasquini, E., Canestrari, F., Cardone, F., and Santagata, F. A., Performance evaluation of gap graded asphalt rubber mixtures. *Construction and Building Materials*, 25, 2014-2022, 2011.

Pasupathy, R., Labi, S., and Sinha, K. C., Optimal Reconstruction Periods for Stochastically Deteriorating Infrastructures. *Journal of Computer-Aided Civil and Infrastructure Engineering*, Vol. 22, pp. 389-399, 2007.

Pederson, C. M., Schuller, W. J., and Hixon, C. D., "Micro-surfacing with natural latex-modified asphalt emulsion: a field evaluation," *Transportation Research Record*, no. 1171, pp. 108–112, 1988.

Peshkin, D. G., Hoerner, T. E., and Zimmerman, K. A., "Optimal Timing of Pavement Preventive Maintenance Treatment Applications". *Transportation Research Board*, Washington, DC, 2004.

Peterson "Road Deterioration and Maintenance Effects". A World Bank Publication, 1987.

Putman, B. J., and Amirhanian, S. N., Utilization of waste fibres in stone matrix asphalt mixtures. *Resources, Conservation and Recycling*, 42, 265-274, 2004.

Rajagopal, A. S., and George, K. P., "Pavement maintenance effectiveness," *Transportation Research Record*, vol. 1276, pp. 62–68, 1990.

Ramachandran, V. S., and Beaudoin, J. J., *Handbook of Analytical Techniques in Concrete Science & Technology, Principles, Techniques and Applications*, William Andrew Publishing, 2001.

Read, J., and Whiteoak, D., *The Shell Bitumen Handbook*, 1 Heron Quay, London., Thomas Telford Publishing, 2003.

Reincke, G., Ballou, W. R., Engber, S. L., and O'Connell, T. M., "Studies of polymer modified micro-surfacing materials in highway maintenance," in *Proceedings of the ISSA*, pp. 45–83, International Slurry Surfacing Association, February 1989.

Robinson, R., and Thagesen, B., Road Engineering for Development, London, UK, 2004.

Rojas, M. F. A., and Cabrera, J., The effect of temperature on the hydration rate and stability of the hydration phases of metakaolin-lime-water systems. Cement and Concrete Research, 32, pp. 133-138, 2002.

Rouse, M., "What is aspect ratio?", 2005.

Rubio, M. C., Martinez, G., Baena, L., and Moreno, F., Warm Mix Asphalt: An Overview. Journal of Cleaner Production, 24, 76-84, 2012.

Ruckel, P. J., Acott, S. M., and Bowering, R. H., Foamed-Asphalt Paving Mixtures: Preparation of Design Mixes and Treatment of Test Specimens. Transportation Research Board, Transportation Research Record, 1983.

Ruggles, C. S., "The Efficient Use of Environmentally-Friendly NR latex (NRL) in Road Construction – Past, Present and the Future", Natural rubber 37, pp. 2-4, 1st Quarter, 2005.

Saito, M., and Kawamura, M., Resistance of the Cement-Aggregate Interfacial Zone to the Propagation of Cracks, Cement and Concrete Research, Vol. 16, pp. 653-661, 1986.

Sallam, H. E.M., and Abd-Elhady, A. A. Mixed mode crack initiation and growth in notched semi-circular specimens; three-dimensional finite element analysis. Asian J Mater Sci; 4(2): 34-44, 2012.

Sayers, M., Gillespie, T. D., and Paterson, W., *Guidelines for Conducting and Calibrating Road Roughness Measurements*. Tech. Paper, No. 46. The World Bank, Washington, D.C., 1986.

Schapery R. A., "A Theory of Crack Initiation and Growth in Viscoelastic Media", Int. J. Fract., Part I, Vol. 11, pp. 141-159, 1975.

Schilling, P., Success with Bituminous Emulsions Requires a Well-Balanced Chemistry of Emulsions, Bitumen and Aggregate, International Slurry Surfacing Association Conference, Berlin, Germany, 2002.

Sebaaly, P. E., Bazi, G., Hitti, E., Weitzel, D., and Bemanian, S., Performance of Cold In-Place Recycling in Nevada Transportation Research Record: Journal of the Transportation Research Board, Volume 1896, 2004.

Serfass, J. P., and Samanos. J., Fibre-Modified Asphalt Concrete Characteristics, Applications and Behaviour. *Journal of the Association of Asphalt Paving Technologists*, Vol. 65, pp. 193-230, 1996.

Serfass, J. P., Poirier, J., Henrat, J., and Carbonneau, X., Influence of curing on cold mix mechanical performance. *Materials and Structures*, 37, pp. 365-368, 2004.

Serfass, J. P., Advantages, Peculiarities and Mysteries of Emulsion Cold Mixes. *Emulsion Cold Mixes Specific Features and New Design Methods*. Magny-les-Hameaux, France: Colas S A, 2002.

Shahin, M. Y., *Pavement Management for Airports, Roads and Parking Lots*. Norwell, MA: Kluwer Academic Publishers, 1994.

Shakir, S. F., “Development of New Cold Bituminous Mixtures for Road and Highway Pavements.” Ph.D. thesis, Liverpool John Moores University, Liverpool, UK, 2012.

Sharaf E. A., Eric, R., Mohamed, Y. S., and Sinha, K. C., Development of a Methodology to Estimate Pavement Maintenance and Repair Costs for Different Ranges of Pavement Condition Index. In *Transportation Research Record* No.1123, Transportation Research Board, Washington, D.C., pp. 30-39, 1987.

Sharaf, E. A., Shahin, M. Y., and Sinha, K. C., Analysis of the Effect of Deferring Pavement Maintenance, In *Transportation Research Record* No.1205, Transportation Research Board, Washington, D.C., 1988.

Siddique, R. *Waste Materials and By-Products in Concrete, Chapter 7: Rice Husk Ash*, PP. 235, Springer, ISBN: 978-3-540-74293-7, 2008.

Sivakumar, M., and Manikandan, T. An Experimental Study on Strength Development of Concrete Containing Composite Ash (Fly Ash-F & Rice Husk Ash), *International Journal of Engineering Research & Technology*, Vol. 3 Issue 4, pp. 1140-1144, 2014.

Smith, R. E., and Beatty, K., *Microsurfacing Usage Guidelines*. *Transportation Research Record: Journal of the Transportation Research Board*, No. 1680, Transportation Research Board of the National Academies, Washington, D.C., pp. 13-17, 1999.

Sorlini, S., Sanzeni, A., and Rondi, L., Reuse of steel slag in bituminous paving mixtures. *Journal of Hazardous Materials*, 209–210, 84-91, 2012.

Strategy for Sustainable Construction (SSC), HM Government, June, 2008.

Syed, I. M., Freeman, T. J., Smith, R. E., et al., “Effectiveness of highway maintenance treatments used in Texas,” in Proceedings of the Symposium on Flexible Pavement Rehabilitation and Maintenance, pp. 136–150, ASTM STP 1349, 1999.

Takamura, K., “An Elephant, 30 Cats and 1 million Fleas – How to view a Chip Seal Emulsion”, BASF Corporation, Charlotte, NC, 2002.

Taylor, H. F. W. Cement chemistry, Thomas Telford, 1997.

Temple, W., Shah, S., Paul, H., and Abadie, C., “Performance of Louisiana’s chip seal and micro-surfacing program, 2002,” *Transportation Research Record*, no. 1795, pp. 3–16, 2002.

Thanaya, I., Improving the Performance of Cold Bituminous Emulsion Mixtures Incorporating Waste Materials. PhD thesis, The University of Leeds, 2003.

The Paris Law., Fatigue crack growth theory. University of Plymouth, 21 June, 2010.

Thom, N., University of Nottingham, Department of Civil Engineering, “Materials”, Lecture notes, 2012.

Thom, N., “Principles of Pavement Engineering”, Second Edition, University of Nottingham, Department of Civil Engineering, 2013.

Tolman, F., and Van Gorkum, F., Mechanical Durability of Porous Asphalt, Eurasphalt and Eurobitume Congress, 1996.

TxDOT., “Highway Design Division Operations and Procedures Manual”. Texas Department of Transportation, Highway Design Division. Austin, Texas, 1984.

Tons, E., and Krokosky, E. M., A Study of Welded Wire Fabric Strip Reinforcement in Bituminous Concrete Resurfacing. Proceedings of the Association of Asphalt Paving Technologists. Vol. 29. pp. 43-80, 1960.

Transport and Road Research Laboratory (TRRL), Road Note 39, 2nd Edition “Recommendations for road surface dressing”, 1981.

U.S. Environmental Protection Agency (USEPA), “Air Quality and Energy Conservation Benefits from Using Emulsions to Replace Asphalt Cutbacks in Certain Paving Operations”, USEPA., 1978.

Van Gorkum, F., Lubbers, H.E., Priston, R.A.G., Roos, H., “Exposure to PAC in Bituminous Road Construction”, Eurobitume, Sweden, pp. 430-436, 1993.

Van Kirk, J., "Long lasting slurry pavements," in Proceedings of the International Slurry Seal Association Conference, Amelia Island, Fla, USA, 2000.

Vaughan, K. A., "An Investigation of Cement Coating for Aggregates in Bituminous Material." Ph.D. thesis, Liverpool John Moores University, Liverpool, UK, 1999.

Vivier, M., and Brule, B., Gap-Graded Cold Asphalt Concrete: Benefits of Polymer-Modified Asphalt Cement and Fibres. Transportation Research Record: Journal of the Transportation Research Board, No. 1342, Transportation Research Board of the National Academies, Washington, D.C., pp. 9-12, 1992.

Wajima, T., Haga, M., Kuzawa, K., Ishimoto, H., Tamada, O., Ito, K., Nishiyama, T., Downs, R. T., and Rakovan, J. F., Zeolite synthesis from paper sludge ash at low temperature (90°C) with addition of diatomite. Journal of Hazardous Materials, 132, 244-252, 2006.

Walls, J., and Smith, M. R., *Life Cycle Cost Analysis in Pavement Design - In Search of Better Investment Decisions*. Publ. FHWA-SA-98-079, FHWA, Washington, D.C., 1989.

Walters, G. V., and Jones, T. R., "Effect of Metakaolin on Alkali-Silica Reaction in Concrete Manufactured with Reactive Aggregate," *Durability of Concrete: Proc. Second International Conference*, ACISP 126, Vol. II, pp. 941-953, 1991.

Watson, D., and Jared, D., Georgia Department of Transportation's Experience with Microsurfacing. Transportation Research Record: Journal of the Transportation Research Board, No. 1616, Transportation Research Board of the National Academies, Washington, D.C., pp. 42-46, 1998.

Watson, J., *Highway Construction and Maintenance*, London, UK, Longman Group UK Limited, 1989.

Watson, J., *Highway Construction and Maintenance*, New York, Longman, 1994.

Weatherspark, Leeds Bradford International Airport weather [Online]. Available: <https://weatherspark.com/history/28736/2015/West-Yorkshire-England-United-Kingdom>, 2015 [Accessed 12/10/2015].

Weatherspark, Leeds Bradford International Airport weather [Online]. Available: <https://weatherspark.com/history/28736/2016/West-Yorkshire-England-United-Kingdom>, 2016 [Accessed 14/11/2016].

Whiteoak, D., "The Shell Bitumen Handbook", Shell Bitumen UK, 1991.

Woodside, A. R., Currie, B., and Woodward, W. D. H., “The Use of a Polypropylene Bituminous Composite Overlay to Retard Reflective Cracking on the Surface of a Highway”, 1993.

Wittwer, E., McNeil, S., Bittner, J., and Zimmerman, K., “Asset Management as a Communications Tool” in Key Findings from the 5th National Workshop on Transportation Asset Management, Midwest Regional University Transportation Center, University of Wisconsin-Madison, 2004.

Wu, S. P., Liu, G., Mo, L. T., Chen, Z., and Ye, Q. S., “Effect of fiber types on relevant properties of porous asphalt.” Transactions of Nonferrous Metals Society of China, 16, Supplement, pp.791-795, 2006.

Wu, S., Xue, Y., Ye, Q., and Chen, Y., Utilization of steel slag as aggregates for stone mastic asphalt (SMA) mixtures. Building and Environment, 42, 2580-2585, 2007.

Xiao, F., Amirghanian, S. N., Shen, J., and Putman, B., Influences of crumb rubber size and type on reclaimed asphalt pavement (RAP) mixtures. Construction and Building Materials, 23, 1028-1034, 2009.

Xue, Y., Hou, H., Zhu, S., and Zha, J., Utilization of municipal solid waste incineration ash in stone mastic asphalt mixture: Pavement performance and environmental impact. Construction and Building Materials, 23, 989-996, 2009.

Yi, J., and McDaniel, S., ‘application of cracking and seating and use of fibres to control reflection cracking’, Transportation Research Record, 1388, 150–159, 1993.

Yoder, E. J., and Witczak, M. W., Principles of pavement design, 2nd Edition, John Wiley & Sons, Inc., 1975.

You, Z., Goh, S. W., and Van Dam, T. J., Laboratory Evaluation and Pavement Design for Warm Mix Asphalt. Proceedings of the 2007 Mid-Continent Transportation Research Symposium. Ames, USA, 2007.

Zimmerman K., and Peshkin D. G., “Pavement management perspective on integrating preventive maintenance into a pavement management system”. *Transportation Research Record: Journal of the Transportation Research Board*, 1827, 2003, pp. 3-9.